

Xijun Yan *Editor*

Dan Shen (*Salvia miltiorrhiza*) in Medicine

Volume 1. Biology and Chemistry



人民卫生出版社
PEOPLE'S MEDICAL PUBLISHING HOUSE



Springer

Dan Shen (*Salvia miltiorrhiza*) in Medicine

Xijun Yan
Editor

Dan Shen (*Salvia miltiorrhiza*) in Medicine

Volume 1. Biology and Chemistry



人民卫生出版社
PEOPLE'S MEDICAL PUBLISHING HOUSE



Springer

Editor
Xijun Yan
Tianjin
China

ISBN 978-94-017-9468-8 ISBN 978-94-017-9469-5 (eBook)
DOI 10.1007/978-94-017-9469-5
Springer Dordrecht Heidelberg New York London

Library of Congress Control Number: 2014950646

© Springer Science+Business Media Dordrecht and People's Medical Publishing House 2015
This work is subject to copyright. All rights are reserved by the Publishers, whether the whole or part of the material is concerned, specifically the rights of translation, reprinting, reuse of illustrations, recitation, broadcasting, reproduction on microfilms or in any other physical way, and transmission or information storage and retrieval, electronic adaptation, computer software, or by similar or dissimilar methodology now known or hereafter developed. Exempted from this legal reservation are brief excerpts in connection with reviews or scholarly analysis or material supplied specifically for the purpose of being entered and executed on a computer system, for exclusive use by the purchaser of the work. Duplication of this publication or parts thereof is permitted only under the provisions of the Copyright Law of the Publishers' locations, in its current version, and permission for use must always be obtained from Springer. Permissions for use may be obtained through RightsLink at the Copyright Clearance Center. Violations are liable to prosecution under the respective Copyright Law.

The use of general descriptive names, registered names, trademarks, service marks, etc. in this publication does not imply, even in the absence of a specific statement, that such names are exempt from the relevant protective laws and regulations and therefore free for general use.

While the advice and information in this book are believed to be true and accurate at the date of publication, neither the authors nor the editors nor the publishers can accept any legal responsibility for any errors or omissions that may be made. The publishers make no warranty, express or implied, with respect to the material contained herein.

Printed on acid-free paper

Springer is part of Springer Science+Business Media (www.springer.com)

Preface to *Dan Shen (Salvia miltiorrhiza)* in Medicine

In the 2008 press conference on the publication of the Chinese edition of the *Dan Shen (Salvia miltiorrhiza) in Medicine*, several volume editors suggested that the book should be translated into English and distributed internationally. They all believed that the medical communities are enthusiastic about TCM research, and that among the studies on single herbs, the study of Danshen has taken the lead. Therefore, it was a worthy undertaking to introduce the study conducted by the Chinese people over the past 1,000 years, and especially in the past 30 years, to the world. Meanwhile, I was asked unanimously to be its editor-in-chief. After several years of hard work by nearly 100 professors and research scientists, the translation is finally complete.

The English edition of *Dan Shen (Salvia miltiorrhiza) in Medicine* is based on its Chinese edition. Modifications include changing the five-volume format to one volume and deleting some duplicated portions in the Chinese edition. Since the chapters in each volume of the Chinese edition were written by many individuals, details such as biological properties and ancient literature reviews were repeated many times, and the duplications were deleted in the English edition. Also, the various names of Danshen were unified. The appendix in the fifth volume, the prescriptions or formulas in ancient China, and the chapter on information management in the fourth volume were also deleted. The introduction to the production region, common names, and phytochemical components had appeared in the first three volumes, while this time only their first appearance was preserved. Some typos and oversights were corrected after consulting with volume editors. New progress in Danshen research was included in this book, such as the development of Salvianolate Lyophilized Injection, which finally came on the market in 2011 after 8 years of strict examination, and it was a landmark event in the development of TCM injections. It is unfortunate that we could not include the data on Qishenyiqi Dripping Pills, as the papers have not been published yet. The drug, developed by academician Boli Zhang, passed large-scale, evidence-based medicine clinical research trials in 2010, the first for a TCM drug, and won the 2011 National Science and Technology Progress Award.

In principle, the English edition of *Dan Shen (Salvia miltiorrhiza) in Medicine* is the translation of the Chinese edition, thus preserving the latter's framework. Because the Chinese edition was written by more than 100

scholars and published in five volumes, the styles and layouts were not identical. For example, some references were listed at the end of the chapter, while some were listed at the end of the section. The English edition did not change the style.

Dan Shen (Salvia miltiorrhiza) in Medicine has amassed Danshen research results since the times of ancient China—it is not only a magnificent historical scroll, but also a huge work which shines the light of modern science and technology.

I sincerely thank academicians Yongyan Wang and Boli Zhang. They have given me so much substantive guidance and encouragement despite their busy schedules. Without their help, it would have been impossible to finish the work. I also want to thank every author and volume editor who has participated in the writing and editing of both editions of this book; they have solved various problems which arose during the writing and translating processes. Last but not least, I want to thank the comrades working in the office of *Dan Shen (Salvia miltiorrhiza) in Medicine*, who have worked patiently and diligently over the past 15 years, collecting and organizing data and information.

The publication of the English edition of *Dan Shen (Salvia miltiorrhiza) in Medicine* is a testimony of our sincere desire for the communication and discussion of TCM among international communities. We earnestly welcome suggestions and criticism from our colleagues around the world.

Xijun Yan

Preface to Volume 1. Biology and Chemistry

“Botany of Danshen” systematically introduces the research on and the resource survey for Danshen (*Salvia miltiorrhiza*). It also describes Danshen’s pharmaceutical and biological characteristics, its identification, *distribution* and ecological environment, and its planting, in vitro cultivation, and genetic *breeding*. The content of Part I is based on a large amount of literature research. More importantly, many authors of this section are those who conducted this original research. For example, most of the content from Chaps. 3 to 6 is based on firsthand data; it represents not only the latest research results on Danshen, but also the theoretical foundation for further research.

It is worth pointing out that the writing of this part has received support from Tianjin Tasly Group and from a project sponsored by the National High-tech *development* Program (“863 program”). Special thanks!

Since Danshen is currently a hot topic in Chinese medicinal research, it is sure that more and more research data will be released, and that this part will have room for improvement. We welcome any criticism or comments.

February 2008

Luqi Huang

Editing Committee

Chief Editor

Xijun Yan

Chief Reviewers

Yongyan Wang

Boli Zhang

Associate Chief Editors

Naifeng Wu

Guoguang Zhu

Luqi Huang

Lianniang Li

Houwei Luo

Juntian Zhang

Guanhua Du

Dean Guo

Yiyu Cheng

Xuewen Zhang

Xinde Shi

Zhengliang Ye

Yonghong Zhu

Shuiping Zhou

Hanxi Xue

Editing Office

Director

Renshu Li

Members

Yonghong Zhu

Zhengliang Ye

Hanxi Xue

Ying Zhao

Volume 1. Biology and Chemistry

Chief Editors

Luqi Huang
Lianniang Li
Houwei Luo

Associate Chief Editors

Deyou Qiu
Zongsuo Liang
Min Chen

Editors

Xuefeng Feng
Wenting Liu
Xirong He
Jingyuan Song
Deyou Qiu
Min Chen
Jinda Hao
Lanping Guo
Guanghon Cui
Zongsuo Liang
Luqi Huang
Houwei Luo
Lianniang Li

Volume 2. Pharmacology and Quality Control

Chief Editors

Juntian Zhang
Guanhua Du
Dean Guo

Associate Chief Editors

Xiumei Gao
Shen Ji
Ming Zhu
Rongxia Liu
Haibin Qu

Editors

Lianhua Fang
Yitao Wang

Xiaoying Wang
Yuehua Wang
Dongxia Wang
Xiaoming Wang
Yi Wang
Jinhua Wang
Jie Wang
Xiaoying Wang
Hongmei Guang
Changsuo Liu
Ailin Liu
Yan Sun
Yonghong Zhu
Jinglan Xu
Guorong He
Xiuying Yang
Danshen Zhang
Tiantai Zhang
Ran Zhang
Juntian Zhang
Li Zhang
Lihua Zhang
Bin Zhang
Chuan Li
Guanhua Du
Rong Du
Ping Chen
Yonghong Chen
Xiuping Chen
Ji Chen
Shuiping Zhou
Zhiwei Qu
Xiaoming Zhu
Zhihao Jiang
Minke Tang
Zhiwen Li
Zhixin Guo
Xiumei Gao
Mei Gao
Hongcai Shang
Xinrui Cheng
Guangliang Han
Jingyan Han
Yanqiao Zang
Ying Dai
Linke Ma
Hongzhi Wang

Junquan Wang
Yi Wang
Zhun Feng
Zhengliang Ye
Yonghui Liu
Yan Liu
Rongxia Liu
Shunhang Liu
Aihua Liu
Xuesong Liu
Jianghao Sun
Guoqing Wu
Ling Tong
Yongjiang Wu
Wanying Wu
Xiaoqian Zhang
Xuemin Zhang
Jinlan Zhang
Xian Zhang
Yunfei Li
Manling Li
Min Yang
Yuewu Yang
Bilian Chen
Shen Ji
Jianping Lin
Dean Guo
Guoqiang Fan
Xiaohui Fan
Qiang Zheng
Zhangzhao Jin
Ming Zhu
Jun Gao
Hongfang Cui
Fenglan Cao
Rixin Liang
Shunnan Zhang
Qing Gong
Haiou Dong
Jianping Han
Haibin Qu

Volume 3. Clinical Research

Chief Editors

Guoguang Zhu
Xuewen Zhang

Xinde Shi
Associate Chief Editors

Yi Zheng
Ruizhi Luo
Naifeng Wu

Editors

Xinde Shi
Yan Liu
Jinping Liu
Jia Liu
Yonghong Zhu
Danyong Wu
Naifeng Wu
Xuewen Zhang
Renshu Li
Ruizhi Luo
Yi Zheng
Guoguang Zhu
Jingsheng Zhao
Ying Zhao
Jiaoli Guo
Shunnan Zhang
Keqin Han

Contents

1	Materia Medica and Plant Resource	1
	Jinda Hao, Xirong He, Luqi Huang and Min Chen	
1.1	Nomenclature	1
1.1.1	Common Name	1
1.1.2	Names in Literature [3]	1
1.1.3	Names in Different Regions [3]	1
1.1.4	Commercial Names [3]	2
1.1.5	Prescription Names [3]	2
1.2	Etymology	2
1.3	Materia Medica Studies	2
1.4	Resource Survey	3
1.4.1	Local Varieties and Original Plant of Danshen [6]	4
1.4.2	Species Confused with Danshen [6]	8
	References	10
2	Distribution and Habitat of Danshen	11
	Luqi Huang, Min Chen and Lanping Guo	
2.1	Geographic Distribution	11
2.2	Ecological and Biological Characteristics	11
2.3	Environmental Condition	12
2.3.1	Climatic Conditions	12
2.3.2	Soil Conditions	12
2.3.3	Community	12
2.3.4	Habitat of High-quality Danshen	12
2.4	Geographic Variation and Quality	13
2.4.1	Geographic Variation	13
2.4.2	Genuineness	15
	References	18
3	Biological Characters of Danshen	19
	Zongsuo Liang, Wenting Liu, Xuefeng Feng and Guanghong Cui	
3.1	Morphology and Development	19
3.1.1	Morphological Characteristics	19
3.1.2	Growth and Development	24

3.2	Anatomical Morphological Characteristics of Danshen . . .	27
3.2.1	Morphological Characteristics of Leaves.	27
3.2.2	Morphological Characteristics of Stems	28
3.2.3	Morphological and Structural Characteristics of Roots.	29
3.2.4	Conclusion	30
3.3	The Reproductive Biological Characters of Danshen . . .	31
3.3.1	Phenological Periods of the Flowering of Danshen.	31
3.3.2	The Exterior Appearances of Flowers and Dynamic Flowering Process of Danshen . . .	32
3.3.3	Morphological Characteristics of Danshen Pollen Grains	32
3.3.4	Vitality of Danshen's Pollen Grains.	32
3.3.5	Effects of Pollination Time (Table 3.8) and Pollination Mode on Seed Setting Rate . . .	33
3.3.6	Conclusion	33
3.4	Study on Danshen's Pollen [10, 11].	34
3.4.1	Morphological Characteristics of Pollen in Genus <i>Salvia</i>	34
3.4.2	Morphological Characteristics of Pollen of Different <i>Salvia</i> Groups	35
3.4.3	Morphological Characteristics of Pollen of Species and Cultivated Varieties	35
3.5	Cytological Study on Danshen Plants [13]	35
3.6	Embryologic Study on Danshen.	35
3.6.1	Development of Macrospores and Female Gametophytes [13]	35
3.6.2	Development of Microspores and Male Gametophytes [16]	40
3.7	Molecular Biological Study on Danshen	42
3.7.1	Isozyme Analysis of Danshen	42
3.7.2	Studies on the Molecular Identification of Danshen.	43
3.7.3	Construction of Danshen cDNA Chips and Study on Functional Genomics	44
	References	47
4	A Study on the Cultivation of Danshen	49
	Zongsuo Liang and Wenting Liu	
4.1	Propagation of Danshen	49
4.1.1	Propagation by Seeds.	49
4.1.2	Propagation by Rootstalk Division.	49
4.1.3	Propagation by Root Division.	49
4.1.4	Propagation by Cutting	50
4.1.5	Propagation by Tissue Culture	50
4.2	A Study on the Biological Characters of Danshen Seeds	51

4.2.1	Water Absorption Characters of Danshen Seeds	51
4.2.2	Influences of Environmental Conditions on Germination of Danshen Seeds	52
4.2.3	Conclusion	53
4.3	Influences of Bud Removal on the Yield and Contents of Effective Constituents of Danshen	54
4.3.1	Exterior Characters of Danshen's Roots After Treatments	55
4.3.2	Changes in Yield After Treatments	55
4.3.3	Conclusion	56
4.4	Summer Dormancy of Danshen	56
4.4.1	Growth Characteristics of New Seedlings Growing on Basal Parts of Stems	57
4.4.2	Discussion	59
4.5	Influences of Planting Density on Yield and Contents of Active Constituents of Danshen	60
4.5.1	Influence of Transplanting Density on Survival Rate	61
4.5.2	Influence of Different Densities on Tanshinol and Tanshinone IIA Contents	61
4.5.3	A Comparison of the Yields of Danshen Under Different Densities (In Terms of Fresh Weight)	62
4.5.4	Summary and Discussion	63
4.6	The Effects of Microelements on the Growth of Danshen and the Accumulation of Effective Constituents	64
4.6.1	Relationship Between Microelements and Tanshinol	64
4.6.2	Relationship Between Microelements and Tanshinone IIA	65
4.6.3	Dynamic Growth and Development of Roots Treated with Microelements	66
4.6.4	Summary	67
	References	68
5	Danshen's In Vitro Culture	69
	Deyou Qiu and Jingyuan Song	
5.1	Micropropagation of Danshen	69
5.2	Cell Culture of Danshen	72
5.3	Tissue and Organ Culture of Danshen	74
5.3.1	Culture of Danshen Adventitious Roots	74
5.3.2	Culture of Hairy Roots and Crown Gall Tissues of Danshen	75
5.3.3	Culture of Crown Gall Tissues of Danshen	80
	References	87

6 Genetics and Breeding of Danshen	89
Deyou Qiu and Jingyuan Song	
6.1 The Germplasm Resources and Breeding Studies of Danshen	89
6.2 Mutation Breeding of Danshen	90
6.3 Molecular Breeding of Danshen.	91
6.3.1 Molecular Marker-Assisted Breeding of Danshen.	91
6.3.2 Studies on the Breeding of Danshen by Genetic Engineering	92
References	95
7 Water Soluble Components of Danshen.	97
Lianniang Li	
7.1 Literature Review	97
7.2 Introduction	98
7.3 Chemical Structures of Phenolic Acids	98
7.4 Extraction and Isolation of Phenolic Acids	99
7.4.1 Extraction of Phenolic Acids	99
7.4.2 Isolation of Phenolic Acids.	101
7.4.3 Examples of Phenolic Acid Isolation	102
7.5 Spectral Properties of Phenolic Acids	103
7.5.1 Ultraviolet Spectra.	103
7.5.2 Mass Spectrometry	103
7.5.3 Nuclear Magnetic Resonance Spectra.	103
7.6 Physical and Chemical Properties of Phenolic Acids.	107
7.6.1 General Properties	107
7.6.2 Stability	109
7.6.3 Chemical Transformation	109
7.7 Biosynthetic Pathways of Phenolic Acids	110
7.8 Synthesis of Phenolic Acids	110
7.8.1 Synthesis of Danshensu [22].	110
7.8.2 Synthesis of Salvianolic Acid F [23]	112
7.8.3 Synthesis of Heptamethyl Lithospermate [24]	116
References	117
8 Liposoluble Chemical Constituents in Danshen	119
Houwei Luo	
8.1 Introduction and Classification.	119
8.1.1 Early Records of Chemical Study on Tanshinone	119
8.1.2 Nomenclature and Classification of Liposoluble Constituents in Danshen	121
8.2 Extraction and Isolation of Liposoluble Compounds.	128
8.2.1 Extraction Method.	129
8.2.2 Separation Methods	130
8.2.3 Operating Procedure and Examples of Preparative Isolation	139

8.2.4	Determining Column Chromatographic Conditions Based on Preseparation on TLC	142
8.2.5	Two Forms of Preparative Columns: Comparison Between Dry Column Chromatography and Gradient Elution	143
8.2.6	Examples of Gradient Elution	144
8.3	Spectrum Characteristic of Tanshinone Compounds	145
8.3.1	Ultraviolet Spectrum	145
8.3.2	Infrared (IR) Absorption Spectrum	148
8.3.3	Nuclear Magnetic Resonance (NMR) Spectrum	151
8.3.4	Mass Spectrometry	166
8.4	The Physicochemical Properties of Tanshinones.	173
8.4.1	The Redox Potential of Tanshinones	173
8.4.2	The Chemical Stability of Tanshinones and the Influence of Solvents on Their Structures	177
8.4.3	The Effects of Rings and Conjugation Systems on the Activity of Quinones	177
8.5	The Biosynthetic Pathway of Tanshinone and Its Artifacts	185
8.5.1	The Biosynthesis of Cryptotanshinone	185
8.6	Chemical Synthesis of Tanshinones	190
8.6.1	Total Synthesis of Tanshinone IIA.	190
8.6.2	Diene Addition of 3-methoxyl-benzofuran-4, 7-diketone	190
8.6.3	Total Synthesis of Miltionone	192
8.6.4	Structural Modification of Tanshinone IIA	194
8.6.5	Structural Modification of Tanshinone I.	195
8.7	Triterpenoids of Danshen	198
8.7.1	Isolation and Identification of Przewanoic Acid A and B [87]	198
8.7.2	Isolation and Identification of Trijuganoic and Euscaphic Acids [88].	200
8.7.3	Isolation and Identification of Triterpene Acid from <i>S. Paramiltiorrhiza</i>	202
8.8	The Challenges and Opportunities for the Study of Tanshinones in this Century	204
8.8.1	The Chemical Study of Tanshinone Aims at Finding New Targets	204
8.8.2	The Biological Activities and the Physicochemical Properties of Compounds	204
8.8.3	Chemical–biological Research of Tanshinone.	205
	References	206
	Index	209

About the Chief Editor

Dr. Xijun Yan was born in 1953 in Zhenyuan, Gansu province. Dr. Yan is a chief pharmacist, and enjoys the Special Expert's Allowance from the State Council of China. At present, he is a President of Tianjin Tasly Group; serves as a member of traditional Chinese medicine (TCM) Standardization Technical Committee; the deputy director of Science Popularization Committee of Chinese Pharmaceutical Association; a member of Expert Committee of The National Pharmaceutical Industry Policy Research Project of Chinese Pharmaceutical Association; the vice president of Tianjin Pharmaceutical Association. Dr. Yan is the first person to propose the concept of "modern TCM drugs" and the new mode of TCM R&D, and has engaged for a considerable length of time in research and industrial development of modern Chinese medicine. Dr. Yan has actively undertaken key national projects on the research and development of important new drugs, supervised or participated in 38 projects in the National Key Science and Technology Projects in the 9th and 10th "Five Year Plans"; National Level Promotion Program of Scientific and Technological Achievements; National High-tech Industrialization Demonstration Project, etc. Dr. Yan has 69 patents and more than 50 publications, including *The Standards of Diagnosis, Efficacy, and Medication in TCM's Heart Disorder* (one of the editors-in-chief); *How TCM Drugs Enter the EC Market* (associate editor-in-chief); *The Ideas and Methods of Modernization of TCM Research* (one of the editors-in-chief); *The Reflection and Practice of the Modernization of TCM Preparations*; *On the Trends of Modern TCM Industry*, etc. Dr. Yan has been awarded honorary titles like National Model Worker; National Outstanding Scientific and Technological Worker; National Outstanding Pharmaceutical Entrepreneur; National Health Industry and Enterprise Advanced Individual; National Model Worker in Chinese Medicine System. Dr. Yan has received numerous awards, including the Third National Prize for Scientific Advancement, the Second Prize for Scientific Advancement by the People's Liberation Army, and the First Prize for Scientific Advancement by Tianjin Municipal Government.

Introduction by Chief Editor

After the hard efforts of an entire decade, by nearly 100 experts from home and abroad, the *Dan Shen (Salvia miltiorrhiza) in Medicine* is finally going to the press.

Danshen (*Salvia miltiorrhiza*) has a time-honored history of research, development, and application in China's traditional medicine, and is held in very high esteem by the medical community. We hope that the five-volume series now made available to the readership will make a worthwhile contribution to its research and application.

Salvia Carries the Dream of Internationalization of Traditional Chinese Medicine

In 1996, China began to formulate and implement a strategy for the modernization of traditional Chinese medicine (TCM). However, the question of how in practice to systematically develop traditional medicine passed on from generation to generation over several millennia, remained a real and persistent challenge to the academic and industrial dimensions of TCM. In 1998, a discussion among several TCM experts from home and abroad gave us the idea of compiling the *Dan Shen (Salvia miltiorrhiza) in Medicine*. The experts discussed not only the present state and the future prospects of modernizing Chinese medicine itself, but also the growth of the Chinese medicine industry, and the issues in developing big brand modern TCM drugs. The discussion was especially centered on the utilization of Danshen, and the topics ranged from its collection and processing in ancient times to the widespread application of various Danshen preparation, from its effective components to its pharmaceutical action, from its cultivation and plantation to its modern industry chain, from its compound prescriptions and to modern Compound Danshen Dripping Pill (Dantonic™), from its R&D to the rapid growth of a modern TCM enterprise—the Tasly Group. Is it possible that a unique industrial technology and economy grow out from a single TCM drug and a series of research activities focused on the drug? Is it possible that the unique industrial technology and economy stimulate new lines of thinking and novel approaches to the modernization and internationalization of TCM? Is it possible the unique industrial technology and economy push forward the systematic project of TCM research and development? These and several other questions roused profound interest

among experts in deepening the research on Danshen, and the compilation of the *Dan Shen (Salvia miltiorrhiza) in Medicine* was originated from this initial driving force.

For thousands of years, TCM has made enormous contribution to the health and multiplication of the Chinese people. But why is it so hard for TCM to be accepted and acknowledged in the international community? Why do some people still have doubts about the scientific nature of TCM? To be able to continually promote the modernization and internationalization of TCM, these questions must have affirmative answers. In order to introduce Chinese medicine to the rest of the world, and let the international community understand, accept, and use TCM, we must resort to modern technology to re-develop TCM again. We also have to give TCM a fresh interpretation, using the standardized scientific and digitized languages. It is indeed necessary to select a certain Chinese medicine for an exploratory trial, and this Chinese medicine must meet a number of requirements. First, it should have both a long history of inheritance and deep accumulation of clinical knowledge; second, it has been systemically studied with modern means of science and technology, and its effective substances and the mechanism of action have been elucidated, relatively speaking; third, it has made a comparatively great contribution to human health, especially in terms of satisfactory effects in the treatment of serious diseases; fourth, its industrialization has been successful, having representative name brand products; fifth, it has sufficient resources to ensure the sustainable industrialization; and sixth, it should be conducive to a progressive growth of Chinese medical research. We believe that Danshen meets all these requirements, and it could showcase a wealth of innovative achievements and profound knowledge, and become a model in promoting the modernization and internationalization of TCM.

Hundreds of Scientists Involved in the Work

It is with this underlying ambition in mind that we started data collection, collation, and *compilation of the this book*. Nearly 100 experts from home and abroad have participated in this huge project. The expert team includes both world renowned senior scientists and young scholars with outstanding achievements. Some of them are from prestigious research institutions and universities, others from industrial regulatory bodies, and still others from the frontline of industrial development. Their expertise covers multiple research areas, including medicinal botany, phytochemistry, pharmaceutical analytics, pharmacology, toxicology, medical preparation, medicine reviewing, TCM, and integrative medicine. We have been particularly fortunate in that our research and compilation work has received strong support and guidance from the academicians Yongyan Wang and Boli Zhang, as well as from several relevant leaders and experts. Each writer adhered to the mission of “being responsible for both past and future generations” and followed stringent scientific spirit and serious academic attitude, searching extensively, and studying strenuously and carefully. They referenced nearly 50,000 pieces of literature, including books, research articles, trial reports,

and others, directly quoted 7,235 references, thus laying a solid literature foundation for the work.

Botany of Danshen documents Danshen herbal research, medical source survey, identification of medicinal characteristics, distribution and ecological environment, biological features, in vitro culture, and genetic breeding; describes and reviews research on Danshen germplasm resources and genetic diversity. The detailed research provides guidance for scientific and large-scale cultivation of Danshen, and contributes to the securing of resources for its further development and industrialization.

The phytochemical research of Danshen originated in the 1930s. Centered on the extraction and isolation of the effective components from Danshen, researchers have utilized various techniques and spectral analytical methods, including the 2D nuclear magnetic resonance. These developments are all accounted for in *Phytochemistry of Danshen*. The volume also systematically describes the chemical structure of Danshen's liposoluble ingredients (tanshinones) and water-soluble ingredients (salvianolic acids), methods for extraction and isolation, spectral characteristics, the chemical and physical properties, the biosynthesis pathways, and chemical synthesis. The chemical ingredients of other plants in the genus *Salvia* are also described.

Since the 1930s, domestic and international experts have carried out in-depth, or even spectacular, intensive pharmacological research into the effective ingredients of Danshen. They have analyzed its pharmacological action and mechanisms in the cardio-cerebrovascular system, the nervous system, the digestive system, and its anti-bacterial and anti-inflammatory effects. In the *Pharmacology of Danshen*, the liposoluble and water-soluble ingredients of Danshen are described in detail for their pharmaceutical functions. The lipo-soluble ingredients have the functions of anti-bacteria and regulation of the endocrine, while the water-soluble ingredients have the functions of anti-oxidation, anti-ischemia, and inhibiting the expression of cell adhesion molecules. The multi-target effects of Danshen and its preparations in the treatment of microcirculatory dysfunction have been recognized by the international pharmacological scholars. The volume reviews and summarizes the achievements of these researches in considerable detail, revealing the leaps and bounds of modern pharmacology in recent years.

Quality Control of Danshen is based on research into the pharmacologically effective components of Danshen. The volume introduces a QC system which combines fingerprinting technology with multi-indicator analysis. In fact, this QC system is a full range of Danshen quality control system, integrating modern TCM chemistry, pharmacological pharmacodynamic, and pharmacokinetics, covering Danshen identification, content determination, fingerprinting spectra, in vivo metabolic processes of major ingredients, and the effect of the preparation process on the quality of drugs, etc. The volume shows comprehensively and systematically the present state of Danshen quality control and highlights the most recent achievements.

Clinical Research of Danshen records 1,261 carefully selected Danshen-containing prescriptions from over 2,000 medical works since the Qin and Han dynasties. It reports the summarized results of mathematical and

statistical analysis, showing how Danshen-containing drugs were processed, with which herbs Danshen was combined, and what kinds of preparations were used. The changes in the frequency of other herbs combined with Danshen, and the indications of these prescriptions have been compared. The ancient Chinese pointed out explicitly a long time ago that the basic functions of Danshen are to invigorate blood and dissolve stasis, and clear blood vessels. They also summarized that “the functions of a single Danshen is equal to those of Four Substances.” In the field of modern medicine, Danshen enjoys an even wider application. The authors of the volume have carried out exhaustive documentation and summarization of the clinical applications Danshen, especially the experience from famous TCM doctors. In this volume, the methods of evidence-based medicine have been used to summarize the functions of modern TCM drugs, Compound Danshen Dripping Pill (Dantonic™) in the prevention and treatment of coronary heart disease and its multiple risk factors, and proposes for the first time the multiple-target mechanism of Dantonic™’s effects on the treatment of coronary heart disease and angina. In addition to their wide application in the treatment of cardio-cerebral vascular diseases like coronary heart disease and ischemic stroke, Danshen preparations are used to treat other diseases, and it has proved to be effective for chronic hepatitis, chronic nephritis, chronic kidney failure, type II diabetes, blood diseases, infectious diseases, and skin diseases. All of these are systematically described in the volume. Such an integration will doubtlessly be beneficial to clinical workers in the fields concerned.

Looking at the history, it is safe to say that Danshen has been one of the most extensively used drug in TCM since ancient times, and it is one of the TCM herbs studied with modern techniques the earliest and most thoroughly. Through the research on Danshen in botany, biology, chemistry, pharmacology, and clinical trials, we now have comprehensive understanding of its effective components, clinical effects, and indications. The study on the effective components of Danshen serves as the foundation for the study on its pharmacological effects, and based on the pharmacological study, a batch of widely applied and effective modern Danshen preparations have been developed. Danshen research is a model of multidisciplinary, multi-domain, multi-faceted integration and cooperation, and will surely be an important milestone in the process of modernization of TCM.

New Challenges and Opportunities in the Era of Health Care

Since the 1970s, the spectrum of human diseases has shifted from the infectious to lifestyle diseases, geriatrics, and degenerative diseases. This has brought about significant changes in medical modes and treatment philosophies; from the biological medicine mode to a “biological-psychological-social” mode; from the purely passive disease treatment to the combination of “prevention–healthcare–treatment–rehabilitation.” Also, people are paying more attention to a timely adjustment of, and recovery from, sub-health state. These trends suggest that the society has entered an

era of “enlarged health.” People hope to attain the objective of enjoying a longer and healthier life by means of full care and comprehensive protection. To put it simply, we now strive to have a life journey which consists of “eugenic birth, longevity life, delayed aging, and peaceful departure.” These changes have posed new challenges to medical research, and guided medical R&D into a new age.

Started from searching for the chemical basis of life substances in 1780s, the drug development mode of modern medicine has gradually evolved into looking for chemical compounds. The trends of contemporary drug development show that a new drug can only be successfully developed after screening thousands of compounds, and the cost of R&D for listed drugs increasing annually, while the speed of new drug development is slowing down, which leads to a vicious circle characterized by high input, high risk, and low output. There is urgent need for a fresh drug R&D mode.

Very different from the Western mode, the TCM mode started from a holistic concept, based on individualized diagnosis and treatment and knowledge accumulation, used the resources of plants, animals, and minerals, and developed preparations of pills, powders, pastes, etc. These TCM preparations, tested through clinical application over thousands of years, contained a variety of pharmacodynamic active substances, and their action mechanisms integrated antagonistic, supplement, and regulation as one. Thus, our ancestors have left us a drug resource treasure, which is our unique advantage. This advantage is also a more economical and efficient path to the discovery of new drugs.

The promotion of TCM modernization strategy, and the implementation of policies such as the Scientific and Technological Action of TCM Modernization (Outline), and the Development Outline for TCM Modernization, has enabled the construction of a system for scientific innovation of Chinese medicine. Contemporary high-tech innovations are increasingly used in the field of TCM, engendering a diversified research and development of TCM. Although the most varieties and the most widely used TCM drugs are the traditional preparations, modern TCM drugs have gradually matured, and the exploration of chemical TCM, biological TCM, and metabolic TCM is receiving increasing attention. Modern TCM drugs are those based on TCM formulas and prescriptions, but manufactured using modern technology to extract effective components, using fingerprinting and chromatographic techniques for qualitative and quantitative quality control, using online data collection, analysis and feedback function of information technology to adapt to the new industrialized production requirements. Chemical TCM drugs are drugs obtained using chemical methods to isolate from TCM or herbal drugs single effective ingredients that could not be totally synthesized, and use them as the lead compounds to generate monomer compounds drugs with defined structures after in-depth study of chemical and biological activities, and by structural modification and transformation.

The priorities in the exploration of biological TCM drugs are planting of medicinal plants, extraction of the effective components, and manufacture of the preparations. In addition, bio-techniques could be used to discover or invent new effective components, to improve the effectiveness of TCM

drugs and the recovery of the effective components, as well as to reduce toxic and side effects. The so-called metabolic TCM drugs are to be searched for new active substances (effective components, effective fractions, or new lead compounds) from the metabolic process of TCM drugs in human or animal bodies, and use them for new drug development. It can be predicted that new techniques and new fields of Chinese medicine R&D will keep springing up. The key is to encourage diversified innovation and exploration based on different technical routes.

The aim of *Encyclopedia of Danshen* is not just to focus on a single TCM herb, but to use the rich TCM drugs and prescriptions as a medical resource treasury, to combine innovative thinking in TCM with modern medical techniques, and to explore new modes for pharmaceutical R&D.

Cooperation to Develop a Blockbuster of Traditional Chinese Medicine

Historically, the typical mode of practicing TCM has been to run a mom-and-pop style operation, composed of a storefront and a backroom workshop. The introduction of modern industrialization has changed the modes of both innovation and industrial organization of TCM. Multidisciplinary cooperation and industry—academia—research integration have become the best approaches to TCM pharmaceutical R&D.

China has a large number of TCM preparations, but few have a market sales in excess of 500 million Yuan, and even fewer with a market sales over 1 billion Yuan. For TCM drugs to meet the standards of modernization and internationalization, for TCM enterprises to become large industry, characteristic industry, or even competitive industry, name brand products and large-scale production are essential. Analyzing the knowledge economy, industry economy, and technology economy of TCM from the point of view of economics, we can see both the huge potential of TCM and the gap between TCM industry and modern pharmaceutical industry.

Starting with a single TCM herb Danshen, bringing together the elite researchers at home and abroad, through a comprehensive and systematic study, *Dan Shen (Salvia miltiorrhiza) in Medicine* has demonstrated the quality, effectiveness, safety, and toxicological and pharmacokinetic characteristics of Danshen-containing drugs. Moreover, it has demonstrated the scientific nature of TCM with detailed and accurate research results, which will unquestionably contribute to the understanding, acceptance, and utilization of TCM drugs by more people, and this is in turn laying a scientific foundation for the expansion and further strengthening of the TCM industry.

The comprehensive and systemic study of Danshen shows that a “blockbuster” type of TCM drug can be developed. The industrialization of TCM has a character of close connections among multiple industries, so the key is to actively exert the gathering and coordinating role of TCM industrial chain to promote the technological transformation, standards upgrades, and structural optimization in the entire industry, and realize the economic value of

TCM in various links of the chain, including TCM agriculture, TCM industry, TCM commerce, and TCM knowledge industry.

A single TCM herb can be used in a variety of prescriptions to benefit the health of many patients; a TCM industrial chain can also boost the economy of certain areas. I believe that the *Encyclopedia* can provide inspiration for the development of TCM resources and TCM industry.

Inheritance and Innovation

A comprehensive summary of Danshen research over thousands of years is both a grand event to revitalize TCM and a difficult task. This series contains not only the original research on Danshen by ancient people and contemporary scientists, but is also the fruit of strenuous labor and a large amount of pioneering work on the part of each author. To summarize Danshen research is to shoulder not only the burden of inheriting previous experience, but also the burden of opening the future and deepening innovation.

As the titled Encyclopedia indicated, this series not only strives to be “extensive and comprehensive,” but also attempts to be “excellent and profound.” Therefore, in terms of compilation style, we not only try to maintain the uniformity in style and systematicness in content, but also take into consideration the uniqueness of each volume, so that the characteristics and progress in each field can be reflected. The book is based on a single herb, Danshen, thoroughly going through the literature from ancient till modern times, with the purpose of reflecting from a certain angle the progress and development of TCM through generations. We divide the series into volumes in terms of botany, phytochemistry, pharmacology, quality control, and clinical research, in order to reflect the entire picture of Danshen research on one hand, and extract the essence of the research on the other, so as to reach the goal of integrating the practicality, comprehensiveness, and prospective-ness in one book. We adopted the approach of “breaking down the institution barriers,” bringing together nearly 100 experts from the forefronts of their relevant fields. We advocated brainstorming and free debate, as well as the accumulation of collective knowledge and wisdom to develop the Encyclopedia into a genuine milestone in Danshen research.

Memories pass through thousands of years, and science is an endless frontier. The modernization and internationalization of TCM is an ongoing process, science is being advanced, technology is being innovated, cross-disciplinary achievements are being integrated, and in-depth research into Danshen is being pushed forward in multiple sectors. There is every reason to believe that this research will continue to be enriched and replenished with an ever-increasing number of new and even more in-depth fruits. The modernization of Chinese medicine is of course more than just producing a collection of academic and technical research papers and awards. It also calls for more TCM products to drive the relevant industries, even new cultural and humanitarian philosophies, which in turn pose new themes and topics to Danshen research for our continuously to explore and innovate. With further

research and accumulation of findings, we will no doubt be able to come up with an additional volume or a sequel to this book, bringing Danshen research to ever deeper and higher levels.

The publication of the book is first of all made possible by the creative achievements of our predecessors in various ages, and by the long history and timeless essence of Chinese culture and Chinese medicine. Our most deeply felt gratitude, then, goes to our ancestors, for this precious scientific and cultural heritage.

In the process of compilation, the associate editors of the book, leaders of various institutions and agencies, colleagues, and friends from home and abroad who are enthusiastic about TCM have given strong support and great help. The chief editors, associate editors, and editors of individual volume, as well as colleagues of the *Encyclopedia* compilation office, have made enormously strenuous efforts toward the publication of the book, and it is to them that I hereby extend my sincerest gratitude. A special mention is due to these experts who participated in this project. They themselves are accomplished experts on Danshen research. They bear the heavy research work of their own, and shared the work of writing this book. Thanks go to the experts for their research accomplishment and hard work. The academicians Yongyan Wang and Boli Zhang sacrificed from their precious time to review the manuscript and to author the Prefaces. All of our editors and compilers extend their deepest gratitude to them.

In terms of compilation style, we applied uniform requirements while leaving relatively great room for each volume in order to allow the chief editors of each volume to exercise judgment according to discipline-specific features and the particular status of research. Therefore, it was impossible to achieve perfect coherence in the writing style and length. The research literature on Danshen transcends several millennia and country borders, and covers multiple disciplines. Despite arduous research and diligent search efforts on the part of various editors and compilers, errors and mistakes may still exist. Collective authoring of a five-volume encyclopedic series calls for enormous amounts of work. Therefore, even repeated elaboration and modification by multiple experts may still leave some room for improvement. We sincerely hope that friends and colleagues in the Chinese medicine research and industry, as well as the hopefully vast readership at large will offer their criticism and comments.

Xijun Yan

Jinda Hao, Xirong He, Luqi Huang and Min Chen

1.1 Nomenclature

1.1.1 Common Name

Salvia miltiorrhiza was first recorded as Danshen in the oldest materia medica book in China, *Shen Nong's Classic of the Materia Medica* [1] and was classified as a top-tier medicine. It has ever since been recorded in subsequent materia medica books, including Part I of *Chinese Pharmacopoeia*, 2005 edition [2].

1.1.2 Names in Literature [3]

Danshen has many different names in literature. In *Shen Nong's Classic of the Materia Medica*, it was called Xichan Cao (Xi cicada grass, 猓蟬草). In *Wu Pu's Materia Medica*, it was Chishen (red root, 赤參) or Mu Yang Ru (woody goat's milk, 木羊乳). In *Collective Commentaries on the Classic of Materia Medica*, it was Zhu Ma (chasing horse, 逐馬). In *Ri Hua-zi's Materia Medica*, it was Shan-shen (mountain root, 山參). In *Grand Materia Medica* (大觀本草), it was Haozhou Zishen (purple root of Houzhou, 濠州紫參). In *The*

Grand Compendium of Materia Medica, it was Benma Cao (galloping horse grass, 奔馬). In *Chinese Medicinal Herbs*, it was Zihua Danshen (purple flower Danshen, 紫花丹參). In *Guangxi Herbs* (廣西草藥), it was Chang Shuwei Cao (long sage, 長鼠尾草). In *Icones of Chinese Medicinal Plants* (中國藥用植物志), it was Hong Gen (red root, 紅根).

1.1.3 Names in Different Regions [3]

Danshen has many local names in different regions of China. It is called Zi Danshen (purple Danshen) in Hebei, Shandong, Jiangsu, Zhejiang, Jiangxi, Hubei, Guangdong, Guangxi, and Sichuan; Zishen (purple root) in Beijing, Gansu, and Zhejiang; Zi Dangen (purple Dangen) in Hunan and Guangdong; Hong Danshen (red Danshen) in Zhejiang, Hubei, and Guangxi; Hongshen (red root) and Chi Danshen (red Danshen) in Jiangsu and Zhejiang; Hong Luobo (red turnip) in Zhejiang and Jiangxi; Xueshen (bloody root) in Jiangsu, Henan and Hubei; Kao Shan Hong (foothill red) in Shandong, Jiangsu and Anhui; Ye Suzi Gen (wild perilla root) in Liaoning, Hebei and Beijing; Shan Suzi (mountain perilla) in Hebei and Shaanxi; Xueshen Gen (Xueshen root), ShaoJiuhu Gen (flagon root), and Shan Suzi Gen (mountain perilla root) in Northeast China; Ye Suzi Yanggen (wild perilla sprout root) in Beijing; Da Hong Pao (big red robe), Xue Danshen (bloody Danshen), Zhuangyuan Hong, and Ren Shen in Hebei; Feng Tang Guan

J. Hao · X. He · L. Huang (✉) · M. Chen (✉)
China Academy of Chinese Medical Science,
Beijing, China
e-mail: huangluqi@263.net

M. Chen
e-mail: cm315keke@163.com

(honey jar) in Shaanxi; Mitang Guan (honey jar), Hong Niangzi Ke (pretty lady plant), Zhazha Caigen (Zhazha vegetable root), Zhazha Haogen (Zhazha grass root), Can Lianhua Gen (silkworm lotus root), Zihua Diningzi Gen (purple flower Diningzi root), Hong Suzi Gen (red perilla root), Xue Shan Gen (bloody mountain root), and Zhazha Honggen (Zhazha red root) in Shandong; Zi Dangshen (purple codonopsis root), Da Ye Huoxue Dan (big leaf invigorate blood drug), Honggen Hongshen (red root), and Huoxue Gen (invigorate blood root) in Jiangsu; Shan Hongluobo (wild radish), Tu Danshen (local Danshen), and Sifang Genggen (square root) in Zhejiang; Hong Gu Shen (red bone root) and Shan Danshen (mountain Danshen) in Anhui; Balianma Gen (Balianma's root) and Xia Danshen (summer Danshen) in Jiangxi; Hong Nuan Yao (red warm drug) and Ma Dajie (sister Ma) in Henan; Shan Zicao Gen (wild arnebia root), Jigegu Feng (born-connecting wind), Sifang Lanhua Caogen (quadrangular blue flower grass root), and Mai Shen (grain root) in Hunan; Honggen Chishen (red root Chishen), Chuan Danshen (Sichuan Danshen) in Sichuan.

1.1.4 Commercial Names [3]

Danshen, Zi Danshen.

1.1.5 Prescription Names [3]

Danshen, Chishen, Zi Danshen, Chao Danshen-Danshen (dry-fried Danshen), Jiu Danshen (wine-prepared Danshen), Cu Danshen (vinegar-prepared Danshen), Danshen Tan (Danshen charcoal), and Biexue Danshen (turtle blood Danshen).

1.2 Etymology

Danshen derives its name from ancient Chinese five-phase five-color theory. According to *The Grand Compendium of Materia Medica* [4],

“Five Shens with five different colors match five organs. Ginseng matches the spleen, called Huang (yellow) Shen; Shashen (*Radix Adenophorae*) matches the lung, called Bai (white) Shen; Xuanshen (*Radix Scrophulariae*) matches the kidney, called Hei (black) Shen; Mumeng (*Polygonum bistorta*) matches the liver, called Zi (purple) Shen; Danshen matches the heart, called Chi (red) Shen.”

According to *Four Tones Materia Medica* (四声本草), “Danshen cures weak feet caused by wind. After treatment, the patient could catch up with a galloping horse, so it is called Ben Ma Cao (galloping horse grass). It has been tested, and it was effective.” This record explains the origin of Danshen's other names, Ben Ma Cao or Zhu Ma (chasing horse).

1.3 Materia Medica Studies

As mentioned above, Danshen was first recorded in *Shen Nong's Classic of the Materia Medica* [1], but it provided no information about its morphology, distribution, or habitat.

In *Miscellaneous Records of Famous Physicians*, it is stated that “it is also named Chishen, Mu Yang Ru, and grows in the valleys of Tongbai and Taishan Mountain. Harvest the roots in May, dry them under sunshine.”

In *Collective Commentaries on the Classic of Materia Medica* [1], it is stated that “This Tongbai Mountain is the origin of Huaihe River, located in Yi Yang. It is not the Tongbai Mountain in eastern China. Now it is distributed everywhere in this place, its stems are quadrangular and hairy, flowers purple, people call it Zhu Ma.” This record indicates that the plant's primary habitat was in the Tongbai Mountain area in Henan Province.

In *Wu Pu's Materia Medica* [1], it is stated that “It has small stems and leaves, and its ovary like a perilla's, with trichomes. Its roots are red. The plant blooms in April with purple flowers, and its roots can be collected in February and May and dried in shade.”

In *Materia Medica of Sichuan* [1], it is stated that “Its leaves are similar to those of purple perilla with fine trichomes, and its purple flowers are also similar to perilla. Its roots are red, the larger ones with a diameter of a finger and with a length of more than one foot. One plant has several roots, and it grows everywhere. The roots are collected in September and October.” This record indicates clearly that the leaves and flowers of Danshen are similar to those of perilla.

In *Illustrated Classic of Materia Medica* of Song Dynasty (960–1127 AD), it is stated that “Danshen grows in the valleys of Tongbai Mountain and Taishan Mountain, and is now also found in Shaanxi, Hedong, and Suizhou. Its seedlings appear in February, and the plants can reach the height of more than one foot. Danshen has a quadrangular stem with a green color, and its leaves come in pairs with a shape similar to the leaves of peppermint, and are hairy. It blooms in March with red and purple colors and is similar to those of perilla. Danshen’s root is red, and the larger root is like a finger with a length of more than one foot, like its stem. One plant has several roots.” This record shows a vivid and detailed morphological description.

In *Essentials of Materia Medica Distinctions* of Ming Dynasty (1368–1644 AD), there was an elegant figure of Danshen from Suizhou (Fig. 1.1).

In *The Grand Compendium of Materia Medica*, it is stated that “Danshen is everywhere in the mountains. One branch has five leaves, with the pointed shape similar to perilla, green, with wrinkles and trichomes. Its small flowers form an ear, with the shape of a moth, and inside the ear are small seeds. The root has red skin and purple cortex.” Here, Li Shizhen gave more detailed observations and pointed out that the plants in Lamiaceae have moth-shaped flowers.

All of these records indicate that Danshen has the characteristic flowers and stems of the *Lamiaceae* family. In addition, Danshen has compound leaves with five leaflets and has roots with red skin and purple cortex, with the diameter of a finger. Combining these descriptions with the picture shown in *Essentials of Materia Medica Distinctions*, it can be concluded that plant Danshen is *Salvia miltiorrhiza* Bunge.



Fig. 1.1 Danshen’s appearance as shown in *Essentials of Materia Medica Distinctions*

1.4 Resource Survey

Danshen is a commonly used traditional Chinese medicine in China, so it is an important commodity in domestic and foreign medicinal material markets. According to *Chinese Pharmacopoeia*, 2005 edition [5], Danshen for medicinal use should be the dried roots and rhizomes of plants belonging to the family of *Lamiaceae*,

genus of *Salvia*, and species of *S. miltiorrhiza* Bunge.

1.4.1 Local Varieties and Original Plant of Danshen [6]

In addition to *S. miltiorrhiza*, many other species of *Salvia* plants are used as Danshen for medicinal purposes in some regions of China. Even though these plants are related to Danshen and contain tanshinone, they are not as good as Danshen. According to *Chinese Pharmacopoeia*, the content of tanshinone IIA in medicinal Danshen should not be less than 0.20 % [2].

Below are the other plant species commonly confused with Danshen.

1.4.1.1 Nan (Southern) Danshen (*Salvia Bowleyana* Dunn)

In Jiangxi, Fujian, and Hunan provinces, it is called Danshen, Chishen, and Zi Danshen; in Hunan, it is called Hong Gen and Ben Ma Cao; in Fujian, it is called Qi Li Ma, Qi Li Jiao, and Tu Danshen, etc.

The morphological characteristics of *S. bowleyana* are similar to those of *S. miltiorrhiza*, but with smaller roots and gray-reddish skin. Its leaflet is ovate and lanceolate, with a length of 4–5 cm and width of 2–4.5 cm. The apex of the leaflet is acuminate, the base is cordate or slightly sloping, and the margin is crenate. Both sides of the leaves are smooth, except for the veins on the lower side. The lateral leaflet is relatively small, with an oblique base. The calyx is tubular or cylindrical; the corolla tube is short and ingrowing; and the posterior lip is about 1.2 cm in length.

S. bowleyana is mainly distributed in Zhejiang, Jiangxi, Fujian, Hunan, Guangdong, and Guangxi provinces. It is mainly sold in local areas and often mixed with *S. miltiorrhiza*.

The total tanshinone content of this product is 0.52 %, the cryptotanshinone content is 0.05 %, and the tanshinone IIA content is 0.85 %, which clearly shows that the quality of *Nan Danshen* is inferior to that of Danshen.

1.4.1.2 Gansu Danshen (*S. Przewalskii* Maxim)

This plant is also called Ganxi Shuweï (sage of west Gansu). In Sichuan, it is called Hong Qin-jiao (red large leaf gentian), and in Gansu, Ningxia, Qinghai, and Yunnan's Zhaotong area, it is called Danshen. In Yunnan's Lijiang area, it is called Zi Danshen.

The main botanical characteristics of this plant include its simple leaf, which is deltoid or ovate in shape, with a length of 8–20 cm. The base of the leaf is cordate or hastate, the margin has obtuse teeth, and the lower side is covered by white trichomes.

This product is mainly distributed in Gansu, Ningxia, Qinghai, Sichuan, Yunnan, and Tibet, and is mostly grown in the forest in high mountains.

The total tanshinone content of the root of this plant is 1.99 %, the cryptotanshinone content is 1.60 %, and the tanshinone IIA content is 0.34 %, which shows that this product is of better quality than formal Danshen.

This product is also used as a substitute for large leaf gentian root in veterinary medicine.

1.4.1.3 Da Zi (Bright Purple) Danshen (*S. Przewalskii* Maxim. Var. *Mandarinorum* (Diels.) Stib.)

This plant is also called Ganxi Shuweï and Hemao Danshen (brown hair Danshen). It is called Da Zi Danshen in Yunnan's Kunming City, and called Danshen and Zi Danshen in Gansu Province.

This plant's morphology is similar to that of Gansu Danshen, and the main difference between them is that its base of leaf is auriculate, and the back of the leaf is covered with thick brown trichomes.

It is mainly distributed in Gansu, Ningxia, and Qinghai, and in Yunnan's Lijiang area, and it is used as Danshen.

The total tanshinone content of this product is 1.30 %, the cryptotanshinone content is 0.30 %, and the tanshinone IIA content is 1.06 %. Its quality is better than Danshen's.

1.4.1.4 Dian (Yunnan) Danshen (*S. Yunnanensis* C. H. Wright)

It is also called Yunnan Danshen, Shishi Danshen (stone mountain Danshen), Hong Qinglai, Xiaohong Danshen (reddish Danshen), Xiao Hong Shen (reddish root), Zi Danshen, and it is called Shan Binlang (mountain areaca) in Yunnan's Qujing area.

The plant is relatively short, with a height of about 25 cm. Its stem is erect, quadrangular, and pinkish, with or without hairs. The leaf is aphyllopodic, and simple or tripinnatifid compound. The simple leaf is ovate or oval, with a length of 3–8 cm and a width of 1.5–3 cm. The apex is obtuse, the base is cordate, and the margin is crenate. The upper side of the leaf is green with trichomes, and the lower side is purple with thick trichomes and a notable vein net. The length of the petiole is 4–8 cm. The compound leaf has 3–5 leaflets. The inflorescence of verticillaster has 4–6 alienated flowers to form the terminal racemes or panicles, and the rachis is covered by glandular hairs.

It is mainly distributed in Yunnan Province.

The total tanshinone content of the roots of this product is 0.58 %, the cryptotanshinone content is 0.10 %, the tanshinone IIA content is 0.10–0.16 %, and the tanshinone I content is 0.15 %.

1.4.1.5 Sanye (Three Leaves) Danshen (*S. Trijuga* Diels.)

It is also called Xiao Hong Shen, Zi Danshen, and Sanye Shuwei. It is called Xiao Danshen and Xiaohong Danshen in Sichuan's Xichang region, called Hong Danshen in Yunnan's Yulongshan area, and called Honggen Genyao (red root medicine) and Zi Shen (purple root) in Yunnan's Lijiang area.

The main feature of this plant is its covering of dense pubescences. The leaf normally has 3 leaflets, but could also have 5 leaflets, which have petioles. The length of the corolla tube is about 3 times longer than that of the calyx, with its base enlarging upward, stretching horizontally or bending upward, and the protrusion part of the corolla limbs is shorter than that of the corolla

tube. The epichile stretches straight. There are verticillates in the corolla tube.

It is mainly distributed in Yunnan and western Sichuan.

The total salviol content of the root of this product is 1.06 %, the cryptotanshinone content is 0.16 %, and the tanshinone IIA content is 0.56 %.

1.4.1.6 Baihua (White Flower) Danshen (*S. Miltiorrhiza* Bunge F. Alba C. Y. Wu et H. W. Li)

This plant is very similar to Danshen; the only difference is that its flower is white and sometimes has a slightly purple halo.

It is mainly distributed in Shandong.

The wine soaked with Baihua Danshen has some therapeutic effect in treating thromboangitis obliterans in Shandong Province.

The tanshinone IIA content of the roots of this product is 0.73 %, the methenyl tanshinone content is 0.39 %, and the tanshinone I content is 0.41 %.

1.4.1.7 Danye (Single Leaf) Danshen (*S. Miltiorrhiza* Bunge var. *Charbonnelii* (Léveillé) C. Y. Wu)

This plant is the simple leaf variety of *S. miltiorrhiza*.

It is mainly distributed in Henan Province.

The tanshinone IIA content of the roots of this product is 0.30 %, the methenyl tanshinone content is 0.23 %, and the tanshinone I content is 0.18 %.

1.4.1.8 Baihua Ganxi Shuwei (White Flower Sage of Western Gansu) (*S. Przewalskii* Maxim. var. *Alba* X. L. Huang et H. W. Li)

The difference between Gansu Danshen and this variety is that Baihua Ganxi Shuwei's corolla is white, and its corolla margin is slightly purple. Its inflorescence is solitary, its leaf is lanceolate or oval lanceolate, and the leaf petiole is relatively short.

It is mainly distributed in Yunnan's Lijiang area.

The tanshinone IIA content of the roots of this product is 0.44 %, the methenyl tanshinone content is 0.36 %, and the tanshinone I content is 0.19 %.

1.4.1.9 Shaomao Ganxi Shuweï (Less Hair Sage in Western Gansu) (*S. Przewalskii* var. *Glabrescens* Stib.)

It is also called Dashan (Big Mountain) Danshen. It is called Hong Qinjiao in Sichuan's Maowen area and Ling Lan Xiang in Sichuan's Kangding area.

The difference between Gansu Danshen and this variety is that the lower side of the leaf of Shaomao Ganxi Shuweï has few pubescences, but has dense dark red glands.

It is distributed in Yunnan's Heqing, Zhongdian, Deqin areas, western Sichuan, and south-eastern Tibet.

The tanshinone IIA content of the roots of this product is 0.78 %, the methenyl tanshinone content is 0.82 %, and the tanshinone I content is 0.52 %.

1.4.1.10 Wan E (Anhui and Hubei) Danshen (*S. Paramiltiorrhiza* H. W. Li et X. L. Huang)

In Flora Republicae Popularis Sinicae (中国植物志), this species is recorded as Ni Danshen (para-Danshen).

Its stem is single, rarely clustered, and covered with sparse pubescences. Its stem leaf is a pinnate compound leaf with 5 leaflets, rarely with 3 or 7 leaflets, and the leaflet is ovate with a length of 1.25–7.5 cm and a width of 0.9–3.5 cm. The apex of the leaflet is tapering or sharp, the base is oval or cardioid, sometimes oblique, and the margin is regular crenate. The length of the leafstalk is 1–6.5 cm, and sparse pubescences cover the leaves and leafstalks. The corolla is lemon yellow to yellow.

It is mainly distributed in Anhui and Hubei, and in the central region of Anhui, it is considered as Danshen proper.

The tanshinone IIA content of the roots of this product is 0.13 %, the methenyl tanshinone content is 0.16 %, and the tanshinone I content is 0.22 %.

1.4.1.11 Zhe Wan (Zhejiang and Anhui) Danshen (*S. Sinica* Migo)

The features of this plant are that its leaf is nearly bald, and its leaflet is commonly narrow and round ovate, round lanceolate, or lanceolate. The apex is tapering or sharp. The differences between this product and formal Danshen are that its leaf is nearly bald with 2–3 pairs of narrow leaflets, the raceme is normally compound with small corolla, the labrum is light gray or yellowish, and there are verticillates in the corolla tube.

This product is also similar to Nan Danshen. The difference between them is that in this species, its calyx shows a bell shape, the upper sepal is sharp, the corolla is curved, and the root skin is purple brown.

It is mainly distributed in Tianmu Mountain of western Zhejiang and Anhui's Liu'an, Qingyang, Shexian, and Huangshan areas. In southern Anhui, this species is considered as Danshen proper.

The tanshinone IIA content of the roots of this product is 0.02 %.

1.4.1.12 Qiaomai Di Shuweï (Buckwheat Field Sage) (*S. Kiaometiensis* Lév.)

It is called Danshen and Honggen in Yunnan Province.

The botanical features of this species include a leaf with a round ovate shape, ellipse shape or long ovate shape, with a length of 10–19 cm and width of 5–10 cm. The apex is sharp, the base shows a cordate shape, and the edges have crenatures on which there are small acrocephalies. The leaf has setae, and its back is covered with pubescences or is nearly bald with a dense covering of glandular punctates. The length of the basal leaf's petiole is 6–20 cm. The inflorescence of verticillaster is compact, clustered into a strobiloid shape in the early phase, and is covered by round bracts. The corolla is purple brown with a length of 2.8–3.5 cm, and the corolla tube is stretched straightly with increasing size from the abdomen to the neck.

It is mainly distributed in Yunnan and western Sichuan.

1.4.1.13 Maoye Qiaomai Di Shuwei (Hairy Leaf Buckwheat Field Sage) (*S. Kiaometiensis* Lév. *F. Pubescens* Stib.)

It is also called Di Shuwei, and in Sichuan's Yanyuan, it is also called Tu Danshen.

Its leaflet has a long leaf stalk, its leaf is narrow and long with a triangle to ovate triangle shape, and the margin has coarse teeth. The surface of its leaf is covered by dense pubescences, and its back is covered by short pubescences and glands. The stem, leafstalk, and rachis are all covered by glandular hairs.

It is mainly distributed in western Sichuan.

1.4.1.14 Changguan Shuwei (Long Crest Sage) (*S. Plectranthoides* Griff.)

It is called Danshen in Yunnan's Dali area, called Jinzhi Danshen in Illustrated Reference of Botanical Nomenclature, and called Hong Danshen, Mao Danshen (hairy Danshen), and Sihua Caiye Danshen (four-flower leafy Danshen) in Shaanxi.

Its leaves are grown from the base and stalk, and are triple leaves or odd-numbered pinnately compound leaves with 2–3 pairs of pinnae or pinnule compound leaves. Its leaflet shows nearly reticular to lanceolate shape and is either bald or has lower veins covered by tiny pubescences, with glandular punctuates and a long leafstalk. The corolla is red or purple to royal blue, and rarely white.

It is mainly distributed in Yunnan, Guizhou, Guangxi, Hubei, and Shaanxi.

The tanshinone IIA content of the roots of this product is 0.07 %, the methenyl tanshinone content is 0.03 %, and the tanshinone I content is 0.09 %.

1.4.1.15 Maodihuang Shuwei (Foxglove Sage) (*S. Digitaloides* Diels.)

It is called Yinzi Danshen (silver pink Danshen) and Bai Yuanshen (white radix scrophulariae) in Yunnan's Lijiang area.

The stalk height is 30–60 cm and is covered by dense long pubescences. Its leaf is normally grown from the base, and the leaf is long reticular

ovate with a length of 3.5–11 cm. Its upper side is covered with sparse pubescences and its lower side with dense white short pubescences. Its leafstalk has a length of 6–8 cm. The corolla stretches flat, does not bend upward, and has a yellow color with lavender flecks, with a length of 3–3.5 cm, and there are hairy rings in the corolla tube.

It is mainly distributed in northwestern Yunnan and southwestern Sichuan.

The total tanshinone content of the roots of this product is 0.67 %, the tanshinone IIA content is 0.04 %, the methenyl tanshinone content is 0.01 %, and the tanshinone I content is 0.29 %.

1.4.1.16 Huanghua Shuwei (Yellow Flower Sage) (*S. Flava* Forrest Ex Diels)

It is called Huanghua Danshen or Danshen in Yunnan's Lijiang area.

Its leaves are large, are mostly grown from the base, and show an ovate hastate shape or ovate triangle shape with a length of 3–15 cm and a width of 2–9.5 cm. The apex is sharp or sometimes blunt, the base shows a hastate shape and sometimes shows a cordate shape, the edges have reticular teeth or double reticular teeth, and the basal laminae is very sharp. The upper side of the leaf is covered by short pubescences or nearly bald, and the lower side is covered by short pubescences or sparse pubescences with dense glandular punctuates. The corolla is yellow, the labrum is stretching flatly and is not bending upward, and the labium is purplish red or purple black.

It is mainly distributed in northwestern Yunnan and southwestern Sichuan.

The total tanshinone content of the roots of this product is 0.069 %.

1.4.1.17 Chenghuang Shuwei (Orange Yellow Sage) (*S. Aerea* Lev.)

It is also called Tongse Shuwei (bronzy sage). In Yunnan's Lijiang, Huaping regions, it is called Matiye Hong Xianmao (*marshmarigold red curculigo*). In Sichuan's Xichang, it is called Hong Danshen, Zi Danshen, Daye Danshen, Da Mubang, Hong Qinjiao, etc.

The stem is covered by ganglioneous yellow brown long pubescences, its leaves are large and mostly are grown from the base, and 1–2 leaves are grown from the stem. The leaves grown from the base are commonly large, show an ellipse shape, obovate shape, or round shape, and have a length of 2.5–8.5 cm. The apex is round; the base shows an auritus shape or wedge shape, gradually narrows, and its lower end can reach the leafstalk; the edges have irregular crenatures; the surface of the leaf is covered by long pubescences, and the back of the leaf is covered by sparse or dense brown long pubescences and glandular punctuates; the leafstalk has a length of 2–4 cm with brown long pubescences; the corolla is blue, white, or violaceous; the corolla tube stretches straight and is only bending upward in the lateral side of the calyx.

It is distributed in Yunnan, Sichuan, and Guizhou.

The total tanshinone content of this product is 1.22 %, the cryptotanshinone content is 0.17 %, and the tanshinone I content is 0.92 %.

1.4.1.18 Lise Shuweï (Dark Brown Sage) (*S. Castanea* Diels)

The stem is single and covered by sparse pubescences; the leaflet shows an ovate shape or long ovate shape or long reticular shape, with a length of 9–18 cm and a width of 4–11 cm; the apex is sharp or slightly blunt; the base shows cardioid or nearly hastile shape; the edge has irregular crenatures; the upper part is covered by sparse pubescences; and the back is covered by gossamer-like villus and is covered by dense glandular punctuates. The leafstalk has a length of 2–16 cm. The corolla is castaneous or purple brown with a length of 3.3–3.6 cm. The corolla tube bends with a resupinate or zigzag shape, suddenly increasing its size at the external side of the calyx, and there are incomplete verticillates in its internal surface.

It is mainly distributed in Yunnan and Sichuan.

The total tanshinone content of the root of this plant is 1.6 %, the cryptotanshinone content is 0.40 %, and the tanshinone IIA content is 1.16 %.

1.4.1.19 Xueshan Shuweï (Snow Mountain Sage) (*S. Evansiana* Hand.-Mazz.)

It is called Zihua Danshen in Yunnan's Lijiang area.

The leaflet is triangle ovate or ovate; the apex is sharp or blunt; the base is cardioid or nearly hastile; the edge has small irregular crenatures; and the back is covered by dense glandular punctuates. The stem and leafstalk are covered by long and unfolded brown long pubescences or are nearly bald. The corolla has a length of 2.6–3.5 cm with a purple color, and there are incomplete verticillates in the corolla tube.

It is mainly distributed in Yunnan's Lijiang, Zhongdian, Weixi, Deqin, and Gongshan areas. In addition, it is found in southwestern Sichuan and southeastern Tibet.

The total tanshinone content of its roots is 0.18 %.

1.4.2 Species Confused with Danshen [6]

Because of the wide distribution of wild Danshen and the very good quality of cultivated Danshen, thanks to the early start of research on cultivation of Danshen under standard conditions, there has been no supply shortage of Danshen so far. Thus, no counterfeits of Danshen have been found in medicinal materials markets. However, based on experience, there are some homonym materials of Danshen in some regions of China, which are commonly called "Tu Danshen" (local Danshen), "Cao Danshen" (herb Danshen), "Danshen Cao" (Danshen herb), etc. These homonyms are not related to the real Danshen, so they should not be used as Danshen for medicinal purposes. Since they use the name of Danshen, they could very easily cause confusion.

1.4.2.1 Qiancao (*Rubia Cordifolia* L) (Family: *Rubiaceae*)

The root of this plant is commonly called Tu Danshen in some regions of Fujian, such as Fu'an, and it has been recorded in *Materia Medica of Eastern Min* (闽东本草).

The stem of this plant is quadrangular with spikes. It has 4 verticillate leaves with long leafstalks, and the leaf is ovate cardioid or narrow ovate with a length of 1.5–6 cm and a width of 1–4 cm. The apex is gradually sharp. The cyme is reticular pyramidal with axillary or terminal growth, and the flower is small and amber colored. The plants have many slim and long roots and rootlets, and the skin is yellowish red.

It is grown in the forests and scrubs in plains or mountains. It is found in most regions of China.

1.4.2.2 Zhusha Gen (*Ardisia Crenata* Sims.) (Family: *Myrsinaceae*)

In Hubei's Badong area, people call the root of *Ardisia crenata* Bai Danshen (white Danshen).

This plant is a compact shrub that can reach a height of 1.5 m. The stem is upright and has several branches. The leaf is papyraceous to glossy, ovate lanceolate to oblanceolate in shape, with a length of 6–12 cm and a width of 2–4 cm. The apex is short and sharp or gradually sharp, and both sides have no trichomes, with bossed glandular punctuates. The edge has round-like crenatures. The umbel is axillary or terminal growth, with white or reddish flowers. The root has many branches with reticular cylindrical shape and is slightly bending with dark purple or dark brown skin.

It grows under the forests in the mountains, or near grooves and roads. It is mainly distributed in Zhejiang, Anhui, Jiangxi, Hunan, Hubei, Sichuan, Fujian, Guangdong, and Guangxi.

1.4.2.3 Shuisu Caosu (*Phlomis Betonicoidea* Diels) (Family: *Labiatae*)

It is commonly called Bai Danshen in Sichuan's Xichang area. It is also called Jia Qinjiao (fake gentian), Bai Yangshen (white American ginseng), Bai Yuanshen (white radix scrophulariae), Bai Xuanshen (white figwort), and Tu Gancao (local liquorice).

The plant's stem is upright and quadrangular, is covered by dense asteroid coarse bristles without branches, and has a height of 30–80 cm. The basal leaf is narrow ovate, ovate lanceolate,

triangular, or orbicular ovate, with a length of 7.5–14 cm and a width of 5–10 cm. The apex is blunt or very sharp; the base is cardioid or slight cardioid to cardioid; the edge has crenatures or tooth-like crenatures. The stem leaf is orbicular ovate to lanceolate, with a length of 5–9 cm and a width of 2–4.5 cm; the edge shows an irregularly reticular or tooth-like shape; the verticillaster inflorescence has many flowers and is dense, with pink corolla and Labiatae limb.

It grows in grasslands and forests, under trees or on hillsides, and is distributed in northwestern Yunnan, southwestern Sichuan, and eastern Tibet.

1.4.2.4 Xiaku Cao (Self-Heal) (*Prunella Vulgaris* L.) (Family: *Labiatae*)

In Fujian's Jianyang area, people call it self-heal Danshen and use the whole plant for medicinal purposes.

The stem is square, the base is stoloniform, and the whole plant is covered by dense fine hairs. The leaves grow in pairs, and the leaflet is ovate lanceolate with a full edge or some crenatures. The verticillaster inflorescence is grown in a terminal form, with a spiked shape.

It grows in wild land, beside roads and tussocks on hillsides, and is distributed throughout most parts of China.

1.4.2.5 Tu Huoxiang (Local Ageratum) (*Agastache* Sp.) (Family: *Labiatae*)

In Shaanxi's Ningqiang, plants in the genus *Agastache* of the family *labiatae* are called Danshen.

The stem of the plant is upright, quadrangular, and slightly red, and is covered by sparse pubescences and glands. The leaves are grown in pairs. The leaflet is reticular ovate or ovate, with a length of 2–8 cm and a width of 1–5 cm. The apex is sharp or gradually sharp, the edge has irregular crenate-dentates, and the leafstalk is 1–4 cm in length. The verticillaster inflorescence can form the acrogenous raceme, and the nutlet is in the form of an inverse ovate triangular prism.

It grows in hillsides and near roads and is distributed throughout most parts of China.

1.4.2.6 Weilingcai Gen (*Potentilla* Root) (*Potentilla Chinensis* Ser.) (Family: *Rosaceae*)

Danshen is also called Xueshen, and in Fujian's Xiamen area, people call the roots of *Potentilla* plants (*Rosaceae*) Xueshen.

The stem is upright with a height of 30–60 cm and is covered by dense gray-white tomentum. It has odd-pinnate compound leaves, and the leaf grown from the base has 8–11 pairs of leaflets, where the top leaflet is largest and the lateral leaflets become gradually smaller moving downward; the leaflet shows a narrow oblong shape with a length of 2–5 cm and a width of 8–15 cm; the edge is split deeply in a plumatus form, and the split lobe shows a triangle lanceolate shape with downward rolled edges. The corymbiform cyme is grown acrogenously with 5 yellow petals. The root is large and shows a cone shape. The dried root is cylindrical and sometimes bending; the surface is reddish or dark brown with irregular longitudinal dehiscences.

It grows on hillsides, on near roads and farm lands, and in mountains. It is distributed throughout many regions of China.

1.4.2.7 Huanghua Jiaohao (*Incarvillea* *Lutea* Bur. et Franch.) (Family: *Bignoniaceae*)

In some places in Yunnan, people call this plant Hong Danshen.

The plant is 25–100 cm tall and covered by ravidous pubescences. The leaves grow in pairs in a plumatus form, and the lateral leaflets have

6–9 pairs in an elliptical shape. The raceme is acrogenous and has 6–12 flowers, the calyx is mitriform, and the corolla is amber. It has red flowers as well. The rhizome is fleshy and strong, and the skin is sorrel.

It grows in the dry or rocky land in mountains and is distributed in Yunnan and Sichuan.

References

1. Tang S. Revised and classic classified materia medica for emergency (重修政和经史证类备用本草). Photocopy. Beijing: People's Medical Publishing House; 1957. P. 138.
2. Pharmacopoeia Commission of People's Republic of China. Chinese pharmacopoeia (part I) 2005. Beijing: Chemical Industry Press; 2005. p. 52.
3. Zongwan X, Jinda H, Youqin Y. Handbook for names and secondary names of common Chinese drugs. Beijing: People's Medical Publishing House; 2001. p. 69.
4. Shizhen L. The grand compendium of materia medica, vol. 1. Beijing: Peoples's Medical Publishing House; 1982. p. 758.
5. Shenghe Z. Chinese materia medica merchandising. Beijing: People's Medical Publishing House; 1990. p. 120.
6. Zongwan X. Investigation and identification of varieties of traditional Chinese medicine (Second Version), vol. 1. Shanghai: Shanghai Scientific and Technical Publishers; 1990. p. 114.
7. Liu W. Essentials of materia medica distinctions. Beijing: Huaxia Press; 2004. p. 141.
8. Editorial Board of Compendium of Chinese Traditional Herbal Drugs. *Compendium* of Chinese traditional herbal drugs vol. 1. Beijing: People's Medical Publishing House; 1976. p. 216.

Luqi Huang, Min Chen and Lanping Guo

2.1 Geographic Distribution

Danshen is widely distributed throughout China, from Jiangxi, Hunan in the south, to Liaoning in the north, to Sichuan in the west. It grows in mountainous hill regions with elevations from 120 to 1,300 m.

Danshen can be either wild or domestic. Wild Danshen is mainly distributed in Liaoning, Hebei, Beijing, Shanxi, Shandong, Hubei, Hunan, Jiangsu, Jiangxi, Gansu, Guizhou, and Shaanxi. Domestic Danshen is mainly distributed in Hebei, Tianjin, Jiangsu, Shanghai, Zhejiang, Anhui, Sichuan, Shandong, Henan, and Shaanxi. The main producing areas are as follows: Hebei's Anguo, Funing, Qianxi, Lulong, Pingquan, Zanhuan, and Yixian; Liaoning's Dalian, Xinjin, Gaixian, Jinxi, and Xingcheng; Shanghai's Congming; Jiangsu's Sheyang, Xinghua, Gao-you, and Jurong; Zhejiang's Shengzhou, Sanmen, and Ningbo; Anhui's Boxian and Taihe; Shandong's Juxian, Pingyi, Yishui, Qixia, Laiyang, and Rizhao; Henan's Songxian, Lushi, Luoning, and Songshan; Hubei's Yingshan, Luotian, Qichun, and Suizhou; Shaanxi's Luonan and Shangzhou; Gansu's Kangxian and

Hezheng; Sichuan's Zhongjiang and Chengdu; Yunnan's Ninglang, Lijiang, Yongsheng, and Binzhou.

2.2 Ecological and Biological Characteristics

Danshen grows well in a sunny, mild, and wet environment. It is able to tolerate cold weather, but it is vulnerable to drought and excessive water. Suitable growing conditions for Danshen are found in locations where the annual average temperature is 17.1 °C, and the annual average relative humidity is 77 %. The plant starts growing when the soil temperature reaches 10 °C in spring. When the air temperature reaches 20–26 °C and the relative humidity is 80 %, it grows very well. In autumn, when temperatures fall below 10 °C, its aboveground parts begin to wither. Danshen's roots can overwinter safely even at a soil temperature of –15 °C. It takes the seeds about 15 days to germinate at 18–22 °C. Adventitious buds begin to develop on the root when soil temperatures reach 15–17 °C. Insufficient sunshine and low temperatures during its growing season can slow down the growth and cause maldevelopment [1].

L. Huang (✉) · M. Chen (✉) · L. Guo
China Academy of Chinese Medical Science,
Beijing, China
e-mail: huangluqi@263.net

M. Chen
e-mail: cm315keke@163.com

2.3 Environmental Condition

2.3.1 Climatic Conditions

Danshen's distribution area can be divided into several climatic regions:

2.3.1.1 Liaodong–Jiaodong Peninsula

This region belongs to the warm temperate zone. It is influenced by ocean climate and has plenty of rainfall, and deciduous broad-leaved forests grow well in its mountainous area. This region is appropriate for Danshen's growth. Geologically, this region is the extension of Tai and Changbai Mountains.

2.3.1.2 Shanxi, Liaoning, and Loess Plateau Distribution Region

The region is a narrow zone between Luliang Mountain and Taihang Mountain, ranging from the Yellow River to the south and Yanshan Mountain to the north. As a warm temperate broad-leaved zone, Danshen is widely distributed in this region, making it one of the major production areas.

2.3.1.3 South of Huaihe River and the Lower-middle Reaches of Yangtze River Region

The region refers to the hilly basins of the middle and lower Yangtze River, reaching north to Qinling Mountain, south to Huaihe River, including Qinling, Dabashan, Wudangshan, Shennongjia, Tongbaishan, Dabieshan, Tianmushan, Huangshan, and Lushan Mountains. The region has a varied topography. Its western mountains are 800–2,000 m high, in general, and its eastern mountains, such as Lushan, Huangshan, Tianmu Mountains, are relatively low and isolated. Climatically, the region is hot in summer and warm in winter and has plenty of rainfall in spring and summer. It belongs to the subtropical zone with deciduous and evergreen broadleaf forests.

2.3.1.4 Other Regions

Danshen is also found on Luoxiao Mountain, which is located in the area between Hunan and

Jiangxi, on Daloushan and Wulingshan mountains in Guizhou–Sichuan Plateau, and in hilly areas in Sichuan Basin. Sichuan's Zhongjiang and Pingwu counties are one of the China's main production areas for Danshen [2].

2.3.2 Soil Conditions

Danshen grows well in fertile sandy soil and is capable of adapting to soils with a wide range of pH values, including neural, acidulous, and alkaline soil [3]. Domestic Danshen is mostly cultivated in thick layers of loose soil with good water drainage.

Guided by botanical nutritional ecology and cultivation and soil sciences, Zhang and Cheng [4] have studied systematically the comprehensive techniques for nuisanceless production of high-quality Danshen. The technique can be easy to implement and the effects in yield improvement are significant.

2.3.3 Community

Danshen has a strong adaptability and is often found in sparse forests and brushes, on hillsides and roadsides, and in fresh planted forests. Due to massive digging in recent years, it is no longer easy to find a pure community of wild Danshen. What can be found now is isolated and scattered. In its habitat, Danshen normally grows in the herbaceous layer under the trees. Common community types of Danshen include catalpa bungei forest community, fir-sandalwood community, raspberry-sedge community, etc., in metamorphic rock mountain areas.

2.3.4 Habitat of High-quality Danshen

Sichuan's Zhongjiang County is where high-quality Danshen is produced. After surveying the ecological and soil conditions of this region, Wu and Chen [5] found that most cultivated Danshen is grown in the sloping land to the northwest of the county, where the elevation is about

600–900 m. The climate of that region is warm and humid, and the soil types are medium loamy terra and neutral purple soil. The soil's organic matter, nitrogen, and potassium contents are mid-to low level, but rich in available phosphor. Among the trace elements, there is plenty of available iron, manganese, and copper, but available zinc and boron are insufficient.

2.4 Geographic Variation and Quality

In recent years, many researchers have carried out studies on Danshen's geographic variations across various production regions, but the results are not conclusive. Where is the high-quality Danshen produced? What are the characteristics of that habitat? These questions are discussed below.

2.4.1 Geographic Variation

The qualities of Chinese medicines are affected mainly by intra-species variation. As a result of long-time adaptation to different habitats, plants' variations can be detected at three different levels: individual, intra-community, and inter-community. For the purpose of quality evaluation and control, the geographic variation among communities is more important than the others, and it has received researchers' attention. The same is true for Danshen.

As mentioned above, Danshen is widely distributed on mountainous and hilly land of elevations between 120 and 1,300 m in China. Both wild and domestic Danshen are available in China. This section discusses geographic variations mainly in terms of phenotypic variation, genetic variation, chemical composition variation, and pharmacological and pharmacodynamic variation in different Danshen production regions.

2.4.1.1 Phenotypic Variation

There are many research reports on Danshen, and their descriptions of Danshen are generally the

same: Danshen's rootstalk is short and thick, with residual caudex on the top; long cylindrical in shape; reddish or auburn rough skin with wrinkles; old root with a purple-brown loose skin that comes off in scale-shaped pieces; hard and brittle texture; slight smell and slight bitter taste.

Zhang et al. [6] classified Danshen into three types: big-leaf type (*Salvia miltiorrhiza* Bge. cv. *sativa*), wild type (*S. miltiorrhiza* Bge. cv. *foliolum*), and small-leaf type (*S. miltiorrhiza* Bge. cv. *silcestris*). The big-leaf-type Danshen is suitable for shallow and gentle sloping land; the small-leaf type is suitable for medium hills, and wild type is suitable for deep hills. After a continuous study over three years, they found that there are significant differences ($P < 0.001$) among the three types of Danshen in their biological properties, bio-productivities, disease resistance, and commercial yields. Also, a difference is also noted in ecologic adaptation, plant character, pollen grain, chromosome, isoenzyme, and quality character. These results suggest that different habitats could cause the changes in Danshen's quality. However, no such reports have been found to confirm this speculation.

Lin and Luo [7] showed that in thin and slender Danshen roots, which have a diameter of less than 1 cm, red to brown skin and are yellowish inside, the content of Tanshinone IIA could reach or exceed the standard set forth by the Pharmacopoeia. On the contrary, in the thick and stronger roots, which have a diameter of 1–2 cm, light red-brown skin and are yellowish white or purple brown inside, the content of Tanshinone IIA is lower than the standard. They suggested that Danshen's appearance is related to the content of tanshinone.

2.4.1.2 Genetic Variation

Guo et al. [8] did RAPD analysis of 44 individual plants of Danshen from nine communities in different regions. From more than 100 primers, they selected 11 primers with high polymorphism and good repeatability, and they amplified 129 bands. Their analysis showed that the polymorphic loci in different communities are 20.9–55.0 %, intracommunity genetic variation is 80.44 %, and intercommunity variation is

8.29 %. So, it is evident that Danshen's genetic variations are mainly intracommunity, and the variations among communities are relatively less common. Their cluster diagram also showed that, except for five individuals from Sichuan's Zhongjiang area, which belong to one group, all the individuals from the other eight communities do not cluster, suggesting that Zhongjiang's Danshen has similar genetic backgrounds, and the individuals of the other communities may have greater genetic variations among themselves than among communities. Generally speaking, in a cultivated species, the genetic backgrounds tend to be similar within one community and to be very different among communities due to human interference, such as breeding and vegetative reproduction. However, Guo Baolin's study shows that even Chinese atractylodes cultivated in the same community (e.g., No.6–No.10 samples from Henan's Lushi, No.22–No.25 samples from Shandong's Yinan, and No.30–No.32 samples from Shandong's Yishui) do not cluster to each other, rather, they are mixed with Danshen from other communities. This indicates that intercommunity genetic variation, even for cultivated Danshen, is not significant.

2.4.1.3 Chemical Composition Variation

The effective components of Danshen root include liposoluble phenanthraquinone compounds and hydrosoluble salvianolic acids. In addition, there are flavonoids, triterpenes, and sterols therein. Liposoluble constituents include: tanshinone I, IIA, II-B, V, VI, cryptotanshinone, isotanshinone I, II, isocryptotanshinone, hydroxy-tanshinone IIA, methyl-tanshinonate, methylenetanshinone, dihydrotanshinone, etc. Hydrosoluble salvianolic acids include: Tanshinol, salvianolic acid A, B, C, D, E, F, G, rosmarinic acid, methylrosmarinic acid, monomethyl lithospermate, dimethyl lithospermate, ethyl lithospermate, lithospermic acid B, protocatechuic acid, caffeic acid, and isoferulic acid, etc.

Many studies have shown that the chemical compositions of Danshen have geographical differences. Wu [9] used HPLC method to measure and compare contents of Tanshinone IIA

and protocatechuic aldehyde of Danshen from different places. Chemical compositions of Danshen are different due to different origins, and their Tanshinone IIA and protocatechuic aldehyde contents are very different. Jin et al. [10] used HPLC method to analyze fingerprints of hydrosoluble and liposoluble constituents of Danshen from different production regions, and the results showed that there are differences and that the liposoluble constituent content is not related to the hydrosoluble constituent content. Huang et al. [11] used HPLC method to measure Tanshinol and protocatechuic aldehyde contents in Danshen from five different production places. Their results indicate that there are some differences in Tanshinol and protocatechuic aldehyde contents.

In addition, some researchers ranked Danshen from different regions based on their chemical composition contents. Zhang et al. [12] found that Danshen from four different regions differ in Tanshinone IIA contents; from high to low, the order is: Hebei's Pingshan, Xushui, Anguo, and Sichuan. Lin et al. [13] did qualitative and quantitative analysis of 13 Danshen samples from different regions or different growth modes with thin layer chromatography and HPLC methods and found that they differ in Tanshinone IIA contents: cultivated Danshen from Hebei's Chengde has the lowest content, while wild Danshen from Henan's Lushi County has the highest content. They also found that in Danshen samples from the same region, the wild ones contain more Tanshinone IIA than cultivated ones. Using ultrasonic extraction and HPLC analysis method, Li et al. [14] measured three liposoluble constituents, tanshinone IIA, cryptotanshinone, and Tanshinone I in Danshen from eight main production regions across the country. Their results showed that the contents of constituents in their Danshen samples are as follows: tanshinone IIA: 0.10–0.40 %; cryptotanshinone: 0.04–0.46 %; tanshinone I: 0.03–0.15 %. Danshen samples from Sichuan's Zhongjiang, Liaoning's Lingyuan, and Shandong's Pingyi have the highest contents of these chemicals, and those from Shanghai's Congming have the lowest contents. Chen et al. [15] compared chemical

compositions of Danshen cultivated in Sichuan's Zhongjiang, Shandong, and Henan and came to the conclusion that Tanshinone IIA contents in these samples are roughly the same.

From these studies, we can see that sorting Danshen from different regions is difficult, even though only the content of one component Tanshinone IIA is used as the parameter. For example, for the Tanshinone IIA content of Danshen from Sichuan, Zhang et al. [12] considered its content to be the lowest, while Lin et al. [13] considered its content to be moderate, and Li et al. [14] considered its content to be the highest. Chen et al. [15] showed that the Tanshinone IIA content in some samples was highest and in other samples was lowest. The study results from other places in China are basically similar. As these comparisons were performed based on the data from the same research group, the systematic error caused by study methods and operations factors could be eliminated, and these radically different results need to be re-evaluated.

2.4.1.4 Medical Effect Variation

Li et al. [16] compared the Danshen obtained from different regions and using Tanshinol and tanshinone components to conduct ADP-induced platelet aggregation tests, prothrombin (PT) time tests and MDA detection, performed cluster analysis on these results. They found that of the Danshen samples from eight regions, two extracts had the functions of resisting platelet aggregation, prolonging the PT time and decreasing MDA. The cluster analysis showed that as for the activity of these extracts, the wild and cultivated Danshen from Shanxi were similarly effective and they were superior to those from other places; cultivated Danshen from Sichuan's Zhongjiang, wild Danshen from Shandong, and cultivated Danshen from Henan were similarly effective and were moderate in quality by comparison; and the wild Danshen from Shanxi's Ankang and cultivated Danshen from Henan were relatively poor. The researchers noted the limitation of using limited indicators to evaluate the effectiveness of Danshen, and pointed out that more accumulated data is needed to perform a complete comparison and evaluation. From their EC_{50} data, it seems no

clear relationships exist between Danshen samples from different regions and their medical effectiveness.

2.4.2 Genuineness

2.4.2.1 Indicators and Data Evaluation

A genuine medicinal material is a featured regional product, so the quality of an herb is associated closely with its producing region. From the above review, we can see that the Danshen samples from different regions have similar phenotypic characteristics with little genetic variations, but have differences in chemical constituency and pharmacological and medical effects. However, no generalizations could be made based on this data. This may be the reason why a genuine-producing region or regions of Danshen have not been identified yet.

Chemical constituents are the material basis of pharmacological effects, and they are also the key for any medicine's clinical effects. Thus, chemical constituents should be used to evaluate an herb's genuineness. The following analysis and discussion is based upon this assumption.

In consideration of its multiple chemical constituents and multiple targets among Chinese medicines, as well as the assurance of data quality, we choose the finger-printing data from Jin et al. [10] to make a further analysis. Our rationales are as follows: (1) Their data involved 33 Danshen samples from 18 regions of China, and a total of 7 chemical constituents, including hydrosoluble and liposoluble constituents, were monitored in each Danshen sample, and some of them were tested repeatedly, so it is one of the largest databases available so far. (2) This study was reported in Chinese Traditional and Herbal Drugs in October 2004, and their methods are reliable, so the quality of the data is assured. (3) The relationship between hydrosoluble and liposoluble constituents and geographical environments was one of the major topics of this study; the researchers even did cluster analysis using these constituents as the indicators. They concluded that the hydrosoluble constituents and liposoluble constituents would vary with different

production places of Danshen, so the analysis results of this research can be used directly.

2.4.2.2 Correlation Between Geographical Condition and Chemical Constituents

From the dendrograms provided by Jin et al., we can see that Danshen from all regions are randomly clustered, and the Danshen samples from the same production region are clustered into different groups. For example, with Danshen samples #2–5 and #7–9 from Shiquan, and samples #6 and #10 from Jifeng, both located in Sichuan's Zhongjiang, the difference in chemical constituents among these samples is much larger than those from other provinces.

However, considering that the authors did cluster analysis with data of hydrosoluble constituents and liposoluble constituents separately, which might not be a good way to find the actual relationship between geographical location and chemical constituents; also, from the dendrograms in the report, we can see that the

differences between many samples are not embodied in these dendrograms. For example, in the liposoluble constituent dendrograms, a total of 17 samples, more than one half of total samples were regarded as identical, and the same problem is present in the hydrosoluble constituent dendrograms. As these researchers did not provide specific cluster distance formulas and cluster methods nor the standard data process methods, we cannot conjecture about it, but it gives us the impression that these data were not standardized, which might cause the oversight of some relatively low content variations.

Therefore, we adopted the raw data provided by Jin et al. to carry out the cluster analysis again, and our method as follows: The hierarchical cluster analysis in SPSS software is used to make the cluster analysis on the seven constituents of Danshen from 18 production regions, the data was standardized (0–1), the cluster method is average linkage (Within groups) and the distance formula is Squared Euclidean distance. The results are shown in Fig. 2.1.

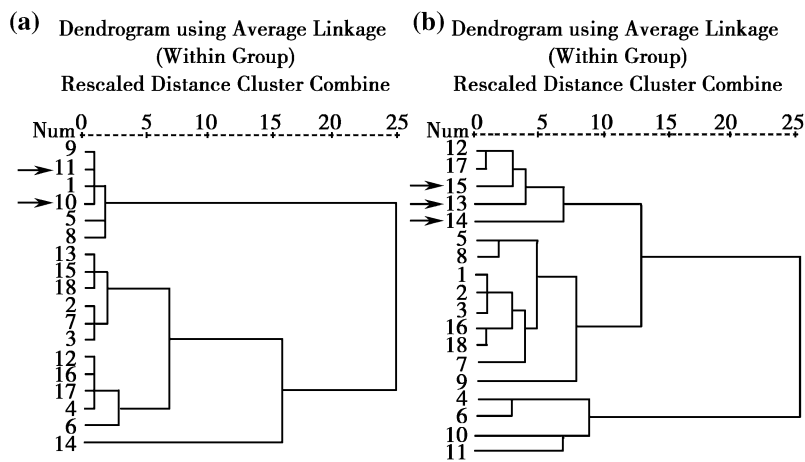


Fig. 2.1 Geographical dendrograms of Danshen's chemical constituents. *Note* **a** Samples #1–14 are from Hebei's Anguo, Hebei's Tangshan, Shandong, Shandong, Shandong's Jijing, Shandong's Laiwu, Laiwu's Liushan, Shanxi, Shanxi's Ruicheng, Sichuan Zhongjiang's Jifeng, Sichuan Zhongjiang's Shiquan, Zhejiang Qing'an's Shenzhe, Zhejiang Qing'an's Xinwo, and Zhejiang Shengzhou's Wangyuan, respectively. **b** The blank item was given the value of zero. Samples #1–18 are from Hebei's Anguo,

Hebei's Tangshan, Henan's Tongbai, Shandong, Shandong's Jijing, Shandong's Laiwu, Shandong's Laiwu, Laiwu's Liushan, Shanxi, Shanxi's Ruicheng, Sichuan, Sichuan Zhongjiang's Jifeng, Sichuan Zhongjiang's Shiquan, Zhejiang Qing'an's Shenzhe, Zhejiang Qing'an's Xinwo, and Zhejiang Shengzhou's Wangyuan, respectively. The arrows indicate Danshen samples from Sichuan Province

Because the original report provided only data on the chemical constituents of Danshen from all production regions, we performed the cluster analysis on Danshen by using the production region as the parameter. From the figure, we can see that the effect of this cluster analysis is very good, and sufficiently presents the differences among the samples. However, the results are basically in accordance with the original report. Except for several Danshen samples from Sichuan being grouped together with samples from other production places, such as Shanxi, Hebei, and Zhejiang, all of the other samples, including the samples from the same province, even from very close production places (e.g., Qing'an County's Shenze, and Qing'an County's Xinwo, Zhejiang Province), were grouped in different clusters. The variations of their chemical constituents among these samples were far larger than those of Danshen samples from other provinces. Thus, the quality variation of Danshen samples from the same province or region may be larger than those from two or more provinces separated by a long distance, which shows that the chemical constituents of Danshen present no geographical correlation; the chemical constituents of Danshen from Sichuan Province have no difference with the chemical constituents of Danshen from other production places (at least including some Danshen samples from Shanxi, Hebei, and Zhejiang provinces), but these chemical constituents have high consistencies in their own species group.

2.4.2.3 About the Genuineness of Danshen

Based upon the above analysis, we have reached the following understandings:

First, the genetic background and small scale ecological factors have a relatively large influence on the accumulation of secondary metabolites in Danshen.

Danshen from all production areas shows no obvious differences, which is the very basic reason why the genuineness of Danshen is unclear, and why the genuine Danshen production region is uncertain. Our study indicates that it would be fruitless to try to establish the genuineness of

Danshen by looking for the relationship between geography and chemical constituents, because on the one hand, Danshen roots from different regions have different constituents, and on the other, there are some overlaps in these components. Overall, these differences have no geographical characters, which is the reason why such studies gave varying results. The fact that Danshen's chemical composition has nothing to do with geographic locations indicates that the large scale ecological factors, such as climate and soil type, do not alter the accumulation of Danshen's secondary metabolites significantly. On the other hand, the fact that Danshen samples from the same province have a greater chemical composition variation between each other than between samples from other provinces suggests that genetic background as well as small scale ecological factors, such as regional soils, microclimates, and human interference, might play a bigger role.

Second, the reason that Zhongjia's Danshen is regarded as genuine might have something to do with its homogeneous quality.

With the modernization and internationalization of Traditional Chinese Medicines, special attention has been paid to the standardization of Chinese medicinal materials. Presently, it has been realized that in addition to its special therapeutic effects, Chinese medicine's homogeneity of quality should be one of the important indicators for its evaluation and quality control. We find an interesting phenomenon in our analysis, i.e., the chemical constituents of Danshen from Sichuan (mainly from Sichuan's Zhongjiang area) have relatively high consistencies in the community group, which is consistent with the conclusion made in the genetic analysis on Danshen by Guo et al. [8]; it means that Danshen from Zhongjiang has relatively high genetic similarity at the community level, which may be the reason why Zhongjiang's Danshen is highly regarded.

The propagation of Danshen is usually done by dividing roots or basal stems, or by sowing the seeds. Among the three methods, the first one is most common. Whether it is intended or not, the process of cultivation and planting is the process of breeding. Recently, Zhongjiang has become the main production place of cultivated

Danshen, characterized by its large cultivation area and matured cultivation techniques. Therefore, the homogeneity of genetic background leads to the consistency of quality of Danshen, which is the reason that Zhongjiang's Danshen has been regarded as a well-known area for medicinal material. Consequently, it can be said that the genuineness of Danshen is associated closely with the planting and processing tradition of a certain location and its cultivation techniques and breeding during the cultivation.

References

1. Xu L. *Anhui Agric.* 2002;10(7):29.
2. Zhou R. *Resource science of chinese medicinal materials.* Beijing: 1993:445–447.
3. China National Corporation of Traditional and Herbal Medicine. *Commonly Used Chinese Traditional Herbal Medicines.* Beijing: Science Press; 1995. p. 132.
4. Zhang G, Cheng F. *World science and technology,* 1999;1(4):36, 42.
5. Wu J, Chen Y. *J Sichuan Agric Univ.* 2000;018 (004):348–351, 373.
6. Zhang X, Wang Y, Luo G, et al. *Chin Tradit Herbal Drugs.* 2002;8:742–7.
7. Lin W, Luo J. *Mod J Integr Chin Tradit W Med.* 2004;2(7).
8. Guo B, Lin S, Feng Y, et al. *Chin Tradit Herbal Drugs.* 2002;33(12):1113–6.
9. Wu S. *Prim J Chin Mater Med.* 2002;16(3):24.
10. Jin Z, Zhu M, Zhang W, et al. *Chin Tradit Herbal Drugs.* 2004;35(10):1174–7.
11. Huang J, Zhang X, Guojun G, et al. *J Anhui Tradit Chin Med Coll.* 2005;24(1):37–40.
12. Zhang Y, Zhao S, Feng Y, et al. *Lishizhen Med Mater Med Res.* 2003;14(1):18.
13. Lin J, Xu L, Li Y, et al. *Chin Tradit Herbal Drugs.* 2002;2:153–4.
14. Li L, Lou Z, Chen W, et al. *Acad J Second Mil Med Univ.* 2000;21(8):571.
15. Chen X, Li W, Xia W, et al. *China J Chin Mater Med.* 1997;22(9):522–4.
16. Li M, Sun H, Lin J, et al. *World Sci Technol—Modernization Tradit Chin Med.* 2002;4(1):33–5.

Zongsuo Liang, Wenting Liu, Xuefeng Feng
and Guanghong Cui

3.1 Morphology and Development

3.1.1 Morphological Characteristics

3.1.1.1 Leaves

Danshen leaves include cotyledon, true leaves, and compound leaves. The cotyledons are leaves that first come out of the ground during the germination of Danshen seeds. The cotyledons are ovoid simple leaves without petioles or stipules. These two leaves look like the Chinese character eight (八) when coming out of the soil. They turn green upon exposure to sunlight and can therefore perform photosynthesis. Nutrient substances both stored in cotyledons and synthesized later are crucial to the growth of Danshen seedlings. (Table 3.1 is the photosynthesis of Danshen leaves.)

Danshen's true leaf is the first simple leaf after the cotyledons. It is oval in shape with a short petiole. There are tiny hairs on the surface of the true leaf. Compound leaves come out after the true leaf. Danshen's compound leaves are odd-pinnate leaves composed of 3–9 leaflets, and the top terminal one is slightly larger than the lateral ones. The petioles of compound leaves include main petioles and petiolules. Main petioles are usually 1–5 cm in length. Petiolules in the middle

are longer than those on the two sides. The lengths of petioles at different nodes differ greatly. The leaflets are obovate, long oval, or lanceolate. Please see Tables 3.2 and 3.3 for the characters of Danshen's leaves.

The tissue of Danshen's leaves is composed of the top and bottom epidermis, palisade tissues, vascular bundle, and spongy tissues. Palisade tissues contain plenty of chloroplast. Figure 3.1 shows the variation of chlorophyll content in Danshen's leaves. As shown in the figure, the change of chlorophyll content comes in the form of a bimodal curve, with the second peak topping the first one. The second peak occurs in early August.

3.1.1.2 Stems

Danshen's stems are quadrangular, 30–100 cm in height, and 3–6 mm in thickness. The stems have branches at the top. The entire stem is densely covered with light yellow soft hairs and glandular hairs. Danshen stems are usually green, and some varieties are light violet. In some plants, the basal parts of the stems are purple. Danshen's stems can be divided into main stems and branches. Rootstalks are developed from hypocotyls underneath the true leaf. A rootstalk usually has 2–4 branches. Danshen has a rather strong branching ability and normally has three-level branches, or even higher. The main stem normally has about six nodes, with shorter internodes at the bottom and top, and longer in the middle (Fig. 3.2).

Z. Liang (✉) · W. Liu · X. Feng · G. Cui
Northwest A&F University, Yangling, People's
Republic of China
e-mail: liangzs@ms.iswc.ac.cn

Table 3.1 Photosynthetic and respiration rates of Danshen leaf

Net photosynthetic rate ($\mu\text{mol CO}_2 \text{ m}^{-2} \text{ S}^{-1}$)	Net respiration rate ($\mu\text{mol CO}_2 \text{ m}^{-2} \text{ S}^{-1}$)	Light saturation point ($\mu\text{E m}^{-2} \text{ S}^{-1}$)	Light compensation point ($\mu\text{E m}^{-2} \text{ S}^{-1}$)
2.12	1.90	295	1,100

Table 3.2 Morphological characteristics of Danshen’s leaves

Shape	Length × width (cm)	Length/width	Phyllotaxis	Petiole length (cm)	Trichome
Ovoid	5–7 × 3–4	1.1–1.6	Opposite	1–5	Silver white

Table 3.3 Morphological characters of Danshen’s seedlings

Cotyledons	Hypocotyl	True leaf	Young roots length (cm)
Oval, green	Cylinder, slim	Long oval	3.6–4.9

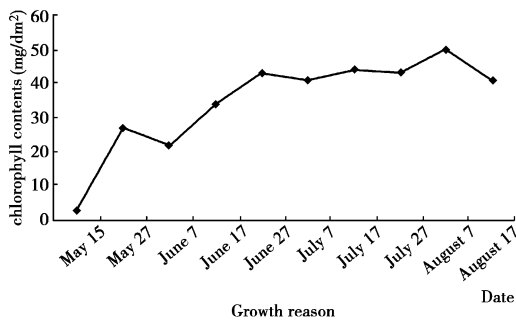


Fig. 3.1 Chlorophyll contents in Danshen’s leaves

The apex of Danshen’s stem is formed by the differentiation of an embryo. The apex is divided into three parts, namely the meristematic zone, the elongation zone, and the maturation zone. The primary structure of Danshen is formed by cell differentiation at the growing point on the top of the stem tip meristematic zone. It comprises three parts, namely the epidermis, the cortex, and the stele (Fig. 3.3).

After the formation of the primary structure, Danshen’s stem starts its secondary thickening. The secondary structure is composed of the epidermis, the cortex, the secondary phloem, the cambium, and the secondary xylem. Please see Table 3.4 for the morphological characteristics of wild and cultivated Danshen stems.



Fig. 3.2 Danshen’s roots and stems

3.1.1.3 Roots

Danshen has a taproot system which is composed of axial and lateral roots. The axial roots are fleshy and grow deep into the soil. The lateral

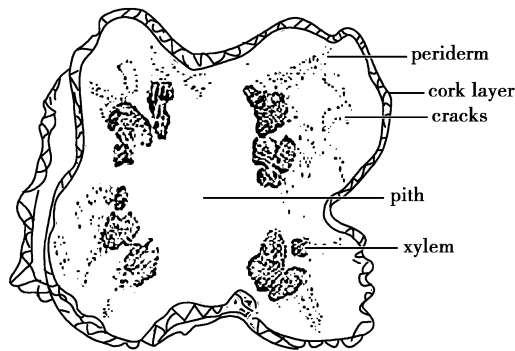


Fig. 3.3 Cross section of Danshen's stem

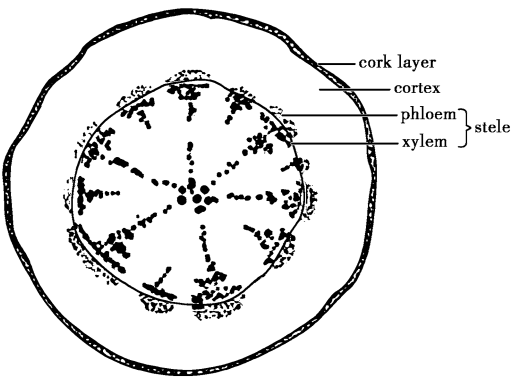


Fig. 3.4 Cross section of Danshen's root

roots are relatively flourishing with three or more levels. The entire root system is distributed in a soil layer ranging 0–60 cm in depth. The experimental measurements showed that in the same year of transplantation, the yield of fresh roots is 1,180 kg/mu (196 kg/acre) and 2,106 kg/mu (350 kg/acre) in the third year after the first winter.

The meristematic tissues on the apex of roots, which are called the growing point, generate new cells by division to form the root cap. By elongation and differentiation, the meristematic tissues also generate the secondary structure of the roots, cork layer, cortex, and stele (Fig. 3.4).

After the primary structure of a Danshen root is formed, the secondary growth in thickness will be started to form the secondary structure of the root. The secondary structure of a Danshen root is composed of the periderm, the phloem, the cambium, and the xylem. It mainly serves to channelize and store nutrients.

3.1.1.4 Flowers

Danshen has a terminal or axillary verticillaster inflorescence (Fig. 3.5). Each whorl has 6–10 flowers, and multiple whorls are arranged in an alienated racemose inflorescence. The inflorescence is usually 13–30 cm in length. Flowerets

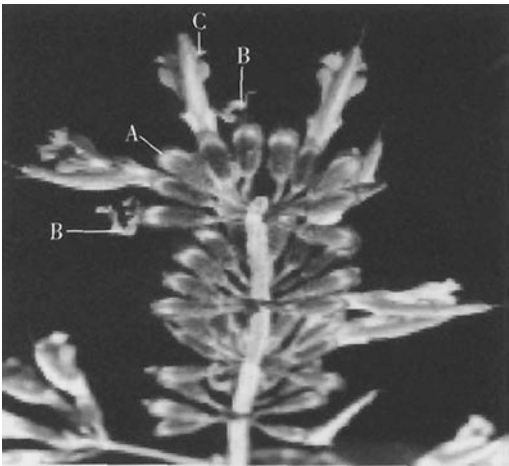


Fig. 3.5 Danshen's verticillaster inflorescence

are arrayed compactly and have short floral shoots. Calyxes are purple and slightly bell-shaped. The terminal is two-lipped, the upper lip being a broad triangle. The terminal is bicuspid. The calyx tube throat is densely covered with white long hair. The corolla is royal purple, long, two-lipped, and 2.5 cm in length. The upper lip is vertical and slightly sickle-shaped. The lower lip is shorter, its terminal being trifid. The central lobe is longer and bigger than both side lobes and

Table 3.4 Morphological characteristics of wild and cultivated Danshen's stems

	Plant height (cm)	Number of branches	Branch diameter	Number of nodes
Cultivated	48	10	Thick	6
Wild	67	4	Thin	11

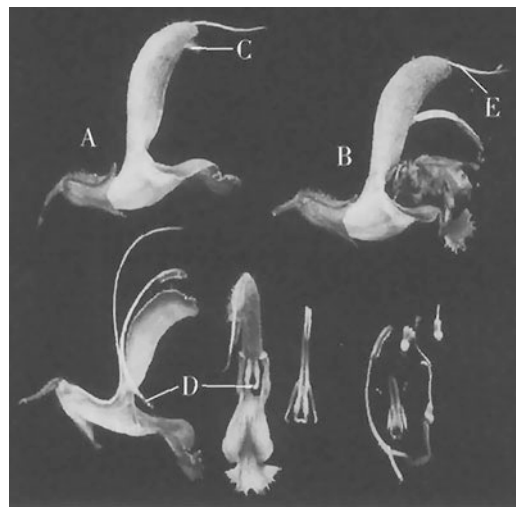


Fig. 3.6 Anatomy of Danshen's flower. (A) Concealed stylus and anther; (B) flattened lower lip serves as a landing place for insects; (C) the anther chamber on top of connective is concealed in the upper lip of corolla; (D) the regressed anther chamber at the bottom of anther becomes a valve of the anther throat; and (E) stigma

is further two-lobed (Fig. 3.6). Two androecia are developed which stick out of the corolla and are covered by the upper lip. Two apandrous grow on both sides of the throat of the upper lip. The anther is line-shaped and unilocular. The ovary is superior and four-lobed. The stylus is longer than the androecia and sticks out of the corolla. The stigma is bifid, and the two lobes are not identical (Fig. 3.7). The basal part of the ovary has a nectary which attracts insects to pollinate (Table 3.5).

Each whorl is composed of two opposite inflorescences. The flower in the middle of each inflorescence blooms first (A). The flower in the picture has already bloomed, and its corolla has already withered, so has the secondary flower (B). The flower on the third level is in bloom.

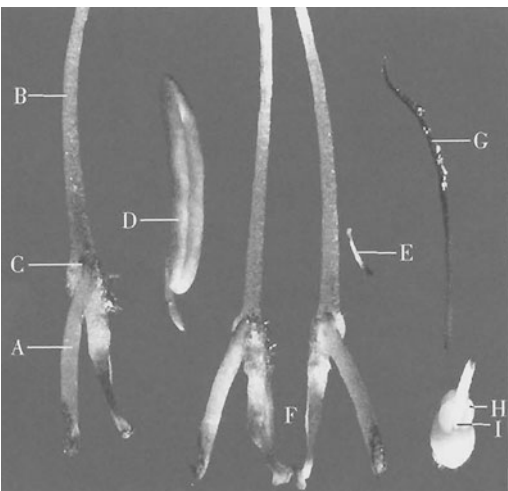


Fig. 3.7 Anatomy of Danshen's androecium and gynoecium. (A) filament; (B) connective; (C) joint formed by filament and connective; (D) fertile anther chamber; (E) infertile androecia; (F) lower end of connective; (G) lobes of gynoecium stigma; (H) four-lobed ovary; and (I) stylus grows at the basal part of ovary crack

3.1.1.5 Seeds

Danshen has small oval seeds 2.5–3 mm in length and 1.3–2 mm in width (Fig. 3.8). The surface of the seed is brownish black and covered by a yellow gray chafflike wax coat. There is a slight hunch-up on the back. The ventral surface has a blunted median ridge which separates the surface into two inclined surfaces. The top and the bottom ends are both blunt. The fruit ridge is located at the lower end of the median ridge. The edge hunches up and is densely covered with ash gray wax spots. There is a C-shaped silver white thin line in the middle (Fig. 3.9). The embryo has no endosperm and is tiny, white, and orthotropic. It has two cotyledons. The 1,000-seed weight is 1.1–1.8 g (Table 3.6).

The seed coat is composed of the exterior epidermis, sub-epidermal tissue, and sclerenchymatous cell layer. The exterior epidermis is made

Table 3.5 Morphological structure of Danshen's flowers

Flower sex	Ovary type	Androecia	Placenta type	Carpel number	Stylus
Monoecism	Superior and four-lobed into four chambers	Two regressed and two fertile	Axile placenta	2	Relatively long

Fig. 3.8 The surface Danshen seeds. **a** Picture of air-dried Danshen seeds. **b**. Picture of Danshen seeds 24 h after water absorption

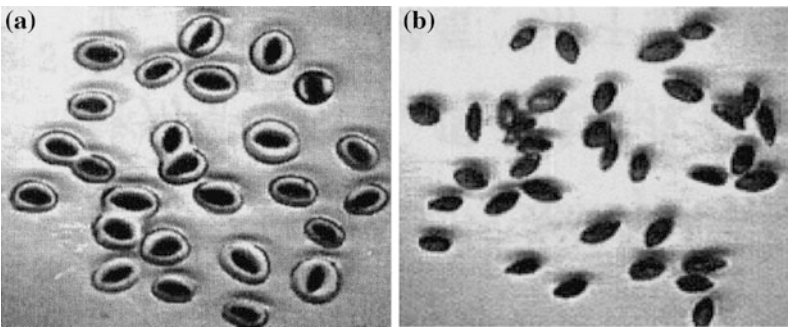


Fig. 3.9 Morphological characteristics of Danshen’s seeds. **a** The back of Danshen’s seed under SEM (×30). **b** Meshed patterns formed by mucus around fruit stalk (×70). **c** Rhombic pattern formed by strumae on the peel (×300). **d** Enlarge view of rhombic mesh structure formed by mucus (×600)

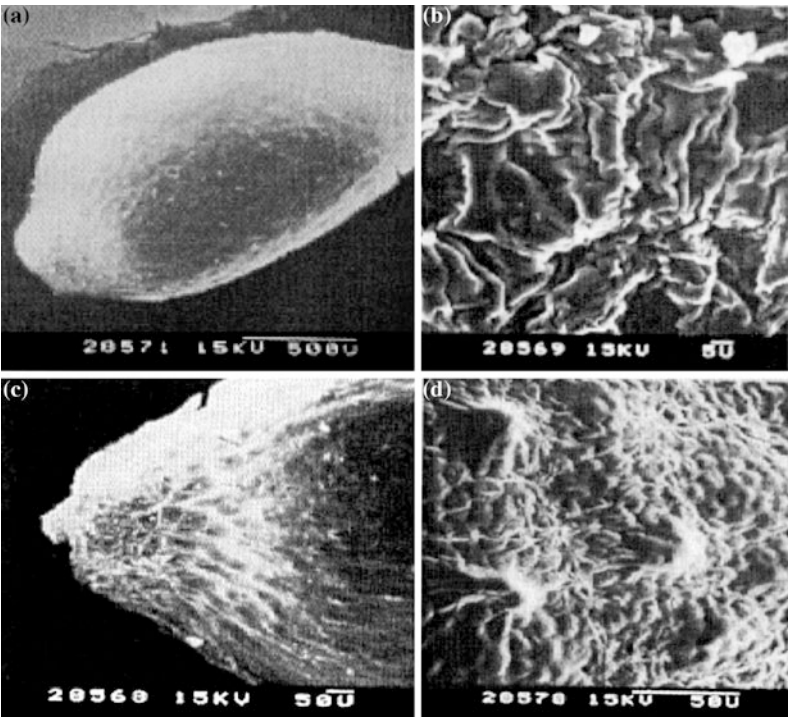


Table 3.6 Morphological characteristics of Danshen seeds

Shape of seed	1,000-seed weight (g)	Color of seed	Seed surface
Oval	1.1–1.8	Brown	Lustrous

up of palisade cells. When the seed matures, the exterior epidermis will be decomposed into a mucuslike substance and disappear from the surface of the seed coat. Although the sub-epidermal tissue is one or two layers of sclerenchymatous cells, the third layer underneath is also made up of sclerenchymatous cells. The fourth layer is a soft tissue made up of asteroid parenchyma cells and spongy parenchyma cells.

3.1.1.6 Life Span of Seeds

The life span of seeds varies with varieties. It is also subject to the influences of various conditions, such as the moisture content, storage temperature, or maturity of the seeds. Danshen seeds have a relatively short life span. Fresh seeds are brownish black and lustrous and have a high germination rate, while old seeds have a lower rate. The germination rate will fall by 10 % after

each month of storage. Under natural conditions, the germination rate will gradually decrease with time. Seeds stored for over 9 months will basically lose vitality.

3.1.2 Growth and Development

Danshen belongs to family *Labiatae*, genus *salvia*. The medicinal part of the plant is its dried roots. Danshen is a perennial herb whose both vegetative growth and reproductive growth are vigorous during growing season. It takes 80–200 days from transplanting to harvesting.

3.1.2.1 Growth of Seedlings

After the cotyledons are unfolded, the leaf primordium will gradually develop on the basal part of the growing point and generate the first true leaf and then compound leaves, one by one. After the emergence of seedlings, the accumulation of dry substances of the aboveground part of the seedling is less than that of the underground part. When the fifth compound leaf of Danshen is unfolded, the cotyledon will begin to turn yellow and then fall off. The seedling grows slowly, with a height of only 3–6 cm in 20 days after emergence. But its root system is more than 10 cm in depth and grows faster than the aboveground part.

3.1.2.2 Growth of Aboveground Part and Root System

Danshen grows vigorously, and the growth is mainly branching vegetative. The sowing is done in July and August of the first year. Seedlings will emerge 2 weeks after sowing and usually enter the vigorous growth period on the 40th day after emergence, or the 15th day after turning green. By the time of Cold Dew (Hanlu, around mid-October), the basal leaves of Danshen will completely wither. This is usually the time for lifting. All of the above combines to about 120 days. In March and April of the next year, the stored Danshen roots and shoots are transferred into a large field where they turn green in just half a month or so. The time between June and July is the vigorous growth period for the

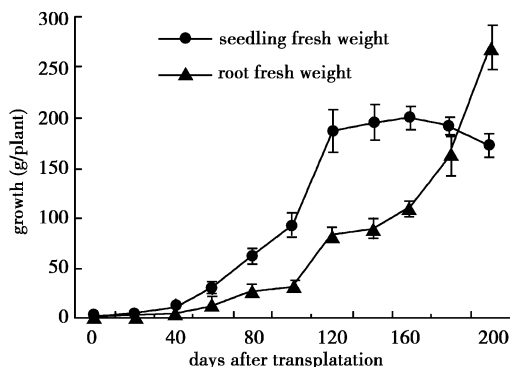


Fig. 3.10 Growth of fresh weights of seedling and root systems after transplantation of Danshen

aboveground part of Danshen, in which the growing points divide continuously, somatic cells grow rapidly, leaves enlarge, internodes elongate, and plants get taller and taller. Leaf buds in the leaf axils on the main stem generate lateral branches, the leaf buds on which will further grow into new branches and gradually form a flourishing plant cluster.

As shown in Figs. 3.10 and 3.11, the growth of the root system is obviously slower than that of the seedling system. Starting on the 40th–45th day after transplantation, the length, quantity, and amount of growth of the root system all enter the rapid growth period and follow a rapid increasing trend for the next 50 days. Starting on the 100th day, the rate of increases in fresh weight and dry weight is significantly greater

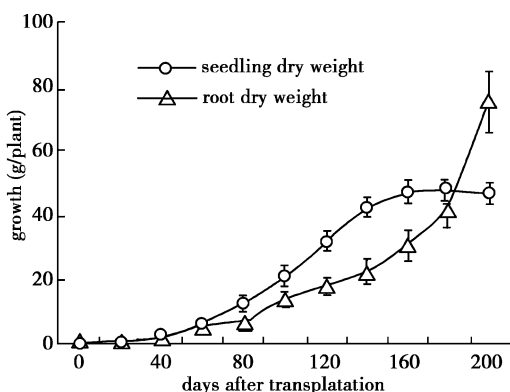


Fig. 3.11 Growth of dry weights of seedling and root system after transplantation of Danshen

than that in the previous period. With regard to the overall growing trend of the root system, the increase rate of fresh weight can be divided into three phases. The first phase is the first 40 days after transplantation. It is called the slow growth period. The increase rate of this period is 1.62 g/40 days. The second phase is between the 40th day and 100th day after transplantation. This phase sees a large increase compared with the first phase, but due to the parallel vegetative growth and reproductive growth, the growth of the aboveground part has a very big influence on the increase in the dry weight of the root system. The increase rate of dry weight in this phase is only 2.5 g/20 days. The third phase ranges from the 100th day to 200th day, in which the dry weight of root system has a total increase of 62.73 g and an increase rate of 20.9 g/20 day, which is 25 times and 8.4 times of those of the first phase and second phase, respectively. Therefore, we can see that the greatest increase in Danshen root weight occurs between the 100th and 200th days after transplantation, i.e., from early September when seeds mature, to early November when Danshen switches from reproductive growth to the second vegetative growth phase. This is a very important period for the accumulation of the dry weight of Danshen root system. The variation of the root quantity of the root system exhibits a double “S” growth curve. The first rapid increase period occurs between the 30th and 70th days after transplantation, followed by a smooth increase period. Then, a second growth peak occurs between the 140th and 200th days. The trend of rapid increase remains thereafter until harvest (Fig. 3.13).

Figure 3.12 shows that the root length begins to increase rapidly from the 40th or 50th days after transplantation. By the 100th day, the increase rate gradually falls and a stable and smooth trend of increase occurs. The changes in roots' thickness can reflect the root system's increase in another dimension. We can see from the curve of root diameter in Fig. 3.13 that starting from the 60th day after transplantation, the root diameter exhibits a stable increase, with the maximum increase rate occurring between the 60th and the 80th days after transplantation,

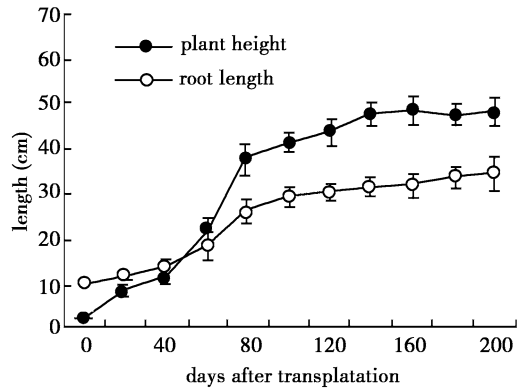


Fig. 3.12 Growth of root length and plant height after transplantation of Danshen

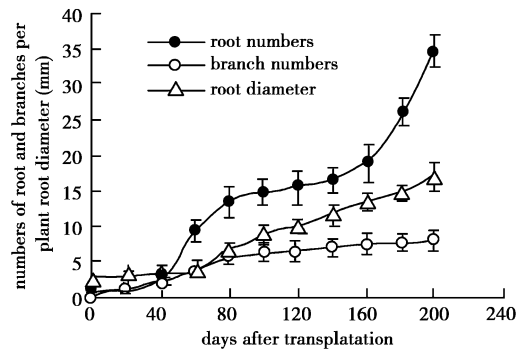


Fig. 3.13 Root and branch numbers and root diameter after transplantation of Danshen

and maintains a trend of constant increase afterward. The results above show that the basic rule for Danshen's growth is this: After the aboveground part enters the vigorous growth period, the root system begins its increase in root numbers, followed by an increase in root length, accompanied by a rapid increase of the diameter of the root system. Thereby, an orderly alternate growth pattern is formed.

The growth and development of Danshen is subject to the topography, water sources, soil fertility, and management measures. The overall growth trend is the growth of the seedling system and the growth of the root system after transplantation are in a mutually promoting and restraining relationship. During the first vegetative growth period after transplantation, the seedling system first has a rapid growth, featured

by the rapid increases in plant height and weight, while the rapid growth period of the root system comes obviously later. In other words, the growth in the first vegetative growing period is mainly in the aboveground part; the root system's growth is mainly occurring in the second vegetative growing period. After bolting and flowering, Danshen enters into the reproductive growing phase, in which both the weight and height of the seedling system have very little increase and the root system exhibits a trend of smooth growth. After maturation of seeds, the plant goes from reproductive growth to the second vegetative growth period in which the growth of the root system prevails.

3.1.2.3 Accumulation of Effective Constituents in and the Yield of Danshen's Roots

Figure 3.14 shows that the tanshinol content in Danshen reached a peak (2.48 %) on July 21 and then gradually decreased. After mid-October, tanshinol reached a relatively stable level, but its content was rather low (1.5 %). The roots harvested on August 12 had a very low tanshinol content, and the reason is still unknown.

Figure 3.15 shows that the tanshinone content in Danshen's roots increased steadily in the initial period, reached the maximum (0.51 %) on September 2, stabilized around 0.4 % between early September and early November, and rapidly fell afterward but still remained higher than 0.2 %.

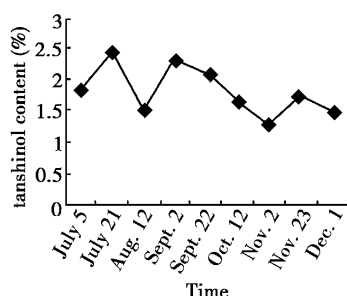


Fig. 3.14 Changes in tanshinol content during growing season

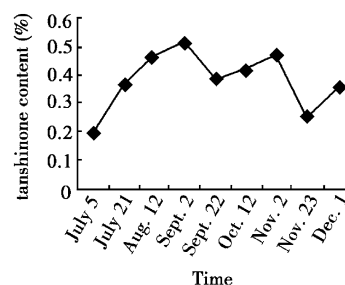


Fig. 3.15 Changes in tanshinone content during growing season

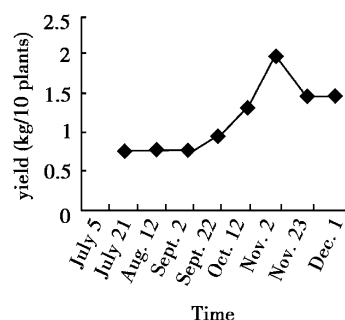


Fig. 3.16 Changes in fresh weight of Danshen's roots during growing season

Figure 3.16 shows that Danshen's fresh root weight increased slowly before September, faster and faster after that, reached the maximum rate in early November, and fell a little afterward. The yield was relatively stable after the end of November, due to the falling temperature.

Based on the above data, we conclude that the best harvesting period for Danshen is in early November.

3.1.2.4 Development of Flowers

Danshen has two types of axillary buds: leaf buds and flower buds. Leaf buds lead to branches and leaves, while flower buds lead to flowers. Shortly after the branching period, Danshen will develop flower bud primordia which differentiate from a single hump into multiple humps and form a racemose inflorescence shaped like a grape cluster containing about 70–80 flowerets. After the meiosis of pollen mother cells, the common peduncle of the racemose inflorescence begins to elongate. According to the sequence of occurrences, the differentiation of each floweret in the

inflorescence is divided into the bracteole differentiation period, the calyx differentiation period, the androecium and gynoecium differentiation period, and the corolla differentiation period.

3.2 Anatomical Morphological Characteristics of Danshen

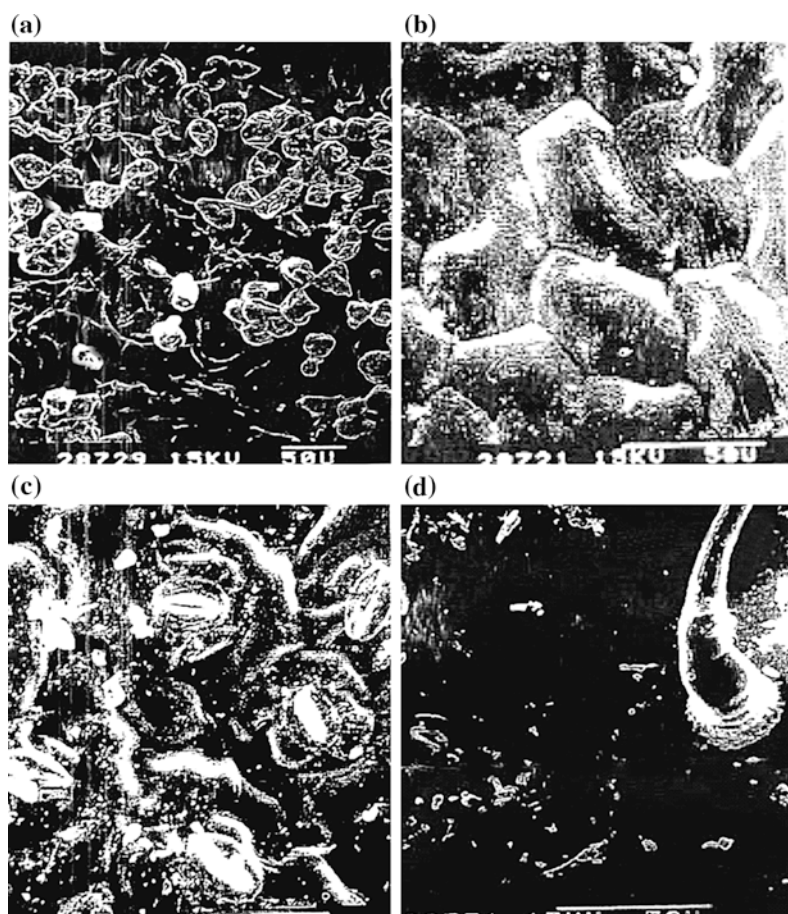
The following materials used for Danshen's anatomical morphological studies were provided by the medicinal source base of Tasly Herbal Medicine Co., Ltd. The well-grown and healthy roots, stems, and leaves were sliced for cross-sectional observation. Conventional paraffin sectioning methods and optical and electron microscopes were used.

3.2.1 Morphological Characteristics of Leaves

3.2.1.1 Microscopic Structure

The upper epidermal cells are flat, with a smooth surface, and without trichomes and stomata (Fig. 3.17a, b). The lower epidermal cells are irregularly shaped, glandular papillary cells, smaller than those in the upper epidermis. The papillae can secrete waxy sediments outward. These sediments are in the form of small balls and grains (Fig. 3.17a). Stomata are irregular, and all located on the lower surface of the leaf. Figure 3.17c shows that Danshen stomata are kidney-shaped pores typical of dicotyledons. The lower epidermis has three trichomes: barbed podetium on the head, no barbed podetium on the head, and spirally bended strip (Fig. 3.17d).

Fig. 3.17 Morphology of leaf epidermis under scanning electron microscope. **a** Upper papilla cells of Danshen leaf ($\times 200$). **b** Upper epidermis of Danshen leaf ($\times 200$). **c** Lower epidermis and stomata of Danshen leaf ($\times 200$). **d** Lower epidermis and a trichome of Danshen leaf ($\times 1000$)



3.2.1.2 Internal Structure

The upper epidermis is made up of a layer of spherical or oval cells. The lower epidermis is made up of a layer of smaller, near-spherical cells (Fig. 3.18). The epidermal cells are compactly arrayed and covered with cuticle. Beneath the epidermis is the mesophyll tissue. The mesophyll tissue is composed of the palisade tissue and spongy tissue. Palisade tissue cells are cylinder-shaped and compactly arranged in 1–2 rows, but still with large intercell spaces. The spongy tissue is irregular in shape and arranged in nets or clusters. The spaces between the cells in spongy tissue are relatively large and are connected to numerous stomata on the lower epidermis to provide a large contact interface between mesophyll tissue cells and intercell air. The mesophyll tissue is rich in chloroplasts. There are small vascular bundles within the mesophyll tissue which are surrounded by vascular bundle sheaths made up of parenchyma cells. The differentiation of mesophyll tissue varies with leaf positions, surrounding conditions, and leaf lengths. For the same plant, sunshine leaves are usually smaller but thicker than shade leaves. They also have smaller cells and cuticle. Sunshine leaves also have thicker palisade cells. Being exposed to more light and

wind, palisade tissues of leaves in the upper part of a plant are thicker than those in the lower part.

3.2.2 Morphological Characteristics of Stems

3.2.2.1 Cross Sections

The cross section of Danshen's stem is near-spherical (Fig. 3.19) and composed of the epidermis, cortex, multiple vascular bundles, pith, and pith rays. The epidermal cells are flat, and their smooth exterior surface is covered by a thin layer of cuticle and trichomes. The trichomes on the epidermis are in the shape of flat ribbons or columns which are sharp at the top. The cortex is thick and has a loose array and collateral vascular bundles. Cells in the middle of the pith are large, while cells in the xylem are smaller and compactly arrayed.

3.2.2.2 Primary Structures

The primary structure of epidermis is composed of a layer of round-shaped living cells which are compactly arrayed and have a few papillae here and there. The epidermis is covered with hairs and other attachments.

Fig. 3.18 Internal structures of Danshen leaves under an optical microscope

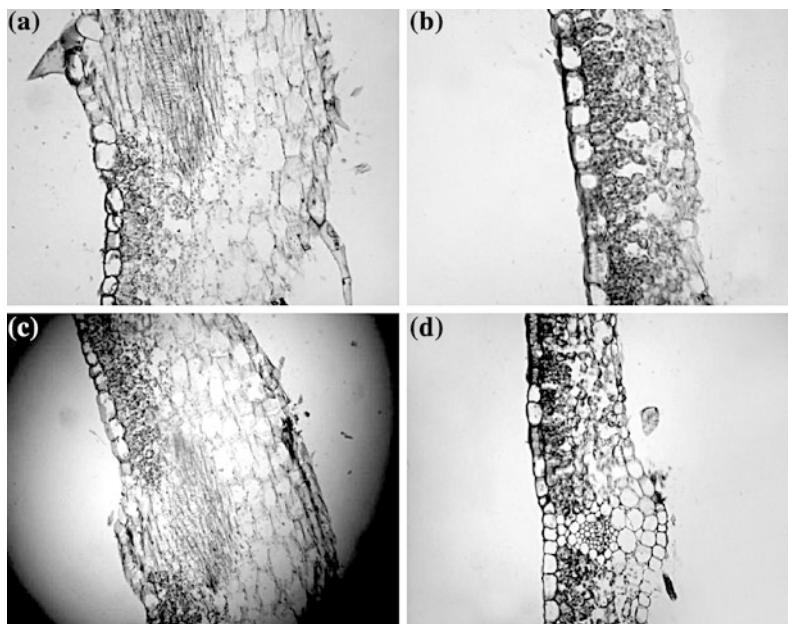
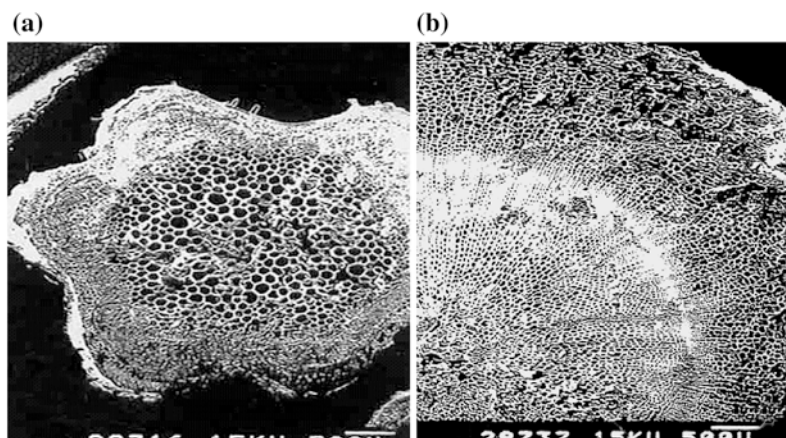


Fig. 3.19 Morphology of Danshen stem under optical microscope ($\times 200$)



The cortex is composed of 5–6 layers of living cells which take up about 1/10 of the entire cross section. The cells are spherical, polygonal, or oval. The two cell layers close to the phloem are compactly arrayed. Other cortex cells are loosely arrayed and have intercell spaces. The cortex cells contain chloroplasts. There is collenchyma in the layer right next to the cortex or in the 2–3 layers at the ridges of the stem to provide mechanical support for the stem.

Danshen's vascular bundles are indefinite collateral type and take up 1/5 of the cross section. The primary phloem is relatively narrow and takes up about 1/3 of the entire area of vascular bundles. It is mainly composed of sieve vessels, companion cells, and parenchyma cells. The primary xylem is relatively broader than the phloem and takes up about 2/3 of the entire area of vascular bundles. It is mainly composed of vessels and parenchyma cells. Inside the parenchyma are scattered 8–9 vessel molecules, which are mostly spiral or annular vessels. The cambium is located between the phloem and the xylem and is made up of a layer of relatively small rectangular cells which are compactly arrayed. The cambium cells have the meristematic ability to thicken the stem.

Pith rays are broad and radial. They are usually made up of 7–8 rows of round parenchyma cells. The pith is located in the middle of the stem and takes up the biggest proportion of the stem, about 7/10 of the cross section. It is made

up of large parenchyma cells which are round and compactly arrayed.

3.2.2.3 Secondary Structures

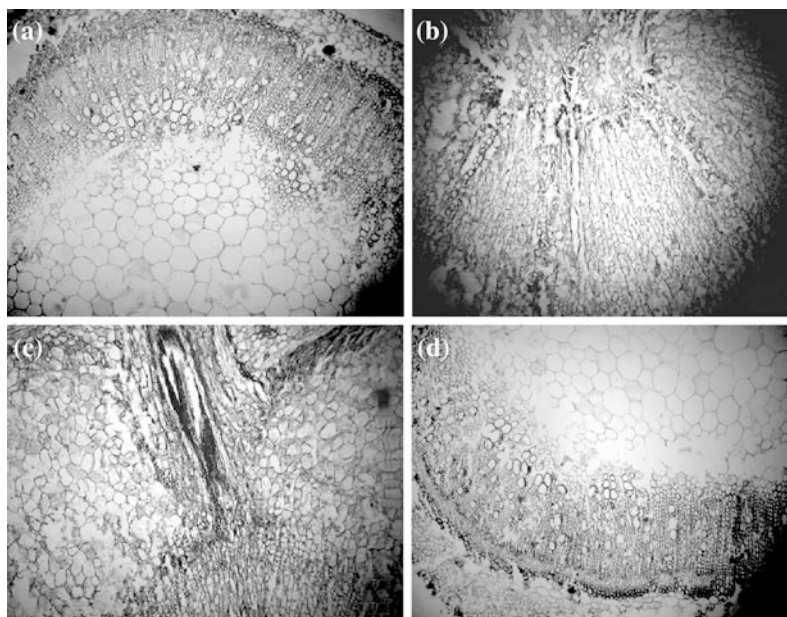
The epidermis of the secondary structure is made up of one layer of cells. The exterior wall of the epidermis is covered with thick cuticle. The cortex is made up of four layers of cells. Vascular bundles have a major change in the secondary structure. Outside the vascular bundles is the primary phloem which is usually made up of sieve vessels, companion cells, phloem fibers, and phloem parenchyma cells. Phloem cells have small diameters and irregular shapes. The phloem rays are not obvious. The phloem basically takes up the same area as the xylem. The secondary xylem is made up of vessels, xylem rays, and xylem fibers.

3.2.3 Morphological and Structural Characteristics of Roots

The primary structure of Danshen's roots is polyarch and consists of mainly epidermis and cortex. The pericycle is not obvious. The phloem is not well developed and is located on both sides of the xylem. The maturation mode of the xylem is exarch.

The emergence lateral roots originate from the pericycle cells right opposite to the primary xylem (Fig. 3.20c). The inner cortex also

Fig. 3.20 Cross sections of Danshen's roots.
a Under scanning electron microscope ($\times 200$).
b–d Under optical microscope ($\times 200$)



participates in the formation of lateral roots. When lateral roots stick out of the seminal roots, the inner cortex also performs anticlinal division simultaneously to accompany the growth of lateral roots. At the same time, the inner cortex is crushed and decomposed, and the vascular tissues within lateral roots perform differentiation.

The secondary structure of Danshen's roots is mainly made up of periderm and secondary vascular bundles. The periderm comprises the cork cambium and the in-cork cambium. The cork layer is located outermost of the roots and made up of 4–5 layers of cork cells, most of which are flat rectangular and compactly arrayed. The cork cambium is made up of 1–2 layers of flat cells. The in-cork layer is made up of 2–3 layers of cells which are near-oval living parenchyma tissue cells. The secondary vascular tissue comprises the secondary phloem, the vascular cambium, and the secondary xylem. The secondary phloem takes up 1/4 of the root radius. The vascular cambium is ring-shaped and has compactly and orderly arrayed flat rectangular cells. The secondary xylem takes up about 1/2 of the root radius. It is made up of xylem parenchyma cells, vessels, and small rays. There are a large number of xylem parenchyma cells. The xylem rays come in single

rows or double rows. Their cells are flat and irregular in shape. There is no pith in the middle of the root (Fig. 3.20a, b, d).

3.2.4 Conclusion

The morphological structures of epidermal hair and stomata are related to the drought resistance of Danshen. Molisch (1954) speculated that epidermal hair can reduce moisture loss [1]. Zhang et al. [2] proposed that epidermal hair has functions in both material exchange and information transmission, as well as a protective function. With regard to the anatomical structure of Danshen's leaves, both the upper and lower epidermises are covered with silver white hair-like substances which are scattered on the upper epidermis and compactly arrayed on the lower epidermis. The upper epidermis is compactly arrayed and covered with a thick layer of cuticle. It has few or no stomata. The lower epidermis has stomata with large pore cavities. These structures indicate that Danshen can withstand strong sunlight radiation. In the growing season, the silver gray hair on the surfaces of leaves and young branches of Danshen

can reflect sunlight, reduce leaf temperature, increase the diffusional resistance of pores, and reduce water loss. In winter, the epidermal hair turns brown and can absorb light energy and form a stable air insulation layer between the leaf surface and cold air, which is a very good adaptive protection measure.

Papilla cells are present in a wide range of angiosperms. Related data show that papilla cells can focus light and eliminate raindrops on the leaf surface [3, 4]. The presence and the amount of papillae are influenced by the environment in which the plant grows, especially by the intensity of illumination and humidity [5, 6]. The papilla cells of Danshen are mainly distributed in the lower epidermis.

The epidermis of Danshen's leaf is a single layer of cells. The upper epidermal cells are irregular and covered by cuticle. The upper epidermis has more cuticle than the lower epidermis. The cuticle has the function of reducing transpiration and to a certain extent resisting the invasion of pathogens and foreign substances. Its strong refractivity can also protect the leaf from being harmed by strong light. A number of glandular cells are also distributed around the epidermal hair of Danshen and can secrete ethereal oils to strengthen the protective effect of the epidermis.

There are small vascular bundles within the mesophyll tissue. The vascular bundles are surrounded by vascular bundle sheaths made up of parenchyma cells. The differentiation of mesophyll tissue varies with different leaf positions, surroundings, and leaf lengths. For the same plant, the sunshine leaves usually have smaller leaf areas but larger thicknesses than shade leaves, and they have smaller cells and cornuums. Sunshine leaves also have thicker palisade cells. Being exposed to more light and wind, palisade tissues of leaves in the upper part of a plant are thicker than palisade tissues of leaves in the lower part.

With regard to the stem structure, the cortex takes up a relatively large proportion of the stem radius. It is generally believed that xerophytes have thicker cortexes so that the protective layers around stems can be thicker. Their vascular

tissues are concentrated around piths. This indicates that Danshen has a strong mechanical support to withstand adverse changes in the external environment.

To sum up, Danshen has obvious stress resistance characters with regard to the structures and functions of roots, stems, leaves, and other organs.

3.3 The Reproductive Biological Characters of Danshen

In the literature on plant cultivation, there are some reports on the introduction, cultivation, and fertilization techniques of Danshen [7–9]. However, no research on the reproductive biological characters of Danshen has been reported. In 2002 and 2003, we studied some of the reproductive biological characteristics of Danshen, including the flowering habits, morphological characteristics of pollen, pollen vitality, and pollination modes, to investigate factors influencing the stock breeding and cross-breeding of Danshen. The results showed that the vitality of Danshen's pollen grains was above 80 %. The pollination time did not have a significant influence on the seed setting rate. The seed setting rate of natural cross-breeding of Danshen was 75.4 %, and the seed setting rate of selfing was 46.16 %, which indicate that Danshen is an often cross-pollinated plant. These studies provided the theoretical basis for the standardized (GAP) cultivation and breeding of Danshen.

3.3.1 Phenological Periods of the Flowering of Danshen

Danshen is an indefinite flowering plant. In Shangluo, Shaanxi, Danshen flowers in late April and remains in bloom until late October when the plant almost withers. The time between June and July is a peak period for flowering. Afterward, the flowers will gradually decrease. The flowerets bloom for 2–6 days, most for 4 days. On the first day of florescence, 9.4 % of flowerets bloom,

Table 3.7 Effects of blooming durations of Danshen flowerets and inflorescences on seed setting rate

Duration (day)	Floweret			Inflorescence				
	1	2	3	3	4	5	6	7
Number	60	90	60	8	8	20	16	4
Ratio (%)	9.4	74.8	16.2	6.3	6.3	13.3	16.7	76.7
Seed setting rate (%)	63.2	51.3	62.5	34.3	29.6	43.3	48.1	59.6

about 75 % on the second day, and 16 % on the third. The greatest number of flowers that bloom occurs between 8:00 and 10:00 a.m. The entire florescence period for a certain inflorescence lasts for 8–11 days.

3.3.2 The Exterior Appearances of Flowers and Dynamic Flowering Process of Danshen

Danshen has a terminal or axillary panicle inflorescence, which is 10–20 cm long. An inflorescence has 6–12 whorls of flowerets. Each whorl has 3–10 flowerets. Calyxes are purple and slightly bell-shaped. The top of the calyx is two-lipped, the upper lip being a broad triangle with a bicuspid tip. The calyx tube throat is densely covered with white long hair. The corolla is royal purple, two-lipped, and about 2.5 cm in length. The upper lip is vertical and slightly sickle-shaped. The lower lip is shorter with a trifid terminal. The central lobe is longer and bigger than both side lobes and is further two-lobed. Two androecia are developed which stick out of the corolla and are covered by the upper lip. Two apandrouses grow on both sides of the throat of the upper lip. The anther is line-shaped and unilocular. The ovary is superior and four-lobed. The stylus is longer than the androecia and sticks out of the corolla. The stigma is bifid, and the stylus is long and exposed, which provides chances for cross-pollination.

Pollination experiments have shown that Danshen flowerets can receive foreign pollen throughout the florescence. However, the seed setting rate differs with when the pollination occurs. The blooming period of Danshen usually lasts 8–11 days and mostly about 11 days. The greatest number of flowerets blooming occurs on

the second of third day after the florescence begins, but it varies with different inflorescences. Please see Table 3.7 for the results.

3.3.3 Morphological Characteristics of Danshen Pollen Grains

Under an optical microscope, the Danshen pollen grains are oval and yellow. Most pollen grains are 30–40 μm in diameter, and some are 60–70 μm in diameter. The grains have a coarse surface and three germinal apertures. By crushing a fresh Danshen pollen grain and enlarging it 400 times, many spherical, oval, and dumbbell-shaped dark particles are found. After being treated with 1 % $\text{I}_2\text{-KI}$ solution, the particles become royal purple, which indicates that these are starch particles. The exterior wall of the pollen grain is dried shortly after flowering, but quickly absorbs moisture when there is high humidity and develops increased adhesiveness which makes it clingy.

3.3.4 Vitality of Danshen's Pollen Grains

Staining Danshen's pollen grains with 0.5 % TTC and observing them under a microscope, we found that the vitality of pollen collected at different times during bloom is almost the same, about 80 %. The result indicates that Danshen pollen comes into vitality before the opening of the anther. This means that the pollen starts to have germination ability in the afternoon of the day before flowering and has a very strong germinating ability by the night. When the maximum germinating potential is reached, the anther will open.

Table 3.8 Effects of pollination time on seed setting rate of Danshen^a

Time	First day			Second day			Third day
	10 o'clock	13 o'clock	17 o'clock	10 o'clock	13 o'clock	17 o'clock	13 o'clock
Flowers pollinated	30	30	30	30	30	30	32
Fruits setting	15	13	15	19	16	16	19
Seed setting rate (%)	50.0	44.4	50.0	63.8	50.5	52.0	59.3

^a Perform emasculation and bagging between 15 o'clock and 17 o'clock on the day before pollination; carry out cross-pollination according to the treatment times on the next day

3.3.5 Effects of Pollination Time (Table 3.8) and Pollination Mode on Seed Setting Rate

During the full-bloom period between June and July, we did a bagging experiment. Tables 3.9 and 3.10 give a comparison between seed setting rates of unbagged and bagged Danshen. Table 3.9 shows the seed setting rate of natural field crossing of Danshen, showing that under natural pollination, Danshen flowers have a seed setting rate of 75.4 %. Table 3.10 shows the seed setting rate after bagging, showing that after being bagged, Danshen flowers have a seed setting rate of about 46 %.

The above results suggest that Danshen is an often cross-pollinated plant. This is probably the result of the morphological structure of Danshen flowers. The stigmas and androecia of Danshen

Table 3.9 Seed setting rate of natural crossing of Danshen in Shangluo, Shaanxi

Serial no.	Floweret numbers	Seeds produced	Seed setting rate (%)
1	36	108	75.0
2	23	76	82.3
3	40	112	70.0
4	43	138	86.0
5	38	128	84.2
6	45	160	88.9
7	56	160	83.9
8	23	68	73.9
9	29	104	89.7
10	17	44	64.7
Average			75.4

Table 3.10 Seed setting rate of self-pollination

Serial no.	Floweret numbers	Seeds produced	Seed setting rate (%)
20	24	20	20.83
21	13	28	53.85
22	27	37	34.26
23	35	79	56.43
24	14	38	67.86
25	20	35	43.75
26	20	50	62.50
Average			46.16

flowers are exposed, and anthers are separated from styluses. Therefore, it is easy to lose their own pollen and increase chances for cross-pollination. So, Danshen has greater chances for cross-pollination within the same plant. In addition, there are many pollinating insects in the field during the florescence, mainly including anthophorids, bees, hornets, flies, and butterflies. Under natural conditions, xenogamous pollination is even easier than cross-pollination within the same plant.

3.3.6 Conclusion

Danshen is monoecious and has an entomophilous inflorescence. Its flowering period starts in late April. Danshen flower buds begin to germinate in the beginning of April in Shangluo, Shaanxi (average atmospheric temperature 5–9 °C). Bolting occurs in early April (average atmospheric temperature 5–14 °C). Bud

formation begins in mid- and late April (average atmospheric temperature 11.5–15 °C). With the increase of atmospheric temperature, the growth and development of inflorescences begins to prevail. Inflorescences have to go through a growth period of 25–30 days. The full-bloom period is in the mid- and late May, in which about 75–90 % of the flowering is completed. The florescence of a Danshen plant lasts for about 12 days. Its full-bloom period is about 8 days. The seeds begin to mature in early June. With regard to Shangluo, Shaanxi, the full-bloom period of Danshen is just a period in which the temperature in this region gradually rises and precipitation is significantly low. The weather conditions in this period are favorable for the release and dissipation of pollen, and it is a time of frequent insect activity. According to field observations, there are many insects on the inflorescences of Danshen plants. Insects move most frequently at noon. The pollination mode is an important evolutionary characteristic in the reproduction process of a species. The three components sustaining the pollination system of a plant are the pollen, the stylus, and the pollinating media. With regard to Danshen, many features of its floral characteristics and pollination biological characters are still worth studying.

Through observation in the Danshen experimental base of Tasly Herbal Medicine Co., Ltd between July and September in 2003, we found that Danshen's florescences are influenced by its growing stages and environments. In the same year, the florescence of two-year-old Danshen is 30–45 days earlier than that of one-year-old Danshen. Danshen grown in a 1,200 m high-elevation region blooms later than those grown in a 700 m low-elevation region. Danshen grown at the borders of forests blooms earlier than those within forests. These results suggest that the nutrition, physiological conditions, and living conditions (conditions of light, water, and heat) of Danshen have significant effects on flowering.

Danshen's flower buds usually begin to differentiate, and the main inflorescence begins to grow when the 7th–9th true leaves come out, which means that the main inflorescence comes up out of the top of the main stem. Once the

growing point becomes a flower bud, their stems can no longer elongate upward. Afterward, a leaf bud will stretch out of the leaf axil right below the main inflorescence on the main stem and become a lateral branch. When 2–3 leaves come up out of the lateral branch, an inflorescence will come out on the top of the lateral branch, i.e., the first lateral branch. The second lateral branch will then grow on the top of the first lateral branch. Although axillary buds at lower positions are relatively weak, they still elongate. According to the observation, the lower the segments on which lateral branches come out, the less developed those lateral branches will be. On the other hand, all twigs on the main stem and its lateral branches have axillary buds that stretch out of their own axils to form lateral branches. Leaf axils close beneath the flower buds have strong axillary buds that stretch out.

The aboveground part of a Danshen plant grows flourishingly. It has many branches, a continuous florescence, and lots of indefinite inflorescences. Its inflorescence axes are usually axillary. Based on observation of aboveground growth, more branching of stems normally results in more axillary inflorescences. Bud removal technique has been used to control the direction of vegetative and reproductive growth, and it is believed that removing buds before florescence can increase the root yield of Danshen [9]. Our experiment has also proved this.

3.4 Study on Danshen's Pollen [10, 11]

3.4.1 Morphological Characteristics of Pollen in Genus *Salvia*

The equatorial view of the pollen grain is near-oblate, oval, or spherical. The polar view is a six-lobed or accidentally eight-lobed oval. The dimensions are $(32.0\text{--}92.4) \mu\text{m} \times (29.9\text{--}77.6) \mu\text{m}$. It has six or accidentally eight germinal furrows which are near-straight, 1–8 μm in width, and reach both poles. The wall is 0.8–3.3 μm in thickness. The outer layer is identical or thicker

than the inner layer. The surface has meshed patterns. Under a scanning electron microscope, we can see meshed triangles, squares, polygons, and ovals. There are 1–20 small holes in the meshes.

3.4.2 Morphological Characteristics of Pollen of Different *Salvia* Groups

The pollen grains of Sect. *Miltiorrhiza* are relatively small and $35\ \mu\text{m} \times 43\ \mu\text{m}$ ($P \times E$) on average. In eight species including Danshen, the large meshes of the pollen have as many as 10–20 small holes (*Salvia trijuga* has only 1–7). Their net ridges are narrow and slim. The Sect. *Eurysphace* has relatively large pollen grains which are $43\ \mu\text{m} \times 54\ \mu\text{m}$ ($P \times E$) in size on average. There are fewer small holes in their large meshes (*Salvia flaua* has more holes), and the net ridges are broader and thicker.

3.4.3 Morphological Characteristics of Pollen of Species and Cultivated Varieties

Please see Table 3.11 for the morphological characteristics of pollen of different *Salvia* plants. Please see Fig. 3.21 for the morphology of Danshen pollen.

Through observation and comparison of pollen grains of different cultivars (large leaf, small leaf, and wild) of Danshen grown in Sichuan (Table 3.12), significant differences are identified [12].

3.5 Cytological Study on Danshen Plants [13]

The literature concerning the cytological study on Danshen is mainly focused on the research on the chromosomes of *Salvia* plants. Studies on the chromosomes of some *Salvia* species have shown that the genus *Salvia* represents a very complicated chromosome type, composed of

various combinations. Chromosomes of some species are rather small and difficult for karyotype studies. The genus *Salvia* exhibits multiple basic numbers of chromosomes (i.e., $n = 9$, $n = 11 \dots$). Its diversity is clearly reflected by the karyotype characteristics. Polyploidization and changes in the shapes of chromosomes are two major factors that contribute to the formation of *Salvia* plant species. Please see Table 3.13 for the chromosome morphology and karyotype study of *Salvia* plants.

3.6 Embryologic Study on Danshen

3.6.1 Development of Macrospores and Female Gametophytes [13]

Danshen has an anatropous ovule, single integument, and thin nucellus. Archegonial cells directly develop into megasporocytes [14] which, after meiotic division, generate four linearly arrayed macrospores. The function megaspore on the chalazal end develops into a polygonum-shaped embryo sac.

At the binuclear embryo sac stage, the nuclei are located in the middle, while vacuoles are located on both ends. When the embryo develops into four nuclei, the embryo sac is significantly elongated and slightly bended. The four nuclei are divided on both ends of the embryo sac, which are separated by a vacuole. The two polar nuclei merge before fertilization. A mature embryo sac is made up of two synergids, one oocyte, one secondary nucleus, and three antipodal cells.

In 1936, Carson and Stuart [15] divided the female gametophytes of six *Salvia* species into two totally different types. One is the *S. splendens* type, whose embryo sac has a longer length than width. One of its sides is significantly convex, while the opposite side is concave, and it has no integumentary tapetum. *S. splendens*, *S. greggii*, and *S. leucantha* belong to this type. The other is the *S. mellifera* type. Its gametophyte is long, slightly bended or not bended. It is divided

Table 3.11 Morphological characteristics of pollen in genus *Salvia*

Plant name	Shape		Size (μm) (P \times E)	Germinal furrow	Exterior wall pattern
	Equatorial view	Polar view			
<i>Salvia miltiorrhiza</i>	Oblate, spherical, or near-oblate	Six-lobed oval	33.4 \times 40.1	Six furrows, arc-shaped or near-straight, reaching both poles, about 3 μm in width	Shallow meshes, several to more than 20 small holes in meshes. Small holes differ in size [10]
<i>S. miltiorrhiza</i> f. <i>alba</i>	Near-oblate, spherical	Six-lobed oval	35.1 \times 41.8	Six furrows, arc-shaped or near-straight, reaching both poles, (1) 5–6 μm in width	Deep meshes, several to more than 20 small holes in meshes [10]
<i>S. bowleyana</i>	Near-oblate, spherical, or oblate	Six-lobed oval	35.1 \times 41.8	Six furrows, arc-shaped or near-straight, reaching both poles, some pollen furrows are discontinued; (2) 5–8 μm in width	Deep meshes, several to more than 10 small holes in meshes. Small holes are deep [10]
<i>S. sinica</i>	Spherical, occasionally oblate	Six-lobed oval	46.6 \times 37.4	Six furrows, broad and long, about (3) 75–5 μm in width	Meshed patterns in nets. Meshes differ in size. 3–6 small meshes in large meshes [11]
<i>S. sinica</i> f. <i>purpurea</i>	Near-oblate, spherical, or oblate	Six-lobed oval	33.4 \times 41.8	Six furrows, arc-shaped or near-straight, reaching both poles, 2–8 μm in width	Shallow meshes, 3–18 small holes in meshes [10]
<i>S. paramiltiorrhiza</i>	Oblate, near-oblate, or spherical	Six-lobed oval	31.7 \times 41.8	Six furrows, arc-shaped, reaching both poles, (2) 5–3.3 μm in width	Deep meshes, 2–17 small holes in meshes [10]
<i>S. paramiltiorrhiza</i> f. <i>purpureoruhra</i>	Near-oblate, spherical	Six-lobed oval, occasionally eight-lobed oval	35.1 \times 46.8	Six furrows, occasionally eight furrows, arc-shaped or straight, about 2 μm in width	Deep meshes, 4–27 small holes in meshes. Small holes are relatively small [10]

(continued)

Table 3.11 (continued)

Plant name	Shape		Size (μm) (P \times E)	Germinal furrow	Exterior wall pattern
	Equatorial view	Polar view			
<i>S. yunnanensis</i>	Near-oblate, spherical, or oblate	Six-lobed oval	36.7 \times 48.4	Six furrows, arc-shaped, reaching both poles, (3) 4 μm in width	Deep meshes, 1–20 small holes in meshes [10]
<i>S. trijuga</i>	Near-oblate, spherical	Six-lobed oval	38.4 \times 45.1	Six furrows. Arc-shaped or straight. Reaching both poles. (1) 7–8. 4 μm in width	Deep meshes, 1–7 small holes in meshes. Small holes are relatively large and deep [11]
<i>S. Priontis</i>	Oval, spherical, or oblate	Six-lobed oval. Slightly wave-shaped outline	39.06 \times 29.95	Six furrows, slim and long. Almost reaching poles, (2) 5 μm in width	Shallow meshes. Thin net ridges, large meshes contain 1–5 deep holes [11]
<i>S. przewalskii</i>	Near-oblate, oblate, or spherical	Six-lobed oval	43.4 \times 55.1	Six furrows. Arc-shaped or straight, reaching both poles, about 5 μm in width	Deep meshes, 1–11 small holes in meshes. Small holes are deep [10]
<i>S. przewalskii</i> var. <i>mandarinorum</i>	Near-oblate, oblate, or spherical	Six-lobed oval	43.4 \times 53.4	Six furrows, straight. About 3–5 μm in width	Shallow meshes, 1–8 small holes in meshes. Small holes are deep [10]
<i>S. flava</i>	Near-oblate, oblate, or spherical	Six-lobed oval	41.8 \times 50.1	Six furrows. Arc-shaped or near-straight. About 3 μm in width	Shallow meshes, 2–17 small holes. Small holes are relatively shallow [10]
<i>S. evansiana</i>	Ellipsoid, occasionally spherical		44.6 \times 36.7	Six furrows, slim and long. Almost reaching poles, 1.25–2.5 μm in width, even in width	Meshes in meshes. Net ridges are thick and waved. Large meshes contain 5–9 small meshes [11]

(continued)

Table 3.11 (continued)

Plant name	Shape		Size (μm) (P \times E)	Germinal furrow	Exterior wall pattern
	Equatorial view	Polar view			
<i>S. aerea</i>	Oblate, spherical, or ellipsoid	Six-lobed oval	92.41 \times 77.62	Six furrows. Almost reaching poles, broad, 3–4 μm in width	Mesher differ in size, 1–6 small holes. Small holes are deep [11]
<i>S. castanea</i>	Ellipsoid, oblate, or spherical	Six-lobed oval	52.6–6.82	Six furrows, reaching poles, broad	Net is made up of holes with different sizes; holes are not evenly distributed [1]
<i>S. smithii</i>	Ellipsoid, spherical, occasionally oblate	Six-lobed oval	44.76 \times 37.13	Six furrows, relatively wide, about 5 μm in width	Shallow meshes differing in size. 2–6 small meshes in large meshes.
<i>S. kiaometiensis</i>	Ellipsoid, spherical, oblate	Six-lobed oval	50.13 \times 45.15	Six furrows, long, almost reaching poles, shallow; coarse grains on furrow bottoms	Single-mesh pattern. Meshes are deep. Net ridges are relatively broad. Meshes are small and seem to be made up of deep holes [11]
<i>S. chinensis</i>	Spherical, oblate, or occasionally ellipsoid	Six-lobed oval	41.94 \times 33.15	Six furrows, relatively wide, about 3.75 μm in width	Shallow meshes. 2–6 small meshes in large meshes
<i>S. japonica</i>	Ellipsoid, spherical, or oblate	Six-lobed oval	32 \times 29.20	Six furrows, relatively wide, almost reaching poles, even in width	Mesher differ in size and shape. Each mesh has a bar sticking out of net ridge [11]
<i>S. liguliloba</i>	Oblate, spherical, or ellipsoid	Six-lobed oval	52.40 \times 74	Six furrows, relatively wide, about 2.5 μm in width	Irregular meshed pattern. Meshes are large. Meshes in meshes. [11]

(continued)

Table 3.11 (continued)

Plant name	Shape		Size (μm) (P \times E)	Germinal furrow	Exterior wall pattern
	Equatorial view	Polar view			
<i>S. splendens</i>	Oblate, occasionally ellipsoid	Six-lobed oval	64.31 \times 41.12	Six furrows, wide and long, 3.75 μm in width. Coarse grains on furrow bottoms	Small meshes in large meshes. 1–5 small meshes in large meshes. Small mesh is surrounded by a ring of even smaller meshes [11]
<i>S. coccinea</i>	Ellipsoid, spherical, or oblate	Six-lobed oval	44.06 \times 36.19	Six furrows, slim and long, almost reaching poles	Meshed pattern. Net ridge is composed of lumps. Meshes are even [11]
<i>S. plebeia</i>	Spherical, ellipsoid, or oblate	Six-lobed oval	39.06 \times 29.94	Six furrows, all vertical to equator. Furrows are long	Shallow meshes. One hole in each mesh. Some meshes have 2–3 small holes [11]

Fig. 3.21 Morphology of Danshen’s pollen (adopted from Ref. [21]). **a** Polar surface. **b** Equatorial surface ($\times 1000$). **c** Equatorial surface ($\times 5000$)

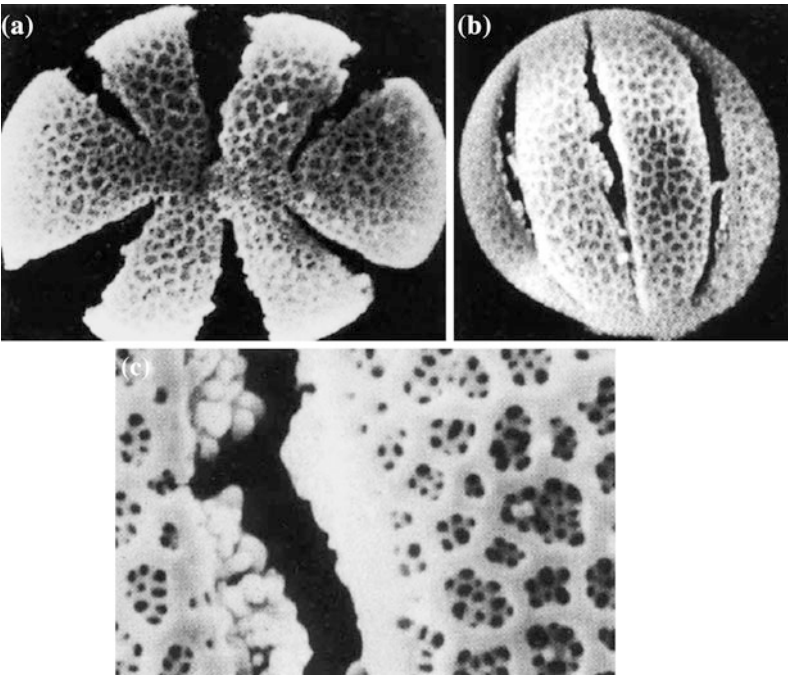


Table 3.12 Pollen’s morphological variations of Sichuan’s Danshen cultivars

Danshen Cultivars	Morphology	Size (μm)	Exterior wall pattern	Mesh holes no.
Big leaf	Oval	22.56 × 30.42	Shallow mesh	1–12
Small leaf	Pumpkin-like	24.62 × 32.16	Two layers overlap	2–12
Wild	Flat ball	28.57 × 32.85	Small nets inside big net	5–20

into two parts after maturation: The chalazal end, which is a little longer, is narrow or tube-shaped and surrounded by an integumentary tapetum, the secondary nucleus is located in the near-micropylar end, and the terminal end is three antipodal cells; the micropylar end is broader and shorter and not surrounded by an integumentary tapetum. *S. mellifera*, *S. apiana*, and *S. columbaria* are similar to this structure. The initial embryo sac of Danshen is significantly long and slightly bended. The integumentary tapetum on the chalazal end is not obvious. The morphology of the female gametophyte of Danshen is more similar to the latter type, except that its micropylar end is not significantly broadened.

3.6.2 Development of Microspores and Male Gametophytes [16]

The division of reproductive cells of Danshen pollen is done within the anther. There is no complete synchronization during division, but all pollen grains have three cells during dissemination. The division of reproductive cells is the same as ordinary mitosis, except that no cell plate is formed in the end. When a reproductive cell is divided into two sperms, cytoplasm flow can be seen within the pollen grain. The sperms can appear in any position within the grain. The observation of Danshen microspores and male gametophytes is as follows:

Danshen’s anther is made up of four pollen sacs. The development of the anther wall belongs to a dicotyledon type. The epidermis of the anther wall is persistent, and the middle layer has a short life. The tapetum has dichotocarpism and is glandular and dinuclear [17]. The inner layer of the anther wall has no fibroid thickening during maturation. Only the original cell walls are thickened.

The pollen grain of Danshen is oblate and has six furrows, and three furrows in each group are close to each other. The interfurrow distance between the pollen walls of two groups is larger. When the single pollen nucleus is close to a side, the nucleus lies against the broader wall on the equatorial plane. A large vacuole takes up the entire pollen. Traces of residual dichotocarpism tapetum still can be seen at this point.

When the pollen performs the first division, the spindle is vertical to the pollen wall. After the division periods, a convex mirror-shaped reproductive cell and a larger vegetative cell are formed. At this point, the vacuole is relatively small in volume. After departing from the pollen wall, the reproductive cell becomes spherical and still remains close to the vegetative nucleus. There is a great difference in the volumes of both cells. The vacuole within the pollen grain becomes smaller and smaller. Starch accumulates within the cytoplasm. When the cytoplasm is fully filled with starch, the reproductive cell becomes a spindle and begins to divide. The division is the same as normal mitosis. There are clear spindle fibers and an equatorial plate, but no cell plate is formed underneath spindle fibers even after the two sperm nuclei are formed in the end. The two daughter nuclei stretch toward both ends and break at the middle to form two sperm cells. The nucleus of the sperm is located in the blunter end. The other end, i.e., the broken end, is sharper and called the “tail.” When sperms are being formed, the two sperms can appear in any position within the pollen grain due to the circular flow of cytoplasm in the grain. Sometimes, the two sperms are not completely separated and still connected at the tails. In this case, the two sperms form an angle.

During the division of reproductive cells, the nucleolus of the vegetative cell nucleus becomes indistinct. When sperms have been formed, the

Table 3.13 Chromosome morphology and karyotype analysis of *Salvia* plants

Plant name	Number of chromosomes	Chromosome type	Morphology and karyotype analysis
<i>Salvia miltiorrhiza</i> Bunge [12, 22]			
<i>Salvia farinaceae</i> Benth. var. <i>royal blue</i>	$2n = 18$	$A_2B_2C_2D_{10}E_2$	Type A: 8.25 μm , two long chromosomes with near-middle primary and secondary constrictions, with long arms Type B: 6.00 μm , two long chromosomes, with primary and secondary constrictions in the middle Type C: 7.00 μm , long chromosomes with primary and secondary constrictions in the middle of near-end centromere Type D: 4.00–3.00 μm , 10 medium chromosomes with near-middle to sub-middle primary and secondary constrictions
<i>S. reflexa</i> Hornem.	$2n = 20$	A_2B_{18}	Type A: 3.75 μm , two long chromosomes, with secondary constrictions on ends Type B: 2.50–1.50 μm , 18 small chromosomes with middle to sub-middle primary constrictions
<i>S. coccinea</i> Juss.	$2n = 22$	$A_2B_6C_{14}$	Type A: 5.00 μm , two long chromosomes with primary and secondary constrictions near the middle Type B: 3.50–3.00 μm , six short chromosomes with sub-middle primary constrictions Type C: 3.25–1.75 μm , 14 small chromosomes with near-middle to sub-middle primary constrictions
<i>S. grahamii</i> (Benth.) Linn.	$2n = 22$	$A_2B_{14}C_6$	Type A: 5.00 μm two long chromosomes with one primary and one secondary constrictions in the middle and sub-middle Type B: 3.50–2.50 μm , 14 medium chromosomes with middle and sub-middle primary constrictions Type C: 3.00–2.50 μm , six short chromosomes with middle primary constrictions
<i>S. nemorosa</i> Linn.	$2n = 14$	$A_2B_8C_4$	Type A: 4.00 μm , two long chromosomes with primary constrictions in the middle and secondary constrictions in the sub-middle of the end of short arm Type B: 3.95–2.50 μm , eight medium chromosomes with sub-middle primary constrictions Type C: 3.25–2.25 μm , four short chromosomes with primary constrictions in the middle
<i>S. horminum</i> Linn.	$2n = 16 + 18$	$A_2B_8C_6$	Type A: 4.25 μm , two long chromosomes with primary constrictions in the middle and secondary constrictions on the end of short arm Type B: 3.50–3.00 μm , eight medium chromosomes with near-middle to sub-middle primary constrictions Type C: 2.50–1.75 μm , six short chromosomes with middle primary constrictions
<i>S. officinalis</i> Linn.	$2n = 14$	$A_2B_6C_6$	Type A: 3.00 μm , two short chromosomes with two primary and secondary constrictions in the sub-middle Type B: 4.95–2.25 μm , six short and long chromosomes with primary constrictions near the sub-middle Type C: 4.00–2.56 μm , six short and long chromosomes with primary constrictions near the middle

(continued)

Table 3.13 (continued)

Plant name	Number of chromosomes	Chromosome type	Morphology and karyotype analysis
<i>S. tiliifolia</i> Vahl.	$2n = 22$	A_2B_{20}	Type A: 4.00 μm , two medium chromosomes with primary and secondary constrictions in the middle and sub-middle Type B: 2.25–1.95 μm , 20 small chromosomes with middle and sub-middle primary constrictions
<i>S. leucantha</i> Cav.	$2n = 22$	A_2B_{20}	Type A: 4.00 μm , two medium chromosomes with primary and secondary constriction in the middle and sub-middle Type B: 2.75–1.95 μm , 20 small chromosomes with middle to sub-middle primary constrictions
<i>S. verbenacea</i> Linn.	$2n = 54$		10 long chromosomes, of which eight have secondary constrictions, one primary constrictions, the longest being 5.67 μm without secondary constrictions. The shortest is 1.25 μm
<i>S. splendens</i> var. <i>fireball</i>	$2n = 44$		All chromosomes are almost identical in length, with unfixed primary constrictions in the middle, 2.66–1.33 μm in size
<i>S. aegyptica</i> Linn.	$2n = 26$		All chromosomes are similar in length, with unfixed primary constrictions in the middle and 2.10–1.00 μm in size
<i>S. pratensis</i> Linn.	$2n = 16$		Chromosomes are rod-shaped. Constrictions cannot be fixed. The longest is up to 5.00 μm , and the shortest is 2.50 μm
<i>S. hispanica</i> Linn.	$2n = 12$		Chromosomes are rod-shaped. Constrictions are not clear. 5.00–3.00 μm in size
<i>S. aethiopsis</i> Linn.	$2n = 22$		Four are longer; others are short. Constrictions are not clear. 5.00–2.00 μm in size

nuclear shape becomes even more irregular and seems to be related to the flow of cytoplasm. A mature pollen grain of Danshen has three cells.

3.7 Molecular Biological Study on Danshen

3.7.1 Isozyme Analysis of Danshen

Huang et al. [18] analyzed the peroxidase isozymes of Danshen and other Labiatae plants using polyacrylamide gel column electrophoresis, and the gel columns were scanned with CS-910 dual-wavelength TLC scanner. The experimental results (Table 3.14) showed that peroxidase isozymes are correlated with morphological evolution and to the expression of diterpenoid

guinone constituents of four sub-generic plants in the *Salvia* genus. The presence and the level of diterpenoid guinone constituents contained by different species in the four sub-genuses are consistent with the expression of zymogram bands of peroxidase isozymes. For example, the diterpenoid guinone content in Danshen is high, and the relative activity of its scanned band of peroxidase isozymes is strong also. *Salvia sinica* Migo and *S. yunnanensis* Wright have low diterpenoid guinone contents, and the relative activity of their zymogram bands is weak as well. *S. plebeia* R. Br. does not contain diterpenoid guinone constituents, and the relative activity of its zymogram band is weak. According to the results, it is believed that the correlation between the expression of peroxidase isozyme zymograms of *Salvia* plants and their chemical constituents can be used as one of the biochemical

Table 3.14 Peroxidase isozymes and total diterpenoid guinone in *Salvia* plants

Family or Genus	Plant name	Total diterpenoid guinone content	Total diterpenoid guinone content ^a	Zymogram band Fig. No.
<i>Salvia</i>	Sub-g. <i>Salvia</i>	<i>S. przewalskii</i> var. <i>mandarinorum</i>	+++	1
	Sub-g. <i>Sclarea</i>	<i>S. miltiorrhiza</i>	++	2
		<i>S. yunnanensis</i>	+	5
		<i>S. sinica</i>	+	6
		<i>S. prionitis</i>	++	7
		<i>S. plebeia</i>	–	Approximately 8
	Sub-g. <i>Jungia</i>	<i>S. splendens</i>	–	3
	Sub-g. <i>Allagospadonopsis</i>	<i>S. chinensis</i>	–	4
		<i>S. substolonifera</i>	–	8
		<i>Ajuga decumbens</i>	–	Approximately 13
<i>Ajugoideae</i>		<i>Ajuga decumbens</i>	–	Approximately 13
		<i>Nepeta cataria</i> Linn.	–	9
<i>Lamioideae</i>		<i>Prunella Vulgaris</i> Linn.	–	10
		<i>Melissa axillaris</i> (Benth.) Bakh. f.	–	13
		<i>Clinodium chinensis</i> (Beath.) O. Ktze.	–	Approximately 14
		<i>Mentha haplocalyx</i> Briq.	–	11
		<i>Lycopus lucidus</i> Turcz.	–	12
		<i>Perilla frutescens</i> (Linn.) Britt.	–	Approximately 11
<i>Ocimoideae</i>		<i>Ocimum basilicum</i> Linn.	–	14

^a +++ stands for more than 0.5 %; ++ stands for 0.3–0.4 %; + stands for 0.1–0.2 %

markers to find resource plants with high contents and to perform directed cultivation of medicinal plants.

Zhang et al. [12] analyzed the isozymes of cultivated Danshen varieties grown in Sichuan by using non-continuous polyacrylamide gel electrophoresis. The results showed macrophyll-type amylase O.1 m, polyphenol oxidase PO. 1 mln, peroxidase Per. 2m2n; microphyll type PO. 2m3n, Per. 4m4n; and wild-type lipase E. 1m, PO. 3 m, Per. 5m6n. They believe that these isozymes can be used as biochemical characteristic markers for the typing of Danshen varieties.

3.7.2 Studies on the Molecular Identification of Danshen

Guo et al. [18] chose 44 samples (nine communities) from the main Danshen-producing areas to study the genetic relationships between main Danshen communities and the genuineness of medicinal materials, using RAPD method. The amplified band data obtained are processed with NTSYS-pc and AMOVA. The experimental results showed that (1) 11 primers with strong polymorphism and reproducibility were selected out of more than 100 primers and obtained 129

bands. (2) The ratios of polymorphic loci in different populations were 20.9–55.0 %. (3) The clustering chart of all samples obtained by using the UPGMA method can be divided into six main branch groups and three out-group individuals, in one of which the five samples from the Zhongjiang communities of Sichuan form a group which has a long genetic distance from other samples. (4) When grouping is done according to production areas, 80.44 % of genetic differences exist within communities, 8.29 % come from different communities within the same group, and 11.27 % come from different groups. It is believed that Danshen has great diversity within communities. The cultivated communities in Shandong and Henan come from local wild populations and are not artificially selected. The decrease in tanshinone IIA and other constituents is due to poor cultivation conditions. The genetic differentiation is not balanced between communities in different areas. Communities from Sichuan's Zhongjiang and Hebei's Chengde are distant from other communities. The determination of Danshen genuineness should be based on modern, superior medicinal material appraisal systems. Danshen produced in Shandong and Henan could be considered as genuine Danshen medicinal material as well.

3.7.3 Construction of Danshen cDNA Chips and Study on Functional Genomics

Using gene chip technology, Cui et al. [19, 20] studied the gene expression profiles of Danshen's hairy roots at different stages and identified some genes involved in secondary metabolism. The results are as follows:

1. Use the CTAB method to extract the total RNA of Danshen root. After separating mRNA by using the QuickprepTM Micro mRNA Purification Kit (Pharmacia Company), synthesize cDNA, add *EcoRI/Not I* adaptors to both ends of the cDNA molecules and ligate to expression vector ZAP Expression Vector, pack using a ZAP-cDNA

Gigapack Gold III cloning kit, and infect *E. coli* XL-Blue MRF to construct a cDNA library. The acquired cDNA library capacity is 3×10^5 . The average insert size is 0.5–2.5 kb. Single phage plaques were isolated for PCR amplification, and aliquots of the PCR reactions were analyzed in a 1.5 % agarose gel to verify the quality of PCR. The remaining cDNA was purified by multiscreen filter plates (Millipore), and aliquots were analyzed by agarose gels again to verify the quality of purification. Clones passing verification were resuspended in 15 μ L 50 % DMSO for arraying. An actin gene from Danshen was used for a positive control. PolyA and 50 % DMSO were used for negative controls. A cDNA chip containing 4354 clones was successfully made. It is the first chip for genuine medicinal material.

2. Growth rate and second metabolites analyses indicated that the period from 30 to 45 days was the growth stage, while the period from 45 to 60 days was the second metabolite accumulation stage. Accordingly, 30 days of hairy root was chosen as a reference, which was hybridized with 45 and 60 days hairy root separately. A total of 203 different expressed genes were obtained. A total of 172 ests were obtained after sequencing, which were joined and clustered into 114 unigenes. By BLASTX analysis, 104 unigenes representing 160 ests were similar to protein sequences logged in NCBI non-redundant protein database, which take up 93.02 % of the total number of ests. Although nine of these genes are isogenous with known sequences, their functions still remain unknown. Sequences not found by BLASTX were put through BLASTN analysis. Only one unigene had a corresponding congener. The other nine unigenes representing 11 ests had no annotating information (i.e., no hits) in the universal protein and nucleic acid databases. According to BLAST similarity, all unigenes are divided into the following four categories: Sixty-two genes whose functions are already known, representing 86 ests; 34 hypothetical proteins whose functions are undetermined, representing 65 ests; nine

Table 3.15 A comparison between Danshen EST BLAST and existing Danshen EST sequences

Category	Total number of ests (%)	Number of unigenes (%)	Comparison with dbEST database		
			Unigene	EST	dbEST database
Genes whose functions are already known	86 (50)	62 (54.38)	40	64	590
Hypothetical proteins whose functions are undetermined	65 (37.79)	38 (29.82)	17	36	75
Unidentified genes with low similarity	10 (5.81)	9 (7.89)	2	2	15
Genes with no significant similarity (NSH)	11 (6.39)	9 (7.89)	3	3	18
Total	172	114	60	105	698

unidentified genes with low similarity representing 10 ests; and nine genes with no significant similarity representing 11 ests. By comparison with known Danshen EST sequences, 62 unigenes representing 105 ests are isogenous with known Danshen EST sequences, and they combine to represent 698 ests (Table 3.15).

- Through GO classification (2006-05-07), a total of 67 genes were annotated, in which there were three Type II genes, 41 Type III genes, 19 Type IV genes, three Type V genes, and one Type VI gene. The three Type II genes participate in two “biological process” branches and have four molecular functions. The 41 Type III genes participate in 27 “biological processes.” Fifteen of them are “in-cell components,” located in cytosol and cytoplasm and have 51 molecular functions, such as ent-copalyl diphosphate synthase activity and cytochrome P450 activity. The 19 Type IV genes participate in 18 “biological processes,” and 13 of them are located in “in-cell components” and have 19 molecular functions, such as protein binding and transcription factor activity. The three Type V genes participate in four “biological processes” and have five molecular functions such as transcription factor and transferase activity. The Type VI gene participates in a “biological process” and is located in the mitochondrial electron transport chain. Its “molecular function” is as an ATP-binding cassette ABC transporter. It can be seen that some genes participate in more than one biological process or have more than one molecular function. Type III genes have more molecular functions which are concentrated in the aspects of catalysis, kinase, and transcription factor activity, while the molecular functions of Type IV genes are concentrated in nucleic acid structures and components and responses to external stimulation.
- By KEGG analysis, a total of 74 genes were annotated. Twenty-six of them have detailed metabolic pathway analyses, in which there is one Type II gene, 14 Type III genes, and 11 Type IV genes, which participate in a total of 29 different metabolic pathways (Table 3.16). The above-mentioned metabolic pathways are categorized according to the KEGG metabolic fingerprint. Of the three Type II pathways, two participate in carbohydrate metabolism and one participates in energy metabolism. Of the 22 Type III pathways, six participate in carbohydrate metabolism, five participate in secondary metabolism, five participate in amino acid metabolism, three participate in decomposition and metabolism of foreign substances, and the remaining three, respectively, participate in lipid metabolism, genetic information transcription, and cell behavior control. Of the four Type IV pathways, two participate in carbohydrate metabolism, energy metabolism, and transcription. It can be seen that Type III genes are of great

Table 3.16 PATHWAY categorization of Danshen differential genes

Type	Contig no.	Gene	Metabolic pathway
II	Chip37c12	Phosphoenolpyruvate carboxykinase [ATP], putative/PEP; carboxykinase , putative/PEPCK, putative	Citrate cycle (TCA cycle) Pyruvate metabolism Carbon fixation
III	Chip16g09	Copalyl diphosphate synthase/CPS/ent-kaurene synthetase A (GA1)	Diterpenoid biosynthesis
	Chip28c03	Cytochrome P450 family protein	Ascorbate and aldarate metabolism
	Chip03a02	Cytochrome P450 family protein	Gamma-hexachlorocyclohexane degradation
	Chip02c03	Cytochrome P450 family protein	
	Chip35f10	Cytochrome P450 family protein	Fluorene degradation Limonene and pinene degradation Stilbene, coumarine, and lignin biosynthesis
	Chip07f09	O-methyltransferase, family 3	Stilbene, coumarine and Lgain biosynthesis
	Chip06f03	2-Isopropylmalate synthase 1	Valine, leucine, and isoleucine biosynthesis Pyruvate metabolism
	Chip41d09	Valyl-tRNA synthetase/valine-tRNA ligase (VALRS)	Valine, leucine and isoleucine biosynthesis Aminoacyl-tRNA biosynthesis
	Chip28h12	Branched-chain amino acid aminotransferase 2/ branched-chain amino acid transaminase 2 (CBAT2)	Valine, leucine, and isoleucine degradation Valine, leucine, and isoleucine biosynthesis Pantothenate and CoA biosynthesis
	Chip04h10	Homocysteine S-methyltransferase 2	Methionine metabolism
	Chip32h7	Isoflavone reductase, putative	1,1,1-Trichloro-2,2-bis(4-chlorophenyl) ethane degradation Tryptophan metabolism Propanoate metabolism
	Chip13d05	Myo-inositol-1-phosphate, synthase-related protein	Streptomycin biosynthesis Inositol phosphate metabolism
	Chip37d07	Phospholipase D beta I/PLD beta 1	Glycerophospholipid metabolism
	Chip35e06	Myb family transcription factor	Circadian rhythm
IV	Chip04e04	Class IV chitinase (CHIV)	Aminosugars' metabolism
	Chip19g04	L-galactono-1,4-lactone dehydrogenase	Ascorbate and aldarate metabolism
	Chip01g10	Carbonic anhydrase	Nitrogen metabolism
	Chip10a03	60S ribosomal protein L21 (RPL21C)	
	Chip35h08	40S ribosomal protein S15 (RPS15D)	
	Chip40d06	60S ribosomal protein L32 (RPL32B)	
	Chip43h02	60S ribosomal protein L34	
	Chip25b10	60S ribosomal protein L37a	Ribosome
	Chip44b10	Large sub-unit ribosomal protein L27	
	Chip15h10	60S ribosomal protein L23 (RPL23C)	
	Chip39h04	60S ribosomal protein L37 (RPL37C)	

importance. Other types of genes are mainly basic metabolic genes related to growth. Some different genes participate in the same metabolic pathway. For example, P450 gene and O-methyltransferase both participate in the biosynthetic pathways of stilbene, coumarin, and xylogen by catalyzing different steps. 2-Isopropylmalate synthase, VAILRS, and BCAT2 all participate in the biosynthetic pathways of valine, leucine, and isoleucine. The annotation of these genes has provided an important basis for the research on the functional genes of Danshen.

References

1. Wang W, Liang Z, Sun Q, et al. *Acta Botanica Boreali-Occidentalia Sinica*. 2003; (23)8: 1406.
2. Zhang J, Zhang X, Zhang G. *Scientia Silvae Sinica*. 1995; 31(5):409–10.
3. Chen Z. *Bull Chin Materia Medica*. 1983;8(1):2.
4. Han J, Liang Z, Sun Q, et al. *China J Chin Materia Medica*. 2004;29(3):207–11.
5. Sun Q, Liang Z, Li S, et al. *China J Chin Materia Medica*. 2004;29(10):934–8.
6. Li H, Liang Z, Chen T. *Northwest Agric J*. 2004;13(1):89–92.
7. Han J, Liang Z, Sun Q, et al. *Acta Botanica Boreali-Occidentalia Sinica*. 2003;23(4):603–7.
8. Tianjing Tasly Group Co., Ltd. *Res Inf Tradit Chin Med*. 2002;1(1):5–7.
9. Jiangsu College of New Chinese Medicine. *Traditional Chinese medicine dictionary*, vol. 1. Shanghai: Shanghai People's Publishing House; 1997. p. 478–82.
10. Xu G, Xu L. A sort-out and study on the quality of commonly used varieties of Chinese medicinal materials, vol. 1 (South cooperation group). Fuzhou: Fujian Science and Technology Publishing House; 1994. p. 140–168.
11. Wang K, Huang X. *Bull Bot Res*. 1986;6(4):55–71.
12. Zhang XG, Wang Y, Luo G. et al. *Chin Tradit Herbal Drugs*. 2002; 33(8):742.
13. Xu R. *Danshen biology and its application*. Beijing: Science Press; 1990. p. 23.
14. Junell S. *Bot Tidsk*. 1937;31:67–110.
15. Carson EM, Stuart H. *New Phytol*. 1936; 35:68–91.
16. Qian N, Wang F. *Acta Botanica Boreali-Occidentalia Sinica*. 1988;8(3):150.
17. Divis OL. *Systematic embryology of the angiosperms*. New York: Wiley; 1966.
18. Huang X, Yang B, Hu Z, et al. *Chin Bull Bot*. 1983; 25(2):145.
19. Cui G, Huang L, Tang X, et al. *China J. Chin. Materia Medica*. 2007;32(12):1137.
20. Cui G, Huang L, Qiu D, et al. *China J Chin Materia Medica*. 2007;32(13):1267.
21. Xu L, et al. *Non-pollution cultivation and processing of Chinese medicine and transgenic engineering*. Beijing: China Press of Traditional Chinese Medicine; 2000. p. 174.
22. Cai Z, Guo B. *J China Pharm Univ*. 1993;24(1):49–52.
23. Guo B, Lin S. *Chin Tradit Herbal Drugs*. 2002;33(12):1113.

Zongsuo Liang and Wenting Liu

4.1 Propagation of Danshen

4.1.1 Propagation by Seeds

Danshen's seeds are very small. The thousand seed' weight is 1.64 g and the germination rate is about 70 %. The germination rate decreases as the storage time prolongs. There are two ways of propagation by seeds: directly sowing and seedling transplantation.

Directly sowing: sow the seeds in bunches or drills in early July. For bunch planting, the distance between two rows should be about 30–45 cm, and the distance between the bunches should be 25–30 cm. The holes should be 1 cm in depth, and 5–10 seeds are sowed per hole. For sowing in drills, the ditch should be 1 cm in depth and use 0.5 kg of seed per mu (about 3 kg/acre). After one half month, the seedlings should be 6 cm high and do the thinning.

Seeding transplantation: Because the seedlings generated by directly sowing are not uniform, the more popular way of using seeds to propagate Danshen is by seeding transplantation. This method has the advantages of low production cost and abundant seeding sources, so it is feasible to do it in large scales. Generally, in mid- to late March in northern China, sow seeds

in drills on seedbeds which are 1.5 m in width. The distance between the rows should be 30–40 cm, and the depth of the ditch should be about 1 cm. After about a half month, when the seedlings are 6 cm tall, do the thinning.

4.1.2 Propagation by Rootstalk Division

Plant division is also a way of propagation. Don [1] of Henan Province has studied the rootstalk division method for Danshen's propagation, the growth and development of Danshen plants after the division, their field management, and pest control.

At the time of harvesting cultivated Danshen, one chooses strong and healthy plants, cuts off their thick roots which can be used as herbal medicine, and uses their thin roots together with the basal parts of their stems and interior leaves as seedlings for planting. Large seedlings can be divided into 2–4 plants according to the natural growth status of their buds and roots before being planted. Wild rootstalks can also be used this way.

4.1.3 Propagation by Root Division

Choose one-year-old red, healthy, and strong lateral roots with a diameter of about 0.3 cm and plant them in soil in February or March, or at the same time as harvesting in November. Row

Z. Liang (✉) · W. Liu
Northwest A&F University, Yangling, People's
Republic of China
e-mail: liangzs@ms.iswc.ac.cn

distances are 30–45 cm, plant distances are 25–30 cm, and hole depths are 3–4 cm. At the time of planting, cut the roots into 4–6 cm pieces and plant them immediately after cutting. Place the root segments upright and plant 1–2 segments in each hole. After planting, cover the holes with about 1.5 cm of soil. It is not advisable to use lignified parent roots as seedlings due to their poor germination power and low yield. It is proven in practical production that using both ends of the roots as seedlings leads to early seedling emergence, while using the middle parts will lead to late seedling emergence. Therefore, it is advisable to plant these parts, respectively, to facilitate field management [2].

4.1.4 Propagation by Cutting

During April to May in southern China, or during July to August in the north, choose strong shoots and cut them into segments of 10–15 cm long. Cut off the leaves on the lower part and retain 2–3 upper leaves. Plant them in tilled plots according to a row spacing of 20 cm and plant spacing of 10 cm. Insert about 1/2–2/3 of the segment into the soil at an inclined angle and insert immediately after cutting; otherwise, its survival will be affected. After planting, water and shade them. After raining, make sure the water is drained in a timely manner to prevent the shoots from rotting. The seedlings will usually take root in 10 days after cutting with a survival rate of over 90 %. Transfer them to fields after their roots grow longer than 3 cm.

4.1.5 Propagation by Tissue Culture

Tissue culture technique can quickly increase the number of high-quality individual Danshen plants, which, after seedling adaptation and transplantation, can be applied to field production. Danshen's tissue culture includes multiplying the seedlings in test tubes, inducing multiploids, producing the active constituents by Cell culture, acquiring transformed plants with

Agrobacteria, and producing Danshen's active constituents in transformed tissues and organs.

Because of the long production period of and low active constituent contents in cultivated Danshen, the clinical application and quality control of Danshen is not an easy task. On the other hand, the wild resource of Danshen is limited, and digging wild Danshen will disturb the ecological balance of the natural habitat. Therefore, Tissue culture technique has the potential of solving these fundamental problems.

The roots, leaves, and petioles of Danshen can all be used as explants. Cai Zhaohui has studied organ differentiation and plant regeneration of Danshen. In 1991, Shimomaro et al. [3] established the conditions for the culture of Danshen's adventitious roots and its high tanshinone yield. In the B₅ liquid culture medium to which IBA_{0.5} is added, the culture of adventitious roots has a relatively slow growth, but a high tanshinone content of over 80 mg/kg, which is 6 times the tanshinone content in the original plant roots. Its major constituents are cryptotanshinone and tanshinone IIA.

Cai et al. [2] conducted more systematic and in-depth studies on the rapid propagation of Danshen. Their results showed that using Danshen leaves as the explants and culturing them on MS medium to which 0.5–1 mg/L 6-BA was added, they achieved 100 % clustered bud occurrence rate. Transferring the seedlings to 1/2 MS medium with 0.2 mg/L IBA, 93 % of them generated roots, and 90 % of these plants survived after transplantation. This method can be used for the mass and rapid propagation of Danshen test-tube seedlings and provides an assurance of seedling supplies for the large-area wide spreading of superior cultivars, which is of course significant for the cultivation and production of Danshen.

Researchers at China Pharmaceutical University studied the multiploid induction technology of Danshen under the condition of tissue culture, and they successfully obtained more than 20 Danshen multiploid strains. Based on agricultural characters, chemical contents of roots, and yield of medicinal parts, a tetraploid strain 61-2-22 is

selected which has superior properties in the field, high yield, good medicinal quality, and high chemical contents. This strain grows vigorously, and uniformly, with high purity. Its medicinal roots have a violet red color, mediate thickness, clustering branching and are relatively long. It has an excellent exterior appearance and meets the Class A plus standard. Its average tanshinone content is 0.5013 %, which is 203.26 % higher than that of the original plants, which is only 0.1653 %. The average tanshinone IA content is 0.1395 %, which is 70.48 % higher compared with the 0.08171 % of the original plants. The average tanshinone IIA content is 0.3155 %, which is 53.16 % higher than that of the original plants, which is only 0.2010 %. The average content of the three tanshinones is 0.9561 %, which is 112 % higher than that of the original plants, which is only 0.4529 %.

So it is obvious that the application of tissue culture techniques to artificially induce multiploids for medicinal plants' breeding has greatly improved the quality and yield of Danshen. The application of recently developed root-inducing (Ri) plasmid transformation technology to generate roots in bioreactors could massively propagate Danshen with high active constituent contents and zero pollution, which has certainly created a vast potential for the development and utilization of Danshen resources.

4.2 A Study on the Biological Characters of Danshen Seeds

Danshen seeds have a low germination rate of 30–40 % under natural conditions. In addition, the emergence of seedlings is uneven [4]. The entire germination process takes about 10–14 days, and the seeds cannot withstand long-term storage [5], all of which bring difficulties to cultivation. In China, there are no official protocols for medicinal plants' germination and cultivation, and few systematic studies have been published. Therefore, research on the biological characters of and germination conditions for Danshen's seeds is a high-priority task in the

standardization of Danshen planting, which is related to seedling culture technology and the quality of seedlings and bears great importance in the cultivation and production of Danshen.

We systematically studied the factors influencing the germination rate of Danshen's seeds. The results showed that Danshen's seeds can absorb water very quickly. After being put into water at 10 and 25 °C, the seeds absorb about 4.5 times of their own weight in water in 10 min and 10.5 and 11.7 times of their original dry weight in 2 h. The temperature had no evident influence on the water absorption process. The most suitable temperature for the germination of Danshen seeds is between 23–28 °C. Under laboratory conditions when filter paper beds were adopted at 25 °C, the germination rate of top-grade seeds could reach up to 83 %, and the germination rate of mixed-grade seeds was 74 %. It was also found that pre-refrigerating, PEG-4000 triggering, and GA₃ seed soaking could significantly boost the germination rate of Danshen seeds. Ultrasonic treatment and PEG triggering technology could make the germination rate of 1-year-old seeds reach over 45 %. Thus, the biological characters and germination conditions of Danshen seeds have been studied, and related technical approaches to the improvement of germination rate and seedling quality are proposed to provide theoretical basis and technical reference for the standardized cultivation of Danshen.

4.2.1 Water Absorption Characters of Danshen Seeds

After being put into water, Danshen seeds can absorb water at about 4.5 times their original weight in 10 min. At 10 and 25 °C, the water absorbed can reach about 10.5 and 11.7 times the original dry weight in 2 h. Temperature has no evident influence on the water absorption velocity of seeds. Results shown in Fig. 4.1 indicate that before the germination of Danshen seeds, the water absorption process can be roughly divided into 3 stages: rapid absorption stage between 0–2 h, slow absorption stage

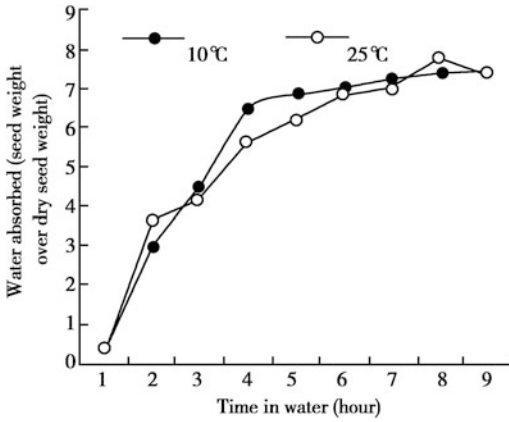


Fig. 4.1 The long-term dynamics of water absorption by Danshen's seeds

between 2–10 h, and stagnancy stage in which water absorption basically stops after 10 h. In order to further understand the water absorption characters of Danshen seeds, we have measured the variation in water absorption velocity at every 10 min for 2 h after soaking. As shown in Fig. 4.2, the greatest water absorption velocities occur within 30 min after soaking, and 86 % of the maximum water absorption rate is reached at 2 h, when the amount of water absorbed can reach up to 10–20 times of the original weight of seeds. In comparison, the water absorption rate of *Pisum sativum*, which is the highest in ordinary field corps, is only 187 % [6]. So there

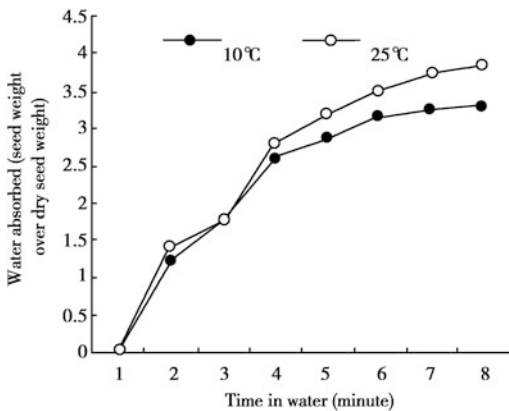


Fig. 4.2 The short-term dynamics of water absorption by Danshen's seeds

is a great difference in water absorption characters between Danshen and ordinary field corps.

4.2.2 Influences of Environmental Conditions on Germination of Danshen Seeds

4.2.2.1 Temperature

Under 25, 30, and 23/28 °C variable temperature conditions, the germinative forces reached 77.3, 81.0, and 80.3 %, respectively, while at 15 and 20 °C the germinative forces were only 45.7 and 69.0 %, respectively. The relative vitality index under the 23/28 °C variable temperature condition was higher than under the condition of 25/30 °C, and it was lower under the condition of 15/20 °C. This indicates that the variable temperature condition is more favorable for the vigorous growth of Danshen seedlings and for a rapid increase in fresh weight. The results also suggest that the most suitable temperature for Danshen seeds to germinate is 23–30 °C and that a variable temperature is more favorable for the growth of seedlings (Table 4.1).

It was also discovered in experimental studies that the uniformity of Danshen seed germination was obviously different under different temperatures. At 25, 30 °C and variable temperature conditions, germination was quite uniform, the germination peak occurred on the fourth day, and the entire germination process took only 6–7 days. When temperature fell below 20 °C, the germination uniformity decreased and the germination process took 10 days.

4.2.2.2 Germination Bed

As shown in Table 4.2, of the 4 germination beds, the filter paper and double-layer gauze bed led to higher germinative forces and germination rates than river sand and soil germination beds did, while the latter two led to higher relative vitality indexes. This is probably because Danshen seeds are small particles which hold limited nutrient substances. When embryo roots sprout, the nutrient contents in soil can appropriately meet the demand of seedlings for nutrients and result in a distinctively higher fresh weight of

Table 4.1 Influence of different temperatures on germination of Danshen seeds

Temperature (°C)	Germinative force (%)	Germination rate (%)	Relative vitality index
15	45.7 ± 1.1	58.3 ± 3.7	0.78 ± 0.13
20	69.0 ± 2.0	72.7 ± 1.8	0.96 ± 0.06
25	77.3 ± 2.4	80.3 ± 1.2	1.00 ± 0.11
30	81.0 ± 2.5	81.0 ± 2.5	0.94 ± 0.10
23/28	80.3 ± 1.8	80.7 ± 1.7	1.12 ± 0.05

Table 4.2 Influence of different germination beds on germination of Danshen seeds (25 °C)

Germination bed	Germinative force (%)	Germination rate (%)	Relative vitality index
Filter paper	68.7 ± 6.3	75.0 ± 8.0	1.00 ± 0.03
Double-layer gauze	69.7 ± 1.5	74.0 ± 2.7	0.98 ± 0.05
River sand	43.3 ± 1.3	73.7 ± 3.7	1.14 ± 0.09
Sandy soil	30.0 ± 4.5	71.3 ± 5.2	1.46 ± 0.26

seedlings than other treatments do. However, to determine the laboratory germination conditions, filter paper or gauze is preferred.

4.2.2.3 Seed Quality

Different classes of seeds have distinctively different germinative forces, germination rates, and relative vitality indexes. The germinative force of Class 1 seeds is higher than those of Class 2 and Class 3 seeds by 14.3 and 34.7 %, respectively. The germination rate is 12.3 and 26.0 % higher, respectively, and the vitality index is 11.5 and 38.6 % higher, respectively (Table 4.3). Therefore, high-quality seeds are the fundamental

Table 4.3 Influence of seed quality on germination (25 °C)

Class of seeds	Germinative force (%)	Germination rate (%)	Relative vitality index
Class 1	83.0 ± 1.5	87.3 ± 1.0	1.15 ± 0.02
Class 2	48.3 ± 7.8	61.3 ± 7.0	0.83 ± 0.10
Mixed-class	68.7 ± 6.3	75.0 ± 8.0	1.00 ± 0.04

Table 4.4 Influence of different seed treatments on germination of Danshen seeds (25 %)

Treatment method	Germinative force (%)	Germination rate (%)	Relative vitality index
Distilled water	68.7 ± 6.3	75.0 ± 8.0	1.00 ± 0.04
Ultrasonic	68.0 ± 3.5	71.0 ± 4.0	0.90 ± 0.04
Pre-refrigerating	65.7 ± 1.2	80.3 ± 1.7	1.34 ± 0.10
PEG-4000	76.6 ± 5.3	79.6 ± 3.2	1.05 ± 0.13
GA ₃	65.0 ± 3.8	80.3 ± 1.7	1.38 ± 0.10

assurance for higher germination rates and strong Seedlings.

4.2.2.4 Pretreatments

Of the 5 treatment methods, pre-refrigerating, PEG triggering, and GA₃ seed soaking treatments led to higher germinative forces and germination rates than those of comparison groups for which other treatment methods were taken, and they significantly boosted germinative forces (Table 4.4), which means such treatments are favorable for the improvement of germination uniformity. Therefore, in the culture of Danshen Seedlings, it is advisable to consider such treatment techniques as appropriate for the local conditions, which will play an important part in the improvement of germination rate and uniformity. Experiments have also shown that the above-mentioned methods were also valid for old seeds that had been stored up to 1 year. The ultrasonic treatment gave the optimal results; the germination rate was increased by 15–49.5 % compared with the comparison rate. PEG triggering treatment also increased germination rate by 12.1 %, while GA₃ only led to an increase of 5 % with regard to that of comparison groups (Table 4.5).

4.2.3 Conclusion

Up until now, there have not existed specific standards or criteria for the germination conditions of any Chinese medicinal seeds except ginseng seeds. Compared with that of the

Table 4.5 Effects of different treatments on germination rates of old Danshen seeds (25 °C)

Item	Comparison	Ultrasonic	GA ₃	Pre-refrigerating	PEG
Fresh seeds	75.0 ± 8.0	71.0 ± 4.0	80.3 ± 1.7	80.3 ± 1.7	79.6 ± 3.2
1-year-old seeds	33.2 ± 3.3	49.5 ± 4.3	38.3 ± 4.5	37.0 ± 2.5	45.3 ± 3.8

cultivation technology of agricultural crops, the research on the standardized cultivation practice of Chinese medicinal materials has just taken off and still needs long-term efforts. As shown in the water absorption characters of Danshen seeds, the reason for their rapid and abundant water absorption is the existence of a mucilage substance on their surfaces. This gelatinous mucilage layer has an excellent water-retaining ability which is very useful for resisting drought and other severe environmental conditions. This water absorption character is quite similar to that of the seeds of *Artemisia sphaerocephala*, a sand-binding plant in northwestern deserts [7]. Therefore, the biological characters of medicinal plants, their metabolisms, and their relationship with environmental conditions require further research. It is generally believed that Danshen seeds are not suitable for room temperature storage. If the storage time exceeds 6 months, the germination rate will fall below 40 % [5, 6] which, after ultrasonic treatment or PEG triggering and restoring, can be significantly increased [8]. So these two seed treatment methods can be used as remedial measures when there is a lack of fresh seeds. Through studies on the germination conditions of Danshen seeds, we propose the following protocol:

1. Germination temperature is a constant 25 °C. Germination bed is made of filter paper or double-layer gauze. Time for collecting statistical data of germinative force is 4 days (96 h) after seed soaking. Time for collecting statistical data of germination rate is 7 days (168 h) after seed soaking.
2. In order to increase the germination rate and uniformity, the following seed pretreatment techniques are recommended: (1) soaking in 100 mg/L GA₃ seed for 24 h; (2) pre-refrigerating at -20 °C for 1 week before sowing; and (3) old seeds that have been stored up to

1 year can be treated with ultrasonic or PEG triggering to increase germination rate.

3. Reference standard for the classification of Danshen seeds: (1) Class 1 seeds: germinative force 70 % and germination rate greater than 75 % and (2) Class 2 seeds: germinative force 60 % and germination rate greater than 70 %.

4.3 Influences of Bud Removal on the Yield and Contents of Effective Constituents of Danshen

Danshen belongs to the *Salvia* plants of Labiatae with indefinite inflorescences. Its flowering period is 80–90 days, during which much of its nutrition is used for the growth of reproductive organs, which inhibits the growth of medicinal roots. In order to make the cultivation of Danshen standardized, we have carried out studies on the effects of bud removal on the yield of Danshen. The results showed that bud removal technique could boost the yield of the medicinal parts of Danshen, but the contents of active constituents in Danshen were not influenced. Therefore, buds should be removed to achieve a high yield of Danshen.

Danshen was planted in the spring, using routine ridge drilling methods. Three treatments were applied to the plants: normal cultivation without bud removal; normal cultivation with bud removal; and bud removal supplemented by foliar fertilization. Each treatment was given a small 4 m × 6 m area and repeated three times. Bud removal method: when the inflorescence is about 1–1.5 cm, cut it off with scissors and repeat this operation every 3–5 days until there is no more exsertion. Supplementary fertilization method: spray EM composite bacterial liquid

onto leaves, starting at the end of August until the harvesting time in November, and a total of four sprays were conducted.

4.3.1 Exterior Characters of Danshen's Roots After Treatments

As shown in Table 4.6, bud removal can significantly increase the number of medicinal roots of Danshen.

4.3.2 Changes in Yield After Treatments

As shown in Table 4.7 and the variance analysis of Table 4.8, significant differences exist between treatments as F is greater than $F_{0.05}$. Through multiple comparisons and a new multiple range method, LSR values are acquired through calculation as shown in Table 4.9. Then, the new multiple range test results of the bud removal experiment of Danshen are acquired, as shown in Table 4.10.

Table 4.6 Exterior characters of medicinal materials of Danshen after different treatments

Item	Root length (cm)	Number of roots	Root diameter (cm)
Bud removal	34.3	19	1.24
No bud removal	31.8	13	1.24
Bud removal and fertilization	33.5	13	1.4

Table 4.7 Yield of dry products after bud removal of Danshen (kg/10 plants)

Replications	No bud removal	Bud removal	Bud removal and fertilization
1	0.274	0.413	0.363
2	0.321	0.465	0.394
3	0.243	0.594	0.299

Table 4.8 Variance analysis of data in Table 4.7

Source of variation	DF	SS	MS	F	$F_{0.05}$
Between treatments	2	0.071	0.036	9	5.14
Error	6	0.025	0.004		
Total variation	8	0.093			

Table 4.9 Calculation of LSR values with the data of Table 4.7

P	2	3	P	2	3
$SSR_{0.05}$	3.46	3.58	$LSR_{0.05}$	0.128	0.132
$SSR_{0.01}$	5.24	5.51	$LSR_{0.01}$	0.194	0.204

Table 4.10 New multiple range test of the bud removal experiment of Danshen

Treatment	Average yield (kg/10 plants)	Significance of difference	
		$F_{0.05}$	$F_{0.01}$
Bud removal	0.49	a	A
Bud removal and fertilization	0.39	a	A
No bud removal	0.279	b	B

Table 4.10 indicates that there is no significant difference in yield between the bud removal group and the bud removal plus EM treatment group, but there is an extremely significant difference in yield between the bud removal group and the no bud removal group. So bud removal can significantly increase the yield of Danshen, and spraying EM composite bacterial liquid on leaves does not play a significant role in this.

4.3.2.1 Changes in Tanshinol Contents (See Table 4.11)

As shown in Tables 4.11 and 4.12, there is no significant difference in tanshinol content between treatments as F is less than $F_{0.05}$. It is therefore clear that different treatments have no significant influence on the tanshinol content in Danshen.

Table 4.11 Tanshinol content after Danshen bud removal

Replications	Tanshinol content (%)		
	No bud removal	Bud removal	Bud removal and fertilization
1	1.36	1.71	1.6
2	1.85	1.41	1.79
3	1.58	1.42	1.52

Table 4.12 Variance analysis of tanshinol content after different treatments of Danshen

Source of variation	DF	SS	MS	F	F _{0.05}
Between treatments	2	0.0236	0.0118	0.326	5.14
Error	6	0.217	0.0362		

4.3.2.2 Changes in Tanshinone Content After Different Treatments of Danshen (See Tables 4.13, 4.14)

As shown in Tables 4.11 and 4.12, there is no significant difference in tanshinone IIA content between treatments as F is less than F_{0.05}. It is therefore clear that different treatment methods have no significant influence on the tanshinone IIA content in Danshen.

Table 4.13 Tanshinone contents after Danshen bud removal

Replications	Tanshinone IIA content (%)		
	No bud removal	Bud removal	Bud removal and fertilization
1	0.3	0.24	0.17
2	0.27	0.37	0.24
3	0.49	0.31	0.42

Table 4.14 Variance analysis of tanshinone IIA contents after different treatments of Danshen

Source of variation	DF	SS	MS	F	F _{0.05}
Between treatments	2	0.0093	0.0047	0.397	5.14
Error	6	0.0702	0.0117		
Total variation	8	0.0795			

4.3.3 Conclusion

Through experimental research and statistical analysis of the results, we have reached the following conclusions with regard to the bud removal issue of Danshen:

1. Cutting off buds significantly increases the number of medicinal roots of Danshen but has no significant effect on the diameter and length of roots; bud removal and fertilization have no significant effect on the diameter and length of roots, but show increases in the number of roots.
2. Compared with not removing buds and removing buds and spraying EM composite bacterial liquid onto leaves, removing buds can lead to a more significant increase in Danshen yield. The yield of fresh roots increased by 12.98–18.75 % compared with that of the not removing treatment, and the yield of dry roots increased by 20–22.22 %.
3. There is no significant difference between removing buds, not removing buds, and removing buds and spraying EM composite bacterial liquid onto leaves in their influence on tanshinol and tanshinone IIA, the effective constituents of Danshen.

The roots of Danshen are the medicinal parts. So it is necessary to inhibit the growth of reproductive organs and enhance the growth of nutritive organs. It has been proved in our experiments in production areas that, with completely identical fertilization, soil preparation, sowing, watering, and other measures, removing buds leads to a greater yield than not removing buds. Therefore, to increase the yield of Danshen, the bud removal technique should be considered. This conclusion is consistent with the research conducted by Xu et al. [9].

4.4 Summer Dormancy of Danshen

Shaanxi's Shangzhou has a mild climate and plenty of rainfall. Its annual precipitation is around 1,000 mm. Its elevation is 700–1,300 m. Danshen produced in this region has a

tanshinone IIA content of 0.21 %, which is higher than the standard specified in Chinese Pharmacopoeia (2000 edition), and a tanshinol content of more than 1.2 %, which is higher than the enterprise standard. So it is a region suitable for the production of commercial Danshen and superior Danshen seeds. Danshen produced in this region has high contents of tanshinone IIA and tanshinol, the two active constituents in Danshen. It has become one of the major bases for Danshen production. We carried out a study in Shangluo Danshen Base and found that the high temperature and drought in the florescence and fructification period (July and August) led to the withering of the aboveground parts of Danshen in this region. When the ambient temperature fell in September, new seedlings sprang up on the basal parts of stems. This is called the summer dormancy of Danshen. Plant withering can also be caused by root rot disease, which leads to the complete death of the whole plant. So in cultivation and production, we have to be able to tell the two different types of withering apart. Our preliminary results showed that Danshen's summer dormancy is a physiological dormancy developed by Danshen to survive in severe environments. This dormancy causes decreases in the yield and quality of Danshen. So certain procedures should be taken to manage this phenomenon, by preventing it from happening or limiting its prevalence.

Danshen sowed in 2002 and transplanted in 2003 in Yangyu River Base of Tasly Herbal Medicine Co., Ltd was used as the study material. Small seedlings (Seedlings growing from the basal parts of stems in September after the aboveground parts of Danshen withered in the high-temperature season of July and August) and old seedlings (Seedlings that did not wither) were taken as the subjects of the research and compared. Our objective was to study the growth dynamics, which include the elongating, thickening, and expanding of the root system, the accumulation of aboveground and underground dry substances, the accumulation of underground active constituents, and the photosynthesis of leaves, the corresponding physiological indexes being: root length, root thickness, number of

branch roots, fresh weight of roots, dry weight of roots, fresh weight of stems, dry weight of stems, tanshinone IIA, tanshinol, chlorophyll, etc. Those small seedlings were labeled, and samples were collected every 15 days.

4.4.1 Growth Characteristics of New Seedlings Growing on Basal Parts of Stems

Figures 4.3, 4.4, and 4.5 show the growth trends of the root length, root thickness, and number of roots. As seen from the comparison between old seedlings and newly generated seedlings, the growth indexes of old seedlings have a slow increasing trend, while the increasing trend of newly born seedlings is greater than that of old seedlings, which means that after the summer dormancy of Danshen, the new seedlings had a vigorous growth.

Figure 4.6 shows that old seedlings have greater increase in the fresh weight and dry weight of roots than new seedlings do, but the latter has a more significant increasing trend. Old seedlings have an average increase of 1.16 g/plant in fresh weight of roots, while new seedlings have an average increase of 1.8 g/plant in fresh weight of roots; old seedlings have an average increase of 0.3 g/plant in dry weight of roots, while new seedlings have an average

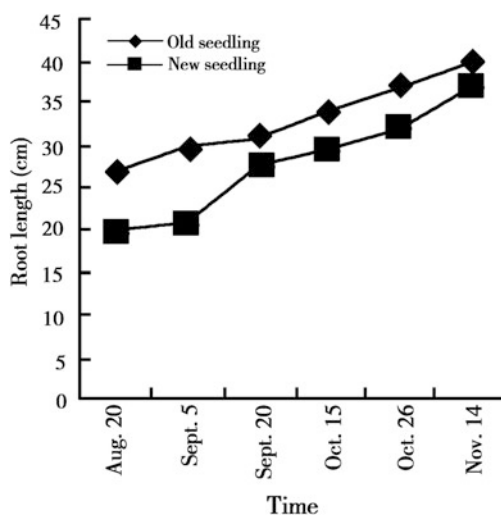


Fig. 4.3 Growth trend of root length

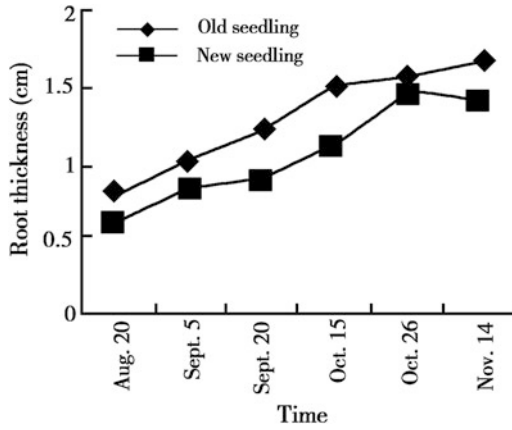


Fig. 4.4 Growth trend of root thickness

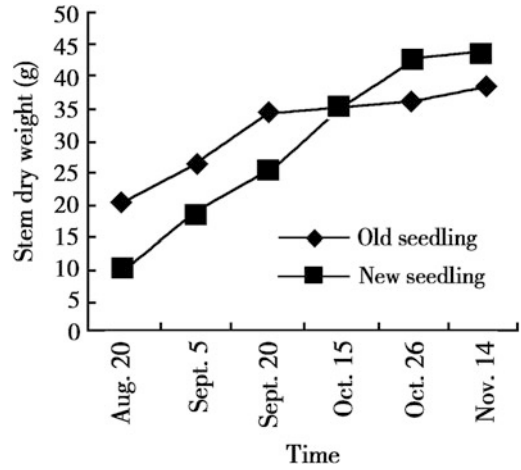


Fig. 4.6 Growth trend of Danshen's stem dry weight

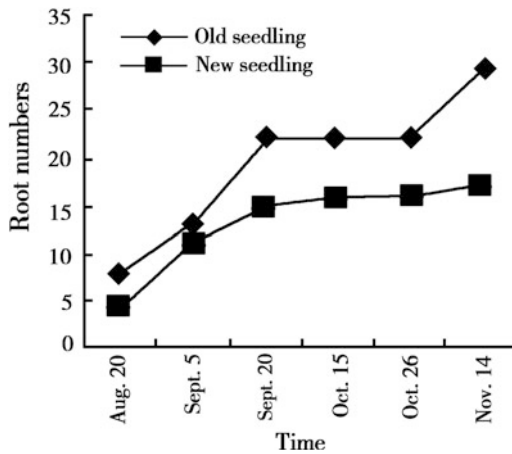


Fig. 4.5 Growth trend of root numbers

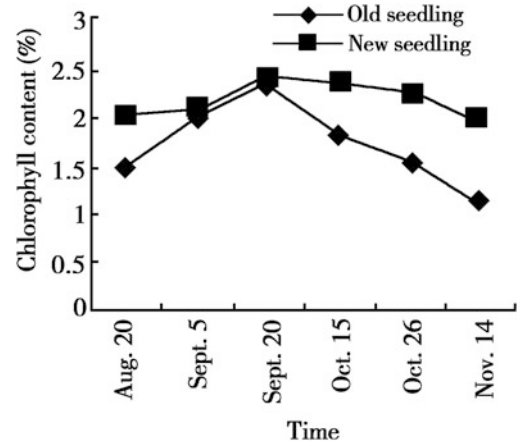


Fig. 4.7 Changes in chlorophyll content in Danshen during growing season

increase of 0.338 g/plant in dry weight of roots. Similarly, old seedlings have greater fresh weight and dry weight of stems than small Seedlings, but generally, new seedlings have a larger increase in growth than old Seedlings.

Figure 4.7 shows the variation of chlorophyll with time. As seen from the variation trend of chlorophyll, before October, the chlorophyll content was overall on the increase, but after October, the chlorophyll content began to fall due to the dropping of temperature. Since new seedlings were leaves developed in July and

August which grew vigorously and old seedlings were original leaves, new seedlings always had higher chlorophyll content than old seedlings.

Figure 4.8 shows the tanshinone IIA content variation curves. The tanshinone IIA content of new seedlings reached its peak on September 20, while the tanshinone IIA content of old seedlings reached its peak on October 5, which means that new seedlings reached the peak of the tanshinone IIA content at an earlier point than old seedlings did. Tanshinone IIA contents of both types had a significant drop after reaching the peaks and then

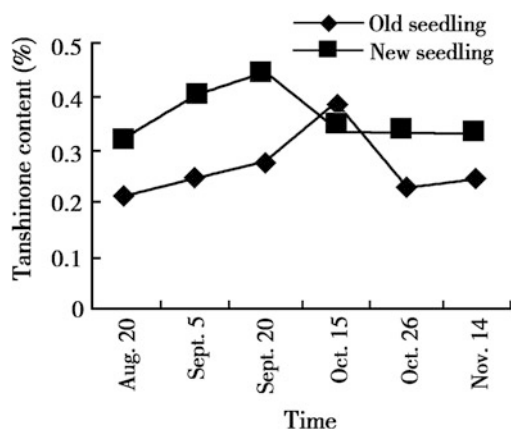


Fig. 4.8 Changes in tanshinone content in Danshen during growing season

a mild increase, but new seedlings still ended up with higher tanshinone IIA content than old seedlings. The tanshinone IIA content of new seedlings stabilized around 0.33 %, while the old seedlings stabilized around 0.23 %.

As seen from Fig. 4.9, tanshinol contents have an increasing declining trend. Old seedlings reach the peak earlier than new seedlings, but in the end, new seedlings have higher tanshinol content than old seedlings.

Table 4.15 shows a yield comparison between old and new seedlings after the harvest of Danshen. Old seedlings have a higher fresh weight of

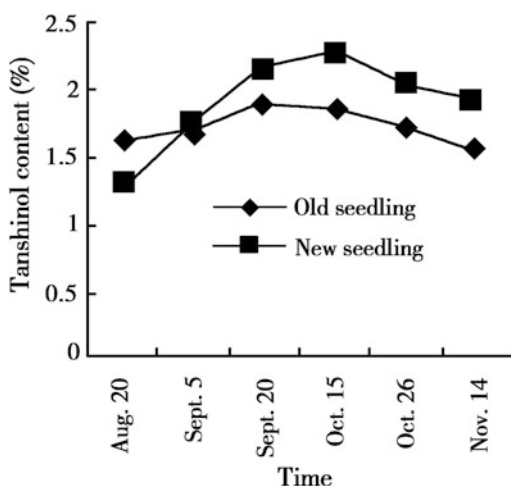


Fig. 4.9 Changes in tanshinol content in Danshen during growing season

Table 4.15 Comparison of yields between old seedlings and new seedlings after Danshen harvesting

Type	Fresh weight of roots (g/plant)	Dry weight of roots (g/plant)	Dry rate (%)
Old seedlings	252	75	30
New seedlings	150	35.4	23.6

roots per plant than new seedlings by 102 g, a higher dry weight of roots by 39.6 g, and a higher dry rate than new seedlings by 6.4 %.

4.4.2 Discussion

When encountering high temperatures during the growing season, the growth of Danshen's young seedlings will be inhibited. This phenomenon is known as the summer dormancy. As indicated by the analysis of the growth indexes and the contents of active constituents of aboveground and underground parts, the new seedlings generated after the dormancy have a faster trend of growth than old seedlings. This is because they grow vigorously, and their leaves have strong photosynthesis effects, which supplies more nutrition for the underground parts and leads them to grow rapidly. On the contrary, under the heat stress, the old seedlings suffered from a decrease in photosynthesis, which led to a slow growth of their roots. The yield analysis indicates that the final yield of old seedlings is more than twice that of new seedlings. The analysis of both yield and growth indexes indicates that both the yield and growth indexes of Danshen will drop after the dormancy, because the aboveground parts of Danshen cease to grow during dormancy, and newly born seedlings after dormancy are only allowed a very short period of growth. Despite their growth indexes and that their active constituent contents have a faster trend than those of old Seedlings, their final yield and growth indexes still fail to match up with the growth of old seedlings.

Dormancy is a halt of development. For the plant itself, it is both an important process of life activities and a beneficial biological character. It is a biological adaptability obtained by the plant over a long period of evolution to environmental conditions and seasonal changes. So dormancy is good for the survival and multiplication of plant species. For example, after forming seeds in autumn, plants in temperate regions can escape being hurt by the bitter cold of winter by dormancy. Due to the short dormancy periods of their seeds, rice crops can prevent their grains from germinating on ears especially when faced with rainy weathers in the harvest season. Trees get rid of their leaves in autumn and form buds that are impenetrable by water or air, which is a precautionary measure against the advent of adverse conditions. All of these are adaptive and protective reactions.

The dormancy of Danshen is a special biological phenomenon that occurs during its growing process. For the plant itself, it is a beneficial biological character and an adaptive behavior in response to adverse environmental conditions. However, as a medicinal material, Danshen should be treated with proper field management to prevent such a phenomenon in production.

4.5 Influences of Planting Density on Yield and Contents of Active Constituents of Danshen

Improper densities in the planting process have an adverse effect on the yield and quality of Danshen. It is required by the state GAP that the production of medicinal materials must be standardized and the cultivating techniques must be optimally combined. In our practice of the construction of a GAP base, we have found that different regions have very different planting densities. Planting density influences not only the yield, but also the contents of effective constituents in Danshen. It is a crucial technical issue in cultivating measures. Studies conducted by our

research group indicate that the thicker the roots are, the lower the total tanshinone content is [10]. This result is consistent with the studies conducted by Chen et al. [11] They believe that Danshen should be planted with a reasonable density. If the density is too low, there will be a serious land exposure problem, which leads to a great waste of light and reduces the yield of Danshen production. However, an excessive density will easily lead to the lodging of above-ground parts and inhibit the growth of under-ground parts. In this case, the root system will suffer a slow growth and the root will become slender, which causes a drop in quality. So, a reasonable planting density is crucial for the growth and production of Danshen. It is an important measure for the high-yield and high-quality cultivation of Danshen. It has become an urgent task to find out how to achieve high-yield and high-quality cultivation of Danshen.

We conducted research on the growth, yields, and effective contents of Danshen in Shangluo Region with different planting densities. Seven different densities were designed for experimental treatments, and they were as follows: 20 cm × 20 cm, 20 cm × 25 cm, 25 cm × 25 cm, 25 cm × 30 cm, 25 cm × 35 cm, 30 cm × 35 cm, and 30 cm × 25 cm. Each treatment was repeated thrice. The arrangement was random. There were 21 small experimental plots in total. The number of surviving Danshen seedlings was collected during the harvest season. After sampling, high-performance liquid chromatography was used to measure their contents of tanshinol and tanshinone IIA. The statistical data of the Danshen yield and individual yield of each plant were collected in each small experimental area. The research results show that the density of 20 cm × 25 cm led to the highest Danshen yield and the greatest effective contents, with a root yield up to 1,631 kg/μ in terms of fresh weight, a tanshinol content up to 2.15 %, and a tanshinone IIA content up to 0.42 %. We conducted studies on the relationships between different planting densities and the effective contents and yield of Danshen, so as to propose the most suitable planting density for the standardized planting of Danshen, to provide a theoretical basis for the

improvement of the quality and yield of Danshen medicinal materials, and to offer scientific data support for the implementation of GAP production of Danshen. For this sake, we aim to provide scientific basis for the standardized cultivation of Danshen.

4.5.1 Influence of Transplanting Density on Survival Rate

A reasonable transplanting density is the key to ensuring the highest survival rate of Danshen. Only if the survival rate is ensured, can a high yield and improved economic benefits be expected. Danshen grown in Shangluo has many branches and prosperous branch stems. If an unreasonable planting density is adopted, when the ground is completely covered by foliage, the plants will thrive and the aboveground parts will grow so prosperously that they will shade each other and reduce the photosynthetic rate of lower leaves. The growth will be seriously hindered, especially in the high-temperature and high-humidity environment of July and August in which this could easily lead to withering and reduce the survival rate of Danshen. The number of surviving seedlings in each small area was recorded during harvesting (see Table 4.16 for results).

Table 4.16 shows that the survival rate of Danshen varies greatly with different planting densities. The survival rate is up to 88 % with the 20 cm × 25 cm density and down to 47 % with the 20 cm × 20 cm density. This indicates that the planting density of Danshen has a great influence on the survival rate and thus on the yield of Danshen.

4.5.2 Influence of Different Densities on Tanshinol and Tanshinone IIA Contents

As shown in Figs. 4.10 and 4.11, different planting densities influence the contents of tanshinol and tanshinone IIA by influencing the distribution of root systems in soil, the number of root branches, and the diameters of roots and by further influencing the surface areas of roots.

Figures 4.10 and 4.11 show that the highest tanshinol contents were achieved with densities of 20 cm × 25 cm and 30 cm × 35 cm; the lowest tanshinol contents occurred with the density of 25 cm × 35 cm. The highest tanshinone IIA contents were achieved with densities of 20 cm × 25 cm and 25 cm × 30 cm; the lowest tanshinone IIA contents occurred with the density of 25 cm × 25 cm. Therefore, to achieve relatively high contents of both tanshinol and

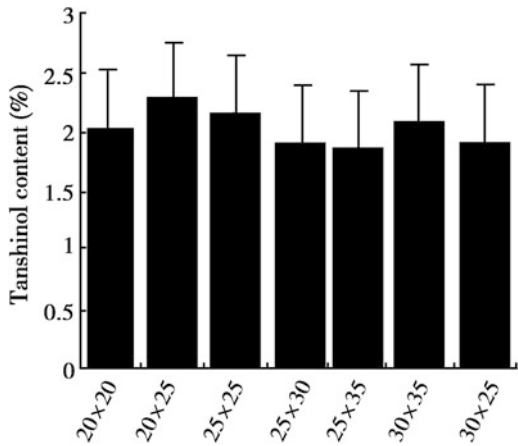


Fig. 4.10 Effect of planting densities on tanshinol contents in Danshen

Table 4.16 Number of surviving seedlings in field during harvesting

Density (cm)		20 × 20	20 × 25	25 × 25	25 × 30	25 × 35	30 × 35	30 × 25
Plants/plot	I	306	416	310	160	180	153	283
	II	274	420	298	150	185	178	263
	III	274	430	314	168	184	144	220
Average		282	422	307	160	183	158	240
Survival rate (%)		47	88	80	50	67	69	75

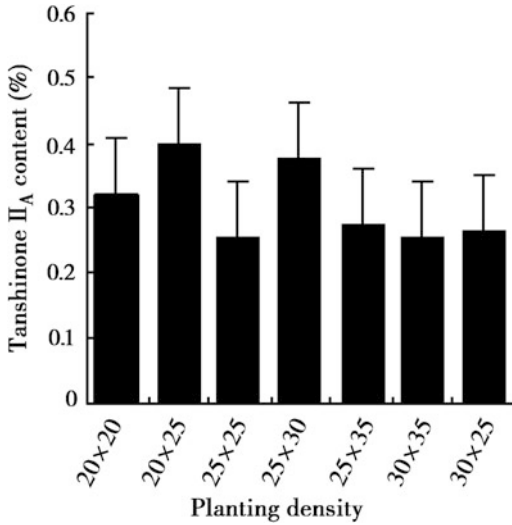


Fig. 4.11 Effect of planting densities on tanshinone IIA contents in Danshen

tanshinone IIA, the density should be 20 cm × 25 cm. Moreover, when the density of 20 cm × 25 cm was adopted, the survival rate also peaked. Therefore, the optimal density of Danshen cultivation is 20 cm × 25 cm.

4.5.3 A Comparison of the Yields of Danshen Under Different Densities (In Terms of Fresh Weight)

Figure 4.12 indicates that the root yield of Danshen grown in the 24 m² experimental area varies greatly with different densities, reaching the

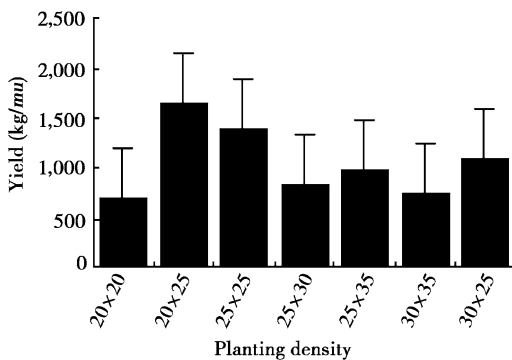


Fig. 4.12 Effect of planting density on Danshen's yield

maximum with 20 cm × 25 cm which is equivalent to 1631 kg/μ, the second highest yield was achieved at the density of 25 cm × 25 cm, which is equivalent to 1,376 kg/μ, and the rests are as follows: the third, 30 cm × 25 cm, 1,084 kg/μ; the fourth, 25 cm × 35 cm, 937 kg/μ; the fifth, 25 cm × 30 cm, 831 kg/μ; the sixth, 30 cm × 35 cm, 746 kg/μ; and the last, 20 cm × 20 cm, 681 kg/μ.

Figure 4.13 shows the variation of individual plant yield with different densities, wherein the individual plant yield reaches the maximum of 215 g/plant at 25 cm × 25 cm density, 187 g/plant at 25 cm × 30 cm density, 179 g/plant at 30 cm × 35 cm, 150 g/plant at 30 cm × 25 cm, 140 g/plant at 20 cm × 25 cm, 134 g/plant at 25 cm × 35 cm, and 80 g/plant at 20 cm × 20 cm.

With regard to the planting densities of 25 cm × 30 cm and 30 cm × 25 cm, even though they have the same density, their differences in plant spacing and row spacing still lead to a large difference in the per-μ yield. The per-μ yield of the latter is 23.3 % higher than that of the former. The individual plant yield of the latter is about 20 % higher than that of the former.

To sum up, the per-μ yield of Danshen is influenced not only by the individual plant yield, but also by the actual number of plants in the field. Under a fixed density in the field, increasing row spacing and decreasing plant spacing can lead to increased nutritive area and spacing area for plants in the field, which are good for the

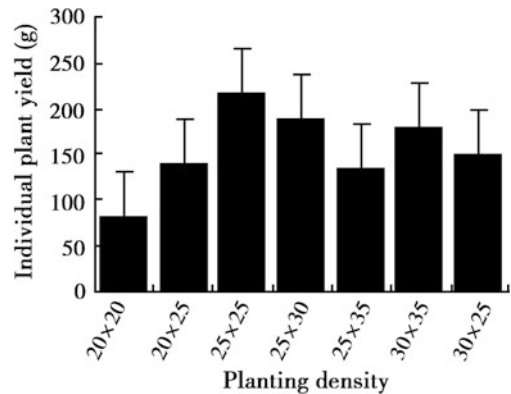


Fig. 4.13 Effect of planting density on individual plant yield of Danshen

elongation of horizontal branch root systems of plants. It is an effective measure to increase the root yield of Danshen.

4.5.4 Summary and Discussion

Based upon the data provided above, we conclude that the survival rate of Danshen differs greatly with different planting densities, reaching up to 88 % at the density of 20 cm × 25 cm and down to 47 % at the density of 20 cm × 20 cm. The highest contents of tanshinol and tanshinone are achieved at the density of the 20 cm × 25 cm. The optimal density for Danshen's cultivation is 20 cm × 25 cm. The highest per-μ yield of Danshen is achieved at the density of 20 cm × 25 cm. The highest individual plant yield is achieved at the planting density of 25 cm × 25 cm. The optimal planting density of Danshen should be set at 25 cm × 25 cm in order to increase the per-μ yield and effective contents of Danshen.

The leaves are the major assimilative organ of Danshen. By photosynthesis, leaves deliver the synthesized organic substances to the root through conducting tissues and finally lead to the yield of the medicinal part and effective constituents. During the seedling period (initial stages of transplanting), there is enough nutritive areas between plants and rows for the development of aboveground parts, especially the leaves. Therefore, the density does not have a large or significant effect. With the continuous growth of leaves, when the full field coverage period arrives, the spaces between plants and rows will gradually shrink and the row spacing will start to close, which will have an inhibitive effect on the growth of leaves. As the density increases, the plant row spacing will have poor ventilation and light admitting quality, which further strengthens the inhibitive effect. The key to reasonably dense planting is to fully expose Danshen to sunlight. First, there must be an adequate level of planting density, which is also dependent on the sunlight area of green leaves of the entire Danshen group

on the unit area. A reasonable planting density and allocation method should be determined to provide the optimal ecological environment for the balanced and coordinated growth of Danshen leaves and root systems and for the high-level accumulation of tanshinol and in tanshinone IIA leaves and thus to fully utilize light energy and land capacity and achieve the highest productivity.

Density effect has always been the focus issue for theoretical ecologists. The influences of different planting densities on plants are mainly due to the competition among plants for environmental resources such as sunlight, water, CO₂ concentration, and fertilization effect. Different planting densities will result in very different yields and the contents. The optimal field density in the Shangluo Region is 20 cm × 25 cm, which could lead to an economic yield up to 1,631 kg/μ and the peak level of effective constituent contents.

The goal of having a reasonable planting density of Danshen is to form a reasonable plant community structure. Therefore, it must be designed according to the characteristics of the growth and development of Danshen and in combination with cultivation measures to ensure the sound development of both individuals and groups and to effectively and economically utilize the natural resources, especially light energy and land capacity which are limited by both local natural conditions and social and economic conditions. Therefore, a reasonable planting density could not only make a full use of natural resources, but also protect resources. With reasonable dense planting, the control measures for cultivation conditions should also be strengthened, meaning to implement scientific management, ensure water supply, carry out reasonable fertilization, promote the normal development of Danshen plants, prevent bad growth or vain growth of Danshen plants, and ensure the high quality and high yield of Danshen. Danshen has very good adaptability, and different places have quite different conditions. So we must take actions that suit the local circumstances.

4.6 The Effects of Microelements on the Growth of Danshen and the Accumulation of Effective Constituents

The environments for the growth of Chinese medicinal plants have direct influences on their growth and contents of microelements. The genuineness of a medicinal material is closely related to its microelement contents. Microelements can influence the formulation and accumulation of chemical contents in a plant by acting as catalysts for certain organic synthetic reactions within the plant or participating in the structural functions of effective constituents of the plant and thus influence the pharmacological activity of the medicinal material [13]. In China, the calcareous soils in the north, salt marsh soils in the coastal region, and part of soils in the south, they all lack in microelements. In regions where microelements are severely lacking, microelements have become the major factors influencing the local agricultural production. Application of microelement fertilizers can influence not only the microelement contents in soil and the microelement supplies for crops, but also the contents and effectiveness of nutritive contents of nitrogen and phosphorus in soil.

Currently, large-scale cultivation of Danshen has already been realized. However, there are no published studies on the effects of microelement fertilization on Danshen's production. We have studied the effects of the application of microelements on the growth of Danshen and the accumulation of effective constituents, in an effort to provide a theoretical basis for the high-quality and high-yield cultivation of Danshen.

4.6.1 Relationship Between Microelements and Tanshinol

Since tanshinol content does not have a large range of variation, the weighted average sum method is adopted for drawing the Figures. Figure 4.14 shows the accumulated values of tanshinol contents influenced by different microelement

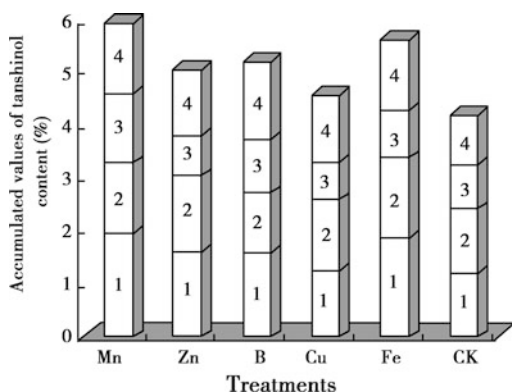


Fig. 4.14 Influences of different microelement treatments on the accumulation of tanshinol contents Note number 1, 2, 3, and 4 in the blocks stand for tanshinol contents at the 150th, 180th, 210th, and 250th days of Danshen's growth, respectively

treatments. Figure 4.15 shows the accumulated tanshinol contents at different stages of growth under the microelement treatments.

From Fig. 4.14, we can see that the accumulated tanshinol content of the group treated with manganese increased by 41 % with respect to the control; the group treated with ferrum increased by 35 %; the group treated with boron fertilizer increased by 25 %; the group treated with zinc fertilizer increased by 21 %. The accumulated value of tanshinol content of the group treated with copper fertilizer was a little higher than the control. This indicates that the application of any

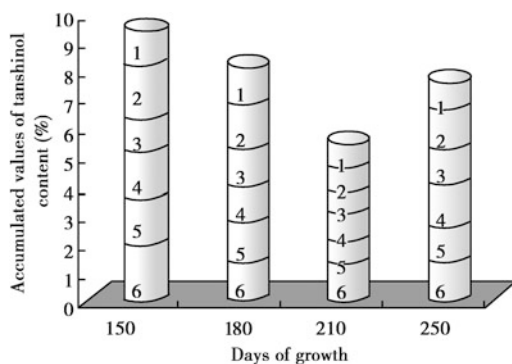


Fig. 4.15 Influences of microelement treatments on the accumulation of tanshinol contents Note number 1, 2, 3, 4, 5, and 6 in the blocks stand for tanshinol contents of the groups treated with manganese, zinc, boron, copper, ferrum, and the control group, respectively

microelement can increase the content of tanshinol, and the increase of the group treated with manganese fertilizer was most significant. As seen from Fig. 4.15, for the treatments in which microelements were applied, the accumulated value of tanshinol content reached its peak of 9.34 % on the 150th day, took a downturn afterward, and increased again to 7.57 by the time of harvesting. This indicates that the peak of accumulated value of tanshinol content does not change with the type of fertilizer applied, but occurs in a fixed stage of growth.

4.6.2 Relationship Between Microelements and Tanshinone IIA

Since the accumulated value of tanshinone IIA does not vary much, the weighted average sum method is adopted for drawing the figures. Figure 4.16 shows the accumulation of tanshinone IIA of treatments at different stages. Figure 4.17 shows the dynamic accumulation of tanshinone IIA of the stages in different treatments. From Fig. 4.17, we can see that the accumulated value of tanshinone IIA content reached its peak (2.77 %) on the 150th day and then gradually went down. Researches have shown that the root diameter is inversely related to the content of tanshinone IIA. In the peak

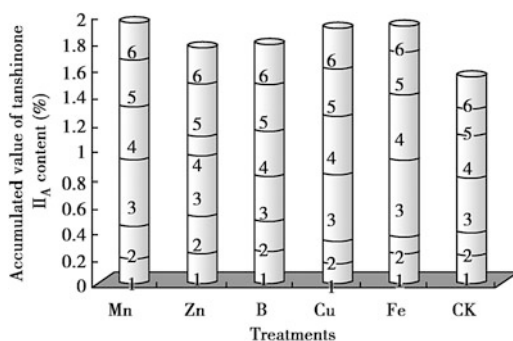


Fig. 4.16 Microelement treatment tanshinone IIA accumulation Note number 1, 2, 3, 4, 5, and 6 in the blocks stand for tanshinone IIA contents of the groups treated with manganese, zinc, boron, copper, ferrum, and the comparison group, respectively

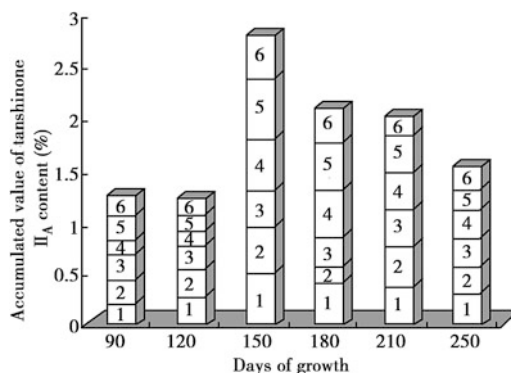


Fig. 4.17 Influences of different microelement treatments on the accumulation of tanshinone IIA Note numerals 1, 2, 3, 4, 5, and 6 in the blocks stand for tanshinone IIA contents of samples taken on the 90th, 120th, 150th, 180th, 210th, and 250th days, respectively

period of tanshinone IIA accumulation, the root system of Danshen has not expanded yet and the root surface area per unit weight is still large. So there is high tanshinone IIA content. After this period, the content of tanshinone IIA will gradually fall with the thickening of roots.

The growth of the aboveground parts of Danshen peaked in July, i.e., somewhere around the 120th day. The accumulation of tanshinol and tanshinone IIA peaked later than the growth peak, around 150th day. This is because both of these chemicals are the products of secondary metabolism. As seen from the biogenesis and biological synthetic pathways of secondary metabolites of plants, some of the key intermediate products of primary metabolism are the building blocks of secondary metabolism. Many experiments have proved that secondary metabolism is regulated by primary metabolism, and the peak of secondary metabolism comes later than that of primary metabolism. From the perspective of energy metabolism, primary metabolism is a process in which the plant obtains energy, and secondary metabolism is a process in which the plant releases energy. The energy-releasing metabolism occurs after the energy-obtaining metabolism.

From Fig. 4.16, we can see that the accumulated value of tanshinone IIA content of the group treated with manganese increased by 27 %

Table 4.17 Microelement contents within plants in different stages of different microelement treatments

Time	Boron content (mg/kg)		Copper content (mg/kg)		Zinc content (mg/kg)		Ferrum content (%)		Manganese content (mg/kg)	
	B	CK	Cu	CK	Zn	CK	Fe		Mn	CK
90th day	138.7	47.6	30.86	24.77	55.77	40.14	0.188	0.16	64.16	55.04
110th day	86	35.9	15.96	15.39	41.88	32.86	0.165	0.1	51.37	41.69
130th day	72.6	–	13.4	–	37.95	–	–	–	48.59	–
150th day	58.8	34.8	13.05	11.65	36.79	30.14	0.141	0.07	31.35	30.12
170th day	48.6	–	11.75	–	33.09	–	–	–	26.9	–

compared with the control group. The tanshinone IIA content of the group treated with ferrum increased by 25 %, with copper increased by 23 %, with boron increased by 16 %, and with zinc increased by 14 %. These results indicate that the application of any microelement fertilizer can increase the accumulation of tanshinone IIA, and the increase of the group treated with manganese fertilizer was most significant.

The amounts and ratios of nutrient elements absorbed by a plant are usually taken as one of the bases for balanced fertilization. Table 4.17 gives the measurement results of microelements absorbed by Danshen plants at different stages. From Table 4.17, we can see that all microelement contents within plants treated with different microelements increased to some extent with respect to the control. The increase of the group treated with boron fertilizer was most significant. The boron content within the plants was 2.9 times of the control on the 90th day, 2.4 times on the 110th day, and 1.3 times on the 150th day, which means the application of boron treatment is good for the boron absorption of plants.

Boron is an essential microelement for the growth of plants. It affects the transportation of sugar, the synthesis of nucleic acids and protein, photosynthesis, pollen germination, fecundation, and fructification of plants [14]. Boron deficiency significantly inhibits the growth and elongation of *Brassica Napobrassica* root tips [2]. After 1 week of boron shortage treatment, the growth of *Brassica Napobrassica*, especially of the root system, was severely inhibited [15]. The experiment conducted by Lou Yunsheng et al. [16] on *Brassica Napobrassica* indicates that boron can boost the growth of the root system and increase

the root volume, the growth rate of root system, and the root–shoot ratio and thus boost the root system and aboveground dry substances.

The quality of Chinese medicines is largely dependent on the variety and contents of chemical elements in the soil in which they grow. Every genuine medicinal material has several characteristic microelement profiles [17]. Zhou Changzheng [18] has proved that the pharmacological activity of *Asarum sieboldi* is somehow related to the microelement contents of genuine medicinal materials. Cultivation of different medicinal materials requires different microelements and different quantities. Of all microelements, boron is needed most by Danshen, and ferrum is need most by rhizoma coptidis [19].

Zinc is a microelement indispensable for the human body. Medicinal materials with high zinc contents are beneficial for the improvement of the human body's immune system. Research has shown that zinc is an important quality index for foods and feeds. Application of zinc can increase the zinc content in stems, leaves, and seeds, which is of great importance for the production of high-zinc food [20, 21]. Danshen roots have a zinc content of 28.7 µg/g tissue, which is relatively high in blood-tonifying medicinal materials such as Chinese angelica and Rehmannia.

4.6.3 Dynamic Growth and Development of Roots Treated with Microelements

From Table 4.18, we can see that root dry weight was significantly higher in groups treated with boron and manganese fertilizers than the control

Table 4.18 A comparison of biomass between different microelement treatments in pot planting

Treatment	Aboveground fresh weight (g/pot)	Aboveground dry weight (g/pot)	Root fresh weight (g/pot)	Root dry weight (g/pot)
CK	144.19	27.18	167.05	39.19
B	162.47	45.88*	228.33**	62.9**
Cu	108.99	22.59	168.22	42.32
Zn	138.19	25.56	148.4	48.19*
Fe	254.72**	52.56**	178.47	43.49

Note ** indicates a significance level of 1 %; * indicates a significance level of 5 %

group, with a significance level of 1 %. The difference in root dry weight between the group treated with zinc and the control reached a significance level of 5 %. The difference in aboveground dry and fresh weights between groups treated with manganese and ferrum fertilizers and the control group reached a significance level of 1 %. These results indicate that the application of manganese and ferrum fertilizers has a positive effect on the accumulation of aboveground biomass.

In Fig. 4.18, the chart on the left shows that Danshen's root dry weights are influenced by microelement treatments. Due to the lack of seedlings, only three samples were taken from the control group and the group treated with ferrum. Five samples were taken from the rest of the treatment groups. The results indicated that boron and manganese led to the fastest accumulation of yield, followed by zinc. The chart on

the right shows the accumulated root dry weight at different stages of microelement treatments under large-field conditions. The accumulated values of root weight in different stages of boron treatment were nearly twice of the control group. The groups treated with manganese and zinc also had some increases over the control group.

4.6.4 Summary

Combined together, the research results of both the pot-planting and large-field experiments indicate that the accumulated value of tanshinol of the group treated with manganese fertilizer increased by 41 % with respect to the comparison value. The accumulated value of tanshinol of the group treated with ferrum increased by 35 % with respect to the comparison value. The accumulated value of

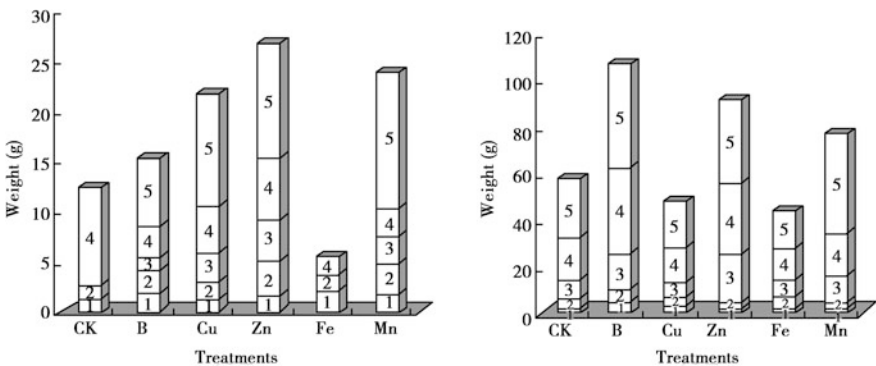


Fig. 4.18 Dynamic accumulation of root dry weight of Danshen under microelement treatments Note the left diagram is the dynamic accumulation of root dry weight in pot-planting experiment. Number 1, 2, 3, 4, and 5 in the blocks stand for the root dry weights of samples taken on the

90th, 110th, 130th, 150th, and 170th days, respectively; the right diagram is the dynamic accumulation of root dry weight in large-field experiment. Number 1, 2, 3, 4, and 5 in the blocks stand for the root dry weights of samples taken on the 90th, 120th, 150th, 180th, and 210th days, respectively

tanshinol of the group treated with boron increased by 25 % with respect to the comparison value. The accumulated value of tanshinol of the group treated with zinc increased by 21 % with respect to the comparison value. The accumulated value of tanshinol of the group treated with copper was a little higher than the comparison value. This means that the application of any microelement can boost tanshinol accumulation, with the application of manganese having the most significant effect. The accumulated value of tanshinol content under the microelement treatments reached a peak of 9.34 % on the 150th day, took a downturn afterward, and increased again to 7.57 % by the time of harvesting. The accumulated value of tanshinone IIA content gradually increased between the 90th day and 150th day, reached its peak (2.77 %) on the 150th day, and then gradually went down. The accumulated value of tanshinone IIA content of the group treated with manganese increased by 27 % with respect to the comparison value. The accumulated value of tanshinone IIA content of the group treated with ferrum fertilizer increased by 25 % with respect to the comparison value. The accumulated value of tanshinone IIA content of the group treated with copper fertilizer increased by 23 % with respect to the comparison value. The difference in root dry weight between groups treated with boron fertilizer and manganese fertilizer and the comparison group reached an extremely significant level of 1 %. The difference in root dry weight between the group treated with zinc fertilizer and the comparison group reached an extremely significant level of 5 %. This reflects the positive effects of the application of boron, manganese, and zinc fertilizers on the Danshen yield.

References

1. Don Z. *Chin Tradit Herbal Drugs*. 1990;21(3):32.
2. Cai Z. *J China Pharm Univ*. 1991;22(2):65–8.
3. Jiangsu College of New Chinese Medicine. *Traditional Chinese medicine dictionary*, vol. I. Shanghai: Shanghai People's Publishing House; 1997. p. 478–82.
4. Kong L, Sun H. *Modern practical chinese medicine cultivation technology*. Beijing: People's Medical Publishing House; 2000. p. 147–9.
5. Ying C. *A Handbook of Practical Chinese Medicinal Seed Technology*. Beijing: People's Medical Publishing House; 1999. p. 31–6.
6. GB/6941-86. *A compilation of agricultural standards of China*. Beijing: Standards Press of China; 1997. p. 6973–6975.
7. Huang Z, Hu Z, Zhang X. *J Plant Ecol*. 2001;25(1):22–8.
8. Liao X, Sun Q, Gao J, et al. *Plant Physiol Commun*. 1995;189–91.
9. Xu L, et al. *Non-pollution cultivation and processing of Chinese medicine and transgenic engineering*. Beijing: China Press of Traditional Chinese Medicine; 2000. p. 174.
10. Han J, Liang Z, Sun Q, et al. *Northwest Agric J*. 2002;11(4):67–71.
11. Chen Z, et al. *China J Chin Mater Med*. 1992;17(3):141.
12. Zhang Z. *J Chin Med Mater*. 1995;18(3):113–5.
13. Xu R. *Danshen biology and its application*. Beijing: Science Press; 1990.
14. Jiangsu College of New Chinese Medicine. *Traditional Chinese medicine dictionary*, vol. I. Shanghai: Shanghai People's Publishing House; 1997. p. 478–82.
15. Gao S. *China J Chin Mater Med*. 1995;20(6):333.
16. Song J. *J Asian Nat Prod Res*. 1999;11(4):86–9.
17. Qian M, et al. *J Chem*. 1978;36(3):199.
18. Pharmaceutical Research Institute of Chinese Academy of Medical Sciences, et al. *Chinese medicine record*, vol. I. Beijing: People's Medical Publishing House; 1979. p. 339.
19. Luo H, et al. *Pharm J*. 1985;20(7):542.
20. Kong D, et al. *Pharm J*. 1984;19(10):755.
21. Kong D, et al. *Pharm J*. 1985;20(10):747.

Deyou Qiu and Jingyuan Song

Cultivated Danshen tends to have low contents of effective constituents and uneven quality, and long-term asexual propagation can easily lead to degeneration. Due to soil pollution by pesticides, heavy metals, and other pollutants in some areas, Danshen produced there could contain higher amounts of these pollutants than standard. These situations add to the difficulty in quality control and clinical use of Danshen. On the other hand, the resources of wild Danshen are limited, and digging wild Danshen will damage the wild resources and bring adverse effects on the ecological balance. Therefore, it is necessary to adopt In vitro culture of Danshen. In vitro culture of Danshen usually involves micropropagation, Cell culture, and tissue and organ culture. Micropropagation is the technique for rapidly propagating Danshen plants through the cloning technology to produce superior seedlings for large-area artificial planting; cell culture is to use solid or liquid media to culture Danshen cells, and then extract active constituents from the cells or media thereby acquired; tissue and organ culture is to use liquid medium to culture Danshen tissues or organs, and then extract the active constituents from the tissues or organs thereby acquired. These techniques are used for industrial production of the effective constituents of Danshen. Since In vitro culture of Danshen is not

affected by climate and environmental factors, it offers a high production efficiency and propagation speed, which can fundamentally solve the current problems in Danshen cultivation such as quality degradation and high levels of pesticides and heavy metals. It is one of the effective measures for Danshen's quality control. For a period of time in the past, some institutions and researchers performed much work with regard to the micropropagation, cell culture, and tissue and organ culture of Danshen and made considerable achievements. These studies are reviewed below.

5.1 Micropropagation of Danshen

The micropropagation of Danshen generally refers to in vitro culture and clonal multiplication of Danshen seedlings in test tubes. This method can be used for mass and rapid propagation of Danshen seedlings, which is certainly of significance for the cultivation and production of Danshen.

Yang [1] studied the organ differentiation and plant regeneration of Danshen. Wang et al. [2] reported a preliminary study on the micropropagation of Danshen. They chose leaves and petioles as explants. In operation, the explants were first cut into small pieces and transplanted onto the following media, respectively: (1) MS medium supplemented with 1.0 mg/L 2, 4-D; (2) MS medium supplemented with 1.0 mg/L 2, 4-D and 2.0 mg/L 6-BA; and (3) MS medium

D. Qiu (✉) · J. Song
Chinese Academy of Forestry, Beijing, China
e-mail: qiudy@caf.ac.cn

supplemented with 0.2 mg/L 2, 4-D and 1.0 mg/L 6-BA. After 7 days, the leaves began to expand, and after 10 days, calli formed where the cuts were made. The calli were then transferred onto MS medium supplemented with 2.0 mg/L 6-BA. Half a month later, these calli generated green buds, which could be turned into clustered seedlings through subculture. Adventitious roots could be induced by cutting down the clustered seedlings and transplanting them to 1/2 MS medium without hormones, and an entire plant could be developed. The regenerated plants could survive when transplanted into soil.

In 1991, Shimomura et al. [3] reported results of Danshen tissue culture. They established a rapid propagation system for Danshen. When *in vitro* seedlings were transplanted to fields, they found that the roots of 6-month-old Danshen produced more tanshinones than commercial Danshen roots (usually coming from plants that were 3–4 years old).

Cai et al. [4] reported detailed results of Danshen tissue culture in 1991. They conducted experiments concerning the effects of different explants, basic media, and different phytohormone combinations on the induction of clustered buds and the rooting of seedlings. It turned out that to induce clustered buds, the optimal effect was achieved by using leaves as the explants on MS medium supplemented with 0.5–1.0 mg/L 6-BA. The optimal condition for inducing roots from the aseptic buds was 1/2 MS medium with pH 5.8 and 3 % sucrose supplemented with 0.2 mg/L IBA, 25 ± 1 °C, and 12 h/day of lighting. Therefore, the mass cloning and rapid multiplication of Danshen seedlings is feasible. The detailed method for the mass cloning and multiplication of Danshen seedlings is as follows: First, select Danshen seeds and put them into 75 % ethanol for 1 min, and then, transfer them into 2 % sodium hypochlorite for 15 min for sterilization. After washing them five times with sterile water, put them onto 1/2 MS medium for germination. Aseptic seedlings can be obtained in a month. Put the aseptic seedlings onto MS medium supplemented with 1 mg/L 6-BA and 0.5 mg/L IAA for subculture. Then,

select nodes and internodes 0.5 cm in length of Danshen seedlings and small pieces of leaves with the size of 0.5 cm × 0.5 cm, and transplant them onto MS, B5, N6, and SH basic media with pH 5.8 and 3 % sucrose supplemented with 1 mg/L 6-BA and 0.5 mg/L IAA. They cut the leaves of seedlings into small pieces of 0.5 cm × 0.5 cm and transplanted them onto MS media supplemented with different phytohormone combinations to carry out the induction experiment of clustered buds. They also transferred rootless seedlings to 1/2 MS medium supplemented with different phytohormones to induce their roots. The experimental culture conditions were as follows: 12 h of lighting per day, light intensity of 1,200 Lux, and culture temperature of 25 ± 1 °C.

It turned out that several days after the Danshen nodes and internodes were transplanted onto the media, 1–2 axillary buds grew on each node, and both the nodes and internodes expanded. After 10 days, callus was induced on both ends and buds or clustered buds were redifferentiated on callus; 10 days after, the small leaf pieces were transplanted to the media; they began to crimple and thicken, and callus was induced on the incision edges of leaves. Then, buds or clustered buds were induced on callus. They also found that on some of the media, cluster buds could be directly induced on the leaf edges. It was also revealed by the results that the most suitable basic medium varied with different explants. When nodes or internodes were taken as the explants, although they could develop buds, the percentage rate of clustered buds further generated was not high. Of all the media in the experiment, the B5 medium led to the highest rates and good results of axillary bud germination and clustered buds. If leaves were used as explants, the MS basic medium offered the greatest speed and best effect of the induction of clustered buds. In this case, clustered buds could be directly induced on the leaf edges without having to go through the callus stage. This result shows that when leaves are used as explants, MS medium can serve the purpose of rapid propagation.

In order to find the most suitable phytohormone combination for the induction of clustered buds on MS medium, they further conducted a ratio experiment with eight cytokinin and auxin combinations. It turned out that 6-BA had a significant bud induction effect, and with the increase of 6-BA concentration, the percentage rate of induction increased. The highest percentage rate of the induction of clustered buds, which could reach up to 100 %, was achieved on the MS medium which contained only 1 mg/L 6-BA and no auxin, and the induction of buds on such medium needed only 16 days. However, when 0.2 mg/L NAA was used, the induction rate of clustered buds exhibited a falling trend, and germination was delayed by 4 days. This result indicates that NAA has some adverse effect on the occurrence of buds. They found that NAA has a significant effect on callus induction. When the NAA concentration increases to 1 mg/L, it strongly inhibits the occurrence of clustered buds and generates a great deal of calli. 1 mg/L IAA also has some effects on callus induction, but to a lesser extent than NAA. Adding 0.5–1 mg/L 6-BA or IAA below 0.5 mg/L to MS medium is favorable both for the induction and occurrence of clustered buds. The induction rate in this case can reach above 95 %. When seedlings are transferred to rooting medium, the rooting rate of adventitious buds will fall with the increase in IBA, IAA, or NAA concentration. The optimal result is achieved with a relatively low concentration of 0.2 mg/L, but only the low-concentration IBA has a promoting effect on rooting. The rooting rate of 0.2 mg/L IBA was 93.1 %, and all of the other phytohormones exhibited an inhibitive effect on rooting. Without the addition of any auxin, the seedlings of Danshen can still achieve a rooting rate of around 70 %.

Cai Zhaohui et al. also conducted multiple transplantation experiments on the plantlets formed from the roots of seedlings. The results indicate that the following steps can lead to the best transplantation result: wait until the roots on the seedlings grow up to 1–2 cm, and then, open the bottles and let the seedlings to adapt to the environment for 3–5 days. Then, carefully take out the plantlets with forceps and wash the agar

off the roots with warm water. Bury them in sterilized sand soil culture pans for 20 days, keeping them moisturized by spraying water throughout the process. After rooting, transplant them together with the nutritive soil to the field. The survival rate of transplantation with this method can reach about 90 %.

Liang et al. [5] studied the effects of growth-regulating substances on the dedifferentiation of leaves and the differentiation of roots and buds of Danshen. It turned out that the dedifferentiation rate of leaves induced by 0.5–5.0 mg/L NAA, 0.5–1.5 mg/L IBA, or 0.2–1.0 mg/L 4PU-230 could reach up to 97–100 %; the differentiation rate of buds induced by 0.1–0.5 mg/L NAA or 0.5–2.0 mg/L IBA was 93–100 %; of the 3 types of cytokinins in the experiment, 4PU-230 had the best effect on the bud differentiation and 6-BA and KT took the second place with regard to the effectiveness; with the increase in concentrations of 4-D, NAA and IAA, the root differentiation rate of callus or regenerated seedlings increased as well. Zhao et al. [6] from the same research team further studied the effects of light qualities and temperatures on the activation rate of leaves and the formation rates of calli and buds of Danshen and found that they had different effects; the induction of buds by green light had the highest frequency, which could reach up to 96 %, and the induction frequency of buds under 30 °C was relatively high and could reach up to 99 %. The experiment indicated that it usually takes only 30–40 days from the inoculation of Danshen leaves to the regeneration of plants. Each 0.5-cm² leaf can generate 20–30 adventitious buds, and the survival rate of seedlings after transplantation is 90–95 %.

Duan et al. [7] found that the induction of clustered buds from *Salvia bowleyana* budlets had the highest frequency of up to 100 % on MS medium supplemented with 2.0 mg/L 6-BA and 0.2 mg/L IAA. Each piece of leaf and petiole could grow up to 20–30 clustered buds, and the survival rate of transplantation was 90 %. On MS medium supplemented with 2.0 mg/L 6-BA, 0.2 mg/L IAA, and 0.2 mg/L 2,4-D, the leaf edges and petioles could develop green buds or light brown calli which, after multiple rounds

of subculture, still had the ability of plant differentiation.

Tian et al. [8] systematically studied tissue culture and plant regeneration of Danshen by using the stems, leaves, buds, and anthers of Danshen as explants. It turned out that stems and leaves easily form calli on MS medium supplemented with different BA and 2, 4-D combinations, and the calli were fast growing. MS medium supplemented with 1.0–2.0 mg/LBA and 0.1 g/L NAA was best for the multiplication of buds, and MS medium supplemented with 1.0 mg/L BA and 0.1 mg/L NAA could be used to induce leaves and anthers to produce adventitious buds.

Liu and Wang [9] studied the rapid propagation techniques of Danshen by using the young leaves of large-leaf Danshen grown in Zhongjiang. Their results showed that the 1/2 MS medium supplemented with 3 % sugar, 0.7 % agar, and 3 mg/L 6-BA had the best effect on primary culture. A bud–seedling differentiation rate of 63.13 % could be achieved after 60 days of culture on this medium, and the 2/3 MS + 3 % sugar + 0.7 % agar + 0.4 mg/L 6-BA medium had the best effect on continuous culture. Plant tissue could multiply 5.4 times every 4 weeks on this medium. The rootless seedlings could generate roots outside the culture chambers through soaking the basal parts of the seedlings in a liquid containing 50 mg/L IBA and 50 mg/L NAA for 5 min, and placing them in a shady and moist plastic shed with loose and fertile soil as the base material. A rooting rate of 86 % could be achieved in 6 weeks.

5.2 Cell Culture of Danshen

Danshen's cell culture is mainly used for the production of active constituents. Many research teams have successfully induced callus of Danshen. Li Ying et al. and Huang Xiulan et al. were the earliest to carry out studies on the cell culture and the generation of active constituents of Danshen. In 1981, they confirmed that the callus of Danshen contained the active constituent of

protocatechualdehyde and that the callus of *S. miltiorrhiza* var. *alba* could generate many diterpenoid guinone compounds [10, 11].

Afterward, Japanese scientists conducted further studies on the cell culture of Danshen. In 1983, Tsutomu et al. [12] established 6 Danshen cell lines on a MS medium containing 1 mg/L 2, 4-D, and 0.1 mg/L KT. They cultured the cells in liquid suspension and then transferred them into MS liquid medium with 1 mg/L KT, without 2, 4-D. Only Cell Line A generated two terpenoids, cryptotanshinone and ferruginol, while Cell Lines B–F and other cell lines only generated a certain amount of ferruginol.

In 1985, Hitoshi et al. [13] further studied the production of ferruginol by using Cell Line B. They found that the production of ferruginol using Cell Line B is subject to the influence of 2, 4-D and lighting. In a medium without 2, 4-D, ferruginol is generated only in the lag phase and stationary phase of growth, and it is inversely related to the division of active cells. 2, 4-D can promote the growth of cells but significantly inhibits the generation of ferruginol. Unlike 2, 4-D, IAA does not promote the growth of cells but boosts the production of ferruginol. Lighting has little influence on cell growth but inhibits the production of ferruginol. After 33 months of successive subculture, a naturalized cell line that could grow normally without any auxin was obtained from Cell Line B. The growth of that cell line requires only kinetin and does not need 2, 4-D. However, ferruginol did not keep increasing throughout the culturing process as expected, but continuously increased only in the lag phase of cell growth and fell to a low level afterward. However, when 3 % sugar was added to the medium on the 12th day (i.e., before cell growth reached the stationary phase), the content of ferruginol rapidly increased again, and climbed up to about 8.7 times of the ferruginol content in the control. This result suggests that for naturalized cell lines, sugar mainly affects the biosynthesis of ferruginol. Ferruginol is synthesized only in the lag phase of naturalized suspension culture cells. When sugar is added to the naturalized culture, the generation of ferruginol will be resumed in the stationary phase [14].

In addition, they also established a two-step culture method. From Cell Line A by using the cell aggregate selection method, they first obtained a Cell Line A5 for the production of cryptotanshinone and ferruginol, and cultured the naturalized cells of Cell Line A5 on MS medium containing 0.1 mg/L 2, 4-D plus 0.1 mg/L KT. Then, they transferred them into an MS medium in which Fe-EDTA or Fe had been depleted and 1 mg/L KT added, without 2, 4-D. Thereby, the cell growth was almost completely inhibited, while ferruginol could be continuously generated throughout the entire culturing process.

Hitoshi et al. [15] also studied the immobilized culture of Danshen cells. They found that when immobilized A5 cells were cultured in production medium, cryptotanshinone and ferruginol could be generated continuously for 25 days. By the 25th day, the majority (about 74 %) of cryptotanshinone was secreted into the medium, while the majority of ferruginol (about 47 %) still remained in cells and 38 % was secreted into the medium. Cryptotanshinone and ferruginol generated by immobilized cells were 39 and 61 % of those generated by suspension-cultured cells, respectively. The research on the immobilized cells also showed that with an increase in the length of time the immobilized cells were used, their capability of secondary metabolite synthesis gradually fell. However, this was not caused by the death of immobilized cells, but likely by the negative feedback effect generated by the accumulation of lipophilic secondary metabolites. When they transferred the immobilized cells into growth medium, the cells would exhibit active cell division again, which meant that they still had high vitality.

In 1987, Hitoshi et al. [16] carried out a detailed study on the influences of different nutrient components in MS medium on the synthesis of cryptotanshinone and ferruginol in suspension cells of Danshen. It turned out that sugar, nitrogen sources, and thiamine (VB₁) were necessary for the production of such compounds, while phosphates, MnSO₄, and kinetin only exhibited slight and beneficial influences. They believed that all other components of the MS medium were nonessential and even inhibitive.

Thereby, they designed a simplified medium for the production of cryptotanshinone and discussed the possible mechanism for the biosynthesis of cryptotanshinone in suspended cells of Danshen.

Yu et al. [17] studied the effects of plant phenylalanine ammonialyase (PAL) on the cell differentiation of Danshen. They found that 2 PAL activity peaks occurred in the differentiation process of Danshen callus. The first peak existed in both differentiation and non-differentiation media and the seemed unrelated to tissue differentiation. The second peak only existed in the differentiation medium. PAL has the highest level of activity in tissues that are about to differentiate or have just differentiated. It can be used as an enzyme indicator for the start of tissue differentiation.

Tao et al. [18] studied the immobilization of callus tissue cells and the characteristics of their converted products. They first embedded callus tissue cells with alginate and then shook the culture at room temperature for a month in LS liquid medium supplemented with 0.1 mg/L KT and 1 mg/L NAA. Analysis of the medium with TLC and HPLC showed that the system could continuously secrete Tanshinone IIA and cryptotanshinone, the two major constituents of Danshen. In addition, they also carried out comparison studies on the suspension culture of Danshen callus, the alginate embedding conditions, the stability of immobilized cells, and the characteristics of secreted products. Their results showed that immobilized cells were obviously superior to suspension culture with regard to stability, product content, and feasibility of downstream processing.

Hu et al. [19] successfully induced callus from the roots, stems, leaves, and petioles of Danshen. All calli contained cryptotanshinone, tanshinone IA, and tanshinone IIA. Callus induced from roots had the highest percentage content of these compounds, which was 4.1 times of that of the original plants.

In 1994, Zhu Weihua et al. [20] used the aboveground parts of 1-year-old Danshen cultivated in Beijing as the experiment materials, cut them into small segments of about 1 cm, and transplanted them onto 67-V medium containing

1 mg/L IAA, 1 mg/L 2, 4-D, and 0.1 mg/L KT or 1 mg/L IAA, 1 mg/L NAA, and 0.1 mg/L T. After dark culture, mutagenesis, naturalization, and selection, they obtained red variants and from which they found a new clone of red callus containing tanshinone. They found that the total tanshinone content varied significantly with different cultures. The highest content could reach up to 5.07 %, which was 3.6 times of that of the original Danshen medicinal material.

Recently, Wang et al. [21] studied the influences of phytohormone on the synthesis of secondary metabolites. They found that on MS medium, 2, 4-D could inhibit the formation of total hydrosoluble phenolic constituents, while KT could increase the total content of tanshinone [21].

Huang et al. [22] also investigated the influences of phytohormone on the synthesis of secondary metabolites. They found that 2, 4-D in MS medium could promote cell growth but inhibit the formation of lithospermic acid B, but 2, 4-D did not have any significant effect on rosmarinic acid. GA₃ could inhibit cell growth but promote the formation of the two compounds mentioned above. The effect of BA was intermediate between 2, 4-D and GA₃, and there was a synergistic effect between BA and GA₃.

5.3 Tissue and Organ Culture of Danshen

Using suspension cells to produce second metabolites of plants often comes with problems such as low contents and poor stability. In order to overcome such problems, untransformed organs (such as adventitious roots) and cultures of transformed tissues and organs are used for culture. This method is also used for the production of active constituents of Danshen. Using untransformed organs (such as adventitious roots) and the culture of transformed tissues to produce active constituents of Danshen has been a hot topic in biotechnology of Danshen in recent years. We will briefly review the progress in this area below.

5.3.1 Culture of Danshen Adventitious Roots

In 1991, Shimomura et al. [3] reported the production of tanshinone in the adventitious root culture of Danshen. They used Gamborg B5 agar medium with different hormone combinations to establish a culture system for Danshen adventitious roots and established the culture conditions for a high yield of tanshinone. They found that under different culture conditions, Danshen adventitious roots could generate four major tanshinones. In Gamborg B5 medium supplemented with IAA or NAA with or without BA, the adventitious roots grew very quickly. When IBA was added to the medium, the tanshinone yield peaked. In Gamborg B5 liquid medium supplemented with 0.5 mg/L IBA, the culture of adventitious roots grew slowly, with an increase of only 20 times in 8 weeks; however, the tanshinone content was high, equivalent to 80 mg/g in terms of dry weight, which was 6 times of the tanshinone content in original plant roots. The major constituents in tanshinone are cryptotanshinone and tanshinone IIA.

By establishing an RP-HPLC fingerprinting analysis method for Danshen adventitious roots, Wang et al. [23] analyzed the influences of inorganic ions on the production of secondary metabolites in Danshen adventitious roots, the detailed method being high-performance liquid chromatography, RP-Waters C18 (150 mm × 3.9 mm, 5 μm), gradient elution with mobile phase 0.5 % ethylic methanol and 0.5 % ethylic acid water, flow rate 1.0 ml/min, detection wavelength 270 nm, and column temperature 30 °C. Fingerprinting of Danshen adventitious roots was also analyzed, and it turned out that 11 common peaks with stable relative positions were detected from nine samples in three groups of adventitious roots under this chromatographic condition. Nine of them were confirmed as indicator peaks for changes in constituents, and five known constituents were confirmed. The results show that inorganic metal ions can significantly increase the contents of salvianolic acids in adventitious roots, but they do not have

any significant effect on the liposoluble constituents such as tanshinone. This method is stable, reliable, and repeatable. It can be used as a basis for the evaluation of changes in the secondary metabolic constituents of Danshen adventitious roots and provide a foundation for the culture and further research of Danshen adventitious roots.

Guo et al. [24] carried out studies on the influences of different media, salt concentrations, and organic substances on the growth of Danshen adventitious roots and the synthesis of Tanshinone IIA and protocatechualdehyde. They used Tissue culture techniques in combination with HPLC approaches to investigate the influences of different media, salt concentrations, and organic substances on the growth of Danshen adventitious roots and the contents of Tanshinone IIA and protocatechualdehyde. By investigating the influences of MS, LS, B5, White, and SH media on the culture of Danshen adventitious roots and considering the growth velocity and effective constituents, they confirmed that MS was a good basic medium. By changing the salt concentration of the medium, they found that high salt concentration was favorable for the growth of adventitious roots, while low salt concentration promoted the synthesis of Tanshinone IIA and protocatechualdehyde. The interactions between the five organic substances in MS medium did not have a significant effect on the growth of Danshen adventitious roots: Glycine was favorable for the synthesis of tanshinone IIA. When missing any one of the four chemicals, i.e., inositol, glycine, VB₁, and VB₆, the synthesis of protocatechualdehyde would be hindered. This experiment confirmed that MS was a good basic medium for the suspension culture of Danshen adventitious roots, and pointed out that the salt concentration and treatment of organic substances in the medium both had significant influences on the growth of Danshen adventitious roots and the synthesis of secondary metabolites.

Guo et al. [24] studied the influences of carbon sources, nitrogen sources, and phosphor sources on the growth and effective constituents (Tanshinone IIA and protocatechualdehyde) of Danshen adventitious roots. They used Tissue culture techniques in combination with HPLC analytic approaches to study the influences of

different types and concentrations of carbon sources and different concentrations of nitrogen and phosphor sources on the growth and contents of Tanshinone IIA and protocatechualdehyde of Danshen adventitious roots. They found that carbon sources, nitrogen sources, and phosphor sources were essential for the culture of adventitious roots. The highest propagation result of adventitious roots was achieved by using sucrose as the carbon source: When adding 30 g/L sucrose and culturing for 20 days, the adventitious roots multiplied the most. Sucrose at 60 g/L was most suitable for the synthesis of tanshinone IIA. Low-concentration sucrose was more favorable for the synthesis of protocatechualdehyde. By intermittently adding sucrose for 25 days after culture, they achieved a multiplication rate of adventitious roots which was 2.3 times greater than the control and a Tanshinone IIA content which was 2.4 times greater than the control. When the concentration of NH₄⁺ and NO₃⁻ in the medium remained at 60 mmol/L and the NH₄⁺-NO₃⁻ ratio was 1:4, 1:4, and 1:1, the highest propagation multiple of adventitious roots and the greatest contents of tanshinone IA and protocatechualdehyde could be achieved, respectively. When the KH₂PO₄ concentration in the medium was changed, the growth of Danshen adventitious roots was more vigorous than that of the control, but highly concentrated KH₂PO₄ inhibited the biosynthesis of tanshinone IIA. This experiment determined the best types and concentrations of carbon sources, best ratios of nitrogen sources, and best concentrations of phosphor sources for the suspension culture of Danshen adventitious roots, and indicated that different carbon sources, nitrogen sources, and phosphor sources had significant effects on the growth of Danshen adventitious roots and the biosynthesis of secondary metabolites.

5.3.2 Culture of Hairy Roots and Crown Gall Tissues of Danshen

In as early as 1930s, it was found that plants could develop crown gall nodules and hairy roots

when infected by *Agrobacterium tumefaciens* and *A. rhizogenes*, respectively. These phenomena were considered pathological. In order to find out the causes, scientists have conducted research on their mechanisms.

Scientists have found that the occurrence of crown gall tissues on plants after they are infected by *A. tumefaciens* is due to a special segment of transferred DNA, namely T-DNA on the tumor-inducing plasmid of *A. tumefaciens*. T-DNA contains two genes *iaaM* (*tms1*) and *iaaH* (*tms2*) which encode for enzymes involved in auxin synthesis, and a gene *ipt* (*tmr*) encoding for an enzyme for cytokinin synthesis. When *A. tumefaciens* infects plants, it can transfer its T-DNA into the genomes of plant cells. In a plant cell, *iaaM* and *iaaH* genes, respectively, express tryptophan oxygenase and indolylacetic acid (IAA) amidohydrolase, which participate in the biosynthesis of IAA, and the *ipt* gene can express isopentene transferase which participates in the biosynthesis of isopentenyladenine (iPA), a cytokinin. This synthesis of auxin and cytokinin guided by T-DNA causes the transformed plant tissues to form crown gall. On the other hand, the formation of hairy roots is related to the root-inducing plasmid of *A. rhizogenes*. The root-inducing plasmid also contains a segment of transferred DNA, and in some cases, a non-transferred DNA segment of about 15 kb is inserted in the middle to divide the T-DNA into TR-DNA and TL-DNA. The T-DNA of root-inducing plasmid also contains segments that share the same resources as *tms1* and *tms2* genes on the T-DNA of *A. tumefaciens*. In addition, its T-DNA has four loci *rolA*, B, C, and D that are related to the morphogenesis of roots. These loci and the isogenous segments of *tms* genes (*tms1* and *tms2*), when expressed in plant cells, can lead to the occurrence of hairy roots. Conventional cell culture often needs the addition of a certain amount of phytohormone and has shortcomings such as low growth and unstable products. By contrast, transgenic tissue and organ culture can provide fast growth without the addition of foreign phytohormones and offer stable genetic and biosynthetic abilities which can steadily produce effective constituents. In

addition, hairy roots originate from individual cells, which is very suitable for large-scale strain screening.

The reason that T-DNA of plasmids contained by *Agrobacteria* can be transferred into the genomic DNA of plants is closely related to the expression of chromosomal virulence and the virulence region (Vir) of plasmids. Vir region is composed of 7 combined genes from *virA*–G. The entire process through which *Agrobacterium* infects a plant cell is comprised of the attachment of *Agrobacterium* to plant cell wall, the cutting, transferring, and integrating of T-DNA, and other steps, whose molecular mechanisms are already known.

The culture of transgenic tissues and organs mainly refers to the culture of hairy roots and crown gall tissues. However, it was not until the late 1980s that people actually began to apply hairy roots and crown gall as an approach to in vitro culture of plant tissues and organs for the production of secondary metabolites. In the 1990s, culture systems of hairy roots and crown gall were widely applied. The culture system of hairy roots, in particular, have already involved more than 160 plants and produced secondary metabolites and effective constituents including indoles, quinolines, tropanes and other alkaloids, panaxsaponin, galactinol and the glycosides, flavonoids, chinones, trichosanthin, etc. Many of the research subjects are medicinal plants. Up until now, small-scale culture of hairy roots has been successful with *Nicotiana rustica*, *Datura stramonium*, *Atropa belladonna*, *Catharanthus roseus*, *Lithospermum erythrorhizon*, *Anisodus tanguticus*, *Ammannia rusticana*, and *Tagetes patula*. Large-scale hairy root culture has been conducted on *Panax ginseng* and *Coptis chinensis*. It is fair to say that the application of hairy root culture technology to the mass production of useful medicines has a very encouraging future. Hairy roots and crown gall have certainly provided an ideal system for research on the approaches to the biosynthesis of secondary metabolites. After being modified and supplemented with genes and expression-regulating units of foreign proteins, the plasmids of *Agrobacteria* can transform plants through a bivector

system and thus obtain transgenic tissues, organs, and even plants that express the foreign proteins. Therefore, since the late 1990s, the transgenic tissue and organ culture system has also been applied to the production of medical antibodies, vaccines, and other important immunoreactive substances, and has demonstrated the tremendous potential of plant expression systems in the production of immunoreactive substances.

5.3.2.1 Culture of Danshen Hairy Roots

Efforts have been made to use Danshen hairy roots to produce the effective constituents. In 1993, Hu and Allrermann [27] used different strains of *A. rhizogenes*, LBA 9402, ATCC 15834, TRI05, R1601, and A41027, to infect aseptic Danshen seedlings, and established an in vitro culture system for Danshen hairy roots. They found that acetosyringone had a boosting effect on the genesis of Danshen hairy roots induced by *Agrobacterium* and carried out a detailed study on the liposoluble active constituents. Using HPLC, they found that not only the hairy roots but also the liquid medium contained tanshinone I, tanshinone IIA, tanshinone IIB, tanshinone V, dihydrotanshinone I, cryptotanshinone, and tanshinone VI, and colorless diterpene ferruginol. They studied the effects on culture conditions on the growth of hairy roots and the production of diterpenoids. They cultured the S9402 strain of hairy roots in MS medium without ammonium salt, added sugar on the 12th day to a concentration of 3 %, and harvested related hairy roots after 8 days. It turned out that the dry weight of hairy roots increased by 22 times, and the total tanshinone content reached the level of 43 mg/g dry weight, of which the content of cryptotanshinone was 20 mg/g dry weight.

In 1995, Zhang et al. [28] successfully established an in vitro culture system for Danshen hairy roots in flask. They used elicitor technology to achieve tanshinone content close to the level of crude drugs. They found that when hairy roots were treated with *Armillaria mellea* Karst, the induction treatment was extremely favorable for the accumulation and secretion of tanshinone in hairy roots. Three to four days after the elicitor treatment, the total tanshinone content

in the hairy roots could reach up to the level of crude drugs. The roots secreted 44 mg/L red colorant into the medium.

In 1997, Huang et al. [29] reported that Danshen hairy roots could generate hydrosoluble phenolic compounds. They found that *A. rhizogenes* ATCC 15834 could induce Danshen leaves to develop hairy roots. After HPLC analysis, they confirmed that the Danshen hairy roots contained hydrosoluble active constituents such as protocathechualdehyde, salvianolic acid A, and salvianolic acid B, in which the content of salvianolic acid A was 0.15 % of the dry weight, which was 2.17 times of the content in crude drugs. Their work has laid a foundation for the industrial production of Danshen hairy roots.

Chen et al. [30] studied the hydrosoluble phenolic contents in Danshen hairy roots and found that they could generate rosmarinic acid and lithospermic acid B. They also studied the hairy roots generated from Danshen's embryonic cells by *A. rhizogenes* ATCC 15834 and found that Danshen hairy roots could produce a small amount of tanshinone and a certain level of phenol compounds. They studied the influences of yeast extracts on the growth and secondary metabolism of hairy roots. It turned out that yeast elicitors could increase the growth rate of Danshen hairy roots from 3.9 g/L (dry cell weight) to 7.3 g/L (dry cell weight). They also found that yeast elicitors could increase the contents of both types of constituents mentioned above. For example, the rosmarinic acid content in the phenol category was increased from 1.24 to 2.89 % in terms of dry cell weight; lithospermic acid B content was increased from 2.59 to 2.98 %; and cryptotanshinone content was increased from 0.001 to 0.096 %. By using LC-MS, they extracted, separated, and identified the tanshinones and phenol compounds from the hairy roots after yeast elicitor treatment. In addition to the above constituents, they also found tanshinone I, Tanshinone IIA and IIB, dihydrotanshinone I, methylene tanshinone, and an unknown tanshinone constituent with a molecular mass of 280. This unknown tanshinone constituent was one of the major tanshinones produced in the hairy roots [31].

Zhang et al. [32] found that induction by Ag^+ and addition of certain nutrient components could further increase the tanshinone content in Danshen hairy roots.

Wang Xueyong et al. used 67-V medium for the suspension and shaking culture of Danshen hairy roots induced by *Agrobacterium* ATCC 15834. After 18 days of culture, they added a chemical elicitor, methyl jasmonate (MJ), to the liquid medium. By adopting the HPLC method, they studied the influences of MJ on the accumulation of tanshinone constituents and their release into the medium. By measuring the contents of cryptotanshinone and Tanshinone IIA and their contents in the medium at different periods of time after MJ treatment, they found that the cryptotanshinone content reached 0.039, 0.204, and 0.572 mg/g on the 2nd, 6th, and 9th days, respectively, which were 2.2, 8.5, and 23.8 times of the contents without MJ treatment. The content of Tanshinone IIA reached up to 0.251, 0.601, and 1.563 mg/g, which were 1.9, 4.1, and 6.2 times of the comparison contents without MJ treatment in the corresponding periods, respectively. This indicates that MJ can significantly promote the accumulation of tanshinone constituents in Danshen hairy roots and help release them into the medium [33].

Wang Xueyong et al. also studied the effects of elicitors YE (yeast extract) and YE + Ag^+ on the accumulation of tanshinone constituents in different periods after the suspension culture of Danshen hairy roots and found that YE and YE + Ag^+ could rapidly stimulate the accumulation of tanshinone constituents, with the YE + Ag^+ providing the optimal results, which means that YE + Ag^+ has some synergic action. In addition, they found that the increase in the cryptotanshinone content was most significant, with an amplitude of up to 35.8-fold. All of this work has laid a material foundation for further molecular-level research on the effects and mechanisms of elicitors on the expression of enzyme genes related to the secondary metabolism of tanshinone [34].

The culture of transgenic tissues and organs has some problems, such as the difficulty of inducing hairy roots or crown gall tissues of

some plants, great difficulty of sterilization, low growth rate, callus formation and/or its vitrification, low contents of effective constituents, requiring massive strains for massive screening, requiring well-ventilated special reactors with low shearing force, etc. All of these factors are closely related to the cost of target products. In other words, the key to the commercialization of target products of transgenic tissue and organ production is the production cost. But with regard to the market, the commercialization of target products of transgenic tissue and organ production is also dependent on the prices of products or commodities, because even though the production cost is high, they still have a potential for industrialization as long as their prices are acceptable to consumers. Therefore, the other key to the industrialization of transgenic tissue and organ culture is to turn the products into valuable commodities in the market.

Culturing in flasks is mainly used to determine the culture conditions for the growth of transgenic tissues and organs and the accumulation of active constituents, and to determine the formula of optimal media. Culturing in reactors is mainly used for the industrial production of related target products. The growth in reactors is obviously different from the growth in flasks. Therefore, before industrial production, the culture conditions of bioreactors, the growth of the culture, and the dynamics of the accumulation of target constituents must be studied.

The key to large-scale culture of Danshen hairy roots lies in its bioreactor culture technology. Since Danshen hairy roots are highly differentiated organs and have a certain form and structure, their culture is different from the suspension cell cultures. All research on Danshen hairy roots is still at the stage of laboratory triangular flask or shake-flask cultures at present. There has not been any report on the application of bioreactors to the large-scale culture of Danshen hairy roots. In order to quickly realize the industrial mass production of Danshen hairy roots and solve the problems in current Danshen production such as inadequate yield and difficult quality control, Qiu et al. [35] studied the bioreactor culture of Danshen hairy roots. They used

ball-type bubble bioreactors (BTBBs) to carry out experiments on the large-scale culture of Danshen hairy roots and conducted a comparison study on the biomass and contents of effective constituents (total tanshinone) in the BTBB culture and triangular flask culture of Danshen hairy roots. It was found that the propagation multiple of Danshen hairy roots cultured in BTBB was 241.71, which was higher than the propagation multiple of Danshen hairy roots cultured in triangular flasks. Also, the total tanshinone content of Danshen hairy roots cultured in BTBB was equal to the total tanshinone content of Danshen hairy roots cultured in triangular flasks and to the total tanshinone content of crude drugs. This result indicates that it is feasible to use BTBB to scale up Danshen hairy roots culture. This work has laid a foundation for the future culture and scale-up (i.e., pilot tests and industrial production) of Danshen hairy roots and will probably lead to a new approach to the sustainable development and utilization of rare Chinese herbal medicinal resources such as Danshen, and the production of green raw medicinal materials.

Their detailed method is as follows [35]: To use aseptic Danshen seedlings as the experimental material and conduct Ri-plasmid Transformation and induction of hairy roots by directly infecting them with *A. rhizogenes* 15834, please refer the papers by Zhang Yinlin et al. Thus, obtained Danshen hairy roots were successively transferred to 67-V agar medium for subculture. Use BTBB with a capacity of 10 l for the bioreactor culture of Danshen hairy roots, and fill them with 7,500 ml 67-V liquid medium. Connect the entire reacting device, and sterilize it with 0.12 M Pa, 121 °C high pressure vapor for 20 min. After it is cooled down, put it on an ultra-clean work table and put 3.68 g Danshen hairy roots into the reactor. A 1,000-ml triangular flask filled with 250 ml 67-V liquid medium is adopted for triangular flask culture. The ventilation volume is 0.05 vvm (the ratio of actual liquid material volume in the tank to the ventilation volume per minute). The sterilization method and the inoculating method for hairy roots are the same as those of the BTBB culture. The inoculum is 0.12 g. Conduct shaking culture

on a shaking table at a rotating speed of 150 rpm/min. All culture work must be done at 25 °C and in dim light. After 50 days of culture, harvest their respective hairy roots and media, measure their fresh weights, and measure their dry weights after drying them at 70 °C until constant weights are reached. Use the ultraviolet spectrophotometric method to measure the total tanshinone content in the Danshen hairy roots and their media.

During the experiment, Qiu et al. [35] found that Danshen hairy roots grew quickly and had many branches in culture. When Danshen hairy roots were connected into the BTBB, they tumbled in the top of reactor liquid with the circulating currents formed by the incoming gas, while Danshen hairy roots in triangular flask culture rotated with the shaking bed. In the first 7 days, Danshen hairy roots cultured in both BTBB and triangular flask grew slowly, but entered the rapid growth period afterward. By the 25th day, Danshen hairy roots cultured in BTBB developed a great deal of white hairy roots and gradually bifurcated and intercrossed to form hairy root balls. A part of the hairy roots began to stick out of the liquid surface. Afterward, the Danshen hairy roots cultured in BTBB grew significantly faster than those cultured in the triangular flask. By the 40th day, the hairy roots filled the entire reactor, and by the 50th day, the colors of the hairy roots and the medium darkened further to a reddish brown. Qiu Deyou et al. also observed that compared with the plant hairy roots cultured in other bioreactors, Danshen hairy roots cultured in BTBB rarely generated any bubbles. When soaked in liquid medium, the Danshen hairy roots cultured in the triangular flask had thicker hairy roots and fewer branches than the hairy roots cultured in BTBB. Danshen hairy roots cultured in the triangular flask and their medium had the same changes in color as those cultured in BTBB. After 50 days, it was measured that the propagation multiple of hairy roots cultured in BTBB reached up to 241.71, which was much higher than the propagation multiple of 203.33 of hairy roots cultured in the shake flask. The total tanshinone content in the hairy roots harvested in bioreactor culture and

their medium was close to the total tanshinone content in the hairy roots harvested in shake-flask culture and their medium, and almost close to the total tanshinone content in crude Danshen drugs. The shape of BTBB was wide at the top and narrow at the bottom. When Danshen hairy roots cultured in the ball-type bubble bioreactor developed a great deal of white hairy roots and gradually bifurcated and intercrossed to form hairy root balls, some of the hairy roots began to stick out of the liquid surface, while others still remained in the medium. This could both obtain sufficient nutrient supplies and greatly improve the ventilation conditions. In addition, Danshen hairy roots cultured in BTBB rarely generated any bubbles throughout the entire culturing process, and being always soaked in medium, Danshen hairy roots cultured in the triangular flask had significantly worse ventilation conditions than Danshen hairy roots cultured in BTBB. This was very likely the cause of the difference in the multiplication.

In 1983, Mugnier et al. [36] conducted hairy root culture in a bioreactor for the first time. Milton and Rhodes [37] conducted hairy root culture in an improved agitating bioreactor. Dilorio et al. [38] supplied the nutrient substance needed for the growth of hairy roots to *Beta vulgaris* and *Carthamus tinctorius* hairy roots in the form of fogs, and the hairy roots grew well. Zheng et al. [39] used 3–10-L aerated culture flasks to carry out laboratory-scale experiments on the culture of *Astragalus membranaceus* hairy roots. The culture of hairy roots has been conducted in bioreactors in the forms of agitating, gas-lift, trickle bed, and atomization bioreactors. In already published reports using bioreactors for hairy root culture, the propagation multiples are generally in the range of dozens, rarely in hundreds, and they are usually lower than the results of triangular and shake-flask experiments. Qiu Deyou et al. found through experiments that the propagation multiple of Danshen hairy roots cultured in the BTBB was 241.71, which was higher than that obtained from shake-flask culture. The total tanshinone contents in BTBB and the triangular and shake-flask cultures were equivalent to the total tanshinone content in

crude Danshen drugs. This result indicates that it is quite feasible to use BTBB to carry out the scale-up culture of Danshen hairy roots. The BTBB system has many advantages that ordinary bioreactors do not have, such as that the height of the bioreactor is greatly reduced, that few bubbles are created during the entire culturing process, and that the biomass and effective constituents of roots in the bioreactor can reach the maximum values in a very short period of time and become comparable to the results of shaking cultures and to the contents in crude drugs. In the future, when combined with induction technology, this bioreactor is likely to achieve higher contents of target constituents than those in the original plants. Since BTBBs are very suitable for the growth of Danshen hairy roots and the production of tanshinone, it can be predicted that in the near future, people are likely to realize the sustainable Development and exploitation of rare Chinese herbal medicinal resources such as Danshen, and the production of green raw medicinal materials.

5.3.3 Culture of Crown Gall Tissues of Danshen

Using crown gall Tissue culture of Danshen to directly acquire the effective constituents of Danshen will help solve the current problems in Danshen cultivation and the quality control. The detailed method for the induction and culture of Danshen crown gall tissues is as follows:

Sterilize Danshen seeds with 0.1 % corrosive mercuric chloride for 10 min, and rinse them with aseptic distilled water three times. Then, inoculate them onto 1/2 MS agar medium. Aseptic seedlings can be obtained right after germination. Culture the aseptic seedlings under the conditions of 25 °C and 16 h/day of lighting. After a month, cut down the stem tips and inoculate them to fresh medium for subculture. Before the induction of crown gall, inoculate nopaline-type *A. tumefaciens* strain C58 onto YMB agar medium and culture them 27 °C for 2 days until they grow well. Then, store them in a refrigerator at 0–5 °C. The bacteria should be

successively subcultured every 2 months. Before using for Transformation, take them out and activate at 25 °C for several hours.

Induction and sterilization: Select well-grown aseptically Danshen seedlings about 6 cm in height. Retain the terminal buds and three leaves, and remove other leaves. Smear the activated C58 bacteria at the nodes, and pierce the surface with a dissecting needle. Incubate the tissue under scattered light at 25 °C. After crown galls emerge, cut them down and transfer them onto MS agar medium containing 500 mg/L carbenicillin. After multiple transfers, aseptically crown gall tissues can be obtained. Subculture the crown gall tissues on MS agar medium in the dark at 25 °C.

Measurement of opine in crown gall tissues: Use 5 % methanoic acid and 15 % ethanoic acid (volume ratio) in water as the electrophoretic buffer. When measuring, grind the plant material, collect the supernatant, and spot the sample on Whatman 3-MM filter. At the same time, also spot 0.1 M arginine, octopine, and nopaline aqueous solution and methyl green aqueous solution onto Whatman 3-MM filter paper, allowing at least 1 cm between neighboring spots and 4.5 cm away from the bottom edge. This is used as the positive electrode. Use cotton balls that have been dipped in the electrophoretic buffer to wet the filter paper, and conduct electrophoresis under 20 v/cm. Stop electrophoresis before methyl green runs out, and dry the filter paper with a hot-air fan. Finally, dip the filter paper into a staining solution. When making the staining solution, first make 0.02 % phenanthrenequinone (Sigma) using absolute alcohol, and then, use 60 % alcohol to make 10 % NaOH. Mix equal amounts of both solutions before use. Put the filter paper into the solution while agitating. After drying the filter with a cool-air fan, observe the sample spots under an ultraviolet lamp at 254 nm.

Selecting the basic media: Place the Ca strain of Danshen crown gall tissue into MS, B5, 67-V, and WP basic media without phytohormones for liquid culture. The composition of 67-V and WP used in the experiment is slightly modified: NaH_2PO_4 and NaH_2PO_4 are replaced by equal amounts of

$\text{NaH}_2\text{PO}_4 \cdot 2\text{H}_2\text{O}$ and $\text{NaH}_2\text{PO}_4 \cdot 2\text{H}_2\text{O}$; the amount of nicotinic acid is reduced to 0.5 mg/L; the amount of thiamine hydrochloride (VB1) is reduced to 0.1 mg/L. The culture conditions are 25 °C without light, shaking table rotating at 140 rpm. Hundred milliliter medium is put into a 500-ml round-bottom flask; the pH value of medium is 5.71. The inoculum for each flask is 248 mg. Five repetitions are designed for each medium, and the culture lasts for 31 days.

The study on the dynamics of the growth of crown gall tissues in liquid medium and the production of effective constituents: The tested strain is the Ca strain of Danshen crown gall tissues. MS and improved 67-V liquid media are used as the basic media. The inocula are 600 mg/flask and 400 mg/flask, respectively. The culture conditions are 25 °C, dark, and rotating at 150 rpm. A 500-ml round-bottom flask is loaded with 100 ml medium with a pH value of 5.71. Culture lasts for 35 days. Harvest samples every 5 days, measure samples' fresh and dry weights, and observe the growth status of the culture. When the color of the medium changes, use chloroform to extract its liposoluble constituents, and analyze the total tanshinone content in the culture and the medium. Repeat three times. The harvesting method for the culture and the medium is as follows: When harvesting, use double-layer gauze to filter, use filter paper to absorb the moisture on the surface of the tissue, measure its fresh weight, and then, dry it at 70 °C until a constant weight is reached. Then, grind it into powder with a mortar for the measuring of total tanshinone content. Extract the media with 1/10 volumes of chloroform. In order to separate cell debris from chloroform into different layers, centrifuge the samples for 20 min at 4,000 rpm. Collect the chloroform layer, and after the chloroform is completely evaporated, measure its weight or directly dilute it to an appropriate concentration, and then, measure the absorbance at 270 nm to calculate the total amount of tanshinone.

Before measuring total tanshinone amount and conducting TLC analysis, a standard curve must be drawn. The method is as follows: Weigh 2.26 mg Tanshinone IIA, and put it into a 1-ml measuring flask. Use ethanol to bring up the volume. As it is not completely dissolved, it is

advisable to transfer it into a 2-ml measuring flask and add a little chloroform to dissolve it completely. Then, adjust the volume to a concentration of 1.13 mg/ml. Use a 100- μ l syringe to transfer 10, 14, 20, 24, and 30 μ l into 5-ml measuring flasks, respectively. Use chloroform to bring up the volume, and use PYE UNICAM PU8800 spectrophotometer to measure their OD value at 270 nm. By regression analysis, the standard linear equation is $C = 10.98049772 \times (\text{OD}) - 0.17122854$, $r = 0.999208$, wherein C is the concentration mg/L of the measured solution and OD is the absorbance of the solution at 270 nm (ranging from 0.2 to 0.6).

Steps of measuring total tanshinone amount in the samples are as follows: Weigh 100 mg and put into a 50-ml triangular flask with a plug. Add 10 ml chloroform and measure the weight. Incubate it at room temperature overnight. Conduct ultrasonic extraction for 20 min. Add chloroform until the original weight is reached. Shake it up and filter it. Transfer 10 ml of the filtrate into a 10-ml graduated test tube. Use chloroform as the blank, and measure the absorbance at 270 nm. If the OD value is not within the range of detection, proper treatments should be carried out. When OD value >0.6 , dilute the sample to a suitable concentration and remeasure it; when OD value is <0.2 , increase the sample amount and remeasure it. Finally, calculate the total tanshinone content in samples. A 10 cm \times 10 cm silica gel thin-layer plate is used for TLC analysis. The developing agent is benzene–methanol (9:1, V/V). The reference standards are cryptotanshinone and tanshinone IIA. Use chloroform to dissolve the reference standards and other samples. Use a capillary needle to apply the samples onto a silica gel thin-layer plate. Sample spots should be about 1 cm away from the bottom edge. Neighboring points should be at least 1 cm away from each other. When sample spots are completely dry, put the plate in the chromatography tank until the solvent reaches the top.

In 1995, Zhang et al. [40] conducted an experiment on the infection of aseptic Danshen seedlings by *A. tumefaciens*. The results showed that 6 days after the C58 strain of *A. tumefaciens* was inoculated onto the nodes of aseptic Danshen seedlings, visible swelling began to appear

where piercings were made. These swellings would grow into crown galls. When a crown gall grew up to 5 mm³ (in about 10 days), they were cut off from the parent tissue and transferred onto MS agar medium containing 500 mg/L carbenicillin for culturing. After five transfers (i.e., about 70 days) on medium containing antibiotics, the sterilization process was completed and aseptic crown gall tissues were obtained. They found that the sterilized crown gall tissues grew well on MS medium without phytohormones, and tissue blocks from different crown galls had significantly different multiplication rates. The Ca strain, which had the fastest growth, was selected out of five crown galls. Opines in the crown gall of Ca and mH strains were detected with high-voltage paper electrophoresis. It turned out that both strains contained nopaline, which indicated that T-DNA had been transferred into Danshen cells and expressed. They also found that the Ca strain's growth and production of total tanshinone differed significantly on different basic media. Crown gall tissues generated a great deal of leaf buds through differentiation on 67-V medium, and their petioles were relatively short, which demonstrated a typical phenotype of teratomas. Leaf differentiation also occurred on WP and B5 media, but to a lesser extent than on 67-V medium and to a greater extent than on MS medium. After 3 weeks of liquid culture of crown gall tissues in 67-V and WP media, the media began to turn orange yellow and then turned orange red. Harvesting was carried out 10 days after the color change. At this point, the crown gall tissues themselves exhibited a light orange red color, while crown gall tissues cultured in B5 and MS media were light yellow and the media were colorless and transparent. After harvesting, the fresh weights and dry weights of crown gall tissues in the basic media were calculated, and the contents of tanshinone in the crown gall tissues were analyzed. The results showed that the growth of crown gall tissues and the accumulation of tanshinone were influenced by the basic medium. B5 and MS media were favorable for the growth of crown gall tissues, and their monthly propagation multiple could reach 102 and 90, respectively, while 67-V and WP media

were favorable for the biosynthesis of tanshinone (see Table 5.1). During the culturing process, tanshinone could be secreted into the media.

In 1997, Song et al. [41] further reported an experiment on the selection of high-yield strains of Danshen crown gall tissues and their production of tanshinone. The results showed that high-yield strains could not be acquired on MS medium, while 67-V medium was favorable for the selection of high-yield strains. They found that although the Ca strain of Danshen crown gall tissues had high and stable tanshinone content, a certain degree of variation (1.13–2.18 %, dry cell weight) still existed. For the purpose of maintaining the stability of the high-yield strain in the long run, they suggested that repeated selections be conducted in the subculture process. In addition, their research also showed that combined with the elicitor technology, liquid stationary culture is favorable for the scale-up culture of high-yield strains of Danshen crown gall tissues, and can achieve a final tanshinone content that is more than three times of the tanshinone content in crude drugs. They also used MS and 67-V media to carry out a comparison study on the growth of Danshen crown gall tissues and the dynamic accumulation of total tanshinone, and found that 67-V medium was superior to MS medium.

Song et al. [42] also studied the growth of the Ca strain of Danshen crown gall tissues in MS and 67-V liquid media and the dynamic production. The results showed that in MS liquid medium, the culture was in the logarithmic phase in days 5–25, and in the stationary phase in days 25–35. The time around the 25th day of culture was a period in which the culture had the best physiological activity and growth (see Table 5.2).

In 67-V liquid medium, the culture of the Ca strain of crown gall tissues was in the stationary phase in days 25–35, while tanshinone did not begin to accumulate in large quantities in the culture and the medium until the 25th day of culture, i.e., the end of the logarithmic phase, and reached a peak by the 35th day. The relationship between the growth of the culture and the accumulation of tanshinone was not parallel, but mutually repellent; that is, the products cannot begin to accumulate in large quantities until cells stop growing and enter the stationary phase. Therefore, timing is very important for harvesting (Table 5.3).

In 2000, Song et al. [43] used a computer software called “Uniform Design Regression Analysis and Optimization System” to study the influences of the concentration of *A. mellea* Karst elicitor, the timing of the addition of the elicitor, and the harvest time on the accumulation of tanshinone in Danshen crown gall tissues. They used 67-V liquid medium as the basic medium. The culture conditions were 25 ± 1 °C, darkness, and a pH value of 5.71. *A. mellea* was cultured in aseptic PDA liquid medium. To make PDA medium, first weigh 50 g wheat bran and mix it with 200 ml water. Boil it for 15 min, and then, filter it. Collect the filtrate and add 20 g glucose, 1.5 g KH_2PO_4 , 10 mg VB_1 , and 20 ml 95 % ethanol into the filtrate. Add water to bring the volume to 1 liter. Then, divide the mixture into 10 500-ml triangular flasks. After high-pressure sterilization, inoculate the PDA liquid medium with 0.5–1 cm of *A. mellea* rhizomorph, and incubate at 25 °C under darkness on a 120 r/min shaking table for about 13 days. Harvest samples when *A. mellea* grows well and forms cocci. Filter the culture with double-layer gauze. Shatter

Table 5.1 Influences of basic media on the growth of Ca strain of Danshen and the production of tanshinone

Basic media	Harvested fresh weight (g/L)	Harvested dry weight (g/L)	Total tanshinone content in the cultures (%/dwt)	Content of liposoluble compounds in the medium (mg/L)
MS	226.90	11.258	0.010	0
B5	254.62	10.518	0.018	0
67-V	160.19	8.880	0.027	24
WP	135.62	6.256	0.084	20

Table 5.2 Dynamic growth of Ca strain of Danshen in MS liquid medium

Culturing time (day)	5	10	15	20	25	30	35
Fresh weight (g/100 ml)	1.81 ± 0.24	4.62 ± 0.44	10.22 ± 0.99	12.97 ± 0.35	17.01 ± 2.86	19.93 ± 0.09	19.12 ± 0.50
Dry weight (g/100ml)	0.112 ± 0.017	0.242 ± 0.016	0.478 ± 0.020	0.582 ± 0.002	0.755 ± 0.081	0.772 ± 0.021	0.783 ± 0.032

Table 5.3 Growth and production of tanshinone of Ca strain in 67-V liquid medium

Culturing time (day)	5	10	15	20	25	30	35
Harvested fresh weight (g/L)	6.4 ± 0.9	17.9 ± 2.4	84.3 ± 1.8	110.0 ± 2.1	140.9 ± 6.9	116.8 ± 1.6	130.9 ± 11.4
Harvested dry weight (g/L)	0.43 ± 0.05	1.08 ± 0.16	4.48 ± 0.47	6.73 ± 0.23	8.72 ± 0.51	7.75 ± 0.15	7.87 ± 0.45
Total tanshinone content in the cultures (%dwt)	/	/	0.008 ± 0.005	0.018 ± 0.005	0.055 ± 0.003	0.215 ± 0.030	0.258 ± 0.066
Total tanshinone output in the cultures G (mg/L)	/	/	/	1 ± 0	5 ± 0	17 ± 2	20 ± 4
Total tanshinone output in the medium L (mg/L)	/	/	/	/	8 ± 1	13 ± 1	40 ± 15
G + L (mg/L)	/	/	/	/	13 ± 1	30 ± 2	60 ± 15
G/(G + L)%	/	/	/	/	38.5	56.7	33.6
L/(G + L)%	/	/	/	/	61.5	43.3	66.4

the filtration residue with a homogenizer, and mix it up with the filtrate. Filter it again, and fully mix up the filtrate and split into 500-ml triangular flasks. After high-pressure sterilization, store it at 25 °C for future use.

In the preliminary study on the range of the concentration of the elicitor, the rotating speed of the shaking table was set at 140 r/min. The detailed method is as follows: Transfer 100 ml medium into 500 ml round-bottom flasks. The inoculum for each flask is 470 mg. Each treatment was repeated 5 times. At the beginning of culturing, add different concentrations of *A. mellea* elicitor: 0, 100, 200, and 300 ml/L. After 23 days of culture, harvest the culture and medium. In the experimental study on the optimization of the elicitor, make the elicitor into parent liquid of a suitable concentration and set the pH value at 5.71. Carry out 10 treatments, each being repeated 3 times. Set the rotating speed of the shaking table at 150 r/min. Add 50 ml medium into 250-ml triangular flasks. 400 mg is inoculated in each flask. The given concentration of *A. mellea* elicitor is 0–18.0 ml/L. Add the elicitor in day 0–27. The harvesting time for treatments is day 20–38. When harvesting, use double-layer gauze to filtrate, use filter paper to absorb the moisture on the surface of the tissue, measure its fresh weight, and then, dry it at 70 °C until a constant weight is reached. Measure its dry weight, and then, grind the sample into powder with a mortar for the measurement of tanshinone content. Use the ultraviolet spectrophotometric method to measure the tanshinone content in the sample. Extract the medium using 1/10 volumes of chloroform. After the chloroform completely evaporates, measure the weight or directly dilute it to an appropriate concentration, and then, measure the absorbance at 270 nm. Calculate the content of tanshinone. The results showed that the *A. mellea* elicitor has a very significant inhibitive effect on the growth of the Ca strain of Danshen crown gall tissues, and with an increase in concentration, the inhibitive effect on the growth of Ca strain is further strengthened. In contrast, the elicitor has a boosting effect on the accumulation and secretion of tanshinone (but a higher concentration does

not necessary provide a better effect). The *A. mellea* elicitor of a concentration of 100 ml/L has less inhibitive effect on the growth of the culture and can significantly boost the accumulation and secretion of tanshinone. The optimal concentration of *A. mellea* elicitor is probably around 100 ml/L. In order to make sure the optimal concentration was included in the experiment, they further considered both the inhibitive effect on the growth of the culture and the boosting effect on the accumulation of tanshinone, and conducted an experimental study on the optimization of *A. mellea* elicitor in an effort to obtain the optimal concentration and application time for the elicitor to promote both the accumulation of Danshen crown gall tissues and the secretion of tanshinone, and to determine the best harvesting time. The results showed that when *A. mellea* elicitor with a concentration of 119 ml/L was added on day 0, the highest output (147 mg/L, $P \leq 0.05$) of tanshinone could be obtained when harvesting the culture and medium on the 29th day. When the elicitor with a concentration of 113 ml/L was added on day 0, the highest output (62 mg/L, $P < 0.05$) of tanshinone could be obtained when harvesting the culture and medium on the 26th day. When the elicitor with a concentration of 87 ml/L was added on day 0, the highest output (94 mg/L, $P \leq 0.05$) of tanshinone could be obtained when harvesting the culture and medium on the 28th day. The use of “Uniform Design Regression Analysis and Optimization System” can greatly reduce the work load, help to make scientific and reasonable experimental designs, process results rapidly and accurately, and provide highly reliable optimal plans that can be easily carried out. It is very effective and convenient for research in which the observed values are subject to the influences of multiple factors.

In 1997, Chen et al. [44] also reported the induction and culture of Danshen crown gall tissues. They successfully obtained Danshen crown gall tissues by using the C58 strain. These crown gall tissues were in the form of cell aggregates 2–3 cm in size in liquid medium. The B5 medium was favorable for the growth of Danshen crown gall tissues, while the 67-V

medium was favorable for the generation of tanshinone. The starting sugar concentration had an effect on the growth of Danshen crown gall tissues. The B5 medium containing 30 g/L sucrose was most favorable for the growth of Danshen crown gall tissues. Although the tanshinone content in the fast-growing crown gall tissues was quite low, it increased rapidly when the tissues were transferred into fresh medium containing yeast extract. This two-step culture method could generate 22 mg tanshinone in each liter of medium. Under the light, these Danshen crown gall tissues turned green and the biosynthesis of tanshinone was inhibited. Using HPLC method, they found cryptotanshinone, tanshinone I, and Tanshinone IIA in the culture.

In 1999, Chen et al. [45] also reported that Danshen crown gall tissues could generate rosmarinic acid and lithospermic acid B. In the same year, they published another report showing the results of a study on dynamic cell growth and secondary metabolism of a Danshen crown gall cell line with high yield of tanshinone [46]. In addition, they also studied the effects of yeast elicitors on the cell growth and secondary metabolism of the Danshen crown gall cell line. Chen et al. used the C58 strain of *A. tumefaciens* to transform Danshen embryonic cells. They selected two crown gall cell strains, of which Strain A only generated trace amount of tanshinones but generated large quantities of phenolic acids, while Strain B generated large quantities of tanshinones which totaled up to 1 % of the dry cell weight. They studied the accumulation of biomass, the formation of phenolic compounds, the pH value and electric conductivity of medium, and the absorption of sugar, nitrates, ferric salts, and phosphates both in the shake-flask culture and bioreactor culture of Strain A, and found that on the 20th day of culture, the contents of rosmarinic acid and lithospermic acid B were 4.59 % (equivalent to 481.5 mg per liter liquid medium) and 0.81 % (equivalent to 85.0 mg per liter liquid medium) of the dry cell weight, respectively. When 67-V medium was used as the medium for Strain B instead of B13, the cells grew quickly and the tanshinone content increased as well. The contents of cryptotanshinone, tanshinone IA, and

Tanshinone IIA were 150 mg/L, 20 mg/L, and 50 mg/L, respectively. In addition, the phenolic constituents were significantly increased too: Rosmarinic acid and lithospermic acid B contents were 530 mg/L and 216 mg/L, respectively. They further treated Cell Strain A transformed by Ti with yeast extract and found that the phenolic contents were decreased, in which the content of rosmarinic acid dropped from 5.0 to 3.0 % of the dry cell weight. But the contents of tanshinones were increased. For example, the cryptotanshinone content increased from traces to 20 mg per liter medium. On the basis of these results, they proposed that rosmarinic acid and lithospermic acid B respectively played a passive role and an active role in response to the invasion of foreign pathogenic bacteria, and they believed that cryptotanshinone was an antitoxin for Danshen plants. When they treated cultured Danshen cells with phenyl alanine deaminase-specific strong inhibitor, it was found that the treatment did not inhibit the formation of tanshinones induced by yeast, but reduced the level of the biosynthesis of rosmarinic acid. For Strain B, they found that the yeast elicitor increased the cryptotanshinone content by 100 %, while the content of rosmarinic acid nearly dropped to zero. The yeast elicitor also inhibited the primary metabolism and greatly reduced the accumulation of biomass [47, 48].

Ying et al. [49] also studied the characters and cell growth of the suspension culture of Danshen crown gall tissues as well as the synthesis of tanshinone. They established a separated-phase dynamic model for the growth, the consumption of substrates, and the accumulation of products of Danshen crown gall tissues. The calculated results of related models were consistent with the experimental results. In the experiment, the Danshen crown gall tissues in suspension culture were composed of light yellow, near-spherical particles 5–10 mm in diameter. The medium was pure and transparent. The growth cycle of Danshen crown gall tissues was 20–25 days, in which day 3–7 was approximately the exponential phase of growth, with a growth velocity of $\mu = 0.16/\text{day}$, day 7–13 was approximately the constant-velocity phase of growth, with a growth velocity of $dC_x/dt = 0.69 \text{ g}/(\text{L d})$, day 13–21 was the velocity-reduction phase

of growth, and the maximum biomass concentration ($C_{x,max} = 10.9 \text{ g/L}$) was reached on the 21st day. The accumulated mass concentration of tanshinone $C_p = 8.4 \text{ mg/L}$.

In summary, encouraging progress has been achieved on the use of cell, tissue, and organ culture of Danshen to directly obtain its active constituents. Through the application of the *Agrobacterium*-mediated Transformation technology and elicitor technology, production of Danshen active constituents by the mass culture of Danshen cells, tissues, and organs will be realized and become a technology with good prospects of development and application.

References

1. Yang N. *Plant Physiol Commun.* 1985;3:53–73.
2. Wang J, Liu D. *Plant Physiol Commun.* 1987;6:46–8.
3. Shimomura K, Kitazawa T, Okamura N, et al. *J Nat Prod.* 1991;54(6):1583–7.
4. Cai Z, Gao S, Xu D. *J China Pharm Univ.* 1991;22(2):65–8.
5. Liang H, He N, Zhao J. *J Central China Normal Univ (Nat Sci).* 1997;31(3):328–31.
6. Zhao J, Chen Z, Wan J. *J Central China Normal Univ (Nat Sci).* 1999;33(1):108–11.
7. Duan Y, Niu Y, Liu Y, et al. *Plant Physiol Commun.* 2003;39(3):201–5.
8. Tian Y, Wang Z. *J Shaanxi Normal Univ (Nat Sci).* 2003;31(1):99–102.
9. Liu X, Wang Y. *J Sichuan Agric Univ.* 2003;21(1):73–5.
10. Li Y, Gu M, Jin J, et al. *Fudan Univ J Med Sci.* 1981;16(3):58–9.
11. Huang X, Hu Z, Yang B, et al. *Chin Pharm Bull.* 1981;16(9):22–3.
12. Tsutomu N, Hitoshi M, Masao N, et al. *Phytochemistry.* 1983;22(3):721–2.
13. Hitoshi M, Masao N, Toshihiko Y, et al. *Phytochemistry* 1985;24(9):1931–33.
14. Hitoshi M, Masao N, Toshihiko Y, et al. *Phytochemistry.* 1986;25(3):637–40.
15. Hitoshi M, Masao N, Toshihiko Y, et al. *Phytochemistry.* 1986;25(7):1621–4.
16. Hitoshi M, Masao N, Toshihiko Y, et al. *Phytochemistry.* 1987;26(5):1421–4.
17. Xu P, Xue Y. *Acta Photophysiological Sinica.* 1987;13(1):14–9.
18. Tao L, Yuan J, Xu J. *Chin J Biotechnol.* 1990;6(3):218–23.
19. Hu Y, Zhang R, Hu Z, et al. *Plant Physiol Commun.* 1992;28(6):424–5.
20. Zhu W, Hu Q, Zhu Z, et al. *J Chin Med Mater.* 1994;17(4):3–4.
21. Wang K, Luo Q, Chen H. *China J Chin Materia Medica.* 1998;23(10):592.
22. Huang L, Liu D, Hu Z. *J Chin Med Mater.* 2000;23(1):1.
23. Wang X, Cui G, He X, et al. *Chin J Exp Tradit Med Formulae.* 2007;13(1):1–4.
24. Guo X, Gao W, Li K. *Chin Tradit Herbal Drugs.* 2007;38(3):429–32.
25. Guo X, Gao Y, Li K. *Chin Tradit Herbal Drugs.* 2007;38(6):907–11.
26. Lin J. *An overview of plant sciences.* Jilin: Northeast Forestry Press; 1993. p. 20–34.
27. Hu ZB, Allrermann AW. *Phytochemistry.* 1993;32:699.
28. Zhang Y, Song J, Lv G, et al. *China J Chin Materia Medica.* 1995;20(5):269.
29. Huang L, Hu Z, Di L. *Plant Physiol Commun.* 1997;33(4):259–61.
30. Chen H, Chen F, Zhang YL, et al. *J Ind Microbiol Biotech.* 1999;22:133.
31. Chen H, Chen F, Chiu FC, et al. *Enzyme Microb Technol.* 2001;28(1):100–105.
32. Zhang C, Yan Q, Cheuk WK, et al. *Planta Med.* 2004;70(2):147–51.
33. Wang X, Cui G, Huang L, et al. *China J Chin Materia Medica.* 2007;32(4):300–2.
34. Wang X, Cui G, Huang L, et al. *China J Chin Materia Medica.* 2007;32(10):976–8.
35. Qiu D, Song J, Ma X, et al. *Mol Plant.* 2004;2(5):699–703.
36. Mugnier J, Jung G, Prious J-L. *Europ. Patent No. EP 0 100 691 A1* (1983).
37. Milton MG, Rhodes MJ. *Appl Microbiol Biotechnol.* 1990;33(2):132–8.
38. Diloriol AA, Cheetham RD, Weathers PJ. *Appl Microbiol Biotechnol.* 1992;37(4):457–62.
39. Zheng Z, Peng G, Liu D, et al. *Plant Physiol Commun.* 1997;33(2):133–4.
40. Zhang Y, Song J, Zhao B, et al. *Chin J Biotechnol.* 1995;11(2):150.
41. Song J, Zhang Y, Qi J, et al. *Chin J Biotechnol.* 1997;13(3):317–9.
42. Song J, Qi J, Ren C, et al. *Acta Pharmaceutica Sinica.* 2000;35(12):929–31.
43. Song J, Qi J, Lei H, et al. *Acta Botanica Sinica.* 2000;42(3):316–20.
44. Chen H, Yuan JP, Chen F, et al. *J Biotechnol.* 1997;58(3):147–56.
45. Chen H, Chen F, Zhang YL, et al. *Proc Biochem.* 1999;34:777.
46. Chen H, Chen F. *Blotech Lett.* 1999;21:701.
47. Chen H, Chen F. *Plant Cell Rep.* 2000;19:710.
48. Chen H, Chen F. *Proc Biochem.* 2000;35:837.
49. Ying P, Xu J, Su Z. *Chin J Appl Environ Biol.* 1999;5(5):478–82.

Deyou Qiu and Jingyuan Song

6.1 The Germplasm Resources and Breeding Studies of Danshen

Genuine Danshen medicinal material comes from the dry roots and rootstalks of Danshen, a *Labiatae* plant. With decreasing wild resources, the supply of medicinal Danshen is already unable to meet the demand. Presently, more than 40 species (including mutants and variants) from the *Salvia* genus have been found whose roots and rootstalks can be used as Danshen. People have studied the chemical contents of nearly 30 species, of which the species with high contents of liposoluble constituents include Ganxi Shuwei Cao (*S. przewalskii*), Sanye Shuwei Cao (*S. trijuga*), Mao-dihuang Shuwei Cao (*S. digitaloides*), Chengse Shuwei Cao (*S. aerea*), Yunnan Shuwei Cao (*Salvia yunnanensis*), Nan Danshen (*S. bowleyana*), Lise Shuwei Cao (*S. castanea*), Huanghua Shuwei Cao (*S. flava*), Honggen Cao (*S. prionitis*), and Wan E Danshen (*S. paramiltiorrhiza*). The hydrosoluble phenolic acids, as important effective constituents of Danshen, have been extensively studied in recent years, and some species with high phenolic contents have been found. Besides serving as new Danshen resources, these species are likely to become germplasm resources for the breeding gene pool of superior Danshen

germplasms. Up till now, two mutants and one variant of Danshen have been reported: original mutants *S. miltiorrhiza* var. *miltiorrhiza* and var. *charbommellii*, and a variant *S. miltiorrhiza* f. *alba*. These germplasms that have variances in morphology need further character appraisal in the future and should be protected [1].

Zhen et al. [1] planted Danshen plants collected from different regions in the same experimental field and found great differences in yield and quality, which indicate that different places of origin have different germplasms. Superior and high-yield varieties that are suitable for various environments can be selected out of them, but research on this aspect is rarely seen in recent studies [2].

Jiayan [3] carried out a comparison analysis of the protocathechualdehyde and tanshinol contents in Danshen medicinal materials of different varieties and different places of origin and found that they had significant differences. However, since the sources, storage conditions, and storage time were not clear, these differences might not be caused by genetic reasons.

Wei et al. [4] from Medicinal Plant Research Center of Hebei Academy of Agricultural Sciences compared the germplasms of Danshen in an effort to select Danshen germplasms with superior characters. By using statistic methods, they compared the biological characters of various Danshen germplasms and their biological yields. It turned out that short-stem Danshen was superior to other germplasms in all production

D. Qiu (✉) · J. Song
Chinese Academy of Forestry, Beijing, China
e-mail: qiudy@caf.ac.cn

characters, individual fruits of round-leaf Danshen had the highest seed-producing rate, and tall-stem Danshen was most susceptible to infections and diseases. They finally selected short-stem Danshen which had superior characters in production.

6.2 Mutation Breeding of Danshen

The mutation breeding of Danshen mainly refers to the artificial induction of polyploids. Polyploid plants usually have larger roots, stems, leaves, flowers, and fruits; stronger resistance to stress; and high contents of medicinal constituents. Therefore, breeding polyploid Danshen has a high value for application and potential for increased production. Gao Shanlin et al. studied the new approaches to the cultivation of superior varieties. They induced Danshen tetraploids by using colchicine and then identified the autotetraploids therein with the chromosome identification method. They reported that adding 10–50 ppm colchicines under the isolated culture condition could effectively induce Danshen to generate polyploids. By microscopic examination of chromosomes in root tips, the polyploids were proved to be autotetraploids. They transplanted test-tube seedlings that were confirmed as tetraploids by more than three times of microscopic examination and carried out preliminary identification of the field agricultural characters and measurement of major chemical contents. The results showed that the individual tetraploid plants had the typical phenotypes of polyploid plants, more or less, and that the contents of major chemical constituents in these plants were generally higher than those of normal plants. This indicates that it is possible to breed them into new varieties through further selection [5].

After studying the agronomic traits in the field for 2 years, Shanlin et al. chose those plants with distinctive polyploid characters and superior agronomic traits for strain comparison experiments. Strain comparison plots were repeated three times and arranged randomly. The roots were harvested in fall (October–November) and

air-dried. Precisely weigh out a 0.5 g sample of each strain, and add 8 ml dichloromethane-methanol (8:2) solvent. Soak the sample at a cold temperature overnight. Next day, perform ultrasonic extraction for 15 min, centrifuge at 3,000 rpm for 15 min, and rinse the debris with the solvent. Combine the extractants and bring the volume to 10 ml. Use HPLC to measure the contents of three tanshinones. After three consecutive years of observation of the agronomic characters in the field, it was found that all these polyploid strains showed distinctive polyploid characteristics such as large roots, stems, and leaves. These results verified the reliability of examination of root tip chromosomes by microscopy. After transplanting the test-tube seedlings, they also found that their major chemical contents were much higher than those of original diploid plants. After that, they carried out a 3-year field strain nursery comparison experiment on more than 20 obtained multiploid strains and selected a superior strain of 61-2-22. This strain has the following features: prosperous growth; large, thick, and coarse leaves; thick and light purple stems; low fertility, some infertile; and thick, purple red root system with many branches. This strain has good field agronomic characters and vigorous growth, and the tanshinone content in the roots is much higher than the tanshinone contents in the original plants and other tetraploid strains [6].

The content of chemical constituents in medicinal plants is an important criterion. Large and flourishing roots, stems, and leaves often have a contradictory effect on the chemical content, and both of them should be considered at the same time. Varieties with large roots, stems, and leaves usually grow quickly and have loose tissues, but they have an adverse effect on the accumulation of chemical constituents. We can see from the results of the study by Gao Shanlin et al. that of more than 20 obtained polyploid strains, most grew quickly and had large and flourishing roots, stems, and leaves, but their content of chemical constituents was not high. 61-2-22 was the only one that did not have roots, stems, and leaves that were too large. Its root system is clustered with multiple roots. Therefore,

it has both high yield and high chemical contents, which meet the ideal standard. After three consecutive years of field test, the average cryptotanshinone content in 61-2-22 strain reached 0.5013 %, which was 203.45 % higher than the content of 0.1652 % in the original plants; the average tanshinone I_A content was 0.1393, which was 70.50 % higher than the content of 0.0817 % in the original plants; the average tanshinone IIA content was 0.3155, which was 53.16 % higher than the content of 0.2060 % in the original plants; the average content of three tanshinones reached 0.956 %, which was 211.1 % higher than the content of 0.4592 % in the original plants. Contents of 3 tanshinones in the 61-2-22 strain were all significantly higher than the contents in the original diploid plants and other tetraploid plants, and the yield of medicinal materials was 71.1 % higher than that of the original diploid plants. This superior strain can be further used in enlarged trial planting for its application and popularization in production [7, 8].

In 2001, Danni et al. [9] used the HPLC method to measure the contents of 3 tanshinones and 2 hydrosoluble phenolic acids in different parts and different years of growth of superior Danshen autotetraploid strain 61-2-22 and Danshen produced in An Hui, Jiangsu, and Shaanxi. The results showed that Danshen strain 61-2-22 had significantly higher contents of effective constituents than the normal Danshen from other places, and the contents of effective constituents in roots were significantly higher than the contents in stems and leaves. Their preliminary pharmacological test results showed that under the same dosage, superior strain 61-2-22 had the best pharmacological activity.

The same research team also reported results of the measurement of field agricultural characters and root yield of polyploids in 2003 and reported results of the HPLC measurement of major effective constituents in the medicinal materials of polyploid roots. It was found that of more than 10 polyploid strains selected, all exhibited typical polyploid characters, and the quality of their roots was greatly improved. Four out of the 10 strains had higher tanshinone contents than the control variety. It was also found

that the yield was significantly related to the contents of tanshinone and tanshinol [10]. They plan to take 3–5 years to carry out large area demonstrative extension by adopting clonal propagation through tissue culture and rapid propagation, so as to gradually replace the degenerated and degraded Danshen varieties currently used in production [11].

Through more than 10 years of experiments, Gao Shanlin et al. proved that the application of tissue culture technology to the mutation breeding of Danshen polyploids is feasible, and the technology is superior to the routine breeding methods. Under the tissue culture condition, the artificial-polyploid-induction breeding method is simple and can treat large quantities of plants, and it provides a high mutagenic efficiency and rapid propagation. Gao Shanlin et al. have created a new approach to the breeding of Danshen. The selected superior strain 61-2-22 can be further used in enlarged trial planting and cultivation to form new Danshen varieties for its popularization and application in production. It must be noted that successful induction of polyploids is only the first step of polyploid breeding. It is more important to screen for the desired types from the multiple types of mutants. Therefore, we have to induce and obtain as many polyploid strains as possible, so as to choose from them the final ideal types in order to help the construction of GAP bases.

6.3 Molecular Breeding of Danshen

6.3.1 Molecular Marker-Assisted Breeding of Danshen

Researchers in China have already carried out genetic diversity analyses of 8 Danshen varieties in five provinces by using the RAPD technology, preliminarily selected RAPD markers that could be used to distinguish and identify Danshen, and found preliminarily molecular markers that are closely linked to genes associated with the biosynthesis of effective constituents in Danshen.

6.3.2 Studies on the Breeding of Danshen by Genetic Engineering

6.3.2.1 Studies on the Mechanism of Biosynthesis of Active Constituents of Danshen

Danshen contains two categories of active constituents: liposoluble diterpenoid guinone compounds and hydrosoluble compounds, of which the liposoluble diterpenoid guinone compounds represented by tanshinone IIA are important medicines for the treatment of cardio-cerebro-vascular diseases. Tanshinones are very similar to abietane compounds and are also called abietane tanshinones. According to the results of the studies on the metabolic pathways of abietane secondary metabolites, we believe that the following pathway is suitable for the study of biosynthetic genes of tanshinone compounds. The gene chip technology is a new technology developed since the 1980s. It can conduct real-time monitoring of all the genes expressed in the entire genome of an organism. It has provided a strong technical tool for the research on the expression of major genes related to the biosynthetic pathway of the main effective constituents in Danshen. Scientists are using this technology to study the relationship between the differences of genuine and non-genuine Danshen in gene expression profiles and the contents of their main effective constituents, especially the content of tanshinone. Their aim is to find out the main genes that participate in the synthesis of many effective constituents in Danshen. After that, the research will be focused on the effects of main environmental factors on the expression level of these genes and fundamentally reveal the nature of how a “genuine Danshen” is formed. In addition, a gene chip containing many major genes involved in the formation of Danshen quality will help for the first time in the world in the detection and monitoring of Danshen quality from the upstream origin and provide brand new research ideas, approaches, and technical tools for the modernization and internationalization of traditional Chinese medicine and pharmacology.

Plants can generate all kinds of secondary metabolites which can be used as drugs or health products. In recent years, studies on the biosynthetic pathways of flavonoid compounds have shown that transcription factors are a very effective new technology in boosting the production of organic compounds with plant genetic engineering technology. The use of specific transcription factors can avoid the time-consuming reaction steps in the multienzyme metabolic pathway and obtain the target products more quickly, because specific transcription factors can control the specific metabolic branches of plant cells. In the future, important transcription factors can be obtained through T-DNA activation tagging, and the effects of transcription factors on gene expression in the biosynthetic pathways of the effective constituents of Danshen will be further studied. In addition, antisense technology is also used for the regulation of the gene expression in the biosynthetic pathway of effective constituents of Danshen, i.e., synthesizing specifically complementary DNA or RNA segments through artificial synthesis or biosynthesis according to the complementary base pairing principle to inhibit or block off certain gene expressions, thus inhibiting the activity of the key enzymes that catalyze a certain branch of metabolism. This can greatly increase the contents of target compounds.

6.3.2.2 *Agrobacteria*-Mediated Danshen Transformation

The *Agrobacteria*-mediated Transformation is the most successful and most widely used method for introducing foreign DNA to plant cells, because *Agrobacteria* can infect most dicotyledons and a small number of monocotyledons, and even gymnosperms, and various explants can be used as the objects of infection. It is simple and easy to repeat and provides a high Transformation frequency.

Transformation of Danshen by *Agrobacteria*

Agrobacteria usually transforms medicinal plants through the generation of adventitious roots or through callus tissue or somatic embryogenesis.

Using *Agrobacteria* to introduce foreign genes into Danshen is an important aspect of the improvement of current Danshen quality and can also be used to study the regulation of the expression of foreign genes in Danshen. In a word, molecular biology is a strong tool for the research on the diversity and regulation of the secondary metabolism of medicinal Danshen and for the genetic engineering of secondary metabolism. Although few transgenic medicinal plants have been obtained, they have already demonstrated great potential in basic research and practical application.

Agrobacteria transformation involves the following steps: the storage and culture of *Agrobacteria* strains, the establishment of an aseptic culture system for medicinal plants, transformation, sterilization and screening, confirmation of Transformation, and other steps. The storage and culture methods for *Agrobacteria* strains are as follows: First, prepare the culture medium. YMB culture medium is used for *Agrobacterium tumefaciens* strain C58, and *Agrobacterium rhizogenes* strains A4 and LBA9402. Its formula includes K_2HPO_4 0.5 g/L, $MgSO_4 \cdot 7H_2O$ 2.0 g/L, NaCl 0.1 g/L, mannite 10.0 g/L, and yeast extract 0.4 g/L. Adjust the medium's pH to 7.0. YEB culture medium is used for *Agrobacterium rhizogenes* strains 15834 and 1601; its formula includes beef extract 5.0 g/L, peptone 5.0 g/L, sugar 5.0 g/L, yeast extract 1.0 g/L, and $MgSO_4$ stock solution (20 mM) 5.0 mL/L. The medium's pH is adjusted to 7.2. Octopine *Agrobacteria* strains include *A. tumefaciens* B6, Ach5, and 15955. Agropine and mannopine strains include *A. tumefaciens* B0542, A281, *A. rhizogenes* 8196, 15834, and A4. Cucumopine strains include *rhizogenes* NCPB2659, and NIAES1724. The above-mentioned strains are inoculated onto corresponding solid culture media for 2 days at 27 °C. When they grow well, store them in refrigerators at 0–5 °C. Subculture them every 2 months. The modification of wild plasmids involves disarming (i.e., remove genes related to the synthesis of phytohormones), retaining the pathogenetic areas and the terminator sequences, adding new foreign genes, and selecting genes, marker genes, and CaMV 35S promoter sequence. Use the modified

plasmids to transform *Agrobacteria*, and thereby, obtain new *Agrobacteria* strains. The binary vector system is also a common plasmid constructing mode and is used to obtain new strains.

The establishment of an aseptic culture system for medicinal plants is an important step in transformation. Seeds can be used to generate seedlings under aseptic conditions through conventional sterilization and tissue culture technology. Other explants can also be used to create regenerated plants under appropriate phytohormone regulation. Hence, a successive subculture system for the medicinal plants can be established under aseptic conditions. Sometimes it is not necessary to establish an in vitro propagation system for the medicinal plant. We can acquire various explants directly from the field or greenhouse and use them directly for transformation after conventional sterilization.

Transformation includes the activation of the bacterial strain, the selection of explants, and the inoculating method (co-cultivation, needling, negative pressure, etc.). Before transformation, take out the *Agrobacteria* strain from the refrigerator and rest it at 25 °C for several hours for activation before use, or transfer it into YEB or YMB liquid medium to which 20–100 $\mu\text{mol/L}$ acetosyringone is added and incubate the culture in a shaker (160 rpm) at 25–28 °C for 30 h before transformation. It is not necessary to add acetosyringone. In a word, the process should be determined according to the effects of transformation. For *Agrobacteria* transformation, there is a wide range of explant options, mainly including the following five major categories: leaves: leaf disks, leaf stems, main leaf veins, and cotyledons; stems: thin sections of internodes and stem segment; hypocotyledon; roots; and buds. Stems and leaves are the most frequently used explants and are most likely to provide successful transformation. The inoculating methods include smearing, co-culture, needle-piercing, and negative pressure. The smearing method is to take leaves, stem segments, seed leaves, hypocotyledonary, roots, and buds as explants, scissor or cut them into pieces, smear the cuts with activated *Agrobacteria*, and finally place them on basic culture media (MS, B5,

67-V, WP, etc.) for several weeks to obtain the transformed tissues and organs. The needling method is to pierce the plant tissues with a dissecting needle coated with activated *Agrobacteria* at the upper ends of aseptically seedling stems, leaf veins, and hypocotyledon of aseptically seedlings and then place them on the basic culture medium for several weeks to obtain the transformed tissues and organs. The co-culture method is to dip aseptically leaf stems, leaf pieces, or root pieces into activated *Agrobacteria* liquid which has been properly diluted with basic medium, wait for about 10 min, take them out and blot up the residual bacteria liquid before putting them back to the basic medium for 2 days, and finally transfer them into the basic culture medium containing 500–1,000 mg/L antibiotic (carbenicillin or cefotaxime is usually used) to obtain transformed tissues and organs; or to co-culture the explants and activate *Agrobacteria* liquid that has been properly diluted with basic culture medium for 24–28 h, take them out and blot up water on surfaces with aseptically paper, and directly place them on solid culture medium containing 500 mg/L antibiotics. If co-culture does not produce a satisfactory inducing effect, negative pressure can be applied to enhance the penetration of activated *Agrobacteria* liquid into the plant tissues when the explants are contacting with the diluted activated *Agrobacteria* liquid. This is commonly known as the negative pressure method.

The transformed tissues and organs must be sterilized and selected. The sterilization of transformed tissues and organs is mostly done on culture medium containing 500–1,000 mg/L antibiotics (carbenicillin or cefotaxime is usually used). Temperature (37–40 °C) sterilization is also used on some occasions. Subculture every 1–4 weeks, and after 3–4 subcultures, transfer the transformed tissues and organs onto a basic culture medium that does not contain antibiotics. If the transformed tissues and organs have resistance to kanamycin, the subculture and screening can be done on a resistance culture medium. Well-grown transformed tissues and organs are subcultured every 4 weeks for future experimental research.

Finally, confirm the results of transformation. The successful transformation of most transformed tissues and organs is confirmed by using high-voltage paper electrophoresis to detect the existence of corresponding opines and by Southern blot hybridization analysis. For conversion involving reporter genes (such as GUS), confirmation is done by detecting the expression (enzyme activity analysis and histochemical staining analysis) of reporter genes. In recent years due to the maturing of the PCR method, the analysis of the existence of *rolB* and *rolC* genes or NPT-II in the converted tissues is mostly used for the confirmation, its amplification primers being *rolB* P1: 5'-GCT CTT GCA GTG CTA GAT TT-3'; *rolB* P2: 5'-GAA GGT GCA AGC TAC CTC TC-3'; *rolC* P1: 5'-CTC CTG ACA TCA AAC TCG TC-3'; *rolC* P2: 5'-TGC TTC GAG TTA TGG GTA CA-3'; *nptII* P1: 5'-TAT GTT ATG TAT GTG CAG ATG ATT-3', *nptII* P2: 5'-GTC GAC TCA CCC GAA GAA CTC GTC-3', respectively. Northern blot hybridization analysis is also used to further confirm the success of transformation in some cases.

6.3.2.3 Breeding of Regenerated Plants from Hairy Roots

Regenerated plants can be obtained from hairy roots and crown gall tissues. The regeneration of plants from hairy roots could be spontaneous or induced by phytohormones. Since the *rol* gene of *agrobacterium* is inserted into the genomes of plants, these regenerated plants usually exhibit a series of paramorphia, which is called “hairy root syndrome.” The contents and constituents of their secondary metabolites may be changed as well. *Agrobacterium rhizogenes* strains 15834 and LBA9402 and *Agrobacterium tumefaciens* strain C58 are used to infect aseptically Danshen seedlings and induce hairy roots and crown gall nodules. The hairy roots and crown gall nodules generate transformed Danshen plants through differentiation on a basic medium without phytohormones under the lighting condition. The regenerated plants are significantly different from the control plants in phenotype whether they are in test tubes or transplanted into soil. The transplanting experiment shows that regenerated

Danshen plants transformed by *Agrobacterium rhizogenes* strains 15834 and LBA9402 have typical characteristics of regenerated hairy root plants, such as shortened internodes, dwarfed plants, and flourishing underground fibrous roots, while the C1 strain of regenerated plants converted by *Agrobacterium tumefaciens* (e.g., C58) grows vigorously and its aboveground plants are taller than the original plants. Its root system is flourishing and thick, and its root yield and total tanshinone content are both higher than those of original plants. The transplanting experiment shows that C1 strain of regenerated plants transformed by *Agrobacterium tumefaciens* has a root yield 41 % higher than the control plants and a total tanshinone content 17 % higher than the control plants. This indicates that genetic engineering can improve the current quality of medicinal materials. Danshen varieties cultivated in recent years have decreasing effective constituents and serious degeneration. The hairy roots of Danshen can spontaneously form regenerated plants without foreign phytohormones. This has provided a new approach for the improvement of Danshen varieties. So far, about 10 superior individual strains have been screened out. Once popularized and applied, such new varieties will create considerable benefits.

The above-mentioned preliminary research shows that some regenerated hairy root plants may have certain advantages, but are far from the goal of mass agricultural production and application and they require further appraisal of agricultural characters. Nevertheless, the results

above still clearly show that the T-DNA insertion method through the *Agrobacteria* transformation system can induce beneficial mutations in Danshen. A batch of superior Danshen plants is thereby obtained. On the basis of these superior plants, if we introduce related key genes on purpose and carry out genetic engineering breeding, the quality and yield of current medicinal materials are likely to be greatly improved.

References

1. Zhen C, Wenjing Y, Hongtao S, et al. Bull Chin Mater Med. 1983;8(1):2.
2. Baolin G, Yuxiu F, Yangjing Z. J Chin Mater Med. 2002;27(7):492–5.
3. Jiayan M. Chin J Rural Med Pharmacy. 2000;7(11):28–9.
4. Wei T, Xiaoliang X, Weixin P, et al. Res Practice Chin Med. 2004;18(1):22–4.
5. Shanlin G, Deran X, Zhaohui C, et al. J China Pharm Univ. 1992;23(4):224–8.
6. Shanlin G, Danni Z, Zhaohui C, et al. China J Chin Mater Med. 1995;20(6):333–5.
7. Danni Z, Shanlin G, Zhaohui C, et al. Pharm Biotechnol. 1996;3(1):22–6.
8. Shanlin G, Danni Z, Zhaohui C, et al. J Plant Res Environ. 1996;5(2):1–4.
9. Danni Z, Shanlin G, Yunyun B, et al. J Plant Res Environ. 2001;10(2):7–10.
10. Jianguo A, Shanlin G. Pharm Biotechnol. 2003;10(6):372–6.
11. Shanlin G. World Sci Technol Modernization Tradit Chin Med. 2001;3(6):58–62.
12. Yinlin Z, Jingyuan S, Jianjun Q, et al. China J Chin Mater Med. 1997;22(5):274–5.

Lianniang Li

7.1 Literature Review

The studies on the chemical constituents of Danshen (*Salvia miltiorrhiza*) were initiated by Japanese researchers in 1930s. They isolated the principle lipophilic components, tanshinone I, cryptotanshinone, and tanshinone IIA, IIB. In 1940s, S. Wang et al. defined the structure of tanshinone I as a diterpenoid quinone, but the relationship between these components and the physiological activity of Danshen was still unknown. During 1970s, the chemistry and pharmacology of the lipophilic constituents of Danshen were studied by the Institute of Materia Medica, Chinese Academy of Medical Sciences, [1] and Shanghai Institute of Materia Medica, [2], and their results showed that the red pigments, i.e., tanshinones, were the effective components for antibacterial activity and for the treatment of coronary heart diseases [4]. Among these, cryptotanshinone was the main antibacterial compound, while tanshinone IIA was the principle compound for the treatment of coronary heart disease.

During the last 20 years, much research on the lipophilic constituents of Danshen has been carried out, more than 60 diterpenoids have been isolated, and the pharmacological activities of

these components have been observed. However, according to traditional Chinese medicinal prescriptions, Danshen has been used as a decoction, and its most popular medicament form in clinical treatments as an injection—both forms contain only water soluble components. Therefore, studies on the biological activities of the water soluble components have attracted a lot of attention. Since the 1970s, studies on the aqueous extract of Danshen have indicated that the water soluble components possess activities in microcirculation improvement, tissue repair, and antithrombosis. However, because the chemical natures of these components were unknown at that time, the pharmacological basis of these activities could not be explained.

In early 1980s, the Institute of Materia Medica, Chinese Academy of Medical Sciences, began systematical studies on the water soluble components of Danshen and isolated 13 phenolic acids, among which salvianolic acid A, B, C, D, E, F, and G were new compounds. Based on these results, the water soluble components of plants in genus *Salvia*, such as *S. yunnanensis*, *S. bowleyana*, *S. flava*, *S. chinensis*, *S. cavaleriei*, *S. cavaleriei* var. *simplicifolia* and *S. prionitis*, were studied, as were the analytical methods for these compounds [3]. The contents of water soluble phenolic acids in 54 samples from 22 plant species belonging to the genus *Salvia*, as well as in many Danshen preparations, were measured using HPTLC scanning and HPLC methods [4, 5]. During this period, the Shanghai First Medical College [6] and Shanghai Institute of Materia

L. Li (✉)
Institute of Materia Medica, Chinese Academy of
Medical Science and Peking Union Medical College,
Beijing, China
e-mail: lilianniang@imm.ac.cn

Medica [7] successfully isolated protocatechuic aldehyde, Danshensu, Danshen acid B and C from injections of Danshen, and the cardiovascular effects of Danshensu were studied. Tanaka et al. isolated magnesium lithospermate B and ammonium–potassium lithospermate B from Danshen, the former showing an improving effect on uremic symptoms [8]. During the recent years, new phenolic acids, yunnaneic acid A, B, C, D, E, F, G, and H, and rabsosiin have been isolated from *S. Yunnannensis* [9, 10].

A large number of studies on the biological activities and mechanisms of the water soluble components of Danshen have been carried out by the Institute of Materia Medica, Chinese Academy of Medical Sciences. It turned out that they all showed strong anti-lipid peroxidation and antithrombic activities; among these, phenolic acids and salvianolic acid A and B were the most potent. These results not only shed light on the water soluble active components of Danshen and their mechanisms from a molecular level, but also provided theoretical information for the development of new medicine from Danshen for the treatment of cardiovascular and cerebrovascular diseases.

7.2 Introduction

The water soluble components of Danshen are mainly phenolic acids. Thirteen phenolic acids from the aqueous extract of Danshen have been isolated with modern separation methods, and 7 of these compounds were depsides. Except for the two known compounds, rosmarinic acid (12) and lithospermic acid (13), these types of depsides were isolated for the first time from plants and were given the names salvianolic acid A (1), B (2), C (3), D (4), and E (5) [11–13].

Salvianolic acid F (6) and G (7) were two new phenolic acids; the former was a stilbene derivative, while the latter possessed an unusual tetracyclic dibenzoxepin skeleton [14]. The other known compounds were protocatechuic aldehyde, protocatechuic acid, isoferulic acid and R-(+)- α -(3,4-dihydroxyphenyl)-lactic acid, named

Danshensu. Of these water soluble phenolic acids, salvianolic acid B was the major component. The genus *Salvia* has more than one hundred species in China, of which about thirty species are used as substitutes of Danshen or as folk medicine. Studies on the water soluble components of nine *Salvia* species led to the isolation of some new depsides besides the former salvianolic acids. Iso salvianolic acid C (11) was isolated from *Salvia chinensis* Benth [15], while a pair of regioisomeric depsides salvianolic acid H (8) and I (9) were isolated from *Salvia cavaleriei* Levl. and *S. cavaleriei* Levl.var. *simplifolia* Peter-Stibál [16, 17]. The main water soluble component of *Sarracenia flava* Forrest was rosmarinic acid; besides this, a minor depside salvianolic acid J (10) [18] and two depsidic glycosides salviaflaside (14) and its methyl ester have also been isolated [19]. Przewalskinic acid (15) [20] was isolated from *Sitta przewalskii* Maxim, and the main water soluble component of *Salvia deserta* Schang was salvianolic acid K (16) [21]. Chemical studies on *Schizothorax yunnanensis* led to the isolation of several phenolic acids with more complicated structural skeleton, namely yunnaneic acid A (17), B (18), C (19), D (20), E (21), F (22), G (23), H (24) and rabsosiin (25). Among them, yunnaneic acid B was the major component.

7.3 Chemical Structures of Phenolic Acids

The chemical structures of the water soluble phenolic acids of Danshen are composed of C_6C_3 units. Danshensu, R-(+)- β -(3,4-dihydroxyphenyl)-lactic acid, is a simple monomeric compound, while most of the phenolic acids are depsides of Danshensu and a caffeic acid derivative or caffeic acid dimer forming several kinds of skeletons. Similar to the free Danshensu, the Danshensu portion of these depsides also possesses an R configuration, while the carbon skeleton of the caffeic acid dimer might be recognized as neolignans. It is noteworthy that most of the lignans obtained naturally are liposoluble

constituents. The water soluble salvianolic acids possess a unique structure of a depside with free hydroxyls in the neolignan skeleton.

Salvianolic acid A and F are stilbene derivatives; it may be formed by decarboxylation of a caffeic acid dimer, which in acidic conditions can be converted to a 2-arylbenzofurane, which is the skeleton of salvianolic acid C. Salvianolic acid B, lithospermic acid and przewalskinic acid possess a 2-aryldihydrobenzofuranoid skeleton with 2*R*, 3*R* configuration and 2β-pseudo-equatorial, 3α-pseudoaxial conformation. Salvianolic acid J has a 2-arylbenzodioxane skeleton, while salvianolic acid G and iso salvianolic acid C possess an unusual dibenzoxepin skeleton.

Rosmarinic acid is a simple depside constructed of Danshensu and caffeic acid, while salvianolic acid E is a dimer of rosmarinic acid; cyclization to a 2-aryldihydrobenzofurane, the skeleton of salvianolic acid B, may occur in acidic conditions. Salvianolic acid H and I are *regio-isomeric* compounds, which may be polymerization products of rosmarinic acid and caffeic acid.

Lithospermic acid B has the same planar structure as salvianolic acid B. However, according to Tanaka, the 2-aryldihydrobenzofuran skeleton possesses a 2*S*, 3*S* configuration. Thus, the absolute configuration of these two phenolic acids needs to be further confirmed.

Yunnaneic acid C and D isolated from *S. yunnannensis* possess a bicyclo [2.2.2] octene skeleton, which might be formed by a Diels-Alder-type addition between rosmarinic acid and caffeic acid. yunnaneic acid A has a dimeric structure composed of yunnaneic acid C and D, which are linked by the formation of a spiroacetal ring. yunnaneic acid B can be regarded as a dimer of yunnaneic acid C. yunnaneic acid E may be generated by oxidative cleavage of the α-diketone part (C-3, C-4) of yunnaneic acid C. yunnaneic acid F is possibly derived from yunnaneic acid C by aldol-type addition of acetic acid to the C-4 carboxyl group. yunnaneic acid G and rabdosiin possess an aryldihydronaphthalene skeleton. yunnaneic acid H has a highly conjugated tetracyclic aryl naphthalene skeleton. The structures of these phenolic acids are shown in Figs. 7.1 and 7.2.

7.4 Extraction and Isolation of Phenolic Acids

7.4.1 Extraction of Phenolic Acids

The phenolic acids of Danshen are polyhydroxy compounds with high polarity, which are easily dissolved in water, methanol, and ethanol and are also soluble in ethyl acetate and acetone, but not soluble in chloroform and ether. According to these characteristics, the total phenolic acid is normally extracted from the medicinal plant materials with water, methanol, ethanol, or aqueous acetone. Besides the total phenolic acid, the extract contains many impurities, such as starches, polysaccharides, proteins, tannins, and pigments, and needs to be purified.

7.4.1.1 Extraction with Water and Precipitation with Ethanol

The dried medicinal plant materials are extracted with water under reflux, and the aqueous extract is concentrated to a volume equal to the weight of the plant material. Ethanol is added to a content of 70 % and the extract is left overnight. The precipitate, which contains starches, polysaccharides, and proteins, is filtered off, and after condensation, the filtrate is extracted with chloroform to remove pigments. The aqueous portion is acidified to pH 3 and successively extracted with ethyl acetate and n-BuOH to obtain the total phenolic acid.

7.4.1.2 Macroporous Resin Chromatography

Macroporous resin can absorb phenolic acids from the aqueous extract and remove polysaccharides, oligosaccharides, and other impurities. The commonly used macroporous resins include HP20 of Mitsubishi, Japan, Amberlite XAD, USA, and other domestic macroporous resins. The concentrated aqueous extract of Danshen is subjected to macroporous resin column chromatography, eluted with water to remove polysaccharides and other impurities, and then eluted with 50 % Ethanol, which yields the total phenolic acid after concentration through drying.

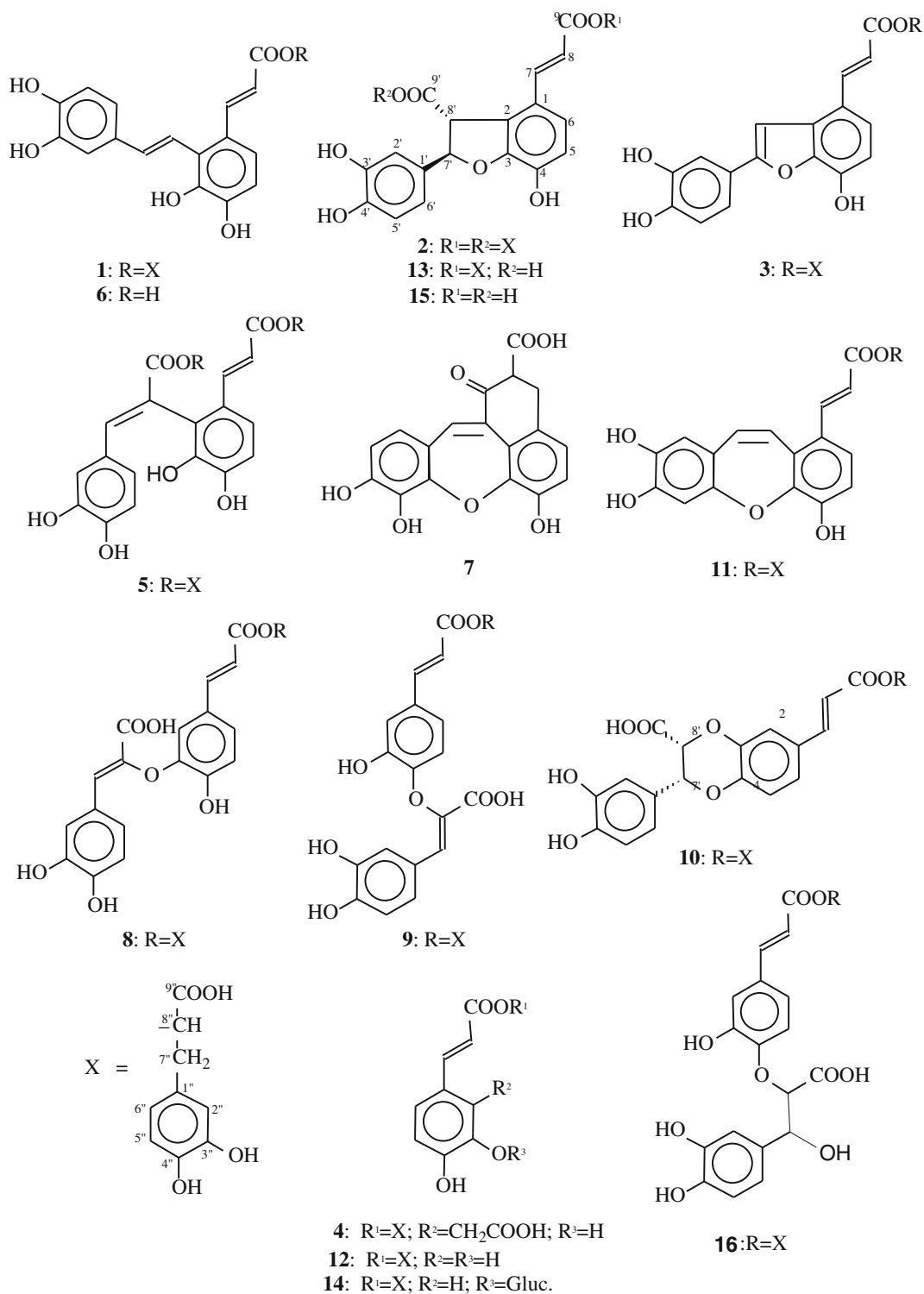


Fig. 7.1 Chemical structures of salvianolic acids

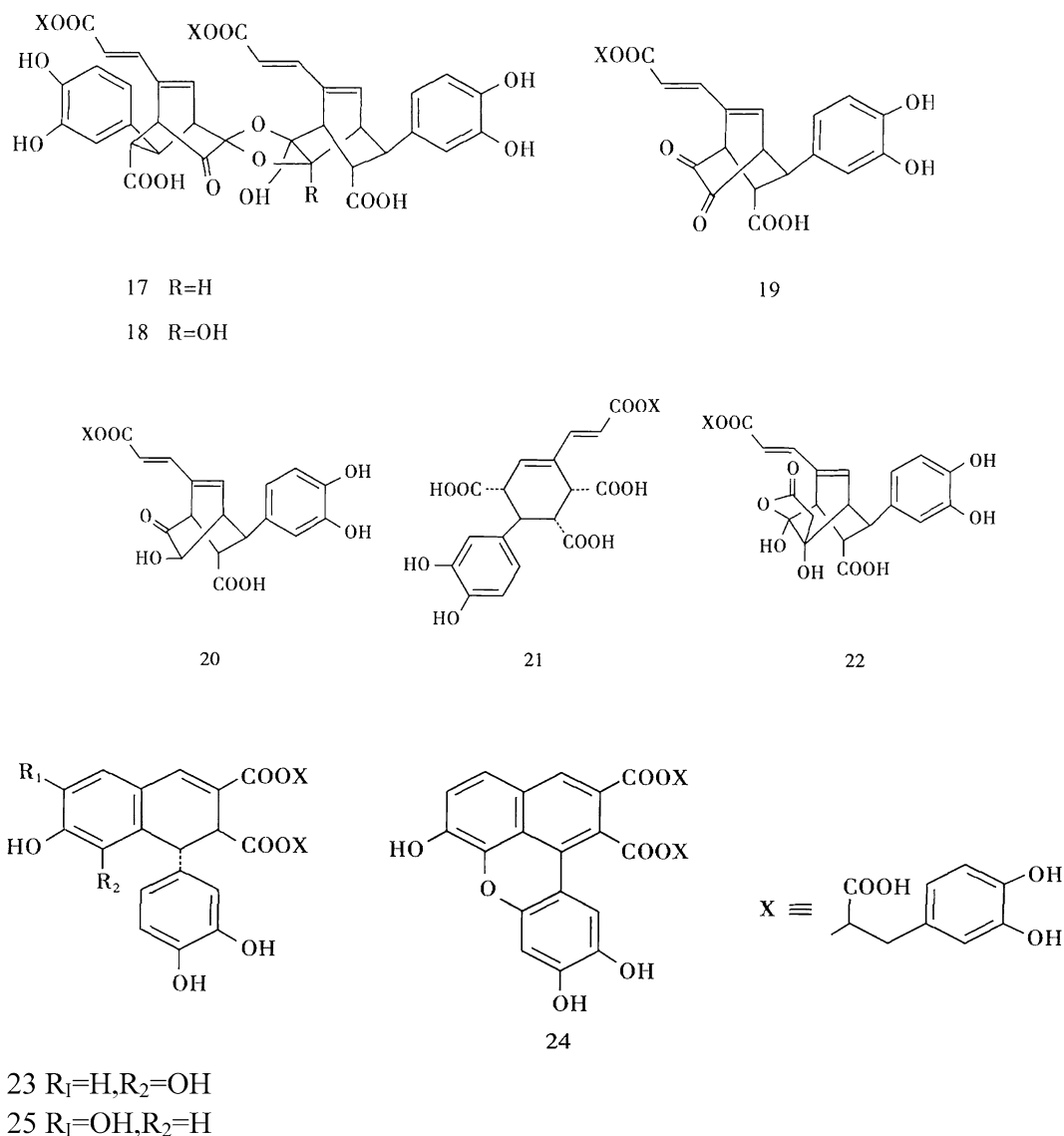


Fig. 7.2 Chemical structures of Yunnaneic acids

7.4.1.3 Extraction with Ethanol and Dissolution in Water

The medicinal plant materials are extracted with 95 % ethanol under reflux. After evaporating the ethanol, the residue is extracted exhaustively with hot H_2O . The concentrated aqueous extract is further extracted with $CHCl_3$ to remove tanshinone and pigments, and then, the aqueous portion is acidified to pH 3 and successively extracted with ethyl acetate and n-BuOH, yielding the total phenolic acid after evaporation.

7.4.2 Isolation of Phenolic Acids

7.4.2.1 Silica Gel Dry Column Chromatography

The total phenolic acids are applied on a silica gel (80–100 mesh) column and separated with $CHCl_3:MeOH:HCOOH$ (85:15:1) as the solvent. The column is divided into several portions and each portion is then eluted with warm ethanol. A rough separation according to polarity is obtained by this method.

7.4.2.2 Flash Chromatography

Silica gel type H is used as the absorbent, and CHCl_3 :MeOH:HCOOH solution at various ratios (95:5:1; 90:10:1; 85:15:1) is used as the solvent. It might be used for further separation of the sections obtained by silica gel dry column chromatography.

7.4.2.3 Preparative TLC

The sections obtained by the above methods can be further isolated by preparative silica gel GF₂₅₄ as the absorbent, using CHCl_3 :MeOH:HCOOH (85:15:1) as the developing solvent. The individual fluorescent bands can be cut and phenolic acids can be eluted with acetone. This method might be used for isolating small amount salvianolic acids.

7.4.2.4 Sephadex LH-20 Column Chromatography

Chromatography over Sephadex LH-20 with methanol as the solvent has the advantage of high recovery of the phenolic acids, while the absorbent can be repeatedly used.

7.4.2.5 High-pressure Liquid Chromatography

Reverse-phase ODS columns could separate phenolic acids, which are difficult to separate by other routine methods, such as salvianolic acid H and I. The moving phase is acetonitrile–water–phosphoric acid (or acetic acid), and the sample is monitored with an UV detector.

7.4.3 Examples of Phenolic Acid Isolation

7.4.3.1 Isolation of Salvianolic Acid A, B, C, D, and E

Danshen (32 kg) was extracted with 95 % ethanol under reflux, yielding the ethanol extract (I). The residue was extracted with water under reflux to obtain the aqueous extract (II). The ethanol extract (I) was concentrated, and then, hot water was added and left overnight, yielding a brown-red precipitate, i.e., tanshinone. After

filtration, the aqueous phase was concentrated and 3 kg of silica gel was added and mixed well and washed sequentially with chloroform, ethyl acetate, and ethanol in a modified Soxhlet apparatus.

The ethanol extract was concentrated under reduced pressure to give a brown powder (1.17 kg) of which 500 g was dissolved in water and extracted with ethyl acetate. The organic extract was concentrated under reduced pressure to yield an amorphous powder (104 g), of which 90 g was divided into two parts and each part was separated by silica gel (2.3 kg) dry column chromatography with CHCl_3 –MeOH–HCOOH (85:15:1) as the solvent. The column was divided into 16 equal sections, which were numbered from the bottom to the top and individually eluted with warm ethanol. After concentration, the eluent of Sects. 13–14 was further separated on Sephadex LH-20 with methanol as the solvent and yielded 2.06 g of salvianolic acid B. The eluent of Sects. 10–12 was further separated with preparative TLC, using CHCl_3 –MeOH–HCOOH (85:15:1) as the solvent, and yielded 0.7 g of salvianolic acid A and 0.4 g of salvianolic acid C. Rosmarinic acid (4.8 g) was obtained from Sects. 7–9 after purification on Sephadex LH-20.

The aqueous extract (II) was concentrated, and ethanol was then added to a concentration of 70 % and left overnight. After filtering and the removal of the solvent under reduced pressure, the extractum (3.95 kg) was mixed with 3 kg of silica gel and sequentially extracted with dichloromethane, ethanol, and water in a modified Soxhlet apparatus. 1,000 ml of the 4,390 ml aqueous extract was acidified with 10 % HCl and extracted with ethyl acetate thoroughly. The organic layer was concentrated under reduced pressure giving a brown powder (35 g), of which 16 g was chromatographed on a Sephadex LH-20 column using methanol as the solvent. Four fractions were obtained. Each fraction was purified by Sephadex LH-20 column chromatography and preparative TLC, obtaining salvianolic acid D (120 mg), salvianolic acid E (80 mg), ethyl lithospermate (600 mg) and isoferulic acid (110 mg).

7.4.3.2 Isolation of Magnesium Lithospermate B and Ammonium–Potassium Lithospermate B [8]

Danshen (1 kg) was extracted twice with 1.5 L of water at 80 °C. The aqueous extract was concentrated under reduced pressure at 40 °C and subjected to a macroporous resin CHP-20P column (7.5 cm × 35 cm). After washing the column with water, the column was eluted with 50 % methanol, yielding 62 g of total phenolic acids, which were further separated by Sephadex LH-20 column chromatography with a gradient solvent of water and ethanol, yielding three fractions: I (4.8 g), II (0.35 g), III (5.9 g), plus magnesium lithospermate B (7.56 g). Fractions I and III were separately chromatographed over Sephadex LH-20 and eluted with water, yielding 1.98 g of ammonium–potassium lithospermate B and another 4.3 g of magnesium lithospermate B.

7.4.3.3 Isolation of Yunnaneic Acid A-H [9, 10]

The dried roots of Danshen were extracted with 70 % acetone. The extract (300 g) was subjected to macroporous resin (1.5 L) column chromatography with water containing increasing proportions of methanol (0 → 100 %, stepwise elution with 10 % increase at each step) to give four fractions, of which the first two were positive to FeCl₃ reagent. The second fraction (19 g) was separated by Sephadex LH-20 (60 → 80 % methanol in water) and macroporous resin CHP20P (30 → 40 % methanol in water) chromatography to yield lithospermate B (1.8 g) and rosmarinic acid (0.3 g). The first fraction was concentrated to give an aqueous solution, which was acidified with 2 M HCl to pH 2 at 0 °C and immediately applied to a Sephadex LH-20 (1.5 L) column with water. After washing the column with water to elute inorganic materials and sugars, the phenolic substances were eluted with aqueous methanol (20 → 40 → 60 %, each 2 L) to obtain 4 fractions. The third fraction was subsequently chromatographed over macroporous resin CHP 20P, Chromatorex ODS with aqueous methanol (30 → 40 %), Sephadex LH-20 (40 → 60 % methanol), and Toyopearl HW-

40F (40 → 80 % methanol) to obtain yunnaneic acid E (209 mg), yunnaneic acid F (370 mg), yunnaneic acid G (113 mg), rabdosiin (74 mg), yunnaneic acid C (610 mg), and yunnaneic acid D (240 mg). The fourth fraction was subjected to Chromatorex ODS chromatography with water containing increasing amounts of methanol to yield yunnaneic acid H (133 mg), yunnaneic acid A (670 mg), and yunnaneic acid B (3.8 g).

7.5 Spectral Properties of Phenolic Acids

7.5.1 Ultraviolet Spectra

The UV spectra of salvianolic acids exhibited characteristic absorptions for a cinnamoyl chromophore at 203, 290, and 310 nm. A shoulder at 220 nm was observed in the spectra of some compounds. A highly conjugated system in the structure increased the intensity at 310 nm and caused an additional absorption maximum at 340 nm. Salvianolic acid B and lithospermic acid, which possess an aryldihydrobenzofuranoid skeleton, revealed absorption peaks at 253 nm. See Table 7.1.

7.5.2 Mass Spectrometry

Due to the fact that salvianolic acids are highly polar compounds, the molecular ions could only be determined by FDMS or FAB-MS. However, the methylated products revealed a diagnostic fragmentation pattern caused by McLafferty rearrangement of β-(3,4-dimethoxyphenyl) lactic ester at m/z 222 and (M^+ -222), and in addition, the characteristic fragment ions at m/z 191, 181, 163, and 151 could also be observed. See Fig. 7.3.

7.5.3 Nuclear Magnetic Resonance Spectra

7.5.3.1 NMR Spectra of ¹H

The ¹H-NMR spectra of salvianolic acids revealed signals of *trans* disubstituted double

Table 7.1 ^{13}C -NMR spectral data of salvianolic acids

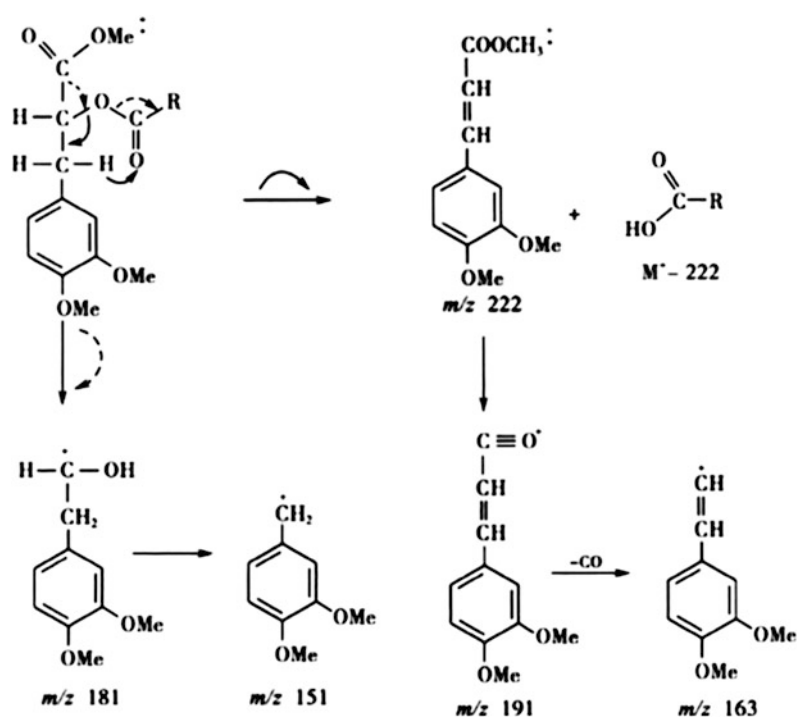
C	Compound									
	2	2a	3b	7	7a	8a	9	10	11b	14
1	126.1	128.0	119.2	127.1	126.7	127.5	130.8	128.0	124.5	125.8
2	133.2	132.5	130.0	127.6	127.0	112.9	116.7	116.7	130.1	116.2
3	146.2	148.7	142.5	139.3	139.6	146.2	146.3	144.0	145.7	145.5
4	148.6	149.5	149.0	144.6	147.1	151.3	148.3	142.9	152.4	149.3
5	117.9	111.4	106.5	140.6	139.1	112.7	116.5	117.1	112.7	116.0
6	118.2	116.4	111.9	120.2	116.3	124.2	122.2	122.5	124.2	124.0
7	142.8	142.0	141.0	40.7	39.2	145.3	146.7	145.0	134.0	144.7
8	113.2	113.4	117.1	37.7	36.9	115.4	116.4	115.5	119.6	116.5
9	166.9	165.8	168.0	173.1	171.2	166.1	168.2	165.9	167.2	166.1
1'	124.4	124.7	125.0	120.1	118.9	125.3	125.8	127.7	121.9	
2'	113.4	108.9	108.3	127.6	132.7	113.0	118.2	114.6	111.6	
3'	146.0	149.5	146.0	140.6	142.2	149.1	146.4	145.3	150.4	
4'	144.2	146.2	150.0	151.9	157.3	150.8	148.8	145.4	146.0	
5'	117.1	117.9	118.0	125.8	123.6	111.3	115.7	115.5	105.3	
6'	121.0	120.5	122.0	129.2	131.4	124.9	124.9	118.2	150.7	
7'	87.5	87.3	157.0	114.4	110.5	128.0	129.2	75.0	131.2	
8'	57.2	55.8	99.7	125.9	124.1	137.8	139.36	76.5	124.4	
9'	170.2	170.2		169.1	167.8	163.9	167.0	169.6		
1''	128.7	128.0				128.6	129.5	127.2		129.8
	129.1	128.5								
2''	116.7	114.4				1,136.0	117.7	116.8		115.9
	116.1	111.4								
3''	144.5	148.1				148.4	146.1	145.0		143.4
	144.6	148.3								
4''	145.5	148.7				149.1	145.2	145.1		144.0
	145.6	149.5								
5''	116.0	112.7				111.7	116.4	116.8		115.4
	116.1	112.7								
6''	121.3	121.1				121.6	121.7	120.0		119.8
	121.7	121.6								
7''	37.1	36.6				37.2	37.9	36.3		37.0
	37.5	37.0								
8''	74.2	73.1				73.1	74.9	73.5		73.4
	75.1	74.1								
9''	171.3	169.3				170.3	173.7	171.2		172.4
	172.1	170.2								
OCH ₃		52.2			51.5	52.2				101.8 ^a
		52.2				52.4				75.5 ^b

(continued)

Table 7.1 (continued)

C	Compound									
	2	2a	3b	7	7a	8a	9	10	11b	14
		55.8	55.7		56.0	55.9			55.9	75.8 ^c
		(×4)								69.9 ^d
		56.1	55.5		56.9	55.6			55.7	77.1 ^e
		(×2)								60.7 ^f
		56.4	55.9		61.3	56.0 (×2)			56.1	
						56.4				
Solvent	C	C	D	A	C	A	D	D	D	D

Note C: CDCl₃; A: (CD₃)₂CO; D: DMSO-d₆; ^{a,b,c,d,e,f} Glu-1'',2'',3'',4'',5''0.6''; a: methylated compound; b: hydrolysis product of methylated compound

Fig. 7.3 MS fragmentation of methylated salvianolic acids

bonds at δ 7.60–8.00 (α -H) and δ 6.20–6.30 (β -H) with coupling constants of $J = 16$ Hz. The 3,4-dihydroxyphenyl lactic moiety showed signals of two methylene proton doublets at δ 3.0–3.5, an oxygen bearing a methine proton at δ 5.18–5.33 ($J = 4/7$ Hz) and three aromatic protons at δ 6.7–6.9. A pair of doublets at δ 4.40–4.50 ($J = 5.4$ Hz) and δ 5.90–6.10 ($J = 5.4$ Hz) indicated the presence of a *trans* disubstituted

dihydrobenzofuranoid skeleton for salvianolic acid B and lithospermic acid. A relative downfield olefinic proton singlet at δ 8.0 ± 0.1 for salvianolic acid E suggested that the two phenyl groups of the carboxystilbene should be *cis* oriented. In the *trans* isomer, this proton signal was less deshielded and appeared at δ 7.2. The dibenzooxepin skeleton of iso salvianolic acid C was deduced from the fact that the two olefinic

signals possessed a coupling constant of $J = 11.5$ Hz. The stereostructure might be determined according to the coupling constant of the proton on the chiral carbon; a coupling constant of $J = 3$ Hz between the two protons on the dioxane ring of salvianolic acid J indicated a *cis* configuration. The methoxyl signals of the 2-aryldihydrofuran of methylated salvianolic acid B and its hydrolysis product appeared at about δ 3.80, indicating that the C-3 methoxycarbonyl on the furan ring was not shielded by the aryl group; thus, the C-3 carboxyl and C-2 aryl possessed *trans* configuration. A coupling constant of $J = 5.4$ Hz indicated a pseudoequatorial aryl and pseudoaxial carboxyl conformation with a dihedral angle of $\sim 135^\circ$ between C-3H and C-2H. Salvianolic acid H and I were two *regioisomeric* compounds, and the linkage of the caffeic acid portion in these two compounds was determined by NOE experiment (Fig. 7.4).

7.5.3.2 NMR Spectra of ^{13}C

The ^{13}C -NMR spectral data of salvianolic acids and related compounds are listed in Tables 7.1, 7.2 and 7.3.

7.5.3.3 Two-dimensional Nuclear Magnetic Resonance

Two-dimensional nuclear magnetic resonance is very useful for elucidating the structure of new salvianolic acids. Through the application of C, H-COSY and C, H-COLOC, the location of the protons and carbons in the structure can be rapidly and unambiguously determined. The structures of salvianolic acid G and iso salvianolic acid C with dibenzoxepin skeleton as well as those of the two minor regioisomeric compounds salvianolic acid H and I were elucidated by these techniques. The locations of the two substitutes on the dibenzoxepin skeleton of salvianolic acid J were determined by HMBC analysis. The calculated chemical shift value of the aryl bearing methine proton should be δ 5.31, while that of the carboxyl bearing methine proton should be δ 4.81. Selective irradiation of δ 5.31 and the aromatic proton doublet at δ 7.28 ($J = 2$ Hz, C-2H) caused enhancement of the C-4 signal at δ 142.9 in both cases. Thus, this carbon (C-4) was coupled individually through three bonds to C-7'H and C-2H. Therefore, the aryl group should be at C-7' and carboxyl group at C-8' of the dibenzoxepin.

Fig. 7.4 Structure of yunnaneic acid A (17) and B (18)

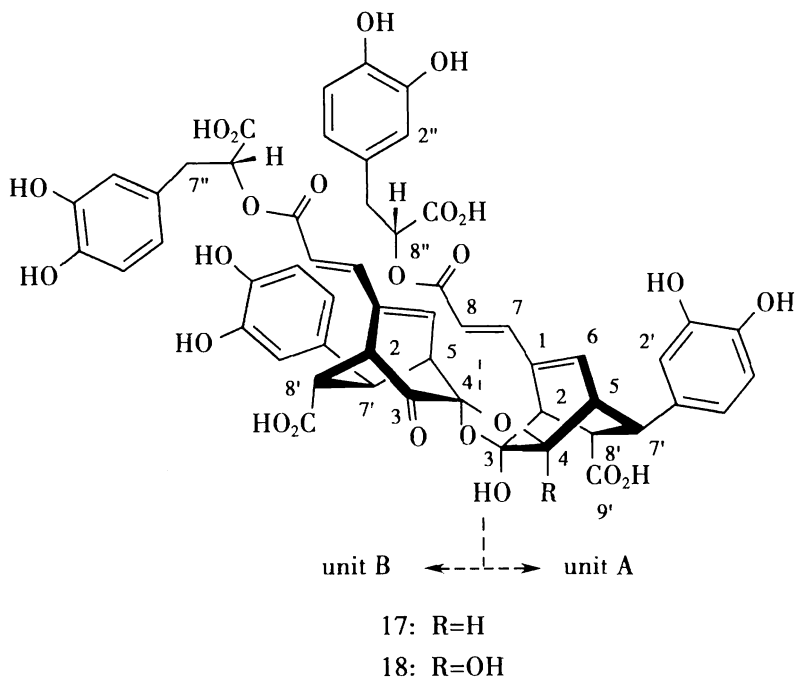


Table 7.2 ^{13}C -NMR spectral data (acetone- d_6) of yunnaneic acid A(17) and B(18)

C	Compound		C	Compound	
	17	18		17	18
A-1	141.9	141.6	B-1	137.9	137.7
A-2	44.9	46.2	B-2	50.6	51.0
A-3	109.1	105.8	B-3	207.5	206.3
A-4	88.1	106.3	B-4	103.0	101.6
A-5	45.5	50.5	B-5	50.9	51.0
A-6	139.0	139.8	B-6	140.6	140.6
A-7	143.6	142.7	B-7	141.5	141.7
A-8	116.7	117.3	B-8	118.7	118.7
A-9	166.9	167.0	B-9	166.3	166.5
A-1'	136.9	137.0	B-1'	135.4	135.3
A-2'	115.4	115.5	B-2'	114.9	115.0
A-3'	145.6	145.6	B-3'	145.7	145.6
A-4'	144.5	144.8	B-4'	144.8	144.5
A-5'	116.0	116.0	B-5'	116.2	116.2
A-6'	119.7	120.0	B-6'	120.2	120.3
A-7'	40.7	40.3	B-7'	43.1	42.6
A-8'	50.0	50.3	B-8'	51.2	50.5
A-9'	173.4	174.0	B-9'	173.6	174.2
A-1''	128.8	128.7	B-1''	128.9	128.9
A-2''	117.5	117.5	B-2''	117.3	117.5
A-3''	145.6	145.7	B-3''	145.7	145.7
A-4''	144.8	144.8	B-4''	144.8	144.8
A-5''	116.0	116.0	B-5''	116.0	116.0
A-6''	121.7	121.7	B-6''	121.6	121.6
A-7''	37.4	37.4	B-7''	37.3	37.4
A-8''	74.1	74.3	B-8''	74.0	74.2
A-9''	171.2	171.4	B-9''	170.9	171.1

7.6 Physical and Chemical Properties of Phenolic Acids

7.6.1 General Properties

Most of the salvianolic acids are colorless or tan amorphous powders. The compounds with a strong conjugated system such as salvianolic acid A, C, G, yunnaneic acid C and H appear as a yellowish amorphous powder, of which yunnaneic acid H, with the strongest conjugated

system, has a dark yellowish color. Due to the presence of a chiral carbon in the structure, these compounds are optically active; their specific rotation is listed in Table 7.4.

Salvianolic acids are easily dissolved in water, ethanol, methanol, and acetone and are also soluble in ethyl acetate, yielding an acidic solution, but are not soluble in chloroform and ether. Magnesium lithospermate B and ammonium--potassium lithospermate B are less soluble in acetone and ethyl acetate, and their aqueous solutions are neutral.

Table 7.3 ^{13}C -NMR spectral data (acetone- d_6) of yunnaneic acid E(21), F(22), G(23) and H(24)

C	Compound			
	21	22	23	24
C-1	133.7	142.4	39.6	126.1
C-2	138.5	45.1	47.6	120.5
C-3	52.9	107.3	135.5	124.9
C-4	38.9	76.2	140.3	130.3
C-5	48.5	51.1	122.7	122.5
C-6	44.6	140.4	114.2	120.9
C-7	146.8	142.5	143.8	143.2
C-8	117.3	118.1	148.4	137.8
C-9	166.7	166.5	124.8	124.4
C-10	172.9		125.3	127.4
C-11	173.1		172.0	170.2
C-12	173.5		166.7	166.1
C-1'	134.5	137.2	121.1	110.4
C-2'	116.5	116.0	115.5	148.9
C-3'	145.3	145.7	145.7	104.7
C-4'	144.5	144.5	143.8	147.7
C-5'	115.8	115.5	116.0	142.2
C-6'	120.4	119.8	119.8	113.4
C-7'		38.3		
C-8'		51.3		
C-1''(C-1''')	128.8	128.9	129.0,129.1	127.9,128.8
C-2''(C-2''')	117.4	117.3	117.5,117.6	117.5,117.7
C-3''(C-3''')	145.6	145.7	145.3,145.5	145.4,145.8
C-4''(C-4''')	144.7	144.8	144.7,144.8	144.7,144.9
C-5''(C-5''')	116.1	116.0	116.0,116.1	115.8,116.1
C-6''(C-6''')	121.5	121.7	121.8,121.9	121.7,122.1
C-7''(C-7''')	37.3	37.4	37.2,37.5	37.2,37.7
C-8''(C-8''')	74.3	74.4	74.2,74.5	74.7,76.1
C-9''(C-9''')	171.8	170.9	170.9,171.1	171.1,172.6
CH ₂		44.2		
COO		173.1		

This type of compound showed the positive color reaction of phenolic hydroxyls, such as a dark green color with ferric chloride and a blue color with a fresh mixture of 1 % ferric chloride and 1 % potassium ferricyanide. Thin layer chromatography showed various fluorescent

spots under 254 nm UV light, such as blue fluorescent for salvianolic acid B, lithospermic acid, and rosmarinic acid, dark yellow fluorescent for salvianolic acid A, bright green for salvianolic acid C, and bright yellow for iso salvianolic acid C.

Table 7.4 Specific rotation of salvianolic acids and related compounds

Compound	Molecular weight	Molecular formula	Specific rotation
Salvianolic A	494	C ₂₆ H ₂₂ O ₁₀	+41° (ethanol)
Salvianolic B	718	C ₃₆ H ₃₀ O ₁₆	+92° (ethanol)
Salvianolic C	492	C ₂₆ H ₂₀ O ₁₀	+70° (ethanol)
Salvianolic D	418	C ₂₀ H ₁₈ O ₁₀	+68° (ethanol)
Salvianolic E	718	C ₃₆ H ₃₀ O ₁₆	+59° (ethanol)
Salvianolic F	314	C ₁₇ H ₁₄ O ₆	
Salvianolic G	340	C ₁₈ H ₁₂ O ₇	−100° (ethanol)
Salvianolic H	538	C ₂₇ H ₂₂ O ₁₂	+63° (ethanol)
Salvianolic I	538	C ₂₇ H ₂₂ O ₁₂	+71° (ethanol)
Salvianolic J	538	C ₂₇ H ₂₂ O ₁₂	+26° (ethanol)
Iso salvianolic acid C	492	C ₂₆ H ₂₀ O ₁₀	+39° (ethanol)
Rosmarinic acid	360	C ₁₈ H ₁₆ O ₈	+67° (ethanol)
Lithospermic acid	538	C ₂₇ H ₂₂ O ₁₂	+12° (ethanol)
Salviaflaside	522	C ₂₄ H ₂₆ O ₁₃	+18.5° (ethanol)
Przewalskinic acid	358	C ₁₈ H ₁₄ O ₈	
salvianolic acid K	556	C ₂₇ H ₂₄ O ₁₃	+31.2° (water)
Yunnaneic acid A	1,078	C ₅₄ H ₄₆ O ₂₄	+86.1° (methanol)
Yunnaneic acid B	1,094	C ₅₄ H ₄₆ O ₂₅	+80.5° (methanol)
Yunnaneic acid C	538	C ₂₇ H ₂₂ O ₁₂	+106.9° (methanol)
Yunnaneic acid D	540	C ₂₇ H ₂₄ O ₁₂	+234.4° (methanol)
Yunnaneic acid E	572	C ₂₇ H ₂₄ O ₁₄	+81.3° (methanol)
Yunnaneic acid F	598	C ₂₉ H ₂₆ O ₁₄	+126.6° (methanol)
Yunnaneic acid G	718	C ₃₆ H ₃₀ O ₁₆	−50.4° (methanol)
Yunnaneic acid H	714	C ₃₆ H ₂₆ O ₁₆	+55.3° (methanol)

7.6.2 Stability

Due to the presence of a 3,4-dihydroxyphenyl in the structure, these types of compounds are easily oxidized in air, polymerized, and deteriorated. These compounds are labile to light and heat and in solution.

7.6.2.1 Effect of pH

The aqueous solution is relatively stable at pH 3–4. In neutral or alkaline solutions, the color turns dark and the content decreases.

7.6.2.2 Effect of Temperature

Salvianolic acid B is easily broken down, producing Danshensu at high temperature. Due to the repeated heating at high temperatures during

the traditional preparation methods of Danshen injection, the content of salvianolic acid B is very low, with the main components being Danshensu and protocatechuic aldehyde.

7.6.3 Chemical Transformation

7.6.3.1 Methylation of Salvianolic Acids

Due to the presence of 3,4-dihydroxyphenol in the structure, salvianolic acids and related compounds are very labile in hot alkaline solutions. Therefore, the methylation of these compounds is carried out under mild conditions with anhydrous potassium carbonate in anhydrous acetone and dimethylsulfate under nitrogen flow and at room temperature, while stirring. Dimethylsulfate can

be added several times in the case of compounds with polyhydroxyl groups, and the reaction time extended to obtain a fully methylated product.

7.6.3.2 Hydrolysis of Methylated Salvianolic Acidss

Most salvianolic acids are depsides of Danshensu and a caffeic acid derivative or caffeic acid dimer. The structure of this moiety can be elucidated by hydrolysis of the methylated salvianolic acid. A mild hydrolysis process is necessary for alkaline sensitive compounds. For example, hydrolysis of methylated salvianolic acid B with 10 % KOH/methanol under reflux causes a base-induced ring opening of the dihydrobenzofuran, yielding a carboxystilbene skeleton. On the other hand, treatment of the same compound with a cool solution of MeONa in CHCl_3 at 0 °C yields a methylated 2-aryldihydrobenzofuranoid compound and a non-optically active racemate of (*R*, *S*)-methyl- β -(3,4-dimethoxyphenyl)-lactate.

7.6.3.3 Transformation of Salvianolic Acid A

Dot 50 mg of salvianolic acid A on a TLC plate impregnated with CHCl_3 -MeOH-HCOOH (85:15:2). Develop the plate twice with CHCl_3 -MeOH-HCOOH (85:15:1). Observe the plate under a UV lamp (254 nm), and a dark yellow fluorescent band of salvianolic acid A and another bright green fluorescent band can be seen. Elution of the individual bands with acetone yielded 20 mg of salvianolic acid C and 10 mg of salvianolic acid A, indicating that salvianolic acid A can be transformed into salvianolic acid C under acidic conditions.

7.6.3.4 Transformation of Salvianolic Acid B

Base-induced ring opening of the dihydrofuran skeleton of salvianolic acid B leads to the formation of the carboxystilbene skeleton of salvianolic acid E. To 70 mg of salvianolic acid B, add 50 mg of anhydrous K_2CO_3 , 0.5 ml of dimethylsulfate, and 5 ml of anhydrous acetone.

The mixture is refluxed under nitrogen flow for 10 h. The usual work-up yields 25 mg of dimethyl heptamethylsalvianolate B and 40 mg of dimethyl octamethyl salvianolate E.

7.7 Biosynthetic Pathways of Phenolic Acids

The biogenesis of the various carbon skeletons of the salvianolic acids might be explained by oxidative coupling of caffeic acid as depicted in Figs. 7.5 and 7.6. The biosynthetic pathways of the yunnaneic acids are illustrated in Fig. 7.7.

7.8 Synthesis of Phenolic Acids

7.8.1 Synthesis of Danshensu [22]

Using protocatechuic aldehyde as the starting material, Xue F. et al. of the Shanghai First Medical College synthesized a racemate of β -(3,4-dihydroxyphenyl)-lactic acid, with an overall yield of 37 %. The synthetic route is depicted in Fig. 7.8. Protocatechuic aldehyde was converted to azlactone (I), then recrystallization in boiling water yielded a ring-opening product (II), and hydrolysis in 1 mol/L afforded an α -ketonic acid (III). Due to the fact that the α -ketonic acid (III) was not stable and required a high vacuum condition under nitrogen flow, the isolation of III was omitted and II was directly hydrolyzed and reduced to the α -hydroxy acid (IV). This reaction condition, refluxed under hydrogen flow, was quite mild and did not require nitrogen flow. So, the procedure was simplified and the yield increased. The free acid was dissolved in methanol and neutralized with 5–7 % Na_2CO_3 solution, and the white precipitate was filtered and washed with a small amount of ether, yielding β -(3,4-dihydroxyphenyl) sodium lactate (Danshensu, yield 65.7 %). The synthesized Danshensu

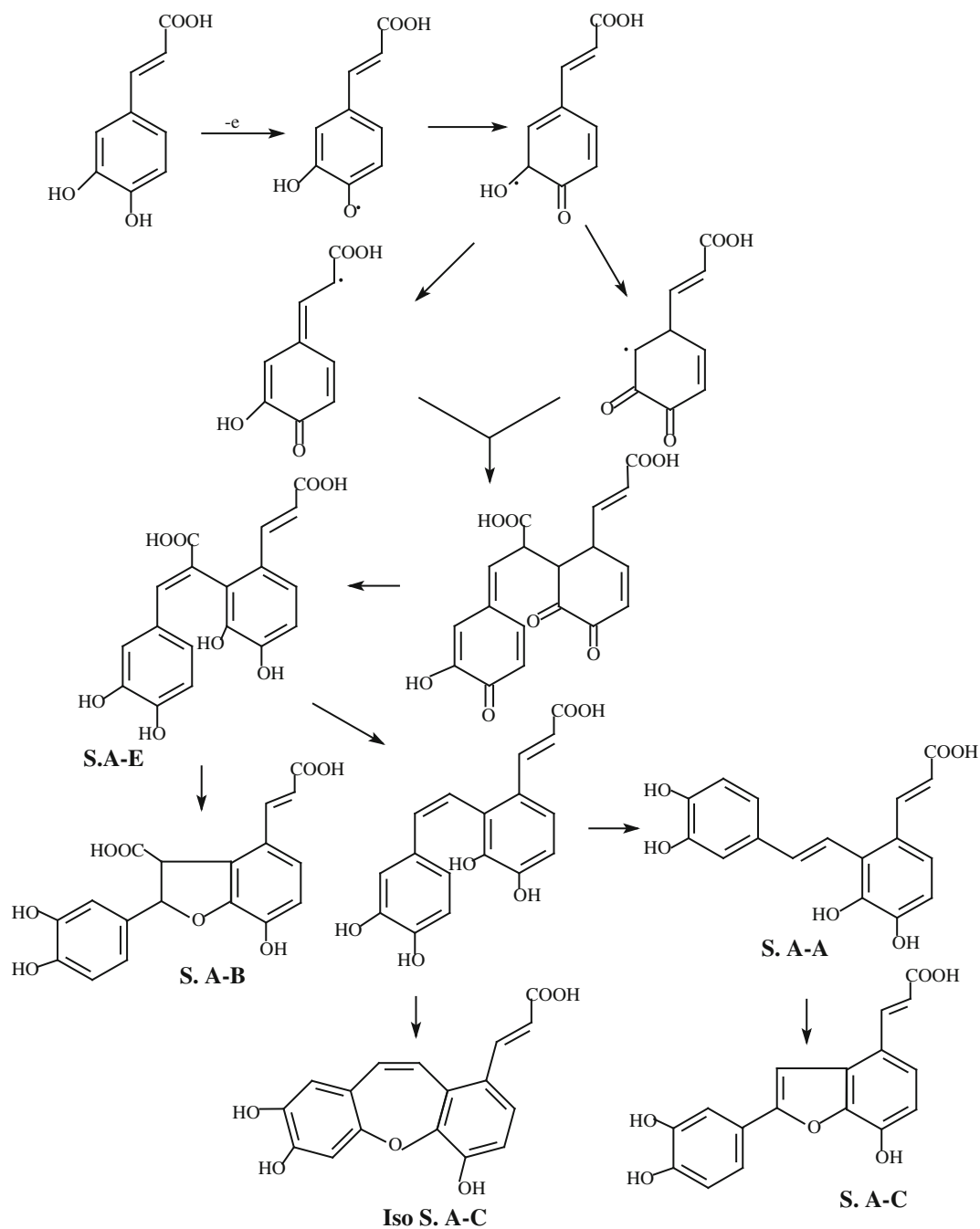
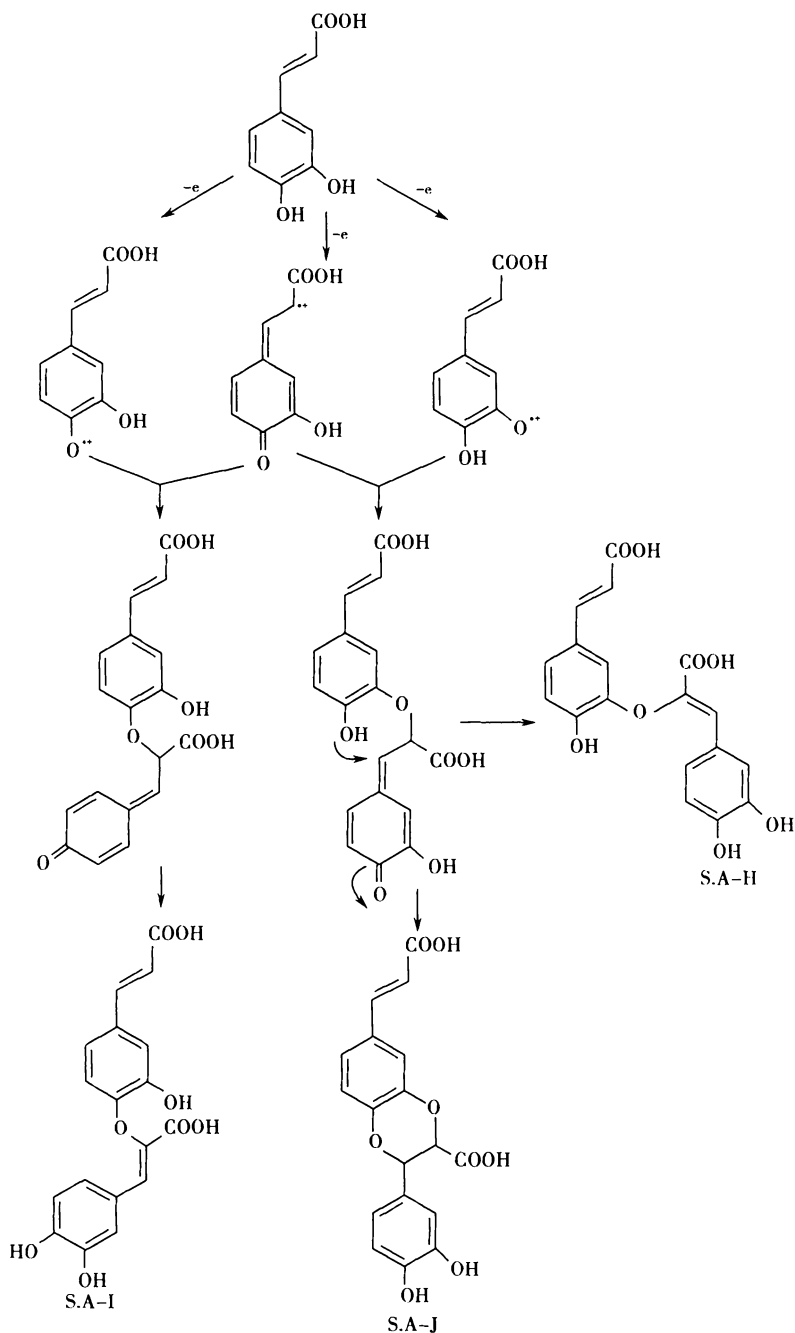


Fig. 7.5 Biosynthetic pathways of salvianolic acid A, B, C, E and iso salvianolic acid C

Fig. 7.6 Biosynthetic pathways of salvianolic acid H, I and J

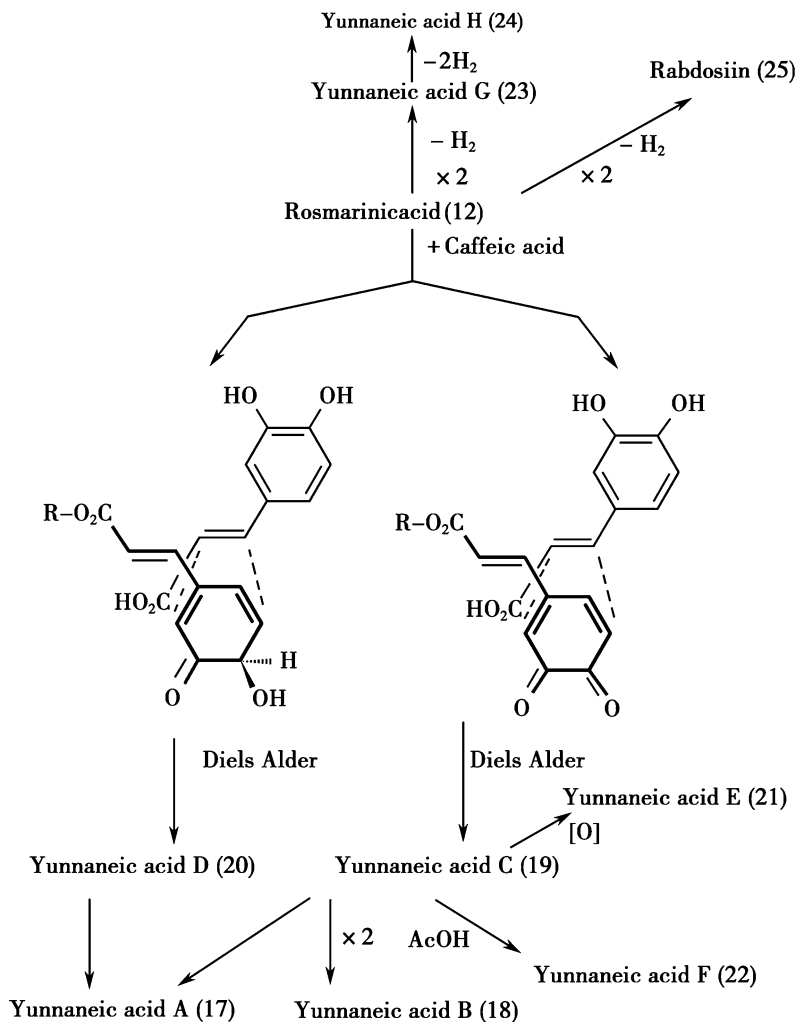


was a racemate; while the natural product was optically active, the IR, $^1\text{H-NMR}$, and MS data of the synthesized product were similar to those of the natural product, except that the melting point was somewhat lower.

7.8.2 Synthesis of Salvianolic Acid F [23]

During the studies on the total synthesis of salvianolic acid A (1), Dalla et al. have successfully

Fig. 7.7 Biosynthetic pathways of Yunnaneic acids



synthesized its biologically active pharmacophore, salvianolic acid F (2) (Fig. 7.9).

Using 2,3-dimethoxybenzyl alcohol (5) as the starting material, tetramethyl salvianolic acid F (3) was obtained in six steps with a 39 % overall yield and was converted into the target molecule (2) using boron tribromide with a 26 % yield. The synthetic route is depicted in Fig. 7.10.

Bromination of 2,3-dimethoxybenzyl alcohol followed by reaction with triphenylphosphine yielded compound 7 in 85 % overall yield. Wittig reaction of compound 7 with 3,4-dimethoxybenzaldehyde yielded the *trans*-stilbene 8 (80 % yield). To a solution of 8 in dry THF, a solution of BuLi in hexane was dripped in at -78°C . The

mixture was stirred for 0.5 h and the temperature was raised to -20°C . DMF in THF was added and the mixture was stirred for 0.5 h, HCl was added until pH 1, and the solution was extracted with ether. The organic layer was dried over anhydrous Na_2SO_4 and evaporated, and the oily residue was purified by silica gel column chromatography and eluted with cyclohexane-EtOAc (1:1) to give compound 9 (85 %) and compound 10 (15 %). Alternatively, compound 9 may also be obtained from compound 8 in a two-step procedure involving a hydroxymethylation reaction which gives compound 11 (75 %), followed by oxidation with Mn_2O with a 95 % yield. Transformation of compound 9 into compound 3

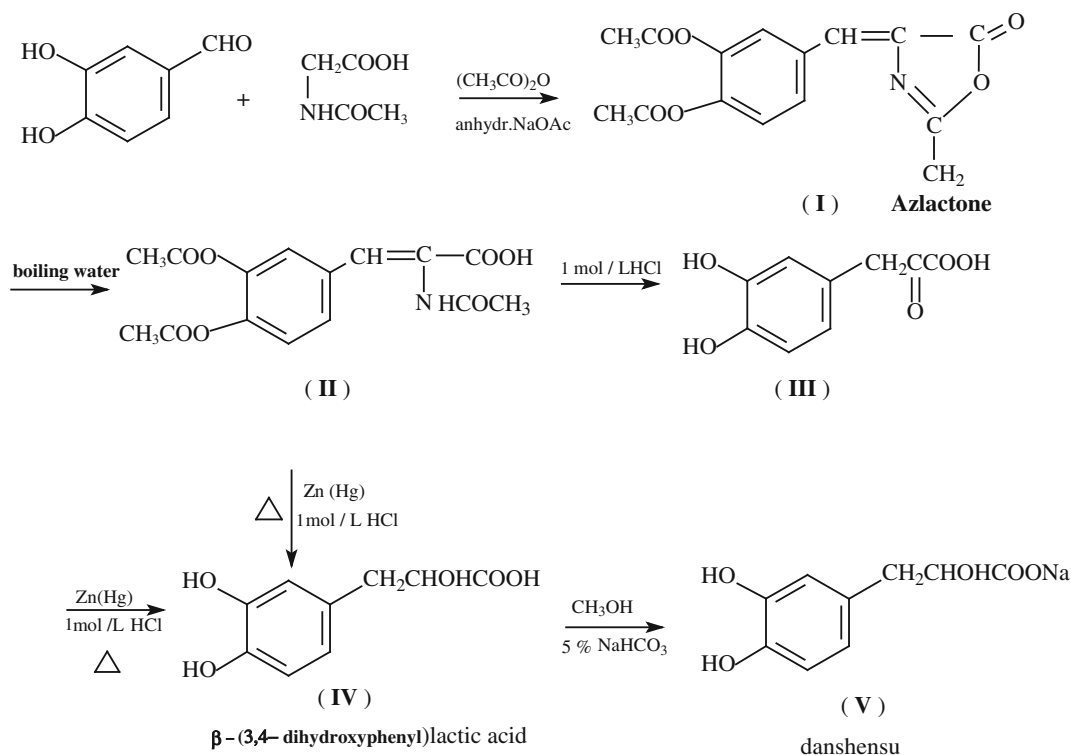


Fig. 7.8 Synthetic route of Danshensu

could be realized via two related methods. Perkin condensation of 9 with malonic acid and a catalytic amount of piperidine in pyridine afforded 3 in a modest yield (20 %). Wittig reaction of 9 in the presence of NaOMe in MeOH afforded a mixture of *E* and *Z* isomers of 12 with a 70 % yield. The isomeric mixture was treated with KOH to give the pure *E* isomer of 3 with a 95 % yield. Demethylation of 3 with borontribromide yielded salvianolic acid F. salvianolic acid F was easily converted to a mixture of 13 and 14 in solution (Fig. 7.11).

Because salvianolic acid A was converted to salvianolic acid C under acidic conditions [13], the transformation of salvianolic acid F could be the result of trace amounts of acid in solution during the reaction. In order to avoid the conversion of compound 2 into compounds 13 and 14, the reaction mixture was poured into a saturated solution of K_2HPO_4 , the aqueous layer was

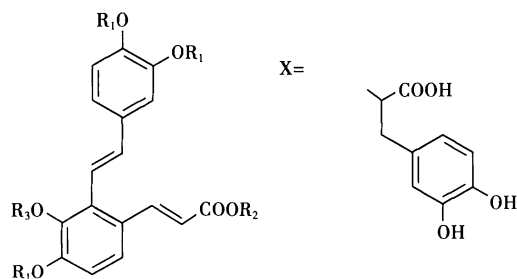


Fig. 7.9 Structures of salvianolic acid A, F and their methylated products 1: $\text{R}_1 = \text{R}_3 = \text{H}$, $\text{R}_2 = \text{X}$; 2: $\text{R}_1 = \text{R}_2 = \text{R}_3 = \text{H}$; 3: $\text{R}_1 = \text{R}_3 = \text{CH}_3$, $\text{R}_2 = \text{H}$

extracted with ether, and the ethereal solution was dried over anhydrous MgSO_4 and evaporated. The residue was dissolved in acetone and purified by silica gel column chromatography with $\text{MeOH}-\text{CHCl}_3-\text{HCOOH}$ (84:15:1) as the solvent to obtain salvianolic acid F (26 %), compound 13 (39 %), and compound 14 (30 %).

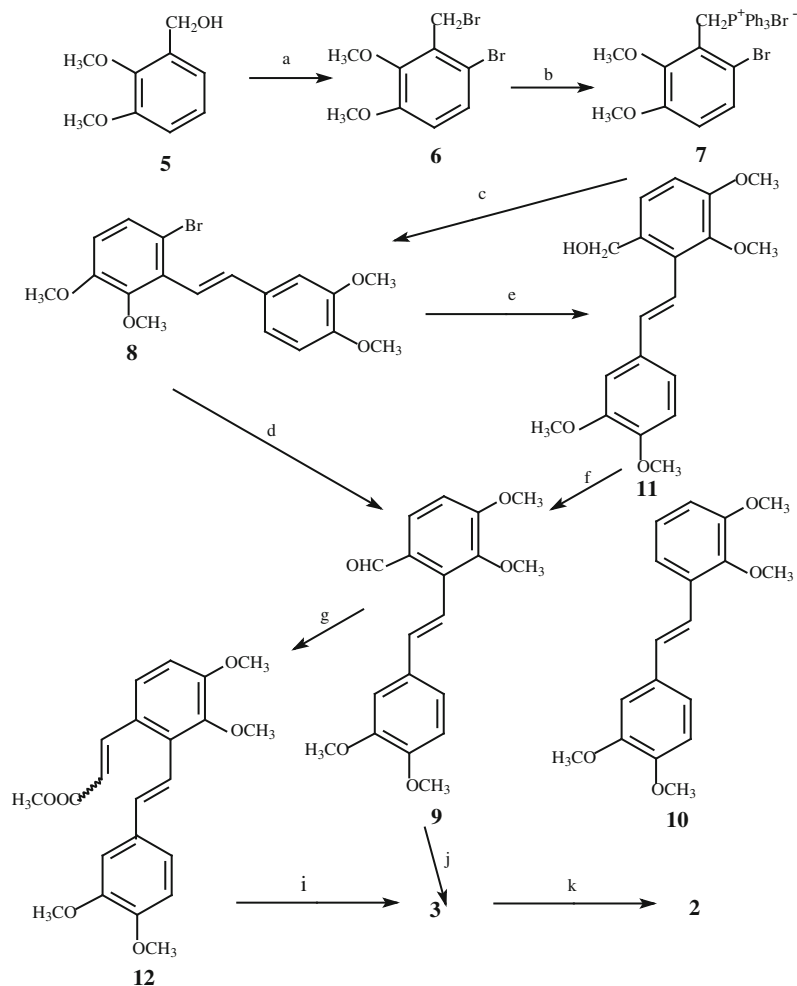


Fig. 7.10 Synthetic route of salvianolic acid F a. Br_2 , CHCl_3 , rt, 1h, 90 %; b. $\text{P}(\text{C}_6\text{H}_5)_3$, toluene, reflux 4 h, 95 %; c. MeOH, MeONa, then 3,4-dimethoxy benzaldehyde, reflux, 5 h, 80 %; d. THF, BuLi, -78°C , 0.5 h, then DMF, -20°C , 0.5 h, 85 %; e. THF, BuLi, -78°C , then gaseous CH_2O , 75 %; f. MnO_2 , CH_2Cl_2 , rt, 16 h 95 %; g. MeOH, MeONa, then $\text{MeOOCCH}_2\text{P}^+(\text{C}_6\text{H}_5)_3\text{I}^-$, reflux, 3 h, 70 %; i. ethanol, KOH, reflux, 4 h, then HCl 3 M, 95 %; j. $\text{CH}_2(\text{COOH})_2$, pyridine, piperidine catalyst, 20 %; k. BBr_3 , CH_2Cl_2 , 20°C , 1h, 26 %

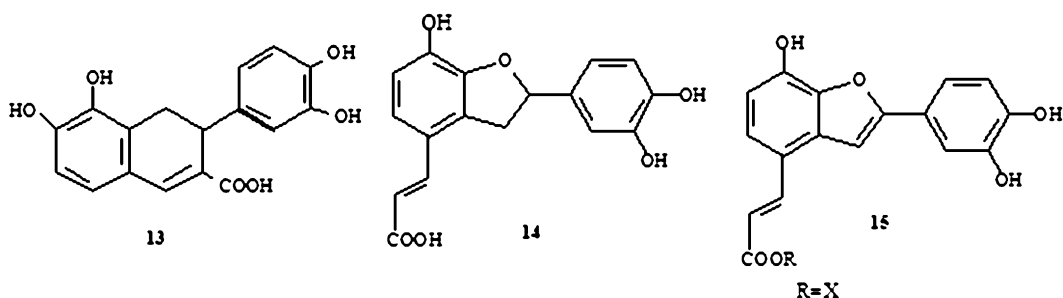


Fig. 7.11 Transformation products of salvianolic acid F

7.8.3 Synthesis of Heptamethyl Lithospermate [24]

Compared with salvianolic acid B, the structure of lithospermic acid (1) lacks one unit of β -(3,4-dihydroxyphenyl) lactic acid. The synthesis of this compound has attracted a lot of attention since 1970s. In 1979, Jacobson et al. reported the synthesis of heptamethyl lithospermate (2) (Fig. 7.12).

Isovanillin was converted into 2-allylisovanillin (3) via Claisen rearrangement of *O*-allylisovanillin. NaBH_4 reduction of compound 3 followed by acetylation yielded compound 5. Ozonolysis of compound 5 followed by reduction with dimethyl sulfide afforded an aldehyde compound (6). Jones oxidation of compound 6 yielded an acidic compound (7). Removal of the acetates on 7 to obtain the diol 8 was accomplished by treatment with MeONa in methanol at

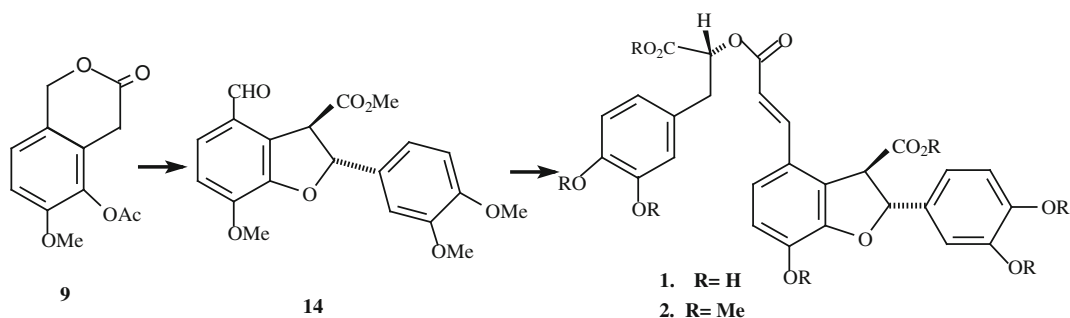


Fig. 7.12 Synthetic route of heptamethyl lithospermate

Fig. 7.13 Synthesis of benzodihydrofuran

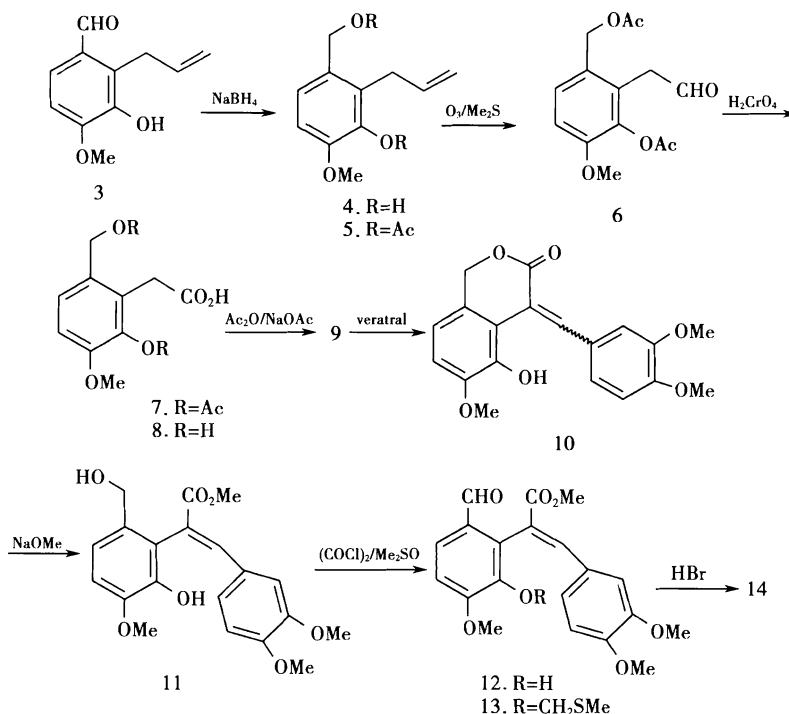
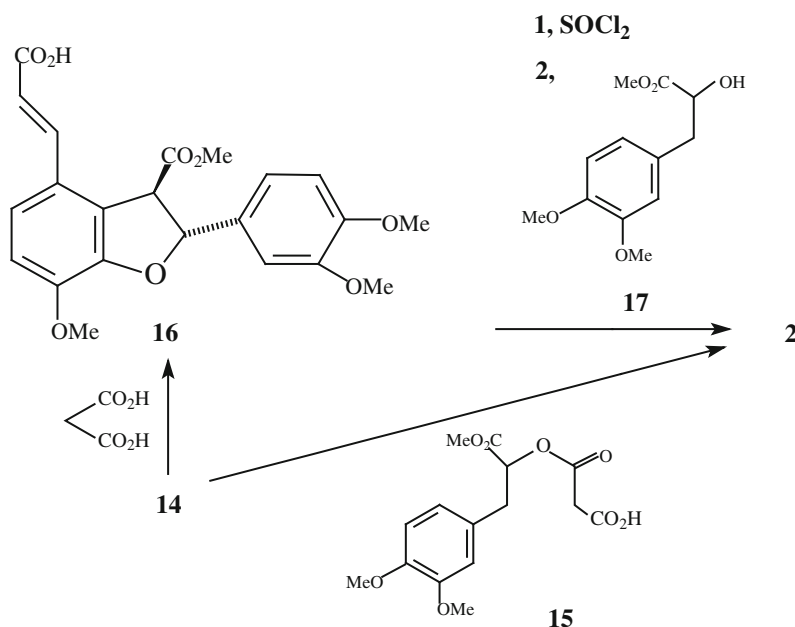


Fig. 7.14 Two synthetic routes of heptamethyl lithospermate



0 °C. Reaction of 8 with NaOAc in refluxing acetic anhydride afforded the benzopyranone 9. Piperidinium benzoate catalyzed condensation of 9 with 3,4-dimethoxybenzaldehyde afforded the aldol product 10 as a mixture of double bond isomers. Opening of the lactone ring in 10 was effected by heating with an excess of MeONa in methanol, yielding the exclusive *E* isomer of the alcohol ester 11. Oxidation of 11 using Me₂SO₄/oxalyl chloride afforded a 78 % yield of *E* aldehyde 12 and a by-product 13 (14 %). Cyclization of 12 with HBr in benzene/CHCl₃ afforded the *trans*-dihydrobenzofuran aldehyde 14 (see Fig. 7.13).

Elaboration of 14 into heptamethyl lithospermate (2) can be realized via two related methods. Knoevenagel condensation of 14 with malonic acid monoester (15) afforded 2 in modest yield. A more efficient procedure involves condensation of 14 with malonic acid resulting in the cinnamic acid 16. Acid chloride formation using thionyl chloride in benzene followed by treatment with methyl 3,4-dimethoxyphenyl lactate (17) afforded heptamethyl lithospermate (2) and its diastereoisomer in 50 % yield (Fig. 7.14).

References

1. Fang Q, et al. Acta Chim Sin. 1976;34(3):197.
2. Qian M, et al. Acta Chim Sin. 1978;36(3):199.
3. Li LN. Chin Pharm Sci. 1997;6(2):57.
4. Li J, et al. Acta Pharm Sin. 1993;28:534.
5. Sun P, He L. Chin J Pharm Anal. 1995;15(supplement):218.
6. Zhang D, et al. Shanghai First Med Coll Acad. 1980;7(5):384.
7. Chen Z, et al. Pharm Bull. 1981;16(9):24.
8. Tanaka T, et al. Chem Pharm Bull. 1989;37(2):340.
9. Tanaka T, et al. J Nat Prod. 1996;59(9):843.
10. Tanaka T, et al. Chem Pharm Bull. 1997;45(10):1596.
11. Li LN, Tan R, Chen WM. Planta Med. 1984;50:227.
12. Ai CB, Li LN. J Nat Prod. 1988;51(1):145.
13. Ai CB, Li LN. Planta Med. 1992;58:197.
14. Ai CB, Li LN. Chin Chem Lett. 1991;2(1):17.
15. Qian TX, Li LN. Phytochemistry. 1992;31(3):1068.
16. Zhang HJ, Li LN. Chin Chem Lett. 1993;4(6):501.
17. Zhang HJ, Li LN. Planta Med. 1994;60:70.
18. Ai CB, et al. Phytochemistry. 1994;37(3):907.
19. Zhao LM, et al. Chin Chem Lett. 1996;7(5):449.
20. Lu XZ, et al. Chin Chem Lett. 1991;2(4):301.
21. Tezuka Y, et al. Chem Pharm Bull. 1998;46(1):107.
22. Xue F, et al. Shanghai First Med Coll Acad. 1983;10(2):133.
23. Dalla V, Cotellet P. Tetrahedron. 1999;55:6923.
24. Jacobson RM, Rath RA. J. Org. Chem. 1979;44(22):4013.

Houwei Luo

8.1 Introduction and Classification

As an herbal medicine, Danshen (*Salvia miltiorrhiza*) has been studied since a long time ago. Particularly, the extraction and application of some liposoluble substances in Danshen were recorded in *Emergency Formulas to Keep Up One's Sleeve* [1], compiled by Ge Hong (281–341) and in *Liu Juan-zi's Ghost-Bequeathed Formulas* [2] (published in the fifth century). At that time, it was used mainly for the therapy of infectious diseases such as abscesses and ulcers, and for soreness of womens' breasts. This is the earliest record that liposoluble constituents were extracted from Danshen and formulated in China, dating about 1,500 years ago. It was already realized that those constituents were liposoluble with a red color. After those constituents were extracted by heating in bitter rice wine, they were dissolved in lard and then cooled to room temperature to give a red paste. The paste could be taken orally with warm wine, of which an oral dose was also described visually to be "as big as a common jujube seed."

8.1.1 Early Records of Chemical Study on Tanshinone

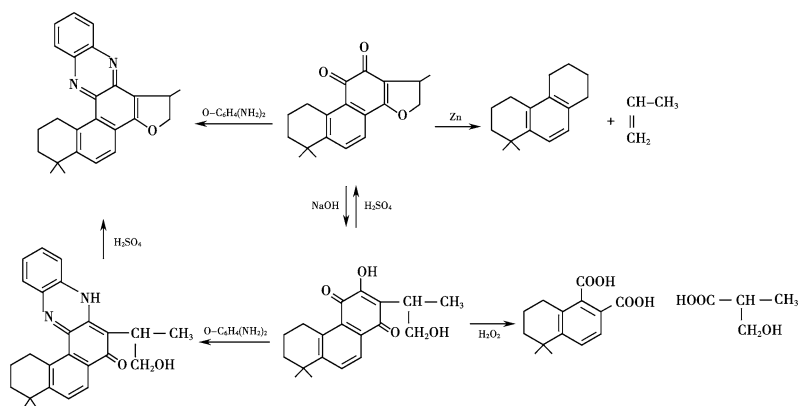
Nakano and Fukushima in Japan initially isolated three pigments from Danshen, which they named

tanshinone I, tanshinone II, and tanshinone III. Of these, tanshinone III is a mixture composed of tanshinone II and another new constituent, cryptotanshinone, as demonstrated by column chromatography performed by Takirua. In 1940, Von Wessely and S. Wang (the Chinese forerunner engaging in chemical studies of Danshen) for the first time confirmed that tanshinone I contained a phenanthrene quinone structure. The chemical nature of cryptotanshinone as an *o*-quinone with tricyclic structure was elucidated by Takiura using chemical method. The presence of 1, 2-orthoquinone in cryptotanshinone was indicated by its formation of quinoxaline with *o*-phenyl diamine. The presence of a tricyclic structure in cryptotanshinone was demonstrated by adding zinc powder to it followed by dry distillation [3]. The presence of a dihydrofuran ring in the cryptotanshinone was demonstrated by adding alkali to it to open the ring and transform it into 1,4-paraquinone. After the dihydrofuran ring was opened, the resulting isopropyl alcohol was ligated to C-loop and adjacent to the paraquinone at the 1 position, which was proved to be a reversible reaction. After acid was added, the original cyclic system of dihydrofuran ring could be recovered (see Fig. 8.1).

Although Von Wessely and T. Lauterbach had performed chemical studies on the chromophore of tanshinone II, they did not elucidate its entire chemical structure. After determining its chemical formula $C_{19}H_{18}O_3$, Okumura and Kakisawa [4] also used the reaction of tanshinone II with *o*-phenyl diamine to form quinoxaline to

H. Luo (✉)
China Pharmaceutical University, Nanjing, China
e-mail: houweiluo@163.com

Fig. 8.1 Structure of cryptotanshinone determined using chemical methods



prove the presence of an *o*-quinone group in its structure, and the presence of a carbonyl group was confirmed by infrared absorption at 1,701 and 1,650 cm^{-1} .

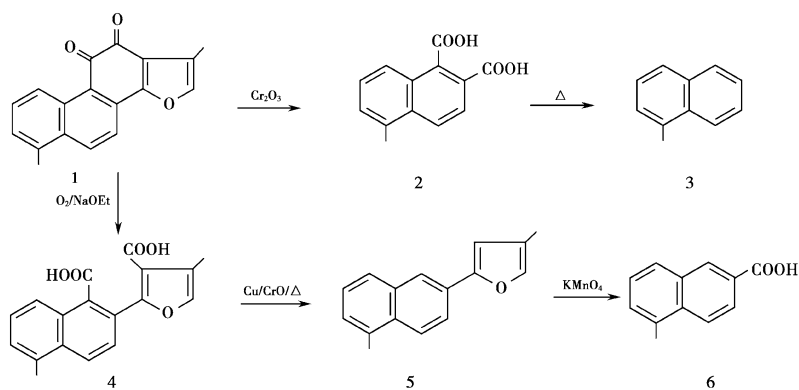
The ultraviolet spectrum showed that tanshinone II had four strong absorption peaks at 223, 268, 344, and 457 nm. In addition, the spectrum revealed that the chromophores in tanshinone I and tanshinone II and in cryptotanshinone were significantly different. This discovery laid the foundation for later studies using UV spectra to differentiate chromophores of different tanshinones. Of the three oxygen atoms in the molecular formula $\text{C}_{19}\text{H}_{18}\text{O}_3$, two atoms were sorted into *o*-quinones and the other was proven to be in a cyclic ether; thus, the chemical structure of tanshinone II was elucidated.

Both tanshinone I and tanshinone IIA belong to an *o*-quinone joined with a furan ring. However, they have differences in ring A: the ring A of tanshinone I is a benzene ring, while the one in

tanshinone IIA is an alicyclic ring. To determine the structure of tanshinone I, it is necessary to confirm the presence of the mother nucleus of 1-methylphenanthrenequinone in the structure, in addition to the 1,2-*o*-quinone group. The method used is shown as below: tanshinone I was oxidized with Cr_2O_3 to give 1-methylnaphthalene dicarboxylic acid (product 2, confirmed by synthesis); product 2 was then heated for decarboxylation to obtain 1-methylnaphthalene (product 3); finally, the alignment position of *o*-quinone group in tanshinone I was determined by oxidizing the tanshinone I with O_2/NaOEt to give product 4; decarboxylating product 4 with Cu/CrO reagent under heating gave product 5; and then, oxidizing product 5 with KMnO_4 gave 1-methylnaphthoic acid. The whole reaction procedure is shown in Fig. 8.2.

The above is the overview of the chemical methods [5] used to determine the chemical structures in the 1940s. Since the 1960s,

Fig. 8.2 Structure of tanshinone I determined using chemical methods



spectrum methods were gradually popularized, from the introduction of ultraviolet and infrared spectra to the application of nuclear magnetic resonance spectrum in the late 1960s. Although the application of these spectrum methods has greatly increased the effectiveness of deducing chemical structures, these methods have some shortcomings, which will be discussed later.

8.1.2 Nomenclature and Classification of Liposoluble Constituents in Danshen

8.1.2.1 Some Explanations

Tanshinone, also known as diterpenoid tanshinone, is a group of compounds synthesized biologically in Danshen. Based on the cyclic systems of the compounds, their major skeleton is composed of a tricyclic diterpene known as an abietane group, so they are also named abietane diterpene (quinone). For example, ferruginol, a compound discovered in Danshen's tissue culture, is a typical abietane diterpene ($C_{20}H_{32}O$) compound [6]. The phenolic hydroxyl group in ferruginol is oxidized easily in air and through a series of oxidation–dehydrogenation reactions, it transforms into compounds mainly composed of diterpenoid tanshinone, such as cryptotanshinone. The latter is then transformed into tanshinone IIA by dehydrogenation of its dihydrofuran ring. Based on its cyclic system, tanshinone I belongs to the phenanthrenequinones. However, it may also be obtained by successive dehydrogenation and demethylation of abietane diterpene with alicyclic ring A.

With respect to its chemical structure, tanshinone has the following characteristics: all chromophores are either 1,2 *o*-quinone furan rings, such as tanshinone IIA or 1,2-*o*-naphthoquinone dihydrofuran rings, such as cryptotanshinone. They are the major liposoluble constituents in Danshen.

The compounds with 1,4 *p*-quinone furan or dihydrofuran rings are referred to as isotanshinones, e.g., isotanshinone I or Isocryptotanshinone, which

are constituents that are present in very low content in Danshen.

In addition, there are some tricyclic diterpene quinones without furan or dihydrofuran rings, whose major characteristic is that the C ring is ligated with an isopropyl side chain, such as miltirone [7] or that the ring A is a benzene ring, such as Ro-09-0680 (miltirone I) [8]. The diterpene quinones are constructed using an isopropyl side chain to substitute for the furan ring in tanshinone I. They have significant activities in anti-oxidation or inhibition of platelet aggregation, which is related to the characteristics in their structures. The constituents have only 2 oxygen atoms in their own molecular formula due to the absence of furan rings and are significantly lower in polarity than the tanshinones containing furan or dihydrofuran rings [9].

In the nomenclature of tanshinone, those with an aromatic ring A (usually toluene) are named tanshinone I; if ring A is alicyclic, in which the position 4 is ligated with a gem-dimethyl group or one methyl group of the gem-dimethyl is oxidized, then they most likely belong to tanshinone II. When tanshinone In alkane is radiated by ultraviolet light, it is easily attacked by an oxygen atom, causing photochemical reactions to insert an oxygen atom between the two adjacent carbonyl groups. As a result, the original absorptions at visible light wavelengths disappear, and it is transformed into a colorless anhydride compound [10]. Oxidative scission may further occur, followed by the formation of a group of oxidative products derived from tanshinone. For example, tanshinone I is oxidized and the ring is split, followed by forming tanshinolactone [11] or Danshenspiroketallactone [12]. These products are considered to be artifact products, unless they are found in plants. In addition, with respect to biogenetic hypotheses, diterpene quinone from Danshen should be formed by a series of metabolic transformations of some diterpene compounds, especially abietane tricyclic diterpene. Therefore, we include these compounds in this chapter for the purpose for further discussion.

8.1.2.2 Classification of Liposoluble Constituents in Danshen

Since the 1930s, chemical studies on Danshen have been ongoing. Although there are many species of *Salvia* whose habitats are in Europe, they contain only some diterpenes, and a few species contain diterpenoid tanshinone. Now, the elucidated chemical structures are divided into five species according to their structures and physicochemical properties or their biogenetic relationships, and they are introduced below.

Early classification of tanshinones was based on their ultraviolet–visible light absorption properties, thus classifying them into three species. This classification system can distinguish different tanshinones based on the characteristic of their chromophores, further reflecting the differences of compounds in conjugated systems. For example, cryptotanshinone and tanshinone IIA differ significantly from each other in the ultraviolet absorption curve. The only reason for the difference is the dihydrofuran ring in cryptotanshinone and the furan ring in tanshinone IIA, that is, the difference is present between the conjugated systems of the two. Therefore, their ultraviolet spectra are different. In addition, the difference between dihydrotanshinone I and tanshinone I is only due to the minute difference between the dihydrofuran ring and furan ring. However, this results in significant differences in many physicochemical properties and even in bioactivities, such as changes in dissolubility, chromatographic behavior, and thermochemistry, and even differences in antioxidative capability, cytotoxicity, or other bioactivities. This demonstrates clearly that bioactivity of a compound is correlated with its physicochemical property and that the physicochemical property of a compound is hidden in its chemical structure. A molecular structure formula contains a host of available information. Therefore, on the surface, the classification is based on the difference in the chemical structure formula, but what is really important are the physicochemical properties revealed by the structural difference.

The following are the major groups of diterpene quinones in Danshen based upon their structural characteristics.

Diterpenoid Tanshinone

The compounds in this group (Fig. 8.3) contain 1,2-*o*-naphthoquinone with furan or dihydrofuran rings as the basic mother nucleus. According to structural differences in ring A, they can be classified as compounds with a benzene ring A, e.g., tanshinone I compounds including tanshinone I (1), dihydrotanshinone I (7) [13], Tanshinolaldehyde I (26) [14], Przewaquinone B (20) [15], Tanshinol (24) [16], etc., and as compounds with an alicyclic ring A which is ligated with different side chains, where position 4 ligated with a gem-dimethyl group is seen most commonly in ring A, e.g., tanshinone IIA (3), or a methyl group is oxidized into a hydroxymethyl group ($-\text{CH}_2\text{OH}$), e.g., tanshinone IIB (4) [17]. In some species, for example *Salvia przewalskii* Maxim, the hydroxymethyl group refers to hydroxymethylation of the methyl group at position C-18 of the furan ring, e.g., Przewaquinone A (19) [15], and in some situations also refers to a methyl group of gem-dimethyl group that is oxidized into formate, e.g., methyl tanshinonate (6). In addition, it is also possible that the hydrogen atom in an alicyclic ring is oxidized directly into a hydroxyl group, e.g., 1-hydroxy-tanshinone IIA (5) [18] and 3 α -hydroxytanshinone IIA (14), that the ring A is ligated with two hydroxyl groups, e.g., tanshindiol A (10), tanshindiol B (11), and tanshindiol C (12) [19], that the gem-dimethyl group at position 4 is deprived of a methyl group and ligated with a hydroxyl group, e.g., Przewaquinone C (21), and that the ring A is ligated with 3-hydroxyl and 4-hydroxymethyl groups, e.g., Przewaquinone F (22) [20].

Another major difference in tanshinone is the structure joined with ring C, either a furan ring or dihydrofuran ring. There are only five compounds joined with a dihydrofuran ring; they are cryptotanshinone (2), dihydrotanshinone I (7), methylene dihydrotanshinone (17) [14], 1,2,15,16-tetrahydrotanshinone (18) [14, 21] and crypto methyl tanshinonate (23) [22], but there are more than twenty compounds joined with a furan ring. In addition, the dihydrofuran ring is transformed easily into a furan ring by

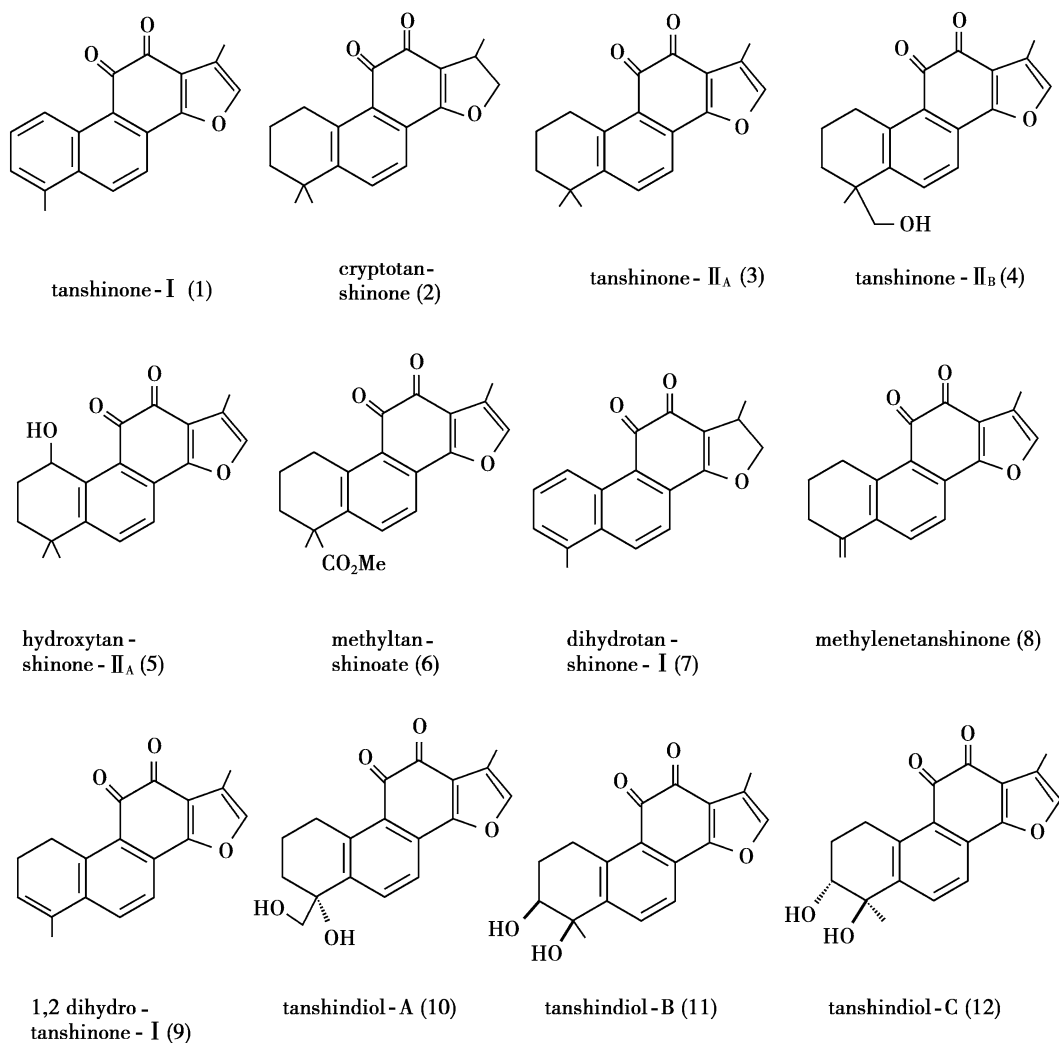


Fig. 8.3 Structural formula of diterpenoid tanshinone

dehydrogenation. For example, the above cryptomethyltanshinonate can also be oxidized automatically into methyltanshinonate [22], and cryptotanshinone can be transformed into tanshinone IIA by dehydrogenation of the dihydrofuran ring, techniques which are used extensively in chemical synthesis.

Some tanshinones belong to neither Class I nor Class II, but to the transition class from Class II to Class I. For example, the compound with an alicyclic ring A is transformed into compounds with an extra cyclic alkene hydrogen, e.g.,

methylenetanshinone (8) and hydroxymethylenetanshinone (25), and the isomers of methylenetanshinone, e.g., 1,2-dihydrotanshinone I (9) [23]. Also, intracyclic dehydrogenation of ring A occurs to form 1,2-dehydrotanshinone IIA (15) [23], and the gem-dimethyl group of tanshinone IIA is substituted by a keto-carbonyl group to form demethyltanshinone (13). In fact, demethyltanshinone can also be obtained by oxidizing tanshindiol A with NaIO_4 [19], or by oxidizing one methyl group in the gem-dimethyl of tanshinone IIA into Tanshinaldehyde (16) [24].

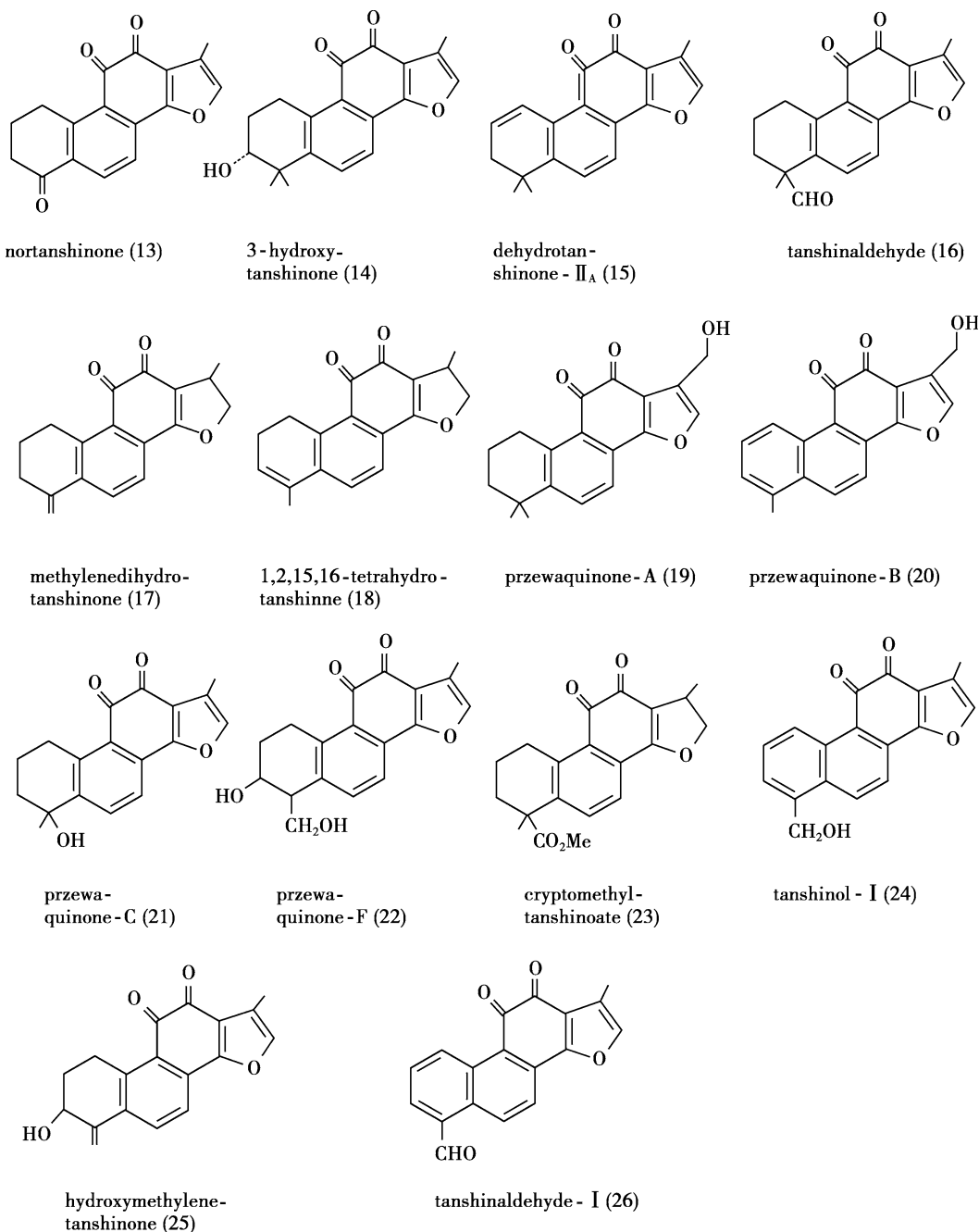


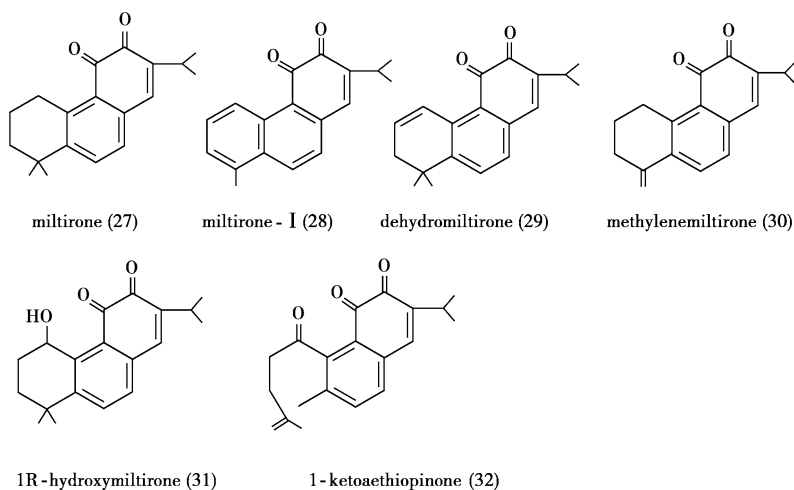
Fig. 8.3 (continued)

Tricyclic Diterpene Quinone

Compounds 27–32 are shown in Fig. 8.4. The common structural feature of this group is that position 13 of ring C is ligated with an isopropyl group instead of a furan or dihydrofuran ring.

Among these tricyclic diterpene quinones, only the ring A of miltirone I (28) is a benzene ring, while the others are alicyclic rings or contain one double bond in the exterior or interior of the ring, e.g., dehydromiltirone (29) [25] and

Fig. 8.4 Structural formula of tricyclic diterpene quinones (27–32)



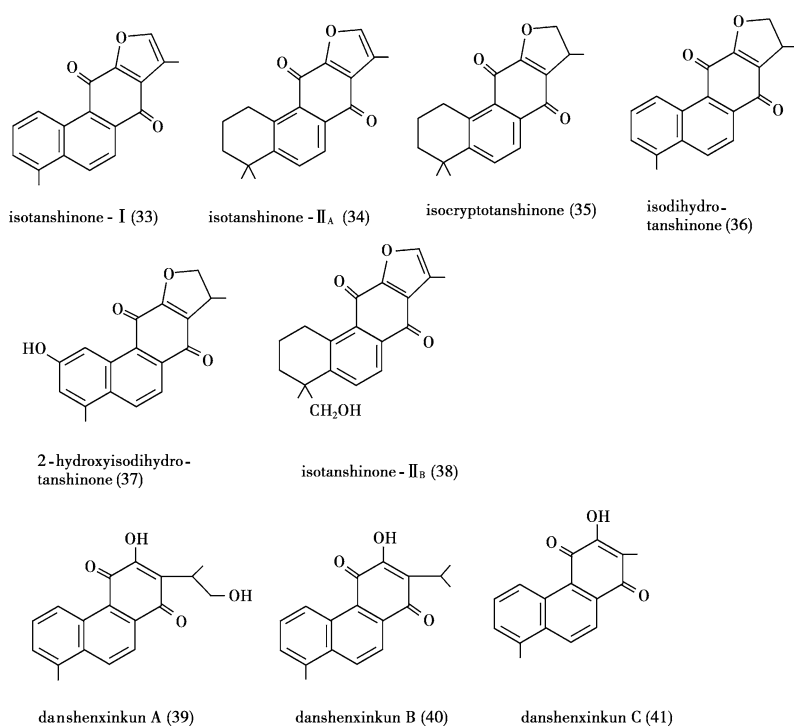
methylenemiltirone (30) [14]. Many of the compounds have various attractive bioactivities, e.g., miltirone functioning on the diazepam receptors in the brain and miltirone I (R0-09-0680) inhibiting platelet aggregation. In addition, the tricyclic diterpene quinones also show very strong anti-oxidative activity [26]. According to initial analysis, it is considered that the anti-oxidative activity of miltirone I is related to

hydrogen free radicals released during homolysis of hydrogen atoms in the isopropyl group [27].

Royleanone Tanshinone

The structures of compounds 33–41 are shown in Fig. 8.5. This group is characterized by 1,4 *p*-quinone. Of these nine royleanone tanshinones, besides six isotanshinones, there are also the paraquinone compounds with an enolic group in

Fig. 8.5 Royleanone tanshinditerpene quinones (33–41)



ring C, e.g., danshenxinkun A, danshenxinkun B, and danshenxinkun C [13]. Danshenxinkun also belongs to the royleanone type of 1,4 *p*-quinone. Judging from thin-layer chromatograms between these and the tanshinones of 1,2 *o*-quinone, although there are three oxygen atoms in the molecular formula $C_{18}H_{16}O_3$ (40) of danshenxinkun B, the adsorption (R_f) reflected by silica gel thin-layer chromatography (TLC) is significantly lower than that of the tricyclic diterpene quinones (e.g., miltirone) of 1,2 *o*-quinone containing only two oxygen atoms. The reason is that the hydroxy group at position 12 of ring C (enolic hydrogen) of danshenxinkun B can react with the quinone of C-11 to form intramolecular hydrogen bonds, thus leading to a reduction in polarity and dissolubility of the compounds and influencing their bioactivities.

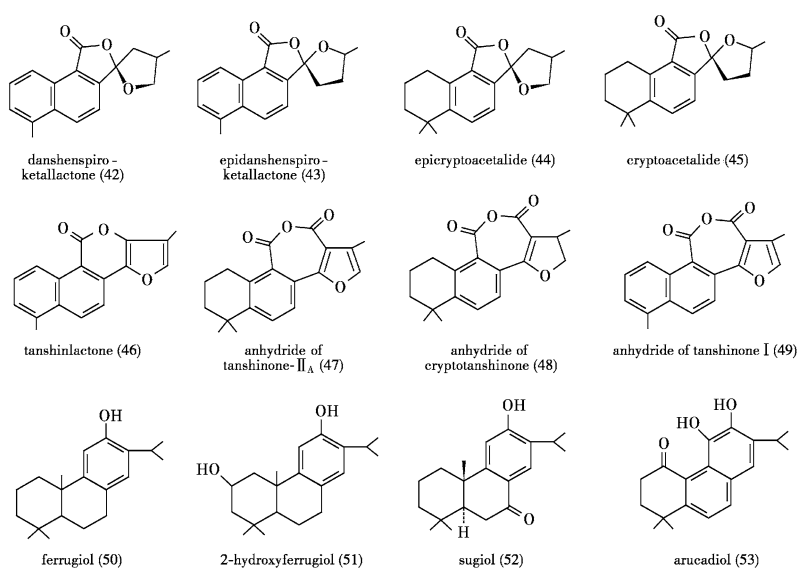
In the royleanone tanshinones, there are also six isotanshinones in very low content; they are isotanshinone I (33), isotanshinone IIA (34), isocryptotanshinone (35) [28], isodihydrotanshinone I (36) [29], iso-2-hydroxy dihydrotanshinone I (37) [21], and isotanshinone IIB (38) [30], of which only a few compounds have been tested for their bioactivities. For example, isotanshinone IIB has an inhibitory effect on platelet aggregation induced by ADP and collagen.

Compounds Related to Biogenesis of Tanshinone

The term biogenesis-related means that the compounds are related to the biosynthesis of tanshinone, i.e., they are the precursors from which tanshinone compounds are derived under catalysis by a series of enzymes in plants. This group also includes some artifact products. For example, when tanshinone I is dissolved in some solvents, especially alkanes or halocarbons, it can be transformed into some artifact products through irradiation by UV light, heat, and oxygen. These compounds are often the oxidative products of quinone, mainly including lactones or anhydrides, which are the colorless compounds that no longer have the visible pigment of quinone and can also show fluorescence, and generally can be detected under fluorescent light. The molecular structures of these compounds are shown in Fig. 8.6.

The reason for naming compound 50 ferrugiol is that there is a phenolic hydroxyl group in its ring C, which is easily oxidized in air into quinone, and the color is transformed from its original colorlessness to a rust-like color. Because it was initially isolated from the tissue culture medium of Danshen and its content in culture medium showed a dynamic change, it was

Fig. 8.6 Compounds related to biogenesis of diterpenoids quinone (42–53)



speculated that it is related to the biosynthesis of cryptotanshinone. Compounds related to ferrugiol are 2-hydroxyferrugiol (51), sugiol (52) [22] and arucadiol (53) [31]. In fact, arucadiol is the same compound as miltiodiol, which was isolated by Kakisawa in early years. The four compounds all have abietane skeletons. The relationships among them can be seen based on comparisons of their structural formulas. For example, the only structural difference between sugiol and ferrugiol is that there is an additional ketone group at position 7 in ring B of Sugiol. Due to the electrophilic effect of the ketone group, the phenolic hydroxyl group in ring C becomes more stable and is not easily oxidized.

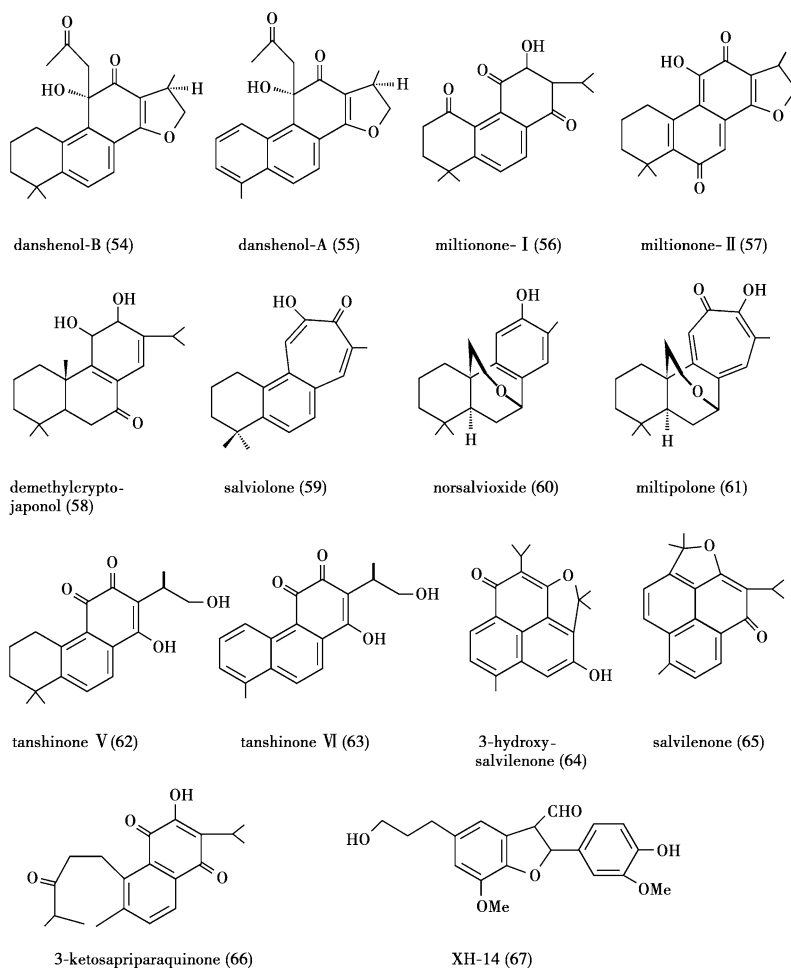
Another group of compounds is the photooxidative products of tanshinone, e.g., compounds 47–49. The reason for including tanshinlactone (46) [11] in this group is based on biogenetic hypotheses. Besides, there are a couple of isomers which cannot be separated completely into monomers, i.e., Danshenspiroketallactone (42, 43) [12]. Asari Fumika et al. subsequently obtained two isomers where ring A is an alicyclic ring, named cryptoacetalide and epi-cryptoacetalide, which could not be separated and were present as a mixture in a 3:1 ratio (44, 45) [32]. Due to further oxidation of the quinoid structure into lactone, the conjugated system is shortened, which affects its chromophore, thus making these compounds colorless. However, under ultraviolet light, they show a blue or purple blue fluorescence, which is helpful in identification. The anhydride of tanshinone IIA (47) [10] is a photochemical product obtained by dissolving tanshinone IIA in hexane and exposing to a 450-W mercury vapor lamp for 2 h. Researchers at the Chinese University of Hong Kong also isolated anhydride of cryptotanshinone (48) and anhydride of dihydrotanshinone I (49) [14] from Danshen, but they did not specify if these two compounds are artifact products. However, from the production of anhydride of tanshinone IIA, not only anhydride of tanshinone IIA but also 1-hydroxytanshinone IIA (5) is obtained from tanshinone compounds under light via free radical reactions and further oxidizing reactions.

Other Compounds

This is a group of cyclic systems compounds which are difficult to classify, including compounds 54–66 shown in Fig. 8.7. Danshenol-A (55) and Danshenol-B (54) [33] are deep yellow needle crystals. They received attention because of their strongly inhibitory effect on aldose reductase, with an IC_{50} of 0.014 and 0.042, respectively. Demethylcryptojaponol (58) [34] is very similar in structure to sugiol (52) and thus may be a transformed product of the latter. To avoid the occurrence of artifact products (for example, the above 1-hydroxytanshinone IIA was demonstrated to be an artifact product) during extraction of Danshen, some research teams in Japan emphasized that the fresh Danshen roots should be soaked immediately in methanol to avoid the production of artifact products. Hence, a colorless salviolone (59) was isolated, which was the firstly isolated diterpene tropolone compound with a seven-membered ring, and has cytotoxicity with a TD_{50} of 3.3 $\mu\text{g/ml}$ for Vero cells.

The compounds biogenetically related to 59 also include norsalviolone (60) and miltipolone (61). After an oxygen atom is taken off the methenyl group of miltipolone, ring B is aromatized to obtain salviolone [35]. During in vitro ischemic reperfusion tests with rats, some scientists in Japan isolated tanshinone V (62) and tanshinone VI (63) [36], which show a certain protective effect on heart muscle. Judging from their structures, they should be the products formed following the opening of the dihydrofuran rings in cryptotanshinone and dihydrotanshinone I. However, TLC results showed that the two constituents were still detected in the liquid extract of fresh Danshen roots, indicating that they are unlikely artifact products but probably the precursor from which cryptotanshinone is derived. miltionone I (56) is a yellow powder and also belongs to the 1,4 *p*-quinone group and can be described with “an additional ketone group is added to position 1 of ring A in danshenxinkun B.” miltionone II (57) [37] is a colorless needle crystal. 3-keto-sapriparaquinone (66) isolated from *Salvia prionitis* is a yellow needle crystal because its broken ring A forms a side chain of

Fig. 8.7 Other compounds (54–67)



3-keto-4-methylpentane. Therefore, based on the chromophore, it should belong to the 1,4 *p*-quinone group. Also isolated from this plant was 3-hydroxy-salvilenone (64) [38], which is also extremely similar in structure to the yellow crystal of salvilenone (65) [39], a microconstituent isolated from Danshen. There is no report on the biological activity of this structure.

8.2 Extraction and Isolation of Liposoluble Compounds

Due to the large time span, the chemical structures elucidated from 1934 until today are numerous in number, and active microconstituents are

discovered continuously. To increase the effectiveness of isolation, certain target compounds should be isolated from total extracts, or the major components of an effective fraction used to control certain illnesses should be isolated. For example, the effective constituents of the “tanshinone capsule” used for curing acne are cryptotanshinone and other tanshinones. Generally speaking, the isolation of certain components from an extract should first be based on the structural features of known compounds and their related “structural information,” especially the relationship between chemical structure and its dissolubility or chromatographic behavior. For instance, the retention time of liquid chromatography as well as the flow rate of adsorption chromatography can provide very useful information.

Table 8.1 Contents of tanshinone compounds in 10 *Salvia* plant species

Name of the plant	Habitat	Content (%)		
		Tanshinone IIA	Methylenetanshinone	Tanshinone I
<i>S. przewalskii</i> var. <i>mandarinorum</i>	Sichuang	0.53	0.035	0.038
<i>S. Przewalskii</i>	Tibet	0.35	0.01	0.12
<i>S. miltiorrhiza</i>	Shandong	0.32	0.15	0.23
<i>S. yunnanensis</i>	Yunnan	0.16	0.13	0.15
<i>S. bowleyana</i>	Jiangxi	0.13	0.07	0.01
<i>S. digitaloides</i>	Yunnan	0.043	0.005	0.292
<i>S. sinica</i>	Anhui	0.02	0.01	0.04
<i>S. prionitis</i>	Zhejiang	–	0.03	0.08
<i>S. kiangsienis</i>	Jiangxi	–	0.04	0.21
<i>Salvia</i> sp	Yunnan	0.05	0.01	0.03

8.2.1 Extraction Method

Currently, the studies on the isolation of Danshen's liposoluble constituents are focused on several major constituents, such as tanshinone IIA, dihydrotanshinone I, and cryptotanshinone. Of course, for the purpose of research or the development of new drugs, one should try to isolate some low-content components with special bioactivities, such as miltirone (27), which has sedative and tranquilizing effects on the brain. Another example is miltirone I (28), which has properties of anti-platelet aggregation or antioxidants. On the other hand, new compounds can be discovered by using different raw materials, or by special improvement of isolation methods. These opportunities should never be overlooked. With respect to the choice of solvents used for the extraction of liposoluble constituents, the theory of "similarity and intermiscibility" is generally followed. The solvents used include ether, ethyl acetate, acetone, ethanol, and methanol. In fact, ethanol is still the most commonly used solvent, as it is safe and economical.

8.2.1.1 Selection of Raw Medicinal Material

To identify plants with a high content of tanshinone IIA and other effective constituents, Huang Xiulan et al. [40, 41] collected roots from 20 species of plants in the genus *Salvia*. The roots were extracted with 95 % ethanol, and the

presence of tanshinone IIA, methylenetanshinone (8), and tanshinone I in the extracts was tested with TLC. The positive samples were further quantitatively measured with ultraviolet spectrophotometry after TLC separation, and the results were summarized in Table 8.1. Subsequent assays on 13 relevant species revealed that the content of tanshinone IIA in some plants grown in Shandong province, such as *S. miltiorrhiza* f. *alba*, *S. trijuga*, and *S. przewalskii*, was more than 0.6 %.

Some researchers measured the major liposoluble constituents in Danshen from 8 major producing areas in China, using ultrasonic extraction methods combined with HPLC. Their results showed that the contents of tanshinone IIA, cryptotanshinone, and tanshinone I in Danshen from different habitats differed significantly. For example, the content of tanshinone IIA was in the range of 0.10–0.40 %; cryptotanshinone, 0.04–0.46 %; and tanshinone I, 0.03–0.15 %. The difference of the total contents of these three major constituents in different species could be as large as fourfold–tenfold. Based on the above results [42], if the contents of these 3 constituents are used as the quality indicator, the highest contents were found in Danshen from Sichuan's Zhongjiang, Liaoning's Linyuan, and Shandong's Pingyi, and the lowest contents were found in Danshen from Shanghai's Chongming. Please refer to Part I of this book for botanical species and quality assessment.

8.2.1.2 Extraction Method Based on Ethanol

Ethanol can extract major liposoluble constituents, as well as some water-soluble substances. The constituents in the ethanol extract can be detected with TLC, with several major tanshinones, e.g., tanshinone IIA, cryptotanshinone, tanshinone I, easily observable. The content of tanshinone IIB is relatively low, but can sometimes also be detected with TLC. The problem with ethanol extraction is that some high-content water-soluble substances in Danshen, such as salvanolic acid A, are also extracted. In order to separate liposoluble constituents from these impurities, ethanol must be recovered stepwise. When the ethanol in the mother solution is concentrated to 1/3 volume, a large number of colloidal substances can be precipitated. After removal of the colloids, crystals can be obtained following cooling of the mother solution, which is the “total-ketone” mixture containing multiple tanshinones. To obtain a single constituent from this mixture, further separation and purification steps are necessary. When designing a particular purification method, the most commonly used way at present is the multifactor, multilevel orthogonal design, as described by Shihui Qian [43]. The factors generally considered include the concentration and amount of ethanol, extraction time, and reflux frequency. Three different levels of each factor are selected, for example, ethanol concentrations of 60, 70, and 80 %; ethanol amounts of sixfold, eightfold, and tenfold; extraction times of 1, 1.5, and 2 h; and reflux frequencies of 1, 2, and 3 times. Finally, when evaluating the most effective method, HPLC can be used for detection. If that is the case, the column is usually silylated silica gel, such as the Bondapak C18 column, methanol–water (75:25) is used as the mobile phase, and the detection wavelength set at 270 nm. According to the test results reported, the concentration of ethanol is a key factor, with the optimal processes as follows: use sixfold 80 % ethanol and extract twice with 2 h for each extraction. Of course, this is only an example for reference, and a specific method must be developed in combination with certain conditions.

8.2.1.3 Supercritical Fluid Technique

When the temperature or pressure exceeds the critical value, common liquid or gas loses its original properties and becomes a high-density liquid, i.e., supercritical fluid. The supercritical fluid has characteristics such as lower viscosity, a greater diffusion coefficient, and better dissolubility. Supercritical fluid can dissolve the liposoluble diterpenoid tanshinone, has a very strong permeability, and can penetrate any micropore of plant tissue. Carbon dioxide is a common gas, and obvious changes in its properties can occur when the temperature is higher than 31.26 °C and the pressure is greater than 7.37 MPa, with its density close to that of liquid, its viscosity close to that of gas, and a diffusion coefficient 100 times that of liquid. It becomes supercritical carbon dioxide at this point, and, due to its agreement with the theory of “similarity and intermiscibility,” it has extraordinary dissolving capabilities for compounds with quinoid structures, such as tanshinones. Zhang Kun et al. [44] reported the supercritical liquid extraction technology of tanshinone IIA, where the extraction pressure was set at 3.00×10^4 , 3.50×10^4 and 4.00×10^4 kPa, respectively; extraction temperature at 35, 40 and 45 °C, respectively; and CO₂ dosage at 450 ml/g. Based on the experiment results, the optimal conditions were as follows: extraction pressure, 3.50×10^4 kPa; extraction temperature, 45 °C; CO₂ dosage, 420 ml/g. Supercritical fluids are inert solvents themselves; they do not react with the extracts, and the extraction temperature is relatively low, which is beneficial for the extraction of those compounds with low melting temperatures and unstable structures, e.g., dehydromiltirone or some diterpenes. In sum, the prominent advantage of this method is that it can maintain the structural integrity of compounds.

8.2.2 Separation Methods

The separation techniques can be divided into two types based on the practical purposes: analytical and preparative. Each type has its own characteristics and applications. They are illustrated with examples as follows.

8.2.2.1 Analytical Method

One characteristic of the analytical separation method is its microquantity ($\mu\text{g}/\mu\text{L}$) capability; a few grams of medicinal material extract or small amounts of preparations are more than enough for the assays. The detection methods are highly sensitive; LC-MS not only can detect at the nanogram level with high accuracies, but also obtain results very quickly. It is used mainly to analyze or solve certain problems such as controlling the quality of raw medicinal materials or some preparations, investigating the mechanisms of development and transformation of the active constituents in Chinese herbs, observing the mechanism of cryptotanshinone formation in tissue culture, as well as selecting and optimizing the tissue culture conditions. These types of methods can also be applied to the study of the pharmacokinetics of Chinese herb drugs, e.g., observing the absorption, tissue distribution, transport, metabolism, and excretion of cryptotanshinone in animals. The wide application of HPLC, especially LC-MS, could promote the progress of such research. Several published examples are given below.

Monitoring the Quality of Medicinal Materials

As specified in Part I of *Chinese Pharmacopoeia* (2005 Edition), the contents of tanshinones should be assayed by HPLC with a C-18 column filled with alkyl-silylated bonded silica gel. The suggested mobile phase is methanol–water (15:5), and ultraviolet detection is suggested at $\lambda_{\text{max}} = 270 \text{ nm}$. For the ethanol extract of Danshen, this method can detect at least 3 major peaks of liposoluble substances with Rt values being 16.47, 20.47, and 25.67 min, which are cryptotanshinone, tanshinone I and tanshinone IIA, respectively. In addition, within Rts of 2.47–12.40 min, more than five different peaks of polymerized phenolic acids can also be detected. However, when using the same column for reverse phase chromatography, the loading amount must be limited, usually to about $0.1 \mu\text{g}$. The main reason for that is for the protection of the column.

Assay of the Active Constituents in Danshen Preparations

Wang Hong et al. [45] analyzed the compound preparations of Danshen manufactured in China,

including compound Danshen tablet, compound Danshen lozenge, compound Danshen dropping pills, and Danshen tablet. Shim-pack CLC-ODS columns ($150 \text{ mm} \times 4.6 \text{ mm}$, $5 \mu\text{m}$, Shimadzu, Japan) were used. Mobile phase for gradient elution is 0.5 % formic acid–water solution (A), acetonitrile (B). The elution program was as follows: 0–15 min, 0–40 % B; 15–40 min, 40–65 % B; 40–55 min, 65 % B; and 55 min, 100 % B. Detection wavelength was 281 nm for 0–25 min and 254 nm for 25–55 min. Column temperature is room temperature. Flow rate is 0.8 ml/min. Separation results in the form of retention time (Rt) showed that there were water-soluble substances within 12.54–22.5 min, including Danshensu (β -D-(3,4-dihydroxyphenyl)-lactic acid), protocatechuic acid, protocatechuic aldehyde, and salvianolic acid B, and liposoluble substances within 30–50 min, including methyl tanshinonate, dihydrotanshinone I, cryptotanshinone, tanshinone I and tanshinone IIA. Their Rt values correlated with the hydrophobicity index of tanshinone, especially with tanshinone IIA having the highest hydrophobicity and also the longest retention time. The contents of these constituents in the 10 Danshen preparations described in this paper were used only as a general reference.

Studies on Tissue Culture

During the 1980s, there were a large number of studies on the tissue culture of Danshen. For example, during the callus culture of Baihua Danshen (*S. miltiorrhiza* f. *alba*), the dynamic changes of the contents of diterpene quinone were monitored. The calluses induced at different time periods (10 days to 6 months) and at different times after transplanting (20 days to 6 months) were used to assay the contents of tanshinone IIA, methylenetanshinone, and tanshinone I. The procedure was as follows: calluses collected under different conditions were extracted with ethanol; silica gel thin layers were used with benzene–chloroform (1:1) and methylene dichloride as developing solvents, and cryptotanshinone and tanshinone IIA were used as controls; and a CS-910 double-wavelength thin-layer chromatogram scanner was used for assaying cryptotanshinone and, in combination with

ultraviolet spectrophotometry, for assaying tanshinone IIA, methylenetanshinone, and tanshinone I. The results showed that the content of tanshinone IIA was 0.02–0.04 % and that of tanshinone I was 0.06–0.17 %. Chen Hui et al. [46, 47] at Hong Kong University used *Agrobacterium tumefaciens* C-58 to transform Danshen, obtaining a fast-growing cell line which can achieve 9.7 g/L in dry weight after 12 days of growth. Active substances in the cell line were extracted with methanol, followed by separation and assaying using HPLC under the following conditions: column: Beckman Ultrasphere C18 (5 μ m), 250 mm \times 4.6 mm; mobile phase: solvent A (0.075 % trifluoroacetic acid) and solvent B (acetonitrile); gradient elution: 0 % B for 0–5 min, 0–70 % B for 5–25 min, 70 % B for 25–40 min, and then 70–0 % B for 40–41 min; flow rate: 1.0 ml/min; detection wavelength: 280 nm. Identified in the extract were rosmarinic acid, salvianolic acid B, cryptotanshinone, tanshinone I and tanshinone IIA. In addition, there were two unidentified compounds. It was of particular significance that the dynamic changes in rosmarinic acid, salvianolic acid B, and the liposoluble compounds of cryptotanshinone, tanshinone I, and tanshinone IIA (total of 5 compounds) in the culture medium were monitored. Rosmarinic acid and salvianolic acid B were up to 532 mg/L and 216 mg/L at day 12, respectively, and the liposoluble tanshinone compounds reached the highest levels at day 20 with cryptotanshinone, tanshinone I, and tanshinone IIA being 146 mg/L, 21 mg/L, and 47 mg/L, respectively, which were significantly lower than the water-soluble constituents of rosmarinic acid and salvianolic acid B. In a further study, they also observed that yeast extract had a significant effect on the formation of secondary metabolites in the culture media of Danshen and reduced the production of rosmarinic acid in the medium from 5 to 3 % of dry cell weight. However, cryptotanshinone in the culture medium followed an increasing trend (from a neglectable amount to 20 mg/L). The authors conjectured that rosmarinic acid and salvianolic acid B might play passive and active defense roles in Danshen, respectively.

Study on in Vivo Metabolism of Tanshinones

The Danshen preparation initially used for clinical therapy of coronary heart disease is the tanshinone IIA—sodium sulfonate preparation. At the early stage, a [35 S]-labeled tanshinone or [3 H]-labeled tanshinone IIA—sodium sulfonate preparation is used to study the distribution, excretion, and metabolism of this preparation in animals. For example, the drug was monitored for its excretion in bile, urine, or stool, that is, assays were performed on bile collected 2 h after administration using silica gel TLC (developing solvent: n-butyl alcohol/glacial acetic acid/water = 4:1:5, V/V) in combination with autoradiography, revealing that the amount of drug excreted via stool was 2–4 times that via urine [48, 49]. In tests with rats, cryptotanshinone was administered via the duodenum, followed by the collection of bile at different post-dose times. The bile was then analyzed with HPLC (5 μ m silica gel, 250 mm \times 2.6 mm ID; mobile phase: n-hexane/dehydrated alcohol = 97.5:2.5; flow rate: 1 ml/min), discovering that there was also dehydrogenated cryptotanshinone, i.e., tanshinone IIA, in addition to cryptotanshinone in the bile. More directly, the purified cryptotanshinone was incubated with rat liver homogenate for 2 h, and then, the reaction was stopped. Subsequently, CHCl_3 extraction was performed on all tanshinone constituents in the homogenate. The extract was then assayed via TLC. The results indicated that besides cryptotanshinone, there was another product in the extract with an R_f value of 0.42, a green color when reacted with concentrated sulfuric acid, and ultraviolet absorption UV λ_{max} (nm) of 212, 223, 250, 268, and 350, which is identical to the properties of the known compound tanshinone IIA [50]. The test indicated that cryptotanshinone can be transformed into tanshinone IIA by the dehydrogenase in liver tissue. In addition, Mingzhi Xie et al. [51] studied the disappearance, tissue distribution, and excretion of cryptotanshinone in the mouse gastrointestinal tract using a double-wavelength thin-layer chromatogram scanner. Also, cryptotanshinone was administered intragastrically to mice, followed by urine collection at 24 and 48 h

post-dose to observe the metabolism of the drug in urine. After being absorbed by gastrointestinal tract, most of the drug can be transformed in the body. The metabolites in bile increased with an increasing duration of administration. Seven metabolites were obtained by the TLC, which were identified based on the R_f value, in combination with the mass spectrum and ultraviolet spectrum. For example, “ $m/z(M^+)$ 296, $R_f = 0.54$ ” represents cryptotanshione and “ $m/z(M^+)$ 294, $R_f = 0.77$ ” represents tanshinone IIA. However, two spots of $R_f = 0.35$ and $R_f = 0.28$ were identical in molecular weight, i.e., $m/z(M^+)$ 310, demonstrating that there should be two compounds that are tanshinone IIA with a hydroxyl group at different substitution positions in the metabolites. The product corresponding to “ $m/z(M^+)$ 452, $R_f = 0.08$ ” had the highest polarity of the metabolites with a high-resolution mass spectrum of 452.1381. According to elemental composition, its molecular formula was deduced to be $C_{24}H_{22}NO_8$, which the authors preliminarily thought to be a condensation product between tanshinone IIA and glutamic acid.

8.2.2.2 Preparative Method

The most significant difference between preparative and analytical separation methods is that for preparative separation, one or more target compounds are obtained for use in further experiments. Whether extracting the effective fractions or a single compound, the most salient example is that of the research team at Hong Kong Chinese University, who isolated 1 mg of XH-14 [52] from 10 kg of raw Danshen. Of course, its bioactivity is also the property which attracted the chemists' attention. According to the requirements for submission of registration and classification of Chinese herbal drugs and natural drugs by the Chinese FDA, the active constituents extracted from natural drugs and preparations should account for more than 90 % of total extracts. In preparations based upon active fractions, the latter should be more than 50 % of the total extract. Furthermore, for the purpose of quality control in drug preparation, it is also necessary to provide qualified control substances or purified compounds. If the control needs to be obtained, it necessarily involves preparative

separation. This requires an effective separation based on the crude extract obtained during extraction. Separation is used to obtain the purified compounds which, in most cases, are separated with column chromatography. When a major constituent is more than 70 % of the crude extract, purification with recrystallization can be performed based on the different dissolubilities of major constituents and microconstituents in different solvents. The following examples are introduced as per the original reports. Considering the technical conditions in different time periods, it is not necessary to follow them exactly. However, the technical principles still have a reference value.

Systemic Chemical Separation

The initial work was reported by Nakao of Japan. Danshen produced in Northeastern China was extracted with ether. After removing the resins, pigment crystals were obtained and treated with acetone, yielding two parts: insoluble and soluble fractions. The insoluble fraction was recrystallized using xylene, obtaining a mixture containing two types of crystals; the one with a large specific gravity and particle size was referred to as tanshinon I, and the one with the smaller specific gravity and particle size was referred to as tanshinon II. The soluble fraction was concentrated and crystallized, followed by repeated recrystallization with acetone to remove the insoluble constituents. The resulting precipitate was a red crystal, named tanshinon III with an unknown structure at that time. In 1941, Takiura used glacial acetic acid and chloroform to repeatedly recrystallize the above tanshinon I and obtained a purple brown crystal with a melting temperature of 231–232 °C, which reveals a blue purple color when reacted with sulfuric acid. Although repeated recrystallization of tanshinon II crystal with acetone or benzene obtained an orange red crystal with a melting temperature of 214–216 °C, its formula was not always consistent with the formula $C_{19}H_{18}O_3$ reported by Nakao.

Based upon the molecular formula $C_{19}H_{18}O_3$, the calculated theoretical values of carbon and hydrogen are C 77.51 and H 6.17, respectively, but the values obtained from experiments were

C 76.42 and H 6.11; the measured carbon value was 1 % lower than that calculated. It was thereby suggested that tanshinon II was still a mixture. Alumina column chromatography was used to separate the mixture: Run the 5 % benzene solution containing tanshinon II through the column, washing with benzene. Two colored bands can be seen clearly on the column. Remove the bands separately, extract with chloroform, and crystallize. The crystal obtained from the upper band (indicating it has stronger adsorbability) melts at 222 °C and is named tanshinon IIB. The one obtained from the lower band (indicating weaker adsorbability) melts at 214 °C and is named tanshinon IIA.

Immediately after the separation of tanshinon II, tanshinon III was separated in a similar way: load the 1 % benzene solution of compound III onto the alumina column to get three color bands of A, B, and C. B and A at the top is a red color. Extract with chloroform, concentrate, and recrystallize in benzene solution. The melting point of the crystal is 222 °C and turns green when reacted with concentrated sulfuric acid. In the alumina column containing bands B and C, elute continuously with a large amount of benzene and collect 200 ml of the liquid with an orange color, followed by concentrating and loading onto another alumina column. Three color bands were obtained; from top to bottom, band D was red, having the highest adsorbability, band E was apricot, turning blood red when reacted with concentrated sulfuric acid, and band F was cardinal red, turning green when reacting with concentrated sulfuric acid. The purified products were recrystallized with benzene to get a red crystal for band F, referred to as tanshinon IIA, with a melting point of 211 °C, and an orange crystal for band E, referred to as cryptotanshinon [3], with a melting point of 191 °C. The top band D was recrystallized to get a crystal with a melting point of 222 °C, i.e., tanshinon IIB. The above experiments reflect the separation techniques used in the 1940s.

TLC Used to Separate Microconstituents

In *TLC: A Laboratory Handbook*, compiled by Egon Stahl, statistical data reveal that since TLC

was used for separation of organic compounds in 1960, its use has grown rapidly from less than 100 papers on TLC in 1960 to more than 1,200 papers in 1964. This trend is also shown in the separation of chemical constituents of Danshen. The representative study is by Kakisawa et al., who isolated two microconstituents from Danshen: 1-hydroxy-tanshinone IIA and methyl tanshinonate, with yields of 0.005 and 0.002 %, respectively [18]. In 1969, Kakisawa et al. again isolated from Danshen three more microconstituents with a 1,4-p-benzoquinone structure, i.e., isotanshinone I, isotanshinone IIA, and Isocryptotanshinone [28]. Because this study was published as a short communication in *Tetrahedron Letter*, it did not provide a detailed procedure, only describing that during the analysis of the crude extract of Danshen with TLC, more than 10 tanshinones were identified; 6 of them were already known, plus the three microconstituents mentioned above. They all belong to royleanone-type isotanshinones containing 1,4-p-benzoquinone.

Chemical Study on Tanshinones in China

Chinese research on the chemical constituents of Danshen began in the 1970s. In a study of isolating active antibacterial constituents from Danshen, a total of 10 compounds were obtained; 7 were tanshinones with an orthonaphthoquinone furan or dihydrofuran ring, and 3 were acidic constituents that were soluble in Na₂CO₃ solution, had an enolic structure, were also royleanone-type compounds with 1,4-p-benzoquinone, and were referred to as neotanshinone A, B, and C, respectively [13]. The procedure they used is described below:

Extraction and primary fraction of liposoluble constituents in Danshen: 2 kg of Danshen root powder was percolated using ether, and the percolate was then treated with 5 % sodium carbonate solution to obtain 30 g of an acidic fraction and 34 g of a neutral fraction insoluble in 5 % sodium carbonate solution.

Separation of chemical constituents in the neutral fraction: 1 kg of silica gel (80–120 mesh) was mixed into benzene and packed in a column by the wet method. 30 g of the neutral fraction was separated on the column, using benzene for

elution. Seven major color strips, i.e., yellow, brownish red, purple red, orange, yellow brown, red and deep brown, could be seen clearly on the column. When the leading strip migrated to the bottom of the column, the column was cut based on the position of the strips, and the fractions were then extracted and eluted with acetone. The eluate was concentrated, separated with preparative TLC, and activated using silica gel (160–200 mesh) at 120 °C for 4 h. The thin layer was a dry plate without adhesive, 30 cm × 40 cm in area, and 3–5 cm in thickness. The developing solvent was benzene:methanol (9:1). After spreading, the solvent was removed, the major strips were eluted with acetone, and the eluate was recrystallized using methanol.

Tanshinone I and tanshinone IIA were isolated from the brown red strip; methyl tanshinonate, 1-hydroxytanshinone IIA, and levo dihydrotanshinone I from the purple red strip; cryptotanshinone from the orange strip; and tanshinone IIB from the red strip.

Separation of the fraction extracted by sodium carbonate solution: the separation was first performed with column chromatography. 800 g of silica gel (80–120 mesh) was packed in a column by the wet method. 30 g of the fraction extracted by sodium carbonate solution was loaded onto the column, and eluted with benzene:methanol (10:1). A deep red strip was obtained. The strip was collected and the solvent removed to get 3 g of red cream. The cream was then separated with preparative TLC using the same conditions as before. Following the spread, multiple complex strips were obtained. The major strips were taken out, eluted with acetone, and recrystallized with methanol to get three compounds, neotanshinone A, B, and C.

Study on Tanshinones Used for Therapy of Coronary Heart Disease

The Institute of Materia Medica team of the Shanghai Chinese Academy of Sciences focused on the isolation and discovery of the active chemical constituents in Danshen that can treat coronary heart disease. Take 6 kg crude drug of Danshen and extract under heating reflux with 95 % ethanol. Decompress and concentrate to get

the extract, then wash with water to remove water-soluble constituents to get 480 g of total liposoluble constituents. Take 260 g for reflux with an appropriate amount of benzene, followed by concentration, and mix with neutral alumina (grade IV). Load onto a 2-kg alumina column for chromatography and rinse with benzene. After the full spread of color strips, remove alumina completely from the column and cut it into three segments according to its color strips; purple red, orange red, and dark red. The three strips are then separated further with chromatography.

Separation of purple red strip: place it into the column again, and continue to wash with benzene. When the benzene solution is slightly concentrated, brown red crystal is precipitated, which is then recrystallized with methanol to obtain tanshinone I with a melting point of 233 °C. Proceed to concentrate the mother solution from the tanshinone I filtration, obtaining a red crystal which is then recrystallized with ethanol to get tanshinone IIA with a melting point of 202–204 °C. Concentrate again the mother solution from which the tanshinone IIA filtration, obtaining a maroon octahedron crystal and a small amount of tanshinone IIA. The maroon octahedron crystal is then recrystallized twice with benzene–ethanol to get a purple red styloid with a melting point of 174–176 °C (decompose), which was identified as methylenetanshinone.

Separation of orange red strip: place again into the alumina column, rinse with benzene, and spread the strip completely. Then, cut it along the strips and collect two segments. One is eluted with acetone and concentrated with acetone to obtain a red linear thin crystal, which is then recrystallized twice with acetone and identified as methyl tanshinonate with a melting point at of 183–184 °C; the other is also rinsed with acetone, and the acetone solution is concentrated to a small volume to obtain macrocrystals, which are then recrystallized twice with acetone to get an orange red needle crystal that was identified as cryptotanshinone with a melting point of 180–182 °C.

Separation of dark red strip: transfer it into the column and rinse with benzene–ethanol (10:1). Dry the eluate by reducing pressure, filter after dissolving with dehydrated alcohol, concentrate,

and place at room temperature. Subsequently, columnar solid matter is precipitated and recrystallized twice with dehydrated alcohol to obtain red fine needle crystals with a melting point of 202–204 °C, which was identified as tanshinone IIB.

The above two strips were isolated with “dried column” chromatography in combination with preparative TLC or repeated-column chromatography and yielded different diterpenoid tanshinones.

Separation Method Based on Bioactivity

In the 1980s, Japanese researchers initiated a new approach to separation, based on bioactivity and combined with chemistry. This approach first identifies a target with special bioactivities, then establishing a rapid and convenient in vitro screening assay, which is comparable to a bioactivity detector. This activity index is used to guide the separation, eventually obtaining the active substances. Many compounds have been isolated with this method, for example, the platelet aggregation inhibitor Ro-09-0680 (miltirone I), the active substance that can bind to the receptors in cerebral nerve cell with a stabilization effect, i.e., miltirone, those that can bind to the adenosine receptor A₁, e.g., XH-14, and the aldose reductase inhibitors against diabetic complication.

Isolation of platelet aggregation inhibitor, Ro-09-0680 [8]: A model of platelet aggregation induced by collagen was used to screen for the active substances in Danshen which inhibit platelet aggregation. The experimental results showed that the methanol extract of Danshen could inhibit platelet aggregation induced by collagen in a rabbit blood test, with an IC₅₀ of 150–450 µg/ml. To further isolate and identify the active constituents, the following steps were taken: 900 g of Danshen roots were extracted with methanol at room temperature, the extract was concentrated to 90 g and dissolved in water and then extracted at pH 8 with ethyl acetate to 22 g with a specific activity 10 times that of the methanol solution, i.e., IC₅₀ = 10–30 µg/ml, but IC₅₀ > 800 µg/ml in water. The results indicate that the active constituents inhibiting platelet

aggregation were mainly present in the ethyl acetate extract. Based on this, further chromatography with silica gel columns was performed to isolate the active constituents soluble in ethyl acetate. A Wakogel C-300 column was used for separation, and methylene dichloride was used for elution. The orange red pigment fraction isolated was loaded onto preparative TLC with Kieselgel 60 F₂₅₄ and spread with methylene dichloride. The purified color strip was removed, eluted with methanol, and recrystallized. A total of 5 purified compounds were obtained; they were compound I (identified as Ro-09-0680, dark red crystal, 26 mg), tanshinone IIA (orange red crystal, 1.0 g), tanshinone I (dark red needle crystal, 1.1 g), dihydrotanshinone I (370 mg), and cryptotanshinone (830 mg). The above 5 compounds all have the basic structure of 1,2-orthonaphthoquinone, and tricyclic diterpene quinone Ro-09-0680 is the compound with the highest activity. Tests showed that it inhibits the activity of CPA with an IC₅₀ of 6.6 µM.

Based on SARs, we suspected that there should be other constituents with an inhibitory effect on CPA in Danshen and that the low-polarity constituents should contain compounds with a structure similar to that of Ro-09-0680. Danshen roots were extracted with ethanol to obtain 270 g total ester, which was then refluxed with ether to obtain 150 g of gelatin form paste. The paste was separated on a Qingdao silica gel (110 mesh) column and eluted with petroleum ether followed by petroleum ether–acetone (98:2–95:5). After concentration, the compounds were detected with TLC and the same constituents were pooled. They were isolated with low-pressure column chromatography using 10–40 µm silica gel. 5 constituents were isolated this way, identified as miltirone, tanshinone IIA, Δ¹-miltirone, Ro-09-0680, Δ¹-tanshinone IIA, and ferruginol. According to the CPA activity assay, the activity was 5.76 µM for miltirone and 2.14 µM for Ro-09-0680.

Isolation of the substance with activity on adenosine receptor: the binding of radioactive ligand to the adenosine receptor A₁ in the nerve cell membrane of calf brain mantle was used as an activity assay [52], and a high-activity

substance XH-14 with a parent nucleus of benzofuran was isolated from Danshen. 10 kg of Danshen roots were used, and only 1 mg XH-14 was finally obtained. The isolation procedure is as follows: boil 10 kg of Danshen roots in water for 2 h and extract the liquid with CHCl_3 . Concentrate the CHCl_3 extraction solution until dry to obtain a red colloid substance (8 g, $\text{IC}_{50} = 15 \mu\text{g/ml}$). Silica gel column chromatography (silica gel, 70–230 mesh; eluant, $\text{EtOH}-\text{CHCl}_3 = 5:95$) was performed with the colloid, and a red product was obtained (400 mg, $\text{IC}_{50} = 2 \mu\text{g/ml}$). Silica gel column chromatography (silica gel, 230–400 mesh; eluant, $\text{EtOAc}-\text{CHCl}_3 = 5:95$) was then performed again on the product to obtain an active product (100 mg, $\text{IC}_{50} = 0.5 \mu\text{g/ml}$). The active product was then treated with semi-preparative HPLC (eluant, $\text{EtOH}-\text{CHCl}_3 = 2:8$) to get a crude compound XH-14 (10 mg, $\text{IC}_{50} = 0.05 \mu\text{g/ml}$). For the final purification, HPLC using gradient elution was used, with $\text{CH}_3\text{CN}-\text{CHCl}_3$ (2:98–15:85) as an eluant, and obtained XH-14 (1 mg, $\text{IC}_{50} = 0.06 \mu\text{g/ml}$) within 30 min. The structural formula of XH-14 is shown in Fig. 8.7 (67).

XH-14 is the least abundant (approximately 0.1 ppm) bioactive compound isolated from Danshen so far. It is notable that the team who isolated the compound also accomplished the total synthesis of XH-14. Furthermore, the bioactivity of synthesized XH-14 also increases significantly with each further purification; its IC_{50} value changes from 15 $\mu\text{g/ml}$ for crude extracts to 0.006 $\mu\text{g/ml}$.

Isolation of aldose reductase inhibitor [33]: Glucose can be transformed into sorbitol via an aldose reduction reaction. Sorbitol is then transformed into fructose by tissue dehydrogenase. Fructose accumulates in the lens, retina, nerve tissue, and kidney tissue and is a biochemical basis for long-term complications leading to diabetes. To block the development of long-term complications leading to diabetes, aldose reductase was used as a target to search for and isolate the active substances from Danshen with an inhibitory effect on aldose reductase. Two active constituents were finally obtained, Danshenol-A (55) and Danshenol-B (54), whose inhibitory

activities were $\text{IC}_{50} = 0.10 \mu\text{M}$ and $\text{IC}_{50} = 1.75 \mu\text{M}$, respectively.

The isolation procedure is as follows: 8 kg of Danshen roots were boiled in water at 80 °C for 3 h with a water extraction yield of 26.2 % ($\text{IC}_{50} = 213.8 \mu\text{g/ml}$). The residues from the water extraction were further extracted with methanol with a yield of 15.9 % ($\text{IC}_{50} = 49.0 \mu\text{g/ml}$). The methanol was concentrated, spread in $\text{EtOAc}-\text{H}_2\text{O}$, and two constituents were obtained, which were either soluble (12.2 %, $\text{IC}_{50} = 8.3 \mu\text{g/ml}$) or insoluble (2.1 %, $\text{IC}_{50} = 30.2 \mu\text{g/ml}$) in EtOAc . The former was treated with CHCl_3 to dissolve itself in a CHCl_3 layer (5.8 %, $\text{IC}_{50} = 5.8 \mu\text{g/ml}$). 27.8 g of the effective fraction dissolvable in CHCl_3 was run with silica gel column chromatography. It was eluted with CHCl_3 –hexane at different gradients, and the following fractions were collected: fraction A with 10 % CHCl_3 –hexane (1.65 g); fraction B with 20–30 % CHCl_3 –hexane (4.76 g); fraction C with 40–50 % CHCl_3 –hexane (2.80 g); fraction D with 60–70 % CHCl_3 –hexane (3.32 g); and fraction E with 80–90 % CHCl_3 –hexane (3.12 g). Fraction F was finally eluted with CHCl_3 (6.92 g). Fraction B (4.76 g) was run with silica gel column chromatography again with EtOAc –hexane (20:80) as the eluant, obtaining successively tanshinone IIA (360 mg, $\text{IC}_{50} = 1.14 \mu\text{M}$) and cryptotanshinone (18 mg, $\text{IC}_{50} = 10.0 \mu\text{M}$). Fractions C and D were run with silica gel column chromatography with EtOAc –hexane (30:70) as the eluant in combination with preparative TLC (EtOAc :benzene = 5:95), obtaining 7 mg of the major active substance Danshenol-A. Fraction E was run with silica gel column chromatography with EtOAc –hexane (40:60) as the eluant in combination with preparative TLC (EtOAc :benzene = 25:75), obtaining 23 mg Danshenol-B, dihydrotanshinone I (7 mg, $\text{IC}_{50} = 1.19 \mu\text{M}$) and sugiol (20 mg, $\text{IC}_{50} > 10 \mu\text{M}$) were obtained from fraction F.

8.2.2.3 General Operations for the Isolation of Known Constituents in Danshen

With more and more chemical constituents being isolated from Danshen, the number of constituents with known structures is also increasing. In

order to study the pharmacological activities of these known constituents or to discover their new applications, the selective isolation of some of them is usually needed. However, in practice, it is not necessary to conduct the isolation according to methods described in the original publication, because techniques are advancing with time. The following is a summary of general principles for isolation, but the more important thing is to master the principles and apply them skillfully.

Separation According to the Structure of a Known Compound

Determine and design an isolation method according to the physicochemical properties (e.g., dissolvability, chromatographic behavior, detection characteristic, spectrum data) provided by the components with known structures. Establish a TLC to explore and optimize column chromatography conditions. This is also currently a common laboratory method. Prior to isolation using a column, one has to choose an adsorbent and eluent. One also has to consider what order the constituents will be eluted in. There are some general rules that can be followed. The elution order for each constituent can be predicted based on their R_f values for “normal-phase adsorption” TLC. However, for chromatography with a silylated ODS reversed-phase column, the order correlates with the hydrophobicity/hydrophilicity ratio. For example, tanshinone IIA is generally eluted after neotanshinone, tanshinlactone, and some tricyclic diterpene quinone, and although tanshinone I is right behind tanshinone IIA in TLC, its dissolvability in benzene, cyclohexane, acetone, or ethanol is much lower than that of tanshinone IIA (dissolvability of crystals also involves non-binding interactions between molecules). Therefore, when organic solvents with low polarity, e.g., benzene or cyclohexane, are used as the eluent, the elution of tanshinone I is difficult compared with tanshinone IIA, but due to the increased polarity provided by the dihydrofuran ring, cryptotanshinone is eluted after tanshinone I. The local negative charge (-0.2210) of the oxygen atom in the dihydrofuran ring is much lower than that (-0.1693) in the furan ring. Therefore,

cryptotanshinone's polarity is higher and it is eluted after tanshinone I.

Another important point is that the R_f value in TLC reflects only the molecular polarity of a compound and does not entirely show the dissolvability of this compound in a solvent because dissolvability is also related to the non-binding interaction between molecules, especially because the stronger the π - π stacking action in the molecule of a compound, the lower its dissolvability. For example, although there is very little difference between the R_f values of tanshinone I and tanshinone IIA in TLC, the dissolvability of the former in benzene, cyclohexane, acetone, or ethanol is much lower than that of tanshinone IIA. If cyclohexane:ethyl acetate (98:2–95:5) is used as the eluent, the isolation will be much easier.

Collection and Detection of Eluent

To determine whether an eluent contains a single component or a mixture, TLC can be used as a preliminary assay. For example, if one wants to isolate from Danshen methyl tanshinonate or hydroxytanshinone IIA, two compounds generally 0.001 % in content, a single round of column chromatography may not finish the job. However, TLC can often discover constituents with very low content, especially from several mother liquors from which tanshinone I has been precipitated, which are then isolated via a second step of column chromatography.

To isolate microconstituents from an extract, it is necessary to identify their locations or fractions first. This information can be obtained by a chromatogram. Collect the mother liquor remaining after crystallization of these locations, including their adjacent locations, and analyze the components and constituents of the mother liquor to isolate these microconstituents. For example, methylenetanshinone is present in the mother liquor of tanshinone IIA and tanshinone I.

Preisolation with TLC

By preisolation with TLC, it is possible to know the composition of multiple components and the ratios of their relative contents. After an isolation condition is explored with TLC, it can be used for

column chromatography as previously described. However, for column chromatography with elution, especially with gradient elution, the isolation condition of TLC cannot be used directly. It must be properly transformed for elution-mode preparative column chromatography, which can be used for large-scale gradient elutions especially.

8.2.3 Operating Procedure and Examples of Preparative Isolation

Now, a complete operating procedure (physicochemical detection, thin-layer isolation and suitable condition of column chromatography-gradient elution) for an entire preparative isolation is described as follows:

8.2.3.1 Physicochemical Detection of Liposoluble Components of Danshen

No matter which chromatography method is used for isolation, the most important thing is to establish a rapid and accurate qualitative detection method. The detection method should be suited for the specific chemical constituents in certain Chinese medicine drugs. For example, the target compounds in Danshen's liposoluble fractions are tanshin diterpene quinone and related terpenes (diterpene, triterpene), and among them, tanshinone diterpene quinone compounds are even more important. From their cyclic skeleton, they are mainly quinones derived from abietane tricyclic diterpene, which are mainly compounds with a 1,2-orthonaphthoquinone furan ring, i.e., so-called tanshinones. Due to differences in chromophores and conjugated chain lengths, different tanshinones can be distinguished according to the position and intensity of their absorption peaks in the ultraviolet-visible light region.

Tanshinones

Tanshinones can show different colors under visible light, which can be distinguished with the naked eye but need to be carefully identified. For example, cryptotanshinone assumes an orange color, tanshinone IIA orange red, tanshinone

I brown (indicating a 1,2-orthophenanthrenequinone structure), and methylenetanshinone purple red due to an additional conjugated double bond after the exocyclic methenyl group of its ring A substituting the gem-dimethyl group in tanshinone IIA. This demonstrates that changes in the colors of different tanshinones under visible light reflect the differences in their chromophores and the length and pattern of their conjugated chains. To further confirm this, dissolve these compounds in chloroform, dot them onto a silica gel plate using a capillary drip tube, and observe the specific color spots. Then, add 1–2 drops of concentrated sulfuric onto the color spots. After dehydrolysis of the sample caused by the concentrated sulfuric acid, further changes in color can be seen. For example, after reacting with concentrated sulfuric acid, tanshinone IIA appears green (including all compounds of tanshinone type II), cryptotanshinone appears orange red, and tanshinone I appears blue (including all compounds of tanshinone type I). Those diterpenes or triterpenes without chromophores cannot be observed by the naked eye under visible light. Also included are the oxidative products of tanshinone (see Sect. 8.6), or some artifact products, e.g., Danshenspiroketallactone and tanshinlactone, which are colorless compounds under visible light but can be distinguished under ultraviolet light due to their conjugated chains of certain lengths. When the silica gel plate used for chromatography is placed under a UV-254-nm or 356-nm ultraviolet lamp, blue or blue purple fluorescent spots can be seen due to different conjugated chains. Compounds with different structures also can be distinguished according to the color tone of their fluorescent spots.

Liposoluble Constituents Containing Only a Single Double Bond

Danshen contains some plant sterols such as β -sitosterol and various triterpenic acids such as ursolic acid. They have no absorption of ultraviolet-visible light. In order to detect these compounds, they need to be spread with a thin-layer plate followed by spraying with water to wet the plate and observe whether or not there are hydrophobic spots. If there are, the thin-layer

plate is dried and sprayed with 5 % phosphomolybdic acid in ethanol and heated to 90 °C. If these hydrophobic spots turn a blue black color after reacting with the above reagents, they indicate the presence of plant sterols or triterpenic acid. Further analysis can be done based on this. In addition, there are also flavonoids in some species of Danshen, which can be identified with the detection reagent used for flavonoids. Some compounds with special cyclic systems, e.g., salvicolone (59) containing a seven-membered ring, were identified initially according to the ultraviolet absorption spectrum [35].

8.2.3.2 Thin-layer Isolation Based on Same Chromophore

The tanshinone II compound family has more than ten members. Aside from tanshinone IIA, it includes tanshinone IIB, hydroxytanshinone IIA, methyl tanshinonate, and tanshindiol A, B, and C. All of these compounds contain the same chromophore; the only difference is that an auxochrome, which usually is a hydroxyl group, may be added. Under visible light, their colors cannot be distinguished by the naked eye, and even their ultraviolet absorption curves are basically the same. However, because they contain different numbers of oxygen atoms, e.g., 1 or 2 more hydroxyl groups in ring A, or hydroxymethylation of the furan methyl group, their chromatographic behaviors and R_f values are different. The principle of chromatography-based isolation of different tanshinone II compounds is based on their different polarities.

8.2.3.3 Adsorbents and Developing Solvent

The isolation of liposoluble tanshiones is still mainly based on adsorption chromatography. Aluminum oxide was the major adsorbent in early years, but silica gel is the choice at present. Silica gel not only offers good separation, but also maintains samples' stabilities. The quality of silica gel made in Qingdao, China is very good. Silica gel plates can be self-made; generally, 0.8 % carboxymethylcellulose sodium is dissolved into boiling water and clarified, and the supernatant is used as the adhesive. Premade

thin-layer plates can also be used. Use home-made silica gel plates (silica gel of <200 mesh with 0.8 % CMC-Na as adhesive, activated at 110 °C for 1 h) or Kieselgel 60 F₂₅₄ (Merck).

Based on the experience of isolating diterpenes or diterpene quinone, it seems very difficult to separate all compounds with different polarities on a thin-layer plate using a single developing solvent. The following six developing solvents are selected to show their compositions, properties, and application scopes [9]:

- (1) $C_6H_6-(CH_3)_2CO$ (95:5);
- (2) $C_6H_6-CHCl_3-(CH_3)_2CO$ (8:2:0.5);
- (3) Petroleum ether–AcOEt (9:1);
- (4) Petroleum ether saturated with MeOH–THF (10:1);
- (5) CH_2Cl_2 –AcOEt– $(CH_3)_2CO$ (9:1:1);
- (6) $CHCl_3$ –AcOEt (3:1).

Solvents 1 and 2 are suitable for conventional isolation of diterpenoid tanshinones. For example, in tanshinone II compounds, there is an additional hydroxyl group in tanshinone IIB compared to tanshinone IIA. The difference in their R_f values is 0.44 for solvent 1, and 0.59 for solvent 2. They can also be used to distinguish whether it is a furan or dihydrofuran ring combined with 1,2-orthonaphthoquinone. For example, comparing cryptotanshinone (combined with dihydrofuran ring) with tanshinone IIA (combined with furan ring), the R_f value in solvent 1 is 0.32, in solvent 2, 0.34. Also, the difference in R_f values between dihydrotanshinone I and tanshinone I was also up to 0.29. One of the reasons for the different R_f is that the local negative charge of oxygen atom in a dihydrofuran ring is significantly larger than that in a furan ring, which makes the polarity of cryptotanshinone, containing a dihydrofuran ring, or dihydrotanshinone I, higher than that of tanshinone IIA and tanshinone I, both containing a furan ring.

However, solvents 1 and 2 are not suitable for the isolation of low-polarity diterpene compounds such as ferruginol, or tricyclic diterpene quinone compounds such as miltirone and miltirone I. They are also unsuitable for the isolation of compounds which only differ in their ring A. For example, the ring A of tanshinone I is a benzene

ring containing a methyl group, but the one of tanshinone IIA is an alicyclic ring containing a gem-dimethyl group. The difference of their R_f values is only 0.03 in solvent 1. The ring A of methylenetanshinone is an exocyclic methenyl group replacing the gem-dimethyl group in tanshinone IIA, and the difference of their R_f values is only 0.02. It is obvious that solvents 1 or 2 cannot separate methylenetanshinone from tanshinone IIA and tanshinone I. Therefore, using low-polarity solvents, e.g., solvents 3 and 4, in which petroleum ether or n-hexane replace

benzene in solvents 1 and 2, can improve the separation. The difference in R_f values between tanshinone IIA and tanshinone I can be up to 0.12 in solvent 3 and 0.11 in solvent 4. In addition, solvent 3 can also be used for the separation of compounds differing only in their ring A. For example, both miltirone and miltirone I belong to tricyclic diterpene quinones, and the difference between their R_f values is 0.14 in solvent 3.

Solvent 5 is a developer with strong selectivity and is used specially to isolate isomers with the molecular formula $C_{19}H_{18}O_4$, e.g., tanshinone IIB, 3 α -hydroxytanshinone IIA, and 3 β -hydroxytanshinone IIA.

Table 8.2 R_f values of diterpenoid tanshinones and related compounds in different solvents [9]

Compound	Molecular formula	Solvent system					
		1	2	3	4	5	6
Ferruginol 50	$C_{20}H_{30}O$	0.77	0.80	0.45			
Danshenxinkun B 40	$C_{18}H_{16}O_3$	0.82	0.83	0.51			
Salviolone 59	$C_{18}H_{20}O_2$	0.62	0.79	0.47			
Miltirone 27	$C_{19}H_{22}O_2$	0.67	0.83	0.43			
Δ^1 -miltirone 29	$C_{19}H_{20}O_2$	0.64	0.82	0.39			
Tanshinlactone 46	$C_{17}H_{12}O_3$	0.69	0.82	0.35			
DanshenSpiroketalactone 42	$C_{17}H_{16}O_3$	0.54	0.76	0.25			
Miltirone I 28	$C_{18}H_{16}O_2$	0.55	0.80	0.29	0.39		
Tanshinone IIA 3	$C_{19}H_{18}O_3$	0.51	0.78	0.33	0.39		
Δ^1 -tanshinone IIA 15	$C_{19}H_{16}O_3$	0.50	0.77	0.28	0.33		
Methylenetanshinone 8	$C_{18}H_{14}O_3$	0.49	0.76	0.29	0.37		
Tanshinone I 1	$C_{18}H_{12}O_3$	0.48	0.73	0.21	0.28		
Methyl tanshinonate 6	$C_{20}H_{18}O_5$	0.35	0.65				
Nortanshinone 13	$C_{17}H_{12}O_4$	0.25	0.55				
Cryptotanshinone 2	$C_{19}H_{20}O_3$	0.19	0.44		0.15		
Dihydrotanshinone I 7	$C_{18}H_{14}O_3$	0.19	0.44		0.13		
Danshenol-A 55	$C_{21}H_{20}O_4$	0.14	0.31				
Tanshinone IIB 4	$C_{19}H_{18}O_4$	0.07	0.19			0.64	0.49
3 α -hydroxytanshinone IIA 14	$C_{19}H_{18}O_4$	0.07	0.18			0.57	0.41
Przewaquinone A 19	$C_{19}H_{18}O_4$	0.06	0.17			0.50	0.43
Przewaquinone B 20	$C_{18}H_{18}O_4$	0.04	0.14				
Danshenxinkun A 39	$C_{18}H_{16}O_4$	0.03	0.17				0.17
Tanshindiol B 11	$C_{18}H_{16}O_5$						0.16
Tanshindiol A 10	$C_{18}H_{16}O_5$						0.10
Tanshindiol C 12	$C_{18}H_{16}O_5$						0.07
Triterpene, salvianolic acid A	$C_{30}H_{46}O_4$						0.80
Triterpene, salvianolic acid B	$C_{29}H_{42}O_4$						0.62
Triterpene, oleanolic acid	$C_{30}H_{48}O_3$						0.54

3 α -hydroxytanshinone IIA, and Przewaquinone A (the methyl group in the furan ring of tanshinone I was oxidized to become a hydroxymethyl group). All three tanshinones contain a hydroxyl group which differs only in its position, thereby changing their polarities. The polarity is highest for Przewaquinone A with an R_f value of 0.50 and is lowest for tanshinone IIB with an R_f value of 0.64, with a difference of up to 0.14 between the two, and is intermediate for 3 α -hydroxytanshinone IIA with an R_f value of 0.57. The tanshinones containing two hydroxyl groups, e.g., tanshindiol A, B, and C, not only have high polarity but are isomers with the same molecular formula ($C_{18}H_{16}O_5$). Considering that their high polarity makes them difficult to dissolve in low-polarity solvents, developing solvent 6 composed of chloroform, $CHCl_3$ –AcOEt (3:1), can be used to isolate the three tanshindioles. The solvent plays a special role in distinguishing between the *cis*- and *trans*-isomers of tanshindioles, e.g., tanshindiol C (3,4-dihydroxyl groups are present in *cis* form with an R_f value of 0.10) and tanshindiol B (3,4-dihydroxyl groups are present in *trans* form with an R_f value of 0.07). The R_f value of tanshindiol A in solvent 6 is 0.16. In addition, Danshen may contain some triterpenes like triterpenic acids, e.g., oleanolic acid, salvianolic acid A, and salvianolic acid B (see Sect. 8.7 for isolation and structural identification of the triterpenic acids), which have a strong polarity due to multiple hydroxyl groups or carboxyl groups and can also be generally isolated in developing solvent 6 (see details in Table 8.2).

8.2.4 Determining Column Chromatographic Conditions Based on Preseparation on TLC

The basis for using TLC preseparation data to determine column elution conditions is that the R_f value of each sample measured with TLC can be converted into its flow rate (R) for column chromatography. It is assumed that the R_f value of samples measured on thin-layers is approximately equal to the flow rate (R) in column chromatography. Because the developing solvent contained

in the thin-layer immobile phase evaporates continuously during development, there are some changes in solvent composition at each site of the thin-layer plate, with the component solvents and their contents adjacent to the initiation points often being higher than those adjacent to the leading edge. However, if the operating conditions of chromatography are strictly controlled, the true R_f value can be obtained.

Components separated using TLC generally have R_f values in the range $0.85 > R_f > 0.05$. Assuming $R_f \approx R$, an approximate formula for the capacity factor k' can be used: $k' = 1/R - 1$. The capacity factor is the reciprocal of the flow rate (R) and can also be considered the reciprocal of the approximate R_f value.

For example, k'_1 is 0.18 for an R_f of 0.85, and k'_2 is 19 for an R_f of 0.05. The capacity factor selected is generally in the range $0.18 < k' < 19$. If the solvent selectivity coefficient α is used to represent the ratio of the two above capacity factors,

$$\alpha_{\max} \approx k'_2/k'_1 \approx 19/0.18 \approx 100$$

When the R_f values of two constituents in TLC are very large, greater than 0.8, and have a small difference between them, for example R_f values of 0.85 and 0.88, the capacity factor is very small under these conditions, i.e., $0.14 < k' < 0.18$.

$$\alpha_{\max} \approx k'_2/k'_1 \approx 0.18/0.14 \approx 1.3$$

It is thereby seen that the value of the isolation coefficient is in the range $100 > \alpha > 1.3$ for TLC.

When the isolation coefficient $\alpha = 1.3$, the theoretical plate number (N) is calculated according to the resolution (R_s) formula:

$$R_s = 1/4 \sqrt{N \cdot \alpha - 1/\alpha \cdot k'/k' + 1}$$

For $R_s = 1$, N is approximately 300.

Figure 8.8 shows that good separation depends not only on the adsorbent but the solvent system used as well. Converting the flow rate from TLC to the capacity factor for column chromatography, as well as increasing moderate capacity factors, will improve the isolation

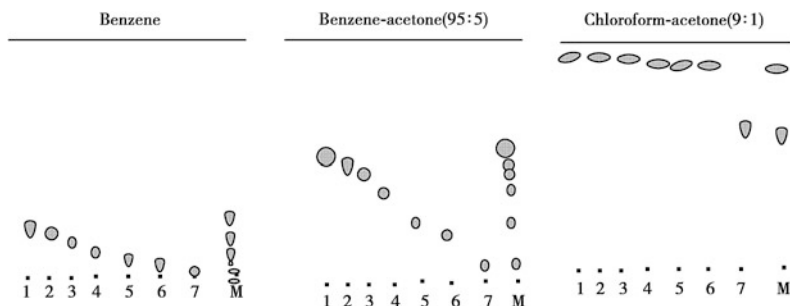


Fig. 8.8 TLC of tanshinones in solvents with different polarities 1 Tanshinone IIA; 2 Methylene tanshinquinone; 3 Tanshinone I; 4 Methyl tanshinonate; 5 Hydroxytanshinone IIA; 6 Cryptotanshinone; 7 Tanshinone IIB; M mixture

effectiveness of column chromatography. For example, when separating tanshinone IIA and tanshinone I, a solution system of chloroform–acetone (9:1) would not be suitable because α is approximately equal to 1 and the capacity factor k' is also close to zero (under these conditions, the adsorbent does not play any adsorptive role). However, if chloroform is replaced by benzene, a much better result is achieved (see Fig. 8.8).

Tanshinone I has an R_f value of 0.13 and k_1' of 6.7, and tanshinone IIA has an R_f value of 0.18 and k_2' of 4.6. Thus, $\alpha = k_1'/k_2' = 6.7/4.6 \approx 1.5$.

It is thereby demonstrated that when using the same adsorbent to separate two similar components, very different separation results can be obtained when using different developing solvents. It is possible using TLC to obtain the flow rates of different compounds in different developing solvents, convert the flow rates into capacity factors, obtain the selectivity coefficient α based on the different capacity factors, and predict the separation effectiveness according to α . This is helpful for selecting a suitable solvent component and gradient, and determining the elution conditions accordingly.

8.2.5 Two Forms of Preparative Columns: Comparison Between Dry Column Chromatography and Gradient Elution

Prior to the 1970s and 1980s, the methods used for the isolation of liposoluble constituents from Danshen were mainly dry column chromatography,

including some preparative thin-layer chromatographies (please refer to “1. Isolation method” in Sect. 2.2 for examples).

8.2.5.1 Dry Column Chromatography

The benefit of this method is that optimal separation conditions can be derived directly from TLC and that nylon bags can be used for packing the column. The nylon bag can be cut after separation, which is much more convenient than pushing the adsorbent out of the glass column. The adsorbent used for dry column chromatography must be inactive or have not too high of an activity. The commonly used adsorbents are of grades II–III. The particle size of the adsorbent should be the same as that used in TLC, which is generally 200–250 mesh. The adsorbent must be presaturated with the eluant used for chromatography. The solvent volume used for presaturation is 10 % of the adsorbent weight; add it to the adsorbent, shake gently to mix, and leave to equilibrate for at least 4–6 h. Pack the presaturated adsorbent into the column. The sample loading method is the same as that of column chromatography, with a sample to adsorbent ratio of 1:70–1:300. The developing solvent is the same as that used for TLC. Because most tanshinones are colored substances, the strips can be viewed directly after chromatography. Colorless constituents can be observed under ultraviolet light for fluorescent strips. Label and cut these strips, then extract with solvent, concentrate, and crystallize. This method’s shortcomings include an easily polluted laboratory environment and a low utilization ratio of the adsorbent. Examples are detailed in previous sections.

8.2.5.2 Gradient Elution

The separation of complex constituents not only depends on the composition of the selected solvent, but also closely depends on the change rate of the solvent gradient. Gradient elution means that during the process of chromatography, the composition of solvents changes gradually so that the strength of elution becomes stronger and stronger. In other words, the purpose of using gradient elution is to make sure that when chromatographic peak 1 and its adjacent peak 2 flow through the full column, their capacity factors k_1' and k_2' are maintained at or approaching a certain optimal value. From the above sections, we can see that the selection of the developing solvent is the key to good separation. The compositions of the developing solvents used in TLC are fixed. For example, the composition of developing solvent 3 is petroleum ether–AcOEt (9:1). However, for column chromatography with gradient elution, the composition of the elution solvent can be flexible. Eluents can be collected according to time span (several minutes, several hours, or dozens of hours) or according to the collecting volume (50, 100, or 500 ml). For example, use plain petroleum ether for the initial elution. After a set amount of time has passed or a certain volume has been eluted, increase the proportion of acetic ether in petroleum ether according to a plan such as the following gradient: petroleum ether, petroleum ether–acetic ether from 99:1, 98:2, 95:5 to 90:10. In manual operation, all constituents in each eluent should be identified individually using TLC before and after increasing the elution gradient. Examples of gradient elution in our laboratory are described in the following section.

8.2.6 Examples of Gradient Elution

8.2.6.1 Separation of Ferruginol, Miltirone, and Ro-09-0680

Onitsuka et al. reported in 1983 that Ro-09-0680 strongly inhibits platelet aggregation [8]. Based on SARs, we thought that the same tricyclic diterpene compound, miltirone, should possess a similar activity, spurring the isolation of this

compound from Danshen. From TLC data, the compound has a large R_f value in developing solvents 1 and 2, but a moderate value in developing solvent 3 (see Table 8.2). Therefore, the solvent composed of petroleum ether is considered to be suitable for gradient elution. The procedure is as follows: first 270 g total ethanol extract from dry roots of Danshen was extracted with ether reflux and concentrated to get 150 g colloidal extract, then mixed with diatomite. Column chromatography was run with silica gel (110–160 mesh) and successive elutions with petroleum ether, petroleum ether–acetone (98:2), and petroleum ether–acetone (95:5), and 250 ml of each eluent was collected.

After concentration, TLC was used to detect and pool like constituents. 2 g of concentrated sample from the petroleum ether–acetone (98:2) eluent was run with low-pressure column chromatography on 10–40 μ m thin silica gel with benzene as the solvent, and 2–5 fractions of 100 ml eluent were collected. 0.46 g of light yellow resin-like substance was obtained, then recrystallized with ethanol after purification, and was identified as ferruginol. Fractions 28–30 in the petroleum ether–acetone (95:5) eluent were pooled, run again with low-pressure column chromatography, and then eluted with petroleum ether–acetone (99:1). Fractions 15–21 were pooled and crystallized to yield a dark red massive crystal, which was determined with TLC to be a mixture. Preparative TLC was then run with silica gel–CMC and the developing solvent petroleum ether–acetic ether (9:1) to get two color strips with R_f values of 0.43 for an orange strip and 0.39 for a red strip. The two strips were then cut off and eluted with chloroform–petroleum ether (2:8). Obtained were a red lamellar crystal, miltirone, and a red oily substance, 1-dehydromiltirone. In addition, this study also isolated Δ^1 -dehydrotanshinone IIA (15) and Ro-09-0680 [25].

8.2.6.2 Isolation of Tanshinlactone [11] and Danshinspiroketallactone

TLC data indicate that both compounds have a lower polarity than tanshinone IIA. Because their 1,2-orthoquinone groups have been oxidized to form lactone structures, they are colorless

compounds. However, under UV light, they can show blue fluorescence. First, fluorescent compounds with an R_f value higher than that of tanshinone IIA were detected by TLC in mother liquor from which 78 g of tanshinone IIA had been recrystallized with ethanol. 15.6 g of the concentrated substance was run on 120 g of silica gel column using cyclohexane and cyclohexane–chloroform (9:1) for the gradient elution, and 40 mg of tanshinolactone and 30 mg of danshinspiroketallactone were obtained. Danshinspiroketallactone was initially isolated by Kong et al. [53] from the water-insoluble fraction of Danshen injection preparation. What we had isolated was a pair of isomers detected by TLC in the mother liquor from tanshinone IIA recrystallization, which was a mixture composed of a 3:1 ratio of danshenspiroketallactone (42) and epi-Danshenspiroketallactone (43), identified by ^1H – ^1H -COSY spectra [12].

8.2.6.3 Isolation of Tanshindiols A, B, and C

Tanshindiols A, B, and C are a group of compounds with high polarity that cannot be observed in conventional developing solvents (e. g., benzene–acetone, 95:5). tanshindiols also belong to tanshinone II type compounds, and the only difference between them is that tanshindiols' ring A has two hydroxyl groups at different positions. They have the same formula of $\text{C}_{18}\text{H}_{16}\text{O}_5$. Due to their high polarity, their R_f values in developing solvents 1 and 2 are close to zero. Obviously, developing solvent 6, CHCl_3 –AcOEt (3:1), must be used to separate these three compounds. Furthermore, their contents are very low, less than 0.0001 %. Therefore, prior to column chromatography, these three compounds must be concentrated first so they can be seen clearly on thin-layer plates and for further isolation. The procedure is as follows: the ethanol extract of Danshen (1.2 kg) was first treated with benzene to get two fractions, i.e., the fraction soluble in benzene (800 g) and the fraction insoluble in benzene (400 g). The fraction insoluble in benzene was dissolved in benzene–methanol (9:1) and run on silica gel with dry column chromatography. Development with

benzene–methanol–formamide (7:3:0.5) isolated the fraction with strong polarity (260 g). Then, the sample was allowed to adsorb to polyamide, washed with water to remove water-soluble impurities, and eluted with 95 % ethanol to get a mixture of red pigments with a very strong polarity (120 g). The pigment fraction was run with silica gel column chromatography again and eluted with dichloromethane–acetic ether (3:1) to get four crude factions, which were then purified with preparative TLC with silica gel and developed with dichloromethane–acetic ether–methanol (15:5:1) to get tanshindiol A (90 mg), tanshindiol B (90 mg), tanshindiol C (30 mg), and 3-hydroxytanshinone IIA (85 mg) [19].

8.3 Spectrum Characteristic of Tanshinone Compounds

8.3.1 Ultraviolet Spectrum

The ultraviolet–visible absorption spectrum can provide structural information about a compound's chromophore such as conjugated systems, carbonyl groups and nitro-groups, as well as other related groups. Ultraviolet absorption spectra give a molecule's structural information through the location of absorption (λ_{max}), absorption strength (molar absorptivity index, ϵ) and the shape of the whole spectrum. Diterpene tanshinone compounds have quinone chromophores and long conjugated chains and show the characteristic absorption in the 350–450 nm visible range. In 1941, Urake first distinguished the three pigments with different ring systems isolated from Danshen by the colors revealed after dehydrolysis of the purified pigments with concentrated sulfuric acid; for example, tanshinone I turned blue, tanshinone II turned green, and cryptotanshinone turned red. The different colors were caused by their corresponding chemical structures or ring systems; for example, the skeleton of tanshinone I is *o*-phenanthraquinone, while tanshinone II has *o*-naphthoquinone binding furan, and cryptotanshinone has *o*-naphthoquinone binding dihydrofuran. In

1961, Okumura first distinguished tanshinone I, tanshinone II, and cryptotanshinone in the UV absorption spectra. The UV spectrum can distinguish well between tanshinones with different long conjugated chains and chromophores. It especially plays an important role in distinguishing ring A as an aromatic ring or alicyclic ring, and whether double bonds appear inner or outer to the alicyclic ring. It can also distinguish between furan and dihydrofuran rings, such as the difference between cryptomethyl tanshinonate [4] (23) and methyl tanshinonate (6).

8.3.1.1 UV Spectrum of Tanshinones

The UV spectra of diterpenoids from Danshen are listed in 5 tables below (Tables 8.3, 8.4, 8.5,

8.6, and 8.7). Table 8.3 lists diterpenoid quinone compounds with the typical *o*-quinone structure of tanshinone. Most of them are tanshinone II type with an alicyclic ring A, and the position and number of the auxochromic group in the compounds have little effect on absorption peaks; therefore, the UV spectra of compounds 3, 4, 5, 6, 10, 11, 12, 14, 16, and 19 in the table are similar. A few compounds which have benzene for ring A are tanshinone I type, of which compounds 1, 20, and 26 have similar UV spectra. However, the difference between types I and II is obvious. The third type of compound consists of cryptotanshinone (2) and cryptomethyl tanshinonate (23). Other tanshinone-type compounds have double bonds in or not in ring A, such as

Table 8.3 UV absorption curves of tanshinone-type diterpenoid quinones (Compound 1–26) λ_{\max} nm EtOH (log ϵ)

Tanshinone I 1	244.5(4.62) 266 sh(4.31) 325(3.68) 417(3.70)
Cryptotanshinone 2	221(4.26) 263(4.47) 272(4.41) 290(3.96) 355(3.41) 447(3.48)
Tanshinone IIA 3	224(4.34) 252(4.30) 269(4.44) 352(3.22) 460(4.30)
Tanshinone IIB 4	224, 252, 269, 272, 348.458
1-hydroxytanshinone IIA 5	220, 250, 272, 348, 461
Methyl tanshinonate 6	223, 252, 269, 352, 465
Dihydrotanshinone I 7	241(4.20) 261(4.16) 291(br,3.33) 335(4.16) 414(3.50)
Methylene tanshinquinone 8	206(4.13),210sh(4.14),226(4.15),281(4.18),288(4.19),470(3.29)
1,2-dihydrotanshinone I 9	205(4.19),227(4.38),291(4.42)
Tanshindiol A 10	The absorption peak is similar to tanshinone IIA
Tanshindiol B 11	222(4.44) 250(4.36) 266(4.50) 348(3.40) 456(3.59)
Tanshindiol C 12	The absorption peak is similar to tanshinone IIA
Nortanshinone 13	220(3.92) 275(3.92) 328(3.32) 423(3.08)
3-Hydrotanshinone IIA 14	The absorption peak is similar to tanshinone IIA
Δ^1 -Tanshinone IIA	213(4.43) 242(4.24) 276(4.36)
Tanshinaldehyde 16	223(4.05) 252(sh 4.00) 270(4.19) 445(3.12)
Methylenedihydro tanshinone 17	
1,2,15,16-Tetrahydro tanshinone 18	220(4.56) 281(4.33) 288(4.39) 335(3.77) 380(3.51) 460(3.06)
Przewaquinone A 19	225(4.17) 252(4.19) 269(4.28) 348(3.24) 460(3.32)
Przewaquinone B 20	245(4.44) 266(4.26) 325(3.68)
Przewaquinone C 21	
Przewaquinone F 22	
Cryptomethyltanshinonate 23	226, 257, 265, 291, 354, 445
Tanshinol I 24	240, 280, 320(sh), 405
Hydroxymethylene tanshinone 25	224(4.47), 278(4.63), 287(4.59), 469(3.65)
Tanshinaldehyde I 26	

Table 8.4 UV absorption curves of three-ring diterpenoid quinones from Danshen (Compound 27–31) λ_{\max} nm MeOH(log ϵ)

Miltirone 27	219(4.17) 258.5(4.34) 360(3.42) 435(3.54)
Miltirone I 28	222(sh, 4.41) 237(4.54) 290(4.06) 425(3.69)
Δ^1 -miltirone 29	241(4.36) 279(4.24) 470(3.44)
Methylene miltirone 30	
1-Hydroxymiltirone 31	226(4.37) 264(4.24) 280(sh, 4.04) 356(3.20) 422(3.38)

Table 8.5 UV absorption curves of royleanone-type tanshinones (Compound 33–41) λ_{\max} nm MeOH(log ϵ)

Isotanshinone I 33	234(4.58) 293(4.45) 346(3.78) 450(3.67)
Isocryptotanshinone 35	251(3.97) 258(4.10) 299(3.79) 365(3.30)
Isodihydratanshinone I 36	284(sh, 4.34) 291(4.39) 340(3.83) 388(3.63)
2-Hydroxy isodihydratanshinone I 37	250(4.6) 300(4.1) 340(sh, 3.5) 457(3.7)
Isotanshinone IIB 38	260(4.40) 284(4.47) 346(3.78) 467(3.47)
Danshenxinkun A 39	287(4.37) 333(3.80) 375(3.56)
Danshenxinkun B 40	217(4.73) 283(4.41) 288(4.44) 330(3.94) 383(3.61)
Danshenxinkun C 41	220(4.68) 242(4.37) 286(4.57) 323(4.58) 380(3.84)

Table 8.6 UV absorption curves of other diterpenoids from Danshen (Compound 42–53) λ_{\max} nm MeOH(log ϵ)

Danshenspiroketallactone 42	226(3.77) 245(4.50) 314(3.85)
Epi-cryptoacetalide 44	
Tanshenlactone 46	242(4.42) 272(4.38) 282(4.48) 308(3.98) 323(4.15) 340(4.02) 357(4.05)
Anhydride of tanshinone IIA 47	237(4.00) 270(3.80) 306(3.97) 325(3.93)
Ferruginol 50	218(3.9) 270(3.2) 275(3.1)
2-Hydroxyferruginol 51	
Sugiol 52	216(3.8) 235(4.0) 283(4.1)
Arucadiol 53	228(4.58) 242(sh, 4.39) 270(4.25) 278(4.24) 362(3.54) 410(3.65)

Table 8.7 UV absorption curves of other diterpenoids from Danshen (Compound 54–66) λ_{\max} nm MeOH(log ϵ)

Danshenol-B 54	214(4.18) 230(4.10) 275(4.06) 287(3.84) 299(3.90) 343(sh) 356(3.42) 372(sh) 403(3.12)
Danshenol-A 55	231(4.32) 265(sh) 275(4.19) 287(4.04) 299(3.90) 343(sh) 356(3.42) 372(sh) 403(3.12)
Miltionone-I 56	232, 242, 275, 315(sh), 340
Miltionone-II 57	222, 265, 308, 320
Demethylcryptojaponol 58	216.5(4.10), 235(3.96), 290(3.90), 364(sh)
Salviolone 59	242(4.18) 249(4.20) 285(4.42) 312(3.60) 3.68(3.28) 388(3.23) λ_{\max} (hexane)
Norsalvioxide 60	
Miltipolone 61	
Tanshinone V 62	256.2(3.91) 273.6(3.99) 351.2(3.22) 467.6(2.83)
Tanshinone VI 63	224.0(4.23) 2.66(sh) 288.8(4.04) 333.4(2.45) 380.2(3.17)
3-Hydroxysalvilenone 64	
Salvilenone 65	212(4.56) 236(4.54) 260(3.96) 331(4.01) 393(3.95) 408(3.75) 440(3.45)
3-Keto-sapriparaquinone 66	205(4.72) 235(sh, 4.35) 277(4.36) 295(sh, 4.19) 340(3.55) 480(3.38)

compounds 8, 9, 13, 15, 18, and 25, and their UV absorption reflects the changes in the conjugated chain length.

Table 8.4 also lists three-ring diterpenoids with *o*-quinone chromophores. The structural characteristic of this group is the isopropyl at C-13 (ring C), which is different from the royleanone-type tanshinone compounds in UV spectra, most of which have a paraquinone structure. The ring systems of some compounds in Table 8.7 are different from abietane ring systems, such as those of salviolone (59), 3-hydroxysalvileneone (64), and salvilenone (65). Sometimes, the UV spectrum can play an important role in distinguishing them.

8.3.1.2 Confirmation of New Ring Systems by UV Absorption [35]

In 1988, Haro Ginda et al. isolated a trace component from Danshen, salviolone 59, which was a yellowish oily substance. They only isolated 0.5 mg and had great difficulty with determining its structure. They finally solved the problem by using a model compound as a reference to compare the ultraviolet absorptions of salviolone with. The reference compound's UV data were λ_{\max} (Hexane) 388(log ϵ 3.23), 368(3.28), 312(3.60), 285(4.42), 249(4.20), and 242(4.18), which were in agreement with those of 2-methyl-4, 5-benzotropolone (see Fig. 8.9). In addition, the IR spectrum absorptions (3,226, 1,615, and 1,260 cm^{-1}) also matched those of the reference. Thereby, a seven-membered ring tropolone chromophore was indicated on the mother nucleus of salviolone, as well as a six-membered

alicyclic ring with a gem-dimethyl group. It was the first tropolone-type compound isolated from Danshen (see Fig. 8.9).

8.3.1.3 The Limitations of the UV Spectrum

Like any other technique, the UV spectrum method has its limitations in application. These limitations can be overcome by combining it with other methods. For example, among the tanshinone diterpenoid quinones from Danshen, there are as many as 14 type II compounds whose UV spectra are almost the same. The main differences between them are the locations and types of auxochromes on the ring, especially the hydroxyl group on ring A, such as in 1-hydroxytanshinone IIA or 3 α -hydroxytanshinone IIA (14). The linking position of the hydroxyl group can be determined by proton chemical shifts in an H-NMR spectrum. In addition, a compound with two hydroxyls on ring A will have a much higher polarity than compounds with only one hydroxyl group, such as tanshinol A, B, and C, which displayed great differences in R_f values on TLC. For example, tanshinone IIA and tanshinone IIB can be distinguished by their respective R_f values of 0.51 and 0.07 (see Table 8.2). Mass spectrum analysis can give the precise molecular weights of compounds, and IR spectra can supply information regarding different functional groups such as hydroxyls and aliphatic carbonyls. In order to avoid unnecessary repetition, the following section will introduce the infrared absorption spectrum method in connection with the UV spectrum method.

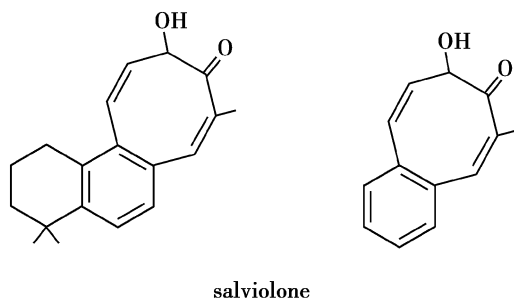


Fig. 8.9 Salviolone and benzotropolone possess the same chromophores

8.3.2 Infrared (IR) Absorption Spectrum

Infrared spectroscopy is based on the vibrational frequency of different groups. Consequently, infrared spectroscopy permits chemists to obtain absorption spectra for compounds in which the position, strength, and shape of peaks are unique reflections of the molecular structure. The infrared spectrum is a kind of molecular vibration

spectrum. The vibrational frequency of groups is attributed to the atomic mass (the type of atom; C, H, O, N, S) and the chemical bond constant (the type of chemical bond). The most important information that can be induced from an infrared spectrum is the identity of the functional groups contributing to the compound. The infrared spectrum mainly contains two regions. The high-energy area of the infrared spectrum contains the high-frequency region with a corresponding frequency range of $4,000\text{--}1,350\text{ cm}^{-1}$, providing the characteristic frequencies of functional groups. The other region is called the fingerprint region, with a corresponding frequency range of $1,350\text{--}400\text{ cm}^{-1}$, and is widely applied to the research of fingerprinting. However, determining the structures of compounds mainly depends on the characteristic absorptions of the vibrational motions of their component atom groups. Therefore, this kind of absorption is limited but marked. In the infrared spectrum, the inverted display of absorption is characteristic, which means that regions of the spectrum with relatively narrow frequency ranges are due to some specific group absorption. For example, the region in the spectrum around $1,700\text{ cm}^{-1}$ is due to carbonyl group absorption. Characteristic absorptions of specific frequencies in the infrared spectrum are used to identify groups, thereby indicating the type of compound.

8.3.2.1 Application of IR Spectrum on the Identification of Tanshinone II

Tanshinone II is an orange red material with a molecular formula of $\text{C}_{19}\text{H}_{18}\text{O}_3$. The quinoxaline derivate, formed by reacting with *o*-phenylenediamine, indicated that a dicarbonyl group exists in tanshinone II. The characteristic absorptions at $1,701$ and $1,650\text{ cm}^{-1}$ confirmed the presence of carbonyl, and the characteristic absorptions in the UV spectrum at 223 , 268 , 344 , and 457 nm were different from those of tanshinone I and cryptotanshinone. In addition, the absorptions at $1,381$ and $1,361\text{ cm}^{-1}$ belonged to a gem-dimethyl on ring A. By combining the above data with chemical studies, especially studies on catalytic

hydrogenation, and comparing with the known structures of compounds such as cryptotanshinone, the structure of tanshinone II was thus elucidated [4].

8.3.2.2 Structure Identification of 1-Hydroxytanshinone II and Methyl Tanshinonate

These are two trace components isolated from Danshen with contents of 0.005 and 0.002% , respectively. The ultraviolet absorption curves of the two compounds almost overlapped that of tanshinone II. The absorptions of 1-hydroxytanshinone II were 462 , 348 , 273 , 252 , and 222 nm , while methyl tanshinonate's were 465 , 352 , 269 , 252 , and 223 nm , which were almost identical to those of tanshinone IIA (EtOH), λ_{max} 460 , 352 , 269 , 252 , and 224 nm .

The UV spectra of the three compounds indicated that they belong to the tanshinone II family, and they differ only in auxochromic groups such as $-\text{OH}$ and CO_2CH_3 . The existence of these auxochromic groups can be confirmed by the characteristic absorptions of functional groups in the IR spectrum. For example, the infrared absorptions of tanshinone II were ν_{max} cm^{-1} (KBr) $3,150$, $1,690$, $1,670$, $1,583$, and $1,535$, and the IR spectrum of hydroxytanshinone II was very similar ($3,150$, $1,685$, $1,670$, $1,580$ and $1,535\text{ cm}^{-1}$), except for a hydroxyl group absorption at $3,525\text{ cm}^{-1}$.

The IR absorptions of methyl tanshinonate were nearly the same as those of tanshinone II, except for the appearance of an ester carbonyl absorption at $1,725\text{ cm}^{-1}$. Nuclear magnetic resonance analyses are needed to further identify the linkage positions of the hydroxyl and ester carbonyl in these compounds [18].

8.3.2.3 Structure Identification of Royleanone-type Compound Isotanshinone

Kakisawa et al. [28] found about 10 quinones from Danshen extract with TLC, of which 3 isotanshinone compounds with a 1, 4-paraquinone skeleton were identified as isotanshinone I, isotanshinone II, and isocryptotanshinone.

The identification of these compounds depended mainly on IR spectroscopy data. isotanshinone I and $C_{18}H_{12}O_3$ had the same molecular formula as tanshinone I. The IR spectrum showed the furan ring (ν_{KBr} 3,150, 1,530, 1,030, and 845 cm^{-1}) and paraquinone carbonyl group (1,660 and $1,585\text{ cm}^{-1}$). The difference between isotanshinone I and tanshinone I was in the different chromophores, which could be distinguished by the UV spectrum. For example, the UV absorptions of tanshinone I were 245 (log ϵ 4.50), 330(3.60), and 420 nm (3.67), while those of isotanshinone I were 234 (4.58), 293(4.45), 346(3.78), and 450 (3.28) nm.

The molecular formula of isotanshinone II is $C_{19}H_{18}O_3$, which was the same as tanshinone II. The IR spectrum showed the furan ring (ν_{KBr} 3,150, 1,530, 1,030, and 845 cm^{-1}) and 1, 4-paraquinone carbonyl group (1,660 and $1,585\text{ cm}^{-1}$). The UV spectrum could also differentiate between them. For example, the UV absorptions of tanshinone II were 224(log ϵ 4.34), 252(4.30), 269 (4.44), 352(3.22), and 460(3.43) nm, while those of isotanshinone II were 227(log ϵ 4.02), 253 (4.33), 256(4.34), 303(3.59), and 361(3.63) nm.

The molecular formula of isocryptotanshinone is $C_{19}H_{20}O_3$. Its UV absorptions were 251(3.97), 258(4.10), 299(3.79), and 365 nm (3.30). The IR spectrum suggested a 1-alkoxyl and 1, 4-paraquinone skeleton by the absorptions at 1,665 and $1,645\text{ cm}^{-1}$. The final determination of the structure of isocryptotanshinone depends on the H-NMR spectrum, which will be described in detail later.

8.3.2.4 Methylene Tanshinquinone [17] and 1, 2-Dihydrotanshinone I [23]

The molecular formula of methylene tanshinquinone is $C_{18}H_{14}O_3$. Compared to tanshinone IIA, there was an additional absorption at 206 nm in the UV spectrum. The IR spectrum of methylene tanshinquinone was 840(s), 910(s), 920(s), 990(s), 1,610(m), 1,630(m), 1,660(s), and $1,680(s)\text{ cm}^{-1}$, while that of tanshinone IIA was 835(s), 910(s), 990 (m), 1,625(w), 1,670(s), and $1,695(s)\text{ cm}^{-1}$, without the absorptions at 920(s) and $1,610(m)\text{ cm}^{-1}$.

Feng and Li [23] purified methylene tanshinquinone by multiple recrystallizations in methanol at room temperature, obtaining an isomeride

of methylene tanshinquinone and 1, 2-dihydrotanshinone from the mother liquor. The UV absorptions of 1, 2-dihydrotanshinone at 227 and 291 nm disappeared. The IR spectrum also indicated an *o*-quinone absorption at 1,685 and $1,665\text{ cm}^{-1}$, the highest absorptions were at 282 nm and $1,635\text{ cm}^{-1}$, the characteristic absorption of the furan ring was at $1,025\text{ cm}^{-1}$, and $\text{CR}_2 = \text{CHR}$ was indicated by the characteristic absorption at 860 cm^{-1} which was not only the unsaturated carbon-hydrogen vibration absorption of the alicyclic ring but also the absorption of the furan ring. Combined with the $\delta 2.05$ shift from the H-NMR spectrum, the data suggested a methyl group linked to an alicyclic ring A. An ethylenic hydrogen proton at $\delta 6.10$ in the alicyclic ring also proved the structure of 1, 2-dihydrotanshinone (16), and the product of catalytic hydrogenation was 4-methyl tanshinone II (one methyl less than tanshinone II), which had the same UV absorptions as tanshinone II at 223, 252, and 268 nm.

8.3.2.5 Structural Identification of Przewaquinone

A and Przewaquinone B [15]

Przewaquinone A, $C_{19}H_{18}O_4$, m.p. 173–175 °C, was an orange red pillar crystal. The UV spectrum was λ_{max} (MeOH) 225 (log ϵ 4.17), 252 (4.195), 269(4.276), 348(3.237), and 460 nm (3.321). Its IR spectrum was ν_{KBr} 700, 835, 920, 1,030, 1,050, 1,200, 1,290, 1,370, 1,422, 1,465, 1,490, 1,540, 1,590, 1,675(s), 1,680(s), 2,860, 2,940, 2,980, 3,410(s), and $3,445(s)\text{ cm}^{-1}$. Przewaquinone A (19) was suggested as a tanshinone II-type compound, with one more oxygen atom in przewaquinone A than in tanshinone IIA. Determining the linkage position of the additional hydroxyl will depend on magnetic resonance spectrum analyses.

Prezewaquinone B was a violet brown lamellar crystal with a molecular formula of $C_{18}H_{12}O_4$, m.p. 242–243 °C (decomposed). It had the same UV spectrum as tanshinone I, and a carbonyl group absorption at 1,660 and $1,670\text{ cm}^{-1}$ in the IR spectrum. Besides peaks at ν_{KBr} 750, 790, 840, 910, 920, 1,000, 1,120, 1,150, 1,160, 1,190, 1,370, 1,590, 1,660(s), and $1,670(s)\text{ cm}^{-1}$, there

were also hydroxyl absorptions at 3,370(s) and 3,440(s). The linkage positions also depend on the analysis of magnetic resonance spectrums.

8.3.3 Nuclear Magnetic Resonance (NMR) Spectrum

^1H -NMR spectroscopy provides structural information via the number of peaks in the spectrum (usually refers to a group of related peaks), their positions (using δ to represent chemical shift), spin coupling (using coupling constant J to represent spin splitting) and the ratio of the heights of integral curves. Together, these four kinds of information show the structures of proton-containing groups, as well as, indirectly, the structures of other groups. The number of peaks in an ^1H -NMR spectrum can suggest how many types of proton-containing groups are in a compound, and based on the ratio of integral curve heights, one can find the ratio of proton numbers between the groups. Take tanshinone IIA for example; there are two groups of peaks referring to two types of methyl groups, δ 1.35 (s, 6H) and δ 2.30 (d, 3H, $J = 1.7$ Hz), which suggests that the two single-peaked methyl groups at δ 1.35 are attached to the same carbon atom, i.e., a gem-dimethyl group, while the double (d) split methyl group at δ 2.30 (d 3H $J = 1.7$ Hz) suggests a methyl at the β -position of a furan ring which is

coupled with the adjacent α -H proton of the furan ring at δ 7.15 (q, 1H $J = 1.7$ Hz), revealing a quartet peak (q). In addition, a wide multiplet peak at δ 1.82 (br m 4H) represents four protons from the integral curve (4H). The triplet peak at δ 3.18 (br t 2H) represents benzyl protons, inferring from the chemical shift. In the low field, there are two double-peaked protons at δ 7.45, 7.58 (dd, 2H, $J = 8.5$ Hz) coupled with one another. Thereby, the precise chemical structural of tanshinone IIA was confirmed, revising the early structure of tanshinone IIA which was determined by UV and IR spectra only (In earlier literature [4], the methyl group was attached at the α -position of furan. It was revised to the β -position because the ^1H -NMR spectrum indicated the existence of a proton at the α -position with a chemical shift δ 7.15.)

8.3.3.1 ^1H -NMR Spectrum of 1-Hydroxytanshinone II

Its molecular formula is $\text{C}_{19}\text{H}_{18}\text{O}_4$ ($M^+ 310$). It possesses only one more oxygen atom than tanshinone IIA. The IR spectrum revealed an extra absorption at $3,525\text{ cm}^{-1}$ corresponding to a hydroxyl group, while the other absorptions were the same as those of tanshinone IIA. The last problem was to determine the linking position of the hydroxyl. H-NMR spectra showed that δ 3.15 (br t 2H) was replaced by δ 4.38 (br s, 1H) and δ 4.98 (br s, 1H), suggesting clearly that the

Table 8.8 H-NMR data of tanshinone IIA-type compounds

	λ EtOH		ν KBr		δ CDCl ₃		$[\alpha]_D$
	max	nm	max cm ^{−1}		NMR ppm		
Tanshinone IIA	460	352	3,150		1.30 (s 6H)	1.7 (br m 4H)	–
	269	252	1,690	1,670	2.25 (d 3H)	3.15 (br t 2H)	
	224		1,583	1,535	7.10 (q 1H)	7.48 (q 2H)	
Hydroxytanshinone	462	348	3,525	3,150	1.28 (s 3H)	1.40 (s 3H)	0°
	273	252	1,685	1,670	2.04 (br m 4H)	2.25 (d 3H)	
	222		1,580	1,535	4.38 (br s 1H) 7.20 (q 1H)	4.98 (brs 1H) 7.62 (q 2H)	
Methyltanshinone	465	352	3,150	1,725	1.62 (s 3H)	1.8 (br m 4H)	−139°
	269	252	1,690	1,670	2.26 (d 3H)	3.25 (br t 2H)	
	223		1,580	1,540	3.66 (s 3H) 7.52 (q 2H)	7.25 (q 1H)	

hydroxyl group must be linked at the benzyl hydrogen of ring A, identifying it as 1-hydroxytanshinone II (5) (see Table 8.8).

8.3.3.2 ¹H-NMR Spectrum of 3 α -Hydroxytanshinone IIA (14)

It has the same molecular formula as 1-hydroxytanshinone II, C₁₉H₁₈O₄ (M⁺ 310). Its UV spectrum is similar to that of tanshinone IIA, and except for hydroxyl absorption, its IR spectrum ν KBr 3,550, 1,665, 1,575, and 1,530 cm⁻¹ is almost the same as that of tanshinone IIA. Only by H-NMR spectroscopy could the attachment position of the hydroxyl be determined. The shifts corresponded to a geminal dimethyl group (δ 1.33, 3H, s) and (δ 1.35, 3H, s); furan methyl (δ 2.26, 3H, near s); α -hydrogen of furan (δ 7.24, 1H, s); methylene of ring A (δ 1.94, 2H, m), (δ 3.31, 2H, m), (δ 3.74, 1H, dd, J = 4.8 Hz); and AB protons of ring B (δ 7.56, 1H, d J = 8 Hz), (δ 7.68, 1H, d J = 8 Hz). A secondary hydroxyl group (δ 3.67, 1H, m) was readily acetylated by acetic anhydride pyridine to give the corresponding acetate (δ 2.05, 3H, s), (δ 5.00, 1H, t, J = 4.9 Hz). The physical data of this compound clearly differ from 1-hydroxytanshinone II. Therefore, the hydroxyl group must be located at C-3. This was also confirmed by the H-NMR spectrum, which showed signals corresponding to the benzylic methylene protons (δ 3.31, 2H).

8.3.3.3 ¹H-NMR Spectrum of Methyl Tanshinonate (6)

Its UV spectrum suggests that its chromophore belongs to a furo-*o*-naphthoquinone mother nucleus. The IR spectrum (3,150–1,500 cm⁻¹) is almost identical to that of tanshinone IIA, and the molecular formula is C₂₀H₁₈O₅ (M⁺ 338), which is one carbon and two oxygen atoms more than tanshinone IIA. The IR spectrum reveals a carbomethoxy group absorption at 1,725 cm⁻¹, and the H-NMR spectrum has a single peak of 3 protons at δ 3.66 (s, 3H) that shows a methyl linking at a carboxyl to form a CO₂CH₃ group. Table 8.8 lists the H-NMR data of tanshinone IIA, hydroxytanshinone IIA and methyl tanshinonate [18].

8.3.3.4 ¹H-NMR Spectra of Isotanshinone I (33), Isotanshinone II (34) and Isocryptotanshinone (35) [28]

Isotanshinone I C₁₈H₁₂O₃ (M⁺ 276). It has the same molecular formula as that of tanshinone I. The IR spectrum shows absorptions from the furan ring at ν KBr 3,150, 1,530, 1,030, and 845 cm⁻¹ and from *p*-quinoid carbonyls at 1,660 and 1,585 cm⁻¹. Even its H-NMR spectrum shows a striking resemblance in many of its features to that of tanshinone I and shows that the former possesses a methyl group (δ 2.35, 3 H, d, J = 2 Hz) attached to a furan ring which is unsubstituted in the -position (-proton appears at δ 7.45, 1 H, q, J = 2 Hz), a methyl group (δ 2.70, 3 H, s) bonded to an aromatic ring, and three aromatic protons (δ 7.50 and 9.50, 3H, m). However, there is a difference between the two spectra: Whereas an AB-quartet of aromatic protons appeared at δ 8.00 (J = 8 Hz) in the spectrum of tanshinone I, the corresponding AB-quartet is downshifted (δ 8.25, q, J = 8 Hz) in that of isotanshinone I, a conspicuous difference in the UV spectra of these two compounds.

Isotanshinone II C₁₉H₁₈O₃ (M⁺ 294). It is a yellow pigment, and IR spectroscopy suggests a furan ring. The H-NMR spectrum is nearly the same as that of tanshinone II; there are a gem-dimethyl (δ 1.30, 6H, s) and a methyl group (δ 2.32, 3H, d, J = 1.7 Hz) bonded to a furan ring unsubstituted in the position (δ 7.50, q, J = 1.7 Hz), and four methylene protons (δ 1.7, m, 4H and 3.35, m 2H). The major difference between isotanshinone II and tanshinone II is the chemical shift of the aromatic ring protons; the central shift of two AB-quartet protons was (δ 7.48) in tanshinone II, while the central shift of the two aromatic protons was further downfield in isotanshinone II (δ 7.90, AB-q, J = 8.5 Hz). In addition, the UV spectrum showed the absorption of a 1, 4-paraquinone chromophore, thus determining the structure of isotanshinone II.

Isocryptotanshinone C₁₉H₂₀O₃ (M⁺ 296). Its UV spectrum showed λ_{\max} EtOH nm (log ϵ) 251 (3.97), 258(4.10), 299(3.79), and 365(3.30). Its IR spectrum showed absorptions at 1,665 and 1,645 cm⁻¹, suggesting the presence of a

1-alkoxyl-1, 4-naphthoquinone group in this compound. The H-NMR spectrum showed a gem-dimethyl (δ 1.30, 6H, s), a methyl (δ 1.35, 3H, d, $J = 7$ Hz), bonded to methyne group (δ 3.65, 1H, m), three methylene groups (δ 1.65, 4H, m, and 3.25, 2H, br t), methylene (δ 4.54, 2H, dq, $J = 10, 9$ and 6 Hz) bonded to an oxygen atom, and aromatic protons (δ 7.75, 2H, ABq, $J = 8$ Hz). This NMR spectrum is similar to that of cryptotanshinone, except that the signals for the AB pattern of two aromatic protons appear further downfield than those of cryptotanshinone (δ 7.60, $J = 8.5$ Hz) and Isocryptotanshinone, which is consistent with its optical activity.

8.3.3.5 ^1H -NMR Spectrum of Isodihydrotanshinone I [29] (36)

$\text{C}_{18}\text{H}_{14}\text{O}_3$ (M^+ 278.0944). The UV spectrum shows an absorption corresponding to a paraquinone carbonyl group and the IR spectrum also shows the paraquinone carbonyl absorption at 1,661 and 1,641 cm^{-1} as well as the characteristic absorption of a furan ring at 1,510, 1,020 and 850 cm^{-1} . The H-NMR spectrum shows a methyl group of a dihydrofuran ring (δ 1.40, 3H, d, $J = 7$ Hz), a methyl bonded to an aromatic ring (δ 2.62, 3H, s), β -H of dihydrofuran ring (δ 3.46–3.82, 1H, br.m) and bonded to an oxygen atom; α -H (δ 4.25, 1H, d $J = 9.6$ Hz) and β -H (δ 4.80, 1H, t, $J = 9$ Hz), aromatic protons of A ring (δ 7.4, 2 H, m), AB protons of ring B (δ 8.0–8.3, 2H, q, $J = 8$ Hz) and aromatic proton (H-1) of A ring (δ 9.25, 1H, $J = 8$ Hz). Dihydrofuran ring groups appeared both in dihydrotanshinone I and isodihydrotanshinone I, while the chemical shifts of H-15, H-16 of the paraquinone

were further upfield due to the anisotropic effect of 1, 4-paraquinone in isodihydrotanshinone I (see Fig. 8.10).

8.3.3.6 ^1H -NMR Spectrum of 2-Hydroxyisodihydrotanshinone I (37) [21]

$\text{C}_{18}\text{H}_{14}\text{O}_4$ (M^+ 294.0907). It has one more oxygen atom than isodihydrotanshinone I. UV spectroscopy indicates a paraquinone group, and IR spectroscopy shows the absorption of paraquinone at 1,657, 1,644 cm^{-1} and of a hydroxyl group at 3,280 cm^{-1} . The H-NMR spectrum shows a methyl group bonded to the dihydrofuran ring (δ 1.32, 3H, d, $J = 8$ Hz), a methyl group bonded to an aromatic ring (δ 2.58, 3H, br s), β -H of dihydrofuran ring (δ 3.51, 1H, br m), α -H bonded to an oxygen atom (δ 4.25, 1H, d, $J = 9.3, 8$ Hz) and β -H (δ 4.79, 1H, t, $J = 9.3$ Hz), an aromatic proton H-3 (δ 7.38, 1H, br.s), AB protons of Ring B (δ 7.62, d, $J = 7.8$ Hz, 8.21, d, $J = 7.8$ Hz) and an aromatic proton H-1 of ring A (δ 9.46, 1H, $J = 1.7$ Hz). The hydroxyl group bonded to C-2 was confirmed by C-NMR data at δ_c 161.5 s (C-2), 184.3 s (C-11), and 176.1 s (C-14).

8.3.3.7 ^1H NMR Spectrum of Isotanshinone IIB [30]

It has the same molecular formula $\text{C}_{19}\text{H}_{18}\text{O}_4$ (M^+ 310) as tanshinone IIB. IR spectroscopy shows the characteristic absorptions of a furan ring at 3,150, 1,540, 1,025, and 845 cm^{-1} . The H-NMR spectrum is also similar to that of tanshinone IIB, with a methyl group bonded to ring A (δ 1.46, 3H, s), a methyl group bonded to a furan ring (δ 2.28, 3H, d, $J = 2.0$ Hz), α -H of furan (δ 7.30,

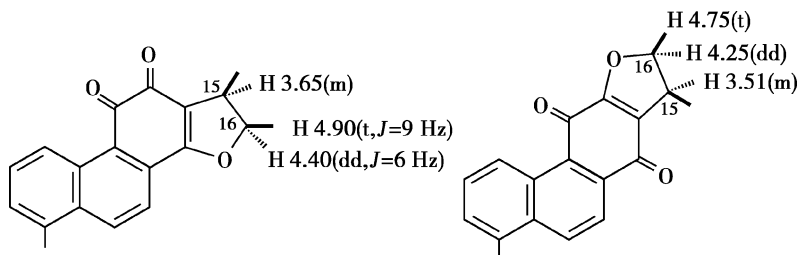


Fig. 8.10 Chemical shift of H-15, 16 in 1,4- ^1H -NMR spectra of known diterpene quinone(right) compared to 1,2-orthoquinone (left)

1H, d, $J = 2.0$ Hz) and four protons of methylene ($\delta 1.87$ – 2.10 , 4H, m), benzylic-proton of ring A ($\delta 3.36$, 2H, br t), and hydroxymethyl CH_2OH ($\delta 3.80$ – 3.98 , 2H, m). The only difference between isotanshinone IIB and tanshinone IIB is the chemical shift of AB protons in ring B; the central chemical shift of tanshinone IIB is ($\delta 7.64$, $\Delta\delta = 0.24$ ppm, $J = 9.0$ Hz), while in isotanshinone IIB, it is further downfield at ($\delta 7.75$, $\Delta\delta = 0.31$ ppm, $J = 8.0$ Hz). What leads to the change is the anisotropic effect of 1, 4-paraquinone on ring B. The absorption curves of the chromophores in paraquinone and tanshinone were easier to distinguish in the ultraviolet-visible spectrum (see Table 8.5).

8.3.3.8 $^1\text{H-NMR}$ Spectra of Danshenxinkun A (39), B (40), C (41) [13]

Danshenxinkun A $\text{C}_{18}\text{H}_{16}\text{O}_4$ (M^+ 296). IR spectrum shows absorptions of the hydroxyl group and carbonyl group in paraquinone, and the UV spectrum shows the absorption of paraquinone at 287, 333, and 375 nm. H-NMR spectroscopy of the acetate of danshenxinkun A shows a methyl group bonded to an aromatic ring ($\delta 2.72$, 3H, s), three aromatic protons of ring A ($\delta 7.5$, 2H, m), ($\delta 9.15$, 1H, $J = 8.0$ Hz), and two aromatic protons of the AB system in ring B ($\delta 8.0$, 8.3, q, 2H, $J = 8.0$ Hz). In addition, it also shows an enol acetate ($\delta 2.0$, 3H, s), and an acetylated isopropyl hydroxyl group ($\delta 1.37$, 3H, d, $J = 7$ Hz, $\delta 2.45$, S, 3H, $\delta 3.1$ – 3.8 , 1H, m and $\delta 4.35$, 2H, $J = 6.0$ Hz) linked to the paraquinone.

Danshenxinkun B $\text{C}_{18}\text{H}_{16}\text{O}_3$ (M^+ 280). IR spectrum indicates the hydroxyl group and carbonyl group in paraquinone, and the UV spectrum shows the conjugate absorption of 1,4-paraquinone which is similar to danshenxinkun A. Comparing its H-NMR spectrum with that of diacetylate danshenxinkun A, the downfield resonance peaks are similar, suggesting they had the same aromatic skeleton, while isopropyl group peaks appeared upfield ($\delta 1.35$, 6H, $J = 7$, 0 Hz), ($\delta 3.3$, 1H, br h) and a hydroxyl group peak at ($\delta 7.88$, 1H, s) could be substituted by heavy water.

Danshenxinkun C $\text{C}_{16}\text{H}_{12}\text{O}_3$ (M^+ 252). IR spectrum indicates a hydroxyl group and carbonyl group, and the UV spectrum shows the conjugate absorption of 1,4-paraquinone which is similar to danshenxinkuns A and B. Comparing its H-NMR spectrum with that of diacetate of danshenxinkun A, the downfield resonance peaks are similar, except for a methyl group peak at $\delta 2.4$ in the H-NMR spectrum of danshenxinkun C and the absence of an isopropyl group. The structure is further confirmed with MS data.

8.3.3.9 $^1\text{H-NMR}$ Spectra of Tanshinlactone (46) [11] and Danshenspiroketallactone (42) [53]

Tanshinlactone $\text{C}_{17}\text{H}_{12}\text{O}_3$ (M^+ 264.0829). The UV spectrum is listed in Table 8.6, and the chromophore is different from that of normal diterpenoid tanshinone in that it fluoresces blue under ultraviolet light. The IR spectrum is (νKBr 1,726, 1,620, 1,580 cm^{-1}). The H-NMR spectrum shows that there are two methyl groups, one bonded to a furan ring ($\delta 2.39$, 3H, d, $J = 1.5$ Hz) and the other bonded to an aromatic ring ($\delta 2.70$, 3H, s). There is also an α -H of furan ($\delta 7.42$, 1H, q, $J = 1.5$ Hz). In addition, there are five protons of ring A ($\delta 8.45$, (H-1) d, $J = 8.3$ Hz), ($\delta 7.51$, (H-2) dd, $J = 7.8$, 8.3 Hz), ($\delta 7.43$, (H-3) d, $J = 7.8$ Hz) and two AB protons of the aromatic ring ($\delta 7.83$, (H-6) d, $J = 9.0$ Hz), ($\delta 7.87$, (H-7) d, $J = 9.0$ Hz) and ($\delta 7.87$, (H-7) d, $J = 9.0$ Hz), ($\delta 7.42$ (H-15, q, $J = 1.5$ Hz). The resonance peaks in this region are similar to that of tanshinone I, but C-NMR spectra clearly showed the differences between the two compounds (see Table 8.9).

Danshenspiroketallactone [53] $\text{C}_{17}\text{H}_{16}\text{O}_3$ (M^+ 268). UV spectrum (see Table 8.6); IR spectrum (νKBr 1,750, 1,340, 1,213, 1,070, and 914 cm^{-1}). The $^1\text{H-NMR}$ spectrum shows a methylnaphthalene fragment ($\delta 7.72$ – 8 , 3H, m), ($\delta 8.53$, 1H, d, $J = 8$ Hz), and ($\delta 9.16$, 1H, d, $J = 8$ Hz). Based on the $^1\text{H-NMR}$ spectra of known diterpene quinone compounds from Danshen, it can be inferred that there must be an electron withdrawing group in the methylnaphthalene nucleus. The absorption at 1,750 cm^{-1} in the IR spectrum suggests an ester

Table 8.9 C-NMR data for tanshinlactone and danshinspiroketallactone

C	Tanshinlactone	Danshinspiroketallactone	C	Tanshinlactone	Danshinspiroketallactone
1	120.6 (d)	118.7 (d)	10	133.1 (s)	133.6 (s)
2	128.8 (d)	130.6 (d)	11	158.4 (s)	183.4 (s)
3	126.8 (d)	128.4 (d)	12	–	175.6 (s)
4	134.4 (s)	135.2 (s)	13	158.4 (s)	121.7 (s)
5	123.4 (s)	123.2 (s)	14	149.4 (s)	161.1 (s)
6	128.8 (d)	132.9 (d)	15	140.4 (d)	142.0 (d)
7	116.6 (d)	124.8 (d)	16	120.3 (s)	120.5 (s)
8	110.3 (s)	129.6 (s)	17	9.0 (q)	8.8 (q)
9	108.0 (s)	126.9 (s)	18	20.0 (q)	19.8 (q)

group. Comparing the high-field region in the ^1H -NMR spectrum with that of dihydrotanshinone I indicates the existence of a dihydrofuran methyl nucleus (δ 1.32, 3H, d, $J = 7$ Hz), (δ 2.16, 1H, dd, $J = 10.6, 13$ Hz), and (δ 2.67, 1H, dd, $J = 7.13$ Hz) and an aromatic methyl group (δ 2.8, 3H, s), (δ 3.0, 1H, m), (δ 3.9, 1H, t $J = 8$ Hz), and (δ 4.6, 1H, t $J = 8$ Hz). The characteristic absorptions at 1,070 and 914 cm^{-1} in the IR spectrum indicate a hydrogenated furan ring. Together with the molecular formula $\text{C}_{17}\text{H}_{16}\text{O}_3$, the structure of (42) was deduced, and the compound, which has a novel skeleton, was named Danshen spiroketallactone. Finally, the results of X-ray analysis show two aromatic rings (A, B) and two rings made of oxygen and carbon atoms (C, D rings). Rings A, B, and C are on the same plane, while ring D appears folded and perpendicular to the main plane.

8.3.3.10 ^1H -NMR Spectra of Miltirone (27), Miltirone I (28) [8], 1-Dehydromiltirone (29) [25]

Miltirone I $\text{C}_{18}\text{H}_{16}\text{O}_2$ (M^+ 264.1150). The UV spectrum is shown in Table 8.4 and is similar to tanshinone, but simpler. IR spectrum: νKBr 1,645, 1,623, 1,582, 1,447, 1,360, 1,220, and 942, 785 cm^{-1} . The ^1H -NMR spectrum (in CDCl_3) shows an isopropyl group with two methyls (δ 1.28, 6H, d, $J = 6$ Hz), one methyl on ring A (δ 2.68, 3H, s), an isopropyl hydrogen (δ 3.15, 1H, m, $J = 6$ Hz), and aromatic protons H-6, -7, -9 (δ 7.0–7.70, 3H), H-10 (δ 8.23, 1H, d,

$J = 8$ Hz), H-5 (δ 9.20, 1H, d, $J = 8$ Hz). In the MS spectrum, there is a strong $M + 2$ ion peak at m/z 266, which is about 5 % higher than the parent ion at m/z 264. Onitsuka et al. [8] regarded it as a typical signal of 1, 2-orthoquinone and further confirmed the structure of miltirone I by preparing a derivative of miltirone I through reacting with *o*-phenylene diamine to form quinoxaline $\text{C}_{24}\text{H}_{20}\text{N}_2$.

Miltirone $\text{C}_{19}\text{H}_{22}\text{O}_2$ (M^+ 282.1588). UV spectrum, see Table 8.4, IR spectrum: νKBr 2,950, 1,680, 1,660, 1,638, 1,580, 1,565, 1,485, 1,390, and 1,380 cm^{-1} . The ^1H -NMR spectrum shows a gem-dimethyl of ring A (δ 1.30, 6H, s), an isopropyl group including two methyls (δ 1.15, 6H, d, $J = 7$ Hz), an isopropyl proton (δ 3.14, 1H, m), AB protons of ring B (δ 7.1, 1H, d, $J = 8$ Hz), (δ 7.6, 1H, d, $J = 8$ Hz), and protons of ring A (δ 3.14, 2H, m), (δ 1.70, 4H, m).

Δ^1 -dehydromiltirone $\text{C}_{19}\text{H}_{20}\text{O}_2$ (M^+ 280.1479). UV spectrum, see Table 8.4, IR spectrum: νKBr 2,958, 1,683, 1,662, 1,647, 1,635, 1,575, 1,560, and 1,382 cm^{-1} . The ^1H -NMR spectrum (in CDCl_3) shows a gem-dimethyl of ring A (δ 1.25, 6H, s), an isopropyl group (δ 1.15, 6H, d, $J = 7$ Hz), an isopropyl proton (δ 3.0, 1H, m), and AB protons of ring B (δ 6.93, 1H, d, $J = 8$ Hz), (δ 7.89, 1H, d, $J = 8$ Hz). The main differences in the ^1H -NMR spectrum between Δ^1 -dehydromiltirone and miltirone are an additional ethylene bond in ring A, and a proton of C-1 (δ 7.85, 1H, d, $J = 11$ Hz), proton of C-2 (δ 6.3, 1H, m), and proton of C-3 (δ 2.25, 2H, dd, $J = 6.1, 2.4$ Hz).

8.3.3.11 ^1H -NMR Spectrum of Anhydride of Tanshinone IIA (47) [10]

The molecular formula of anhydride of tanshinone IIA (6,7,8,9-tetrahydro-1,6,6 trimethylfuro[3,2c] naphth [2,1e]oxepin-10,12-dione) is $\text{C}_{19}\text{H}_{18}\text{O}_4$ (M^+ 310.121). UV spectrum, Table 8.6; IR spectrum: furan (νKBr 3,154, 1,537 cm^{-1}), carbonyl (1,786, 1,735), aromatic ring (1,604); ^1H -NMR spectrum: a gem-dimethyl (δ 1.32, 6H, s), methyl of furan (δ 2.27, 3H, d, $J = 1$ Hz), α -H of furan (δ 7.32, 1H, q, $J = 1$ Hz), protons of ring A (δ 1.10–2.00, 4H, m), (δ 2.89, 2H, t), and aromatic protons of ring B (δ 7.63, 2H, s).

8.3.3.12 ^1H -NMR Spectra of Anhydride of Cryptotanshinone (48) and Anhydride of Tanshinone I (49)

Anhydride of cryptotanshinone $\text{C}_{19}\text{H}_{20}\text{O}_4$ (M^+ 312). IR spectrum: (νKBr 2,962, 2,869, 1,778, 1,719, 1,615, 1,349, 981, 952 cm^{-1}); ^1H -NMR spectrum: a gem-dimethyl (δ 1.31, 3H, s), (δ 1.33, 3H, s), a methyl group bonded to dihydrofuran (δ 1.35, 3H, d, $J = 6.8$ Hz), alicyclic protons (δ 1.60–1.90, 4H, m), (δ 2.70–3.00, 2H, m), β -H of dihydrofuran (δ 3.61, 1H, ddq, $J = 9.8$, 7.1, 6.8 Hz), α -H of dihydrofuran (δ 4.20, 1H, dd, $J = 9.1$, 7.1 Hz), (δ 4.74, 1H, dd, $J = 9.8$, 9.1 Hz), and aromatic proton of ring B (δ 7.60, 2H, s).

Anhydride of tanshinone I IR spectrum: (νKBr 2,967, 2,931, 2,901, 2,872, 1,768, 1,714, 1,603, 1,385, 1,220, 1,197, 1,166, 1,034, 995, 968, 763 cm^{-1}); ^1H -NMR spectrum: a methyl group bonded to dihydrofuran (δ 1.41, 3H, d, $J = 6.7$ Hz), a methyl group bonded to benzene ring (δ 2.74, 3H, s), β -H of dihydrofuran (δ 3.70, 1H, ddq, $J = 10.1$, 7.3, 6.7 Hz), α -H of dihydrofuran (δ 4.29, 1H, dd, $J = 9.1$, 7.3 Hz), (δ 4.84, 1H, dd, $J = 10.1$, 9.1 Hz), and aromatic protons (δ 7.40–7.60, 2H, m), (δ 7.86, 1H, d, $J = 8.9$ Hz), (δ 8.00, 1H, d, $J = 8.3$ Hz), (δ 8.25, 1H, d, $J = 8.9$ Hz).

8.3.3.13 ^1H -NMR Spectra of Tanshindiol a (10), B (11), C (12) [19]

Tanshindiol A $\text{C}_{18}\text{H}_{16}\text{O}_5$ (M^+ 312.0992). The IR spectrum (νKBr 3,530, 3,400, 1,655, 1,570, and 1,530 cm^{-1}) shows the furo-o-naphthoquinone

chromophore as well as hydroxyl groups. Based on the molecular formula, there should be two hydroxyl groups. The problem is the linking positions of these groups; such a problem can be solved by ^1H -NMR spectroscopy. In the ^1H -NMR spectrum, the methene protons of ring A were (δ 1.81, 2H, m), (δ 2.69, 2H, m), and (δ 3.21, 2H, m), respectively. A methyl group bonded to furan (δ 2.26, 3H, d, $J = 1.8$ Hz), α -H of furan (δ 7.39, 1H, q, $J = 1.8$ Hz), AB aromatic protons of ring B (δ 7.64, 1H, d, $J = 7$ Hz), (δ 7.91, 1H, d, $J = 7$ Hz), a primary alcohol and a tertiary alcohol (δ 3.60, 2H, s) which linked at C-4 of ring A instead of the original gem-dimethyl. Further confirmation of the structure of ring A could be carried out through oxidation of tanshindiol A by using NaIO_4 to give Nortanshinone (see 8.3.3.14. ^1H -NMR spectrum of Nortanshinone).

Tanshindiol B $\text{C}_{18}\text{H}_{16}\text{O}_5$ (M^+ 312.0.988). IR spectrum: (νKBr 3,480, 1,660, 1,570, and 1,530 cm^{-1}). ^1H -NMR spectrum: alicyclic methyl (δ 1.46, 3H, s), alicyclic hydroxyl (δ 1.55, 2H, s, OH, the signal disappears when D_2O is added), alicyclic protons (δ 2.16, 2H, m), (δ 3.36, 2H, m), (δ 3.96, 1H, dd, br, $J = 12.4$ Hz, the wide peak becomes sharper when D_2O is added), a methyl group bound to furan (δ 2.27, 3H, d, $J = 1.5$ Hz), α -H of furan (δ 7.26, 1H, q, $J = 1.5$ Hz), AB aromatic protons of ring B (δ 7.64, 1H, d, $J = 8$ Hz), (δ 7.97, 1H, d, $J = 8$ Hz).

Tanshindiol C $\text{C}_{18}\text{H}_{16}\text{O}_5$ (M^+ 312.0987). IR spectrum: (νKBr 3,470, 1,655, 1,570, 1,530 cm^{-1}). ^1H -NMR spectrum: alicyclic methyl (δ 1.50, 3H, s), alicyclic protons (δ 2.14, 2H, m), (δ 3.35, 2H, m), (δ 3.98, 1H, dd, $J = 4.4$, 2.9 Hz), a methyl group bound to furan (δ 2.27, 3H, d, $J = 1.5$ Hz), α -H of furan (δ 7.26, 1H, q, $J = 1.5$ Hz), AB aromatic protons of ring B (δ 7.66, 1H, d, $J = 8$ Hz), (δ 8.03, 1H, d, $J = 8$ Hz).

8.3.3.14 ^1H -NMR Spectrum of Nortanshinone (13) [19]

$\text{C}_{17}\text{H}_{12}\text{O}_4$ (M^+ 280.0711). IR spectrum: (νKBr 3,120, 1,660, 1,570, 1,530 cm^{-1}). No absorption from a hydroxyl group. ^1H -NMR spectrum: methenes of ring A were (δ 2.12, 2H, m), (δ 2.70, 2H, m), and (δ 3.40, 2H, m), respectively; a

methyl group bound to furan (δ 2.30, 3H, d, $J = 1.8$ Hz), α -H of furan (δ 7.31, 1H, q, $J = 1.8$ Hz), AB aromatic protons of ring B (δ 7.77, 1H, d, $J = 8$ Hz), (δ 8.33, 1H, d, $J = 8$ Hz), and there is no hydroxyl group indicated in the $^1\text{H-NMR}$ spectrum. The C-NMR spectrum shows two carbonyl groups of naphthoquinone C-11 (δ 182.8, s) and C-12 (δ 175.5, s), as well as a keto-carbonyl group (C-4) instead of the original gem-dimethyl, so it was named “nortanshinone.” Nortanshinone could also be obtained in the laboratory through oxidation of tanshindiol A (10 mg) with NaIO_4 (20 mg) in methanol-water.

8.3.3.15 $^1\text{H-NMR}$ Spectra of Przewaquinone C (21) and Przewaquinone F (22) [20]

Przewaquinone C $\text{C}_{18}\text{H}_{16}\text{O}_4$ (M^+ 296.1077). The molecular formula weight provided by MS spectrum is 14 less than that of Przewaquinone A. In $^1\text{H-NMR}$ spectroscopy, the peak area of gem-dimethyl at δ 1.35 is 6H in Przewaquinone A, while it is a methyl peak of about 3 protons in Przewaquinone C, and there is a methyl group bond to the furan ring (δ 2.18, 3H, s). Considering the fact that there is absorption from a hydroxyl group in IR spectrum, the hydroxyl and another methyl group must be linked at C-4 of ring A. $^1\text{H-NMR}$ spectrum: alicyclic protons (δ 1.06–2.07, 2H, m), (δ 3.18–3.38, 2H, m), alicyclic methyl group (δ 2.0, 3H, s), a methyl group bound to the furan ring (δ 2.20, 3H, s), α -proton of furan (δ 7.08, 1H, s), AB aromatic protons of ring B (δ 7.22, 7.58, 2H, dd, $J = 8$ Hz).

Przewaquinone F $\text{C}_{18}\text{H}_{16}\text{O}_5$ (M^+ 312.1004). IR spectroscopy gives the absorptions of hydroxyl groups as double peaks ($3,520, 3,480\text{ cm}^{-1}$), as well as absorptions at 2,915, 2,850, 1,675, 1,655, 1,640, 1,570, 1,530, 1,153, 1,000, 906, and 785 cm^{-1} . The $^1\text{H-NMR}$ spectrum showed ring A protons (δ 3.1, 2H, m), (δ 1.8–2.0, 2H, m), (δ 4.0, 1H, m), (δ 2.6, 1H, m), and CH_2 of primary alcohol linking at ring A (δ 3.58, 2H, m), AB aromatic protons of ring B (δ 7.3, 7.4, 2H, dd, $J = 8$ Hz), a methyl group bound to the furan ring (δ 2.0, 3H, s) and (δ 7.0, 1H, s).

8.3.3.16 $^1\text{H-NMR}$ Spectra of Methylene Tanshinone (8) [17] and 1, 2-Dihydrotanshinone I (9) [23]

Methylene tanshinquinone $\text{C}_{18}\text{H}_{14}\text{O}_3$ (M^+ 278). UV spectrum, see Table 8.3. The UV spectrum differs from that of tanshinone IIA mainly in the appearance of a double-bond absorption at 206 nm. IR spectrum: (ν KBr 1,680, 1,660, 1,630, 1,610, 990, 920, 910, and 840 cm^{-1}). The $^1\text{H-NMR}$ spectrum showed ring A protons (δ 3.16–3.40, 2H, t, $J = 11$ Hz), (δ 1.75–2.07, 2H, br, m), (δ 2.40–2.60, 2H, br, t), a double bond outside of ring A (δ 4.05, 4.42, 2H, dd, $J = 1$ Hz), a methyl group bound to the furan ring (δ 2.20, 3H, s), α -H of furan (δ 7.20, 1H, s), AB aromatic protons of ring B (δ 7.64, 2H, dd, $J = 8$ Hz). The structure was finally confirmed by the catalytic hydrogenization of the product in THF followed by $^1\text{H-NMR}$ spectroscopy, which showed a split methyl peak at (δ 1.24, 3H, $J = 7$ Hz), the same position of the methyl on the ring, but with an extra proton peak (δ 2.92, 1H, m). The two protons of methene (δ 4.05, 4.42, 2H, dd, $J = 1\text{ Hz}$) disappeared.

1,2-dihydrotanshinone $\text{C}_{18}\text{H}_{14}\text{O}_3$ (M^+ 278). The highest absorptions are at 227 and 291 nm with the absence of 282 nm in the UV spectrum. In the $^1\text{H-NMR}$ spectrum, there are two methyl groups at (δ 2.05, 3H, d, $J = 1.5$ Hz), (δ 2.25, 3H, d, $J = 1.5$ Hz), respectively, protons of ring A (δ 2.10–2.50, 2H, m), (δ 3.30, 2H, t) and an ethylene proton inside ring A (δ 6.10, 1H, t), AB aromatic protons of ring B (δ 7.52, 2 H, dd, $J = 8$ Hz), and H-furan (δ 7.27, 1H, m).

8.3.3.17 $^1\text{H-NMR}$ Spectrum of Hydroxymethylene Tanshinone (25) [54]

$\text{C}_{18}\text{H}_{14}\text{O}_4$ (M^+ 294.0892). The UV spectrum is similar to that of methylene tanshinone. IR spectroscopy shows absorption of o-naphthoquinone (ν KBr 1,690, 1,675, and $1,650\text{ cm}^{-1}$). Based on the molecular formula, it has one more oxygen atom than methylene tanshinone. Combined with the hydroxyl absorption (ν KBr 3,220–3,500 cm^{-1}) in the IR spectrum, it could

be calculated that the structure has one more hydroxyl group than methylene tanshinone, which could be confirmed by NMR spectroscopy. In the ^1H -NMR spectrum, triple peaks of H-3 (ring A) in methylene tanshinone (δ 2.40–2.60, 2H, br t) are replaced by a dd peak of a proton (δ 4.40–4.59, 1H, dd, $J = 4, 10$ Hz). The complete ^1H -NMR spectrum: a β -methyl group bond to the furan ring (δ 2.22, 3H, s), AB protons of ring B (δ 7.50–7.78, 2H, dd, $J = 8$ Hz), α -H of furan (δ 7.18, 1H, s), two methene protons of ring A (δ 5.39, 5.58, 2H, d), and protons of ring A (δ 1.60–2.19, 2H, m), (δ 3.30–3.50, 2H, t, $J = 12$ Hz) and (δ 4.40–4.59, 1H, dd, $J = 4, 10$ Hz), respectively. When irradiated at δ 1.60–2.19(H-2), the dd peak at δ 4.40–4.59 (H-3) is replaced by a single peak.

8.3.3.18 ^1H -NMR Spectra of Ferrugiol (50) [25], Sugiol (52) and Arucadiol (53) [55]

Ferrugiol $\text{C}_{20}\text{H}_{30}\text{O}$ (M^+ 286.2291). UV spectrum, see Table 8.4, is a typical abietane tricyclic diterpene. Because it was isolated and identified with cryptotanshinone in the process of Danshen tissue culture investigation, this compound has received a lot attention. ^1H -NMR spectroscopy of ferrugiol showed five methyl groups including a gem-dimethyl of ring A (δ 0.89, 3H, s), (δ 0.90, 3H, s), an angular methyl group at (δ 1.26, 3H, d, $J = 1.8$ Hz), an isopropyl group [(δ 1.11, 3H, d), (δ 1.12, 3H, d), proton of isopropyl (δ 3.10, 1H, m)], alicyclic protons [(δ 2.10, 2H, m), (δ 2.76, 2H, m)], and two aromatic protons (δ 6.68, 1H, s), (δ 6.80, 1H, s).

Sugiol $\text{C}_{20}\text{H}_{28}\text{O}_2$ (M^+ 300.2065). UV spectrum, see Table 8.4. IR spectroscopy shows (ν_{KBr} 3,117, 2,863, 1,642, 1,599, 1,585, 1,569, 1,505, 1,460, 1,373, 1,342, 1,267, 1,247, 1,179, 1,090, 879, and 774 cm^{-1}). ^1H -NMR spectroscopy (CDCl_3) shows five methyl groups including a gem-dimethyl of ring A (δ 0.90, 3H, s), (δ 0.98, 3H, s), an isopropyl group [(δ 1.20, 6H, d), proton of isopropyl (δ 3.10, 1H, m)], alicyclic protons (δ 2.59, 1H, d, $J = 5.4$ Hz, Ha-6), (δ 2.64, 1H, d, $J = 7.6$ Hz, Hb-6), and two aromatic protons (δ 6.88, 1H, s), (δ 7.89, 1H, s).

Arucadiol $\text{C}_{19}\text{H}_{22}\text{O}_3$ (M^+ 298.1565). IR spectroscopy shows a hydrogen bond association of phenolic hydroxyl group (ν_{KBr} 3,480, 1,200 cm^{-1}) and an absorption of carbonyl group at 1,640 cm^{-1} . ^1H -NMR shows a gem-dimethyl (δ 1.46, 6H, s), an isopropyl group [(δ 1.33, 6H, d, $J = 7$ Hz), isopropyl proton (δ 3.42, 1H, septet, $J = 7$ Hz)], two methylene protons (δ 2.06, 2H, t, $J = 7$ Hz), (δ 2.92, 2H, t, $J = 7$ Hz), and two ortho aromatic protons [(δ 7.32, 1H, d, $J = 8.5$ Hz) and (δ 7.94, 1H, d, $J = 8.5$ Hz)]. Another aromatic proton at (δ 7.25, 1H, brs) and two hydrogen-bonded phenolic functions at δ 6.88, s and δ 10.65, s disappeared after addition of D_2O , and the absorptions decreased when irradiated at δ 1.5 (signal of H_2O in CDCl_3). Hydroxyl-H (δ 10.65) shifts downfield for hydrogen bonds formed by the carbonyl of ring A. The compound was also isolated from *S. argente* and named arucadiol.

8.3.3.19 ^1H -NMR Spectra of Przewaquinone A (19) and Przewaquinone B (20)

Przewaquinone A $\text{C}_{19}\text{H}_{18}\text{O}_4$ (M^+ 310.1227). The UV spectrum is similar to that of tanshinone IIA, see Table 8.3. IR spectrum: (ν_{KBr} 3,445, 3,410, 2,980, 2,940, 2,860, 1,680, 1,675, 1,590, 1,540, 1,490, 1,465, 1,422, 1,370, 1,290, 1,200, 1,050, 1,030, 920, 835, and 700 cm^{-1}), of which 3,445, 3,410 cm^{-1} are the typical absorptions of a hydroxyl group, and it is important to decide the linking position. ^1H -NMR spectroscopy ($\text{DMSO}-d_6$) shows a gem-dimethyl (δ 1.35, 6H, s), methene of ring A (δ 3.18, 2H, t), (δ 1.72, 4H, m), AB aromatic protons of ring B (δ 7.55, 7.68, 2H, $J = 8$ Hz), a methylene combining with an oxygen atom (δ 4.70, 2H, s, which could be exchanged by D_2O) and α -H of furan (δ 7.38, 1H, s).

Przewaquinone B $\text{C}_{18}\text{H}_{12}\text{O}_4$ (M^+ 292.0747). The UV spectrum is similar to that of tanshinone I, see Table 8.3. Its molecular formula shows that it has one more oxygen atom than tanshinone I. IR spectrum: (ν_{KBr} 3,440, 3,370 cm^{-1}) indicating the existence of hydroxyl absorption. The other absorptions at 1,670, 1,660, and 1,590 cm^{-1} are similar to those of tanshinone I. ^1H -NMR spectroscopy ($\text{DMSO}-d_6$) showed a methyl

group attached to ring A (δ 2.70, 3H, s) and three aromatic protons [(δ 9.15, 1H, d, J = 8 Hz), (δ 7.36–7.78, 2H, m)], AB aromatic protons of ring B (δ 7.85, 8.45, 2H, dd, J = 8 Hz), furan-H (δ 7.78, 1H, s), a methylene combining with an oxygen atom (δ 4.65) and hydroxyl-H (δ 3.57).

8.3.3.20 $^1\text{H-NMR}$ Spectra of Tanshinaldehyde II (16) [24] and Tanshinaldehyde I (26) [23]

Tanshinaldehyde II $\text{C}_{19}\text{H}_{16}\text{O}_4$ (M^+ 308.1057). The UV spectrum shows the characteristic absorption of *o*-quinone (223, 252, 270, and 445 nm). IR spectrum: *o*-carbonyl group (ν_{KBr} 1,690, 1,669 cm^{-1}), an aldehyde group at 1,720 cm^{-1} (2,960, 2,944, 2,922, 1,720), benzene ring (1,576, 1,534), furan ring (1,358, 912, 840). $^1\text{H-NMR}$ spectroscopy shows two methyl groups, one on the furan ring (δ 2.26, 3H, s) and one on ring A (δ 1.44, 3H, s, CH_3 -18); AB aromatic protons of ring B (δ 7.32, 7.60, 2H, dd, J = 8 Hz), α -H of furan (δ 7.24, 1H, s), methene protons [(δ 3.24, 2H, br,m), (δ 1.83, 4H, br,m)], all of which are similar to data from methyl tanshinonate except for the signal at (δ 3.55, 3H, s COOCH_3), are replaced by (δ 9.47, 1HCHO), indicating an aldehyde group.

Tanshinaldehyde I $\text{C}_{18}\text{H}_{10}\text{O}_4$ (M^+ 290.0579). It has a tanshinone I-type skeleton, and the only difference is that the aldehyde group replaces the methyl group bonded to the benzene ring. $^1\text{H-NMR}$ spectroscopy suggests methyl of furan (δ 2.35, 3H, d, J = 1 Hz), α -H of furan (δ 7.40, 1H, J = 1 Hz), protons of aromatic ring [(δ 7.85, 1H, dd, J = 10 Hz), (δ 8.00–8.10, 2H, m), (δ 9.60–9.80, 2H, m)], and proton of aldehyde (δ 10.35, 1H, s).

8.3.3.21 $^1\text{H-NMR}$ Spectra of Methylene-dihydrotanshinone (17) and 1, 2, 15, 16-Tetrahydrotanshinone (18)

Methylene-dihydrotanshinone $\text{C}_{18}\text{H}_{16}\text{O}_3$ (M^+ 280.1087). $^1\text{H-NMR}$ spectroscopy shows a methyl group attached to the dihydrofuran (δ 1.38, 3H, d, J = 6.8 Hz), β -H of dihydrofuran (δ 3.62, 1H, ddq, J = 9.7, 6.8, 6.3 Hz), α -H of dihydrofuran [(δ 4.39, 1H, dd, J = 8.9, 6.3 Hz),

(δ 4.91, 1H, dd, J = 9.7, 9.2 Hz)], methylene proton outside of ring A [(δ 5.10, 1H, s), (δ 5.54, 1H, s)], protons of ring A [(δ 1.80–2.00, 2H, m), (δ 2.50–3.00, 2H, m), (δ 3.32, 2H, t, J = 6.5 Hz)], and AB aromatic protons of ring B [(δ 7.52, 1H, d, J = 8.1 Hz), (δ 7.90, 1H, d, J = 8.1 Hz)]. $^1\text{H-NMR}$ spectroscopy shows that the main difference between methylene-dihydrotanshinone and methylene tanshinquinone is either a furan ring or dihydrofuran ring.

1,2,15,16-tetrahydrotanshinone $\text{C}_{18}\text{H}_{16}\text{O}_3$ (M^+ 280.1113). It has the same molecular formula as methylene-dihydrotanshinone. They also share some identical absorptions in $^1\text{H-NMR}$ spectra: a methyl group attached to dihydrofuran (δ 1.38, 3H, d, J = 6.8 Hz), β -H of dihydrofuran [(δ 3.62, 1H, ddq, J = 9.5, 6.8, 6.1 Hz)], α -H of dihydrofuran [(δ 4.38, 1H, dd, J = 9.5, 6.1 Hz), (δ 4.91, 1H, t, J = 9.5 Hz)], and AB aromatic protons of ring B [(δ 7.43, 1H, d, J = 7.9 Hz), (δ 7.54, 1H, d, J = 7.9 Hz)]. The only difference between them is the disappearance of a methylene outside of ring A, which is replaced by a double bond inside the ring and a methyl group (δ 2.07, 3H, d, J = 1.3 Hz) and an olefinic proton (δ 6.10, 1H, m) attached to it.

8.3.3.22 $^1\text{H-NMR}$ Spectrum of Cryptomethyl Tanshinonate (23)

Cryptomethyl tanshinonate (trijuganone C) $\text{C}_{20}\text{H}_{20}\text{O}_5$ (M^+ 340.1301). The UV spectrum (226, 265, 291, 354 nm) indicates the existence of an *o*-naphthoquinodihydrofurane chromophore. The IR spectrum shows absorptions from *o*-quinone (1,690, 1,646 cm^{-1}), as well as absorption of an ester group (1,730 cm^{-1}). $^1\text{H-NMR}$ spectrum: alicyclic protons (δ 3.26, 2H, br, t); AB aromatic protons of ring B (δ 7.48, 2H, q); three methyl groups, one attached to a dihydrofuran (δ 1.35, 3H, d, J = 6.88 Hz), one attached to ring A (δ 1.56, 3H, s), and one attached to carboxymethyl ester (δ 3.66, 3H, s); α -H of dihydrofuran Ha (δ 4.90, 1H, t, J = 9.46 Hz), Hb (δ 4.36, 1H, dd, J = 5.73, 9.46 Hz). The compound was instable in air, and its oxidized compound can be formed over several weeks' storage. Dissolve 4 mg of cryptomethyl tanshinonate in CHCl_3 and drop

drops on a 15 cm × 15 cm silica gel plate, then add DDQ in benzene, store for 2 h, then develop with benzene-acetone (95:5), take the color band, and elute with methanol. ¹H-NMR spectroscopy of this compound shows a methyl group bonded to furan (δ2.26, 3H, s), α-H of furan (δ7.30, 1H, s). All the other peaks are the same as cryptomethyl tanshinonate.

8.3.3.23 ¹H-NMR Spectra of Tanshinone V (62), and Tanshinone VI (63) [36]

Tanshinone V is an orange powder, $[\alpha]_D^{30} +5.0$ (c 0.1, CHCl₃:MeOH, 1:1). UV spectrum: λ MeOH 256.2(3.91), 273.6(3.99), 351.2(3.22), 467.6 nm (2.83). IR spectrum: (νKBr 3,300, 2,900, 1,660, 1,640, 1,560, 1,460, 1,410, 1,380, 1,330, 1,270, 1,200, 1,170, 1,130, 1,020, 940, 810, 760, 730 cm⁻¹). ¹H-NMR spectrum: a gem-dimethyl (δ1.25, 6 H, s), an isopropyl group (δ1.64, 3H, d, J = 6 Hz, CH-CH₃), a hydroxyl group (δ2.56), (δ3.19, 2H, m, CH₂OH), (δ3.87, 1H, m, CH-CH₃), (δ3.92), and AB protons of ring B [(δ7.60, 1H, d, J = 8 Hz), (δ7.90, 1 H, d, J = 8 Hz)].

Tanshinone VI is an orange red needle crystal, $[\alpha]_D^{30} +47.0$ (c 0.1, CHCl₃: MeOH, 1:1). UV spectrum: λ MeOH 224.0(4.23), 266(sh), 288.8 (4.04), 333.4(2.45), 380.2 nm (3.17). IR spectrum: (νKBr 3,300, 1,680, 1,660, 1,620, 1,590, 1,480, 1,350, 1,310, 1,200, 1,020, 840, 790, and 760 cm⁻¹). ¹H-NMR spectrum: a methyl group at (δ1.50, 3H, d, J = 8 Hz, CH-CH₃), a methyl group attached to benzene (δ2.75, 3H, s), primary alcohol (δ3.20, 2H, m, -CH₂OH), (δ3.80, 1H, m, CH-CH₃), aromatic protons (δ7.02-7.20, 3H, m, C-9,-6,-7-H), protons of ring B (δ8.20, 1H, d, J = 8 Hz, C-10-H), and aromatic protons of ring A (δ9.20, 1H, d, J = 8 Hz, C-5-H).

To determine the structure of some complicated ring systems, C-NMR spectroscopy data are needed. For example, these data were used in elucidating the structures of tanshenlactone and Danshenspiroketallactone. The major information ¹³C-NMR spectroscopy could provide is the number of carbons. Because the chemical shift of ¹³C-NMR spectra has a wide bandwidth

(0–250 ppm) and the spectrum is a proton broadband decoupling spectrum (¹H-complete decoupling, COM) which deletes the coupling of hydrogen atoms to carbon atoms, each line refers to a carbon atom, while determining the type of carbon atom, such as primary carbon, secondary carbon, tertiary carbon, or quaternary carbon, depends on INEPT technology. When taking INEPT/R 1/4 J spectra, different types of carbons can be recognized, for example, signals of CH, CH₃ are upward, while signals of CH₂ are downward. The quaternary carbon will disappear from the spectrum, and the quaternary carbon can be recognized by comparing the INEPT/R 1/4 J spectrum with the ¹H-complete decoupling spectrum. In addition, DEPT (distortionless enhancement by polarization transfer) spectroscopy is a more convenient and reliable technique. Structural identification of the following compounds depends on information from H-NMR spectroscopy as well as ¹³C-NMR spectroscopy.

8.3.3.24 NMR Spectra of Salvionone (59), Miltipolone (61) [35]

Salvionone C₁₈H₂₀O₂ (M⁺ 268.1490). The IR spectrum indicates a phenolic hydroxyl group (νKBr 3,270, 1,240 cm⁻¹), as well as an intense absorption of a carbonyl group at 1,630 cm⁻¹. ¹³C-NMR (δ179.9) data support IR results and show that a highly conjugated system is involved in the carbonyl group. In the H-NMR spectrum, there are two isolated aromatic protons at [(δ7.95, 1H, s) and (δ8.05, 1H, s)] as well as a group of AB protons at [(δ7.53, 1H, d, J = 8.5 Hz), (δ7.58, 1H, d, J = 8.5 Hz)], suggests a pair of ortho aromatic-H, phenolic hydroxyl-H (δ8.45, 1H, brs), benzyl-H of alicyclic (δ3.10, 2H, t, J = 7 Hz) which is coupled with a group of quintet peaks at (δ1.95, 2H), while the peaks are also coupled with (δ1.72, 2H). NOESY spectroscopy suggests a gem-dimethyl group at (δ1.36, 6H). All of the above information shows the existence of a structure like this: Ar-CH₂CH₂CH₂CMe₂. Besides, there is a peak of methyl protons (2.49) in the deshielding field, which becomes sharper when the aromatic proton at δ7.95 is irradiated. At that time, there was

0.5 mg of the compound, and it is very hard to determine the structure with such a small amount of sample. Fortunately, the ring systems were determined as the UV spectrum of salvionone was the same as that of 2-methyl-4,5-benzetropolone, which had a known ring system. After the ring system was confirmed, the deduced structure was accepted.

Miltipolone $C_{19}H_{24}O_3$, FAB mass peak ($M + H^+$ m/e 301.1837), IR spectrum shows a phenolic hydroxyl group associated with hydrogen bonds (ν_{KBr} 3,300 cm^{-1}), and an intense absorption at 1,620 cm^{-1} indicates a conjugated carbonyl group, which is confirmed by ^{13}C -NMR (δ 171.97). There are seven carbons between δ 120–172 in the ^{13}C -NMR spectrum, combined with two aromatic protons at δ 7.28 and δ 7.40, and a methyl group attached to benzene (δ 2.42, s). After reacting with $FeCl_3$, it turns dark violet.

All of the above suggests that it probably has a tropolone skeleton system.

The coupling relation between methyl δ 2.42 and H-15, H-7 was confirmed by C, H-COLOC spectroscopy (see Table 8.10), and the linkage of C-8 and C-15 was also confirmed; thereby, the last oxygen atom is present as an ether linkage. It was confirmed by the correlation between δ 2.99, 4.36(CH_2 -6) and 4.68(H-7) in the H-NMR spectrum as well as the correlation between ^{13}C -NMR: δ 74.38 (d, C-7) and C-16 δ 67.35 (t, C-16). The structure of miltipolone is shown in Fig. 8.11.

8.3.3.25 1H -NMR Spectra of Miltionone I (56), Miltionone II (57)[38]

Miltionone I is a yellow powder, $C_{19}H_{20}O_4$ (M^+ 312.1357). UV spectrum: 232, 242, 275, 315(sh), and 340 nm. The IR spectrum shows a benzene

Table 8.10 Chemical shift of 1H , ^{13}C -NMR spectra and C, H-COLOC spectrum

C	$\delta^{13}C$	δ^1H	δ^1H coupling with J^3 COLOC
1	29.92 (t)	α -H 1.95 (dt, 4.5, 13.4) β -H 1.72 (dtd, 13.4, 3, 1.9)	1.60
2	18.98 (t)	1H 1.62 (m), 1-H 1.70 (m)	
3	40.99 (t)	α -H 1.20 (dt, 4, 13) β -H 1.60 (dtd, 1.9, 3.6, 13)	0.86, 1.23, 1.72
4	34.39 (s)		1.62, 1.66, 2.11
5	41.47 (d)	1H 1.23 (ddd, 2.0, 6.2, 12.0)	0.86, 1.16, 1.60, 1.7, 4.68
6	29.24 (t)	α -H 1.66 (ddd, 2.0, 12.0, 13.9) β -H 2.11 (ddd, 3.8, 6.2, 13.9)	
7	74.38 (d)	1H 4.68 (dd, 2.0, 3.8)	7.28
8	138.67 (s)		2.11, 7.40
9	155.99 (s)		4.36, 4.68, 7.28
10	40.62 (s)		1.7, 7.40
11	120.02 (d)	1H 7.40 (s)	
12	171.97 (s)		
13	166.37 (s)	(OH 9.6 br)	2.42, 7.28, 7.40
14	131.31(s)		2.42
15	136.37 (d)	1H 7.28 (s)	2.42, 4.68
16	67.35 (t)	α -H 2.99 (dd, 2.0, 9.1) β -H 4.36 (d,9.1)	
17	21.3 (q)	3H 1.16 (s)	0.86, 1.23
18	32.7 (q)	3H 0.86 (s)	1.16
19		3H 2.42 (s)	7.28

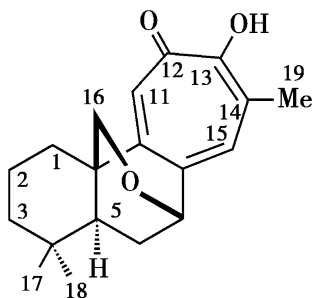


Fig. 8.11 The structure of miltionone

ring ($\nu_{\text{KBr}} 1,570 \text{ cm}^{-1}$), and there is a hydrogen bond between 2-hydroxyl group and 1,4-benzo-quinone. ($\nu_{\text{KBr}} 3,380, 1,670, 1,650 \text{ cm}^{-1}$). In the H-NMR spectrum, there is an isopropyl group linked to the benzene ring [($\delta 3.37, 1\text{H}$, septet, $J = 7.1 \text{ Hz}$, H-15), ($\delta 1.29, 6\text{H}$, d, $J = 7.1 \text{ Hz}$, Me-16 and Me-17)], and two vicinal aromatic protons [($\delta 8.18, 1\text{H}$, d, $J = 8.2 \text{ Hz}$, H-7) and ($\delta 7.68, 1\text{H}$, d, $J = 8.2 \text{ Hz}$, H-6)]. The hydroxyl hydrogen at $\delta 7.38$ disappears when D_2O is added. In

addition, there are also two methylenes at [($\delta 2.95, 2\text{H}$, t, $J = 7.2 \text{ Hz}$, H-2) and ($\delta 2.09, 2\text{H}$, t, $J = 7.2 \text{ Hz}$, H-3)] as well as a gem-dimethyl ($\delta 1.29, 6\text{H}$, s, Me-18 and Me-19). The important thing is the carbonyl group at C-1 of ring A, which is confirmed by ^{13}C -NMR $\delta 199.46$. The alicyclic methylene of miltionone II at C-1 is ($\delta 28.29$, t) (see Table 8.11 for detail).

Miltionone II is a colorless needle crystal, $\text{C}_{19}\text{H}_{20}\text{O}_4$ (M^+ 312.1349), mp $184\text{--}185^\circ\text{C}$, $[\alpha]_{\text{D}}^{30} +114.8^\circ\text{C}$ (CHCl_3). UV spectrum: 222, 265, 308, and 320 nm. The IR spectrum shows an enolic hydroxyl group ($\nu_{\text{KBr}} 3,380 \text{ cm}^{-1}$) and a carbonyl ketone ($1,780, 1,720, 1,615, 1,590$, and $1,550 \text{ cm}^{-1}$). The H-NMR spectrum shows a gem-dimethyl [($\delta 1.31, 3\text{H}$, s, Me-18), ($\delta 1.33, 3\text{H}$, s, Me-19)] and ($\delta 1.35, 3\text{H}$, d, $J = 7.2 \text{ Hz}$, Me-17); alicyclic protons ($\delta 1.82, 2\text{H}$, m, H-2) and ($\delta 2.86, 2\text{H}$, m, H-1); and dihydrofuran ring protons, H-15 $_{\alpha}$ ($\delta 3.61, 1\text{H}$, m), and H-16 $_{\beta}$ [($\delta 4.20, 1\text{H}$, dd, $J = 9.2 \text{ Hz}$), ($\delta 4.75, 1\text{H}$, t, $J = 9.2 \text{ Hz}$)]. The existence of 17-methyl bonded

Table 8.11 ^{13}C -NMR data of miltionone I, miltionone II, and cryptotanshinone

C	Miltionone I (56)	Miltionone II (57)	Cryptotanshinone (2)
1	199.46s	28.29*t	29.65*t
2	36.64*t	19.05*t	19.09*t
3	36.64*t	38.19*t	37.87*t
4	35.39s	34.86s	34.86s
5	135.10s	135.42s	143.66s
6	130.49*d	190.32s	132.52*d
7	129.32*d	130.11*d	122.50*d
8	133.44s	130.41s	128.46s
9	128.77s	122.28s	126.32s
10	153.44s	151.74s	152.39s
11	181.03s	156.51s	184.26s
12	156.83s	183.19s	175.69s
13	127.34s	108.81s	118.32s
14	183.52s	163.75s	170.71s
15	24.64*d	38.46*d	34.66*d
16	19.83*q	78.08*t	81.46*t
17	19.83*q	18.73*q	18.80*q
18	28.73*q	31.65*q	31.89*q
19	28.73*q	31.77*q	31.94*q

* ^{13}C -H correlation based on decoupled ^{13}C -NMR test

to the dihydrofuran ring is confirmed by comparing with cryptotanshinone data (see Table 8.11), plus an enolic hydroxyl group protons (δ 7.27, OH-11) and methylene protons at (δ 7.59, 1H, s, H-7). The carbonyl ketone at C-6 is confirmed by δ 190.32 in the ^{13}C -NMR spectrum.

8.3.3.26 NMR Spectra of Epi-Danshenspiroketalactone (43), Cryptoacetalide (45), Epi-cryptoacetalide (44)

The structure of spiro lactone, named Danshenspiroketalactone [12] (42) was determined by X-ray analysis. We found that it was a mixture of a pair of isomerides through 2D COSY (benzene- d_6) spectroscopy. Protonic signals were almost identical in the aromatic field of the two isomerides, and the only difference was in the alicyclic field. Asari Fumika et al. also isolated a pair of spiroketalactone-type compounds with an alicyclic ring A, named cryptoacetalide and epi-cryptoacetalide, and failed to separate them [32]. cryptoacetalide (45), epi-cryptoacetalide (44), $\text{C}_{18}\text{H}_{22}\text{O}_3$ [HRMS, m/z 286.1571(45:44 = 3:1)]. ^{13}C -NMR spectroscopy shows an ester carbonyl group (δ 168.12) and quadri-substituted benzene ring (δ 148.85 s, 144.50 s, 138.56 s, 132.91 d, 124.07 s, and 119.04 d). Based on calculating the

degree of unsaturation, it was estimated that besides the lactone and benzene rings, there should be another two rings. ^1H - ^1H COSY spectroscopy indicated there were three fragments: $-\text{CH}_2-\text{CH}_2-\text{CH}_2-\text{C}(\text{CH}_3)_2-$, $-\text{O}-\text{CH}_2-\text{CH}(\text{CH}_3)_2-\text{CH}_2$, and $-\text{CH}=\text{CH}-(\text{benzene ring})$. The presence of acetal C was inferred by ^{13}C -NMR δ 112.80. There were correlations between gem-dimethyl (δ 1.27 and 1.28), aromatic proton (δ 7.62, H-7), and aromatic carbon atom (δ 148.85, C-5) in cryptoacetalide (45) shown by 2D COLOC spectroscopy (see Tables 8.12 and 8.13). There were coupling systems existing between an aromatic proton (δ 7.24, H-6), alicyclic methane (δ 3.17, H_2 -1) and another aromatic carbon atom (δ 138.56, C-10). In addition, there were still the following crosspeaks: H-6 and C-8, H-7 and C-9, H_2 -1 and C-9, which suggested the existence of a tetra-naphthyl ring system, and the correlations between methylene proton (δ 1.95, H_a -16) and aromatic carbon atom (C-8) and quaternary carbon (δ 112.80, C-13). The quaternary carbon C-13 is related with H-7, suggesting it must be an acetal carbon.

8.3.3.27 ^1H -NMR Spectra of Danshenol-A (55) and Danshenol-B (54)

Danshenol-A is a dark yellow needle crystal, m. p. 182 °C, $[\alpha]_D-136.4^\circ(\text{CHCl}_3)$, $\text{C}_{21}\text{H}_{20}\text{O}_4$

Table 8.12 ^1H -NMR data for cryptoacetalide (45) and Epi-cryptoacetalide (44)

Cryptoacetalide (45)				Epicryptoacetalide (44)			
H	δ	Num.	Coupling constant	H	δ	Num.	Coupling constant
1	3.17m	2H		1	3.17m	2H	
2	1.80m	2H		2	1.80m	2H	
3	1.68m	2H		3	1.68m	2H	
6	7.62d	1H	$J = 8.1$	6	7.62d	1H	$J = 8.1$
7	7.24d	1H	$J = 8.1$	7	7.20d	1H	$J = 8.1$
14a	3.71t	1H	$J = 8.1$	14a	4.31t	1H	$J = 8.1$
14b	4.36t	1H	$J = 8, 1$	14b	3.81t	1H	$J = 7.0, 8.1$
15	2.86m	1H		15	2.68m	1H	
16a	1.95dd	1H	$J = 10.5, 13.1$	16a	2.58dd	1H	$J = 9.4, 13.3$
16b	2.43dd	1H	$J = 6.8, 13.1$	16b	2.10dd	1H	$J = 4.5, 13.3$
17	1.18d	3H	$J = 7.0$	17	1.24d	3H	$J = 7.0$
18	1.27s	3H		18	1.27s	3H	
19	1.28s	3H		19	1.28s	3H	

Table 8.13 ^{13}C -NMR chemical shift and C,H-COLOC spectrum of cryptoacetalide, Epi-cryptoacetalide ($J = 7\text{ Hz}$, CDCl_3)

	45		44			45		44	
	Carbon	Proton ^a	Carbon	Proton ^a		Carbon	Proton ^a	Carbon	Proton ^a
1	$\delta 25.84$	2,3	$\delta 25.84$	2,3	10	$\delta 138.56$	1,6	$\delta 138.43$	1,6
2	18.30	1,3	18.30	1,3	11	168,12		168.33	
3	39.21	18,19	39.21	18,19	12	–		–	
4	33.98	18,19	33.98	18,19	13	112.80	7,16a	112.80	7,16b
5	148.85	3,7	148.75	3,7	14	76.9	17	76.90	17
		18,19		18,19	15	32.33	16,17	33.23	16,17
6	132.91	7	133.01	7	16	45.34	17	44.37	17
7	119.04	6	118.92	6	17	17.27		17.99	
8	144.50	6,16a	145.30	6	18	31.64	18,19	31.64	18,19
9	124.07	1,7	123.61	7	19	31.64	18,19	31.64	18,19

^a proton and carbon atom on the same line show crosspeaks

(HRMS: 336.1395 m/z 336). It has one $\text{C}_3\text{H}_6\text{O}$ fragment more than the known compound dihydrotanshinone I $\text{C}_{18}\text{H}_{14}\text{O}_3$ (7). Its ^1H -NMR and ^{13}C -NMR spectra (see Table 8.14) show that it has some similarities in data with dihydrotanshinone I.

The ^1H - ^1H and ^1H - ^{13}C 2D correlation NMR spectra showed that compound 55 has the same A, B, and D ring systems as dihydrotanshinone I. In addition, compound 55 generated the signals of a methylene proton ($\text{C}20\text{-H}_2$) and a methyl group ($\text{C}22\text{-H}_3$). ^{13}C -NMR spectroscopy showed a signal of quaternary carbon linked with an oxygen atom $\delta c 79.3$ (C-11) and two carbonyl carbons [$\delta c 204.8$ (C-21), 196.1 (C-12)] shifting toward the low field obviously (see Fig. 8.12). The above data suggested the ring system of Danshenol-A belonged to abietane skeleton, except the presence of the C3 unit ($\text{CH}_3\text{-CO-CH}_2$) linked with its ring C, and the precise linking position of the C3 unit was confirmed by heteronuclear multiple bond correlation (HMBC) spectroscopy. The HMBC spectrum showed that the C3 unit was linked at C-11, so the plane structure of the compound was known. When irradiated at 17-H_3 in NOE test, the signal of 22-H_3 was gained, and vice versa; thereby, the *cis* form of $\text{CH}_3\text{-CO-CH}_2$ with the methyl group was confirmed. On the other hand, the retro-aldol reaction between dihydrotanshinone I and Eu

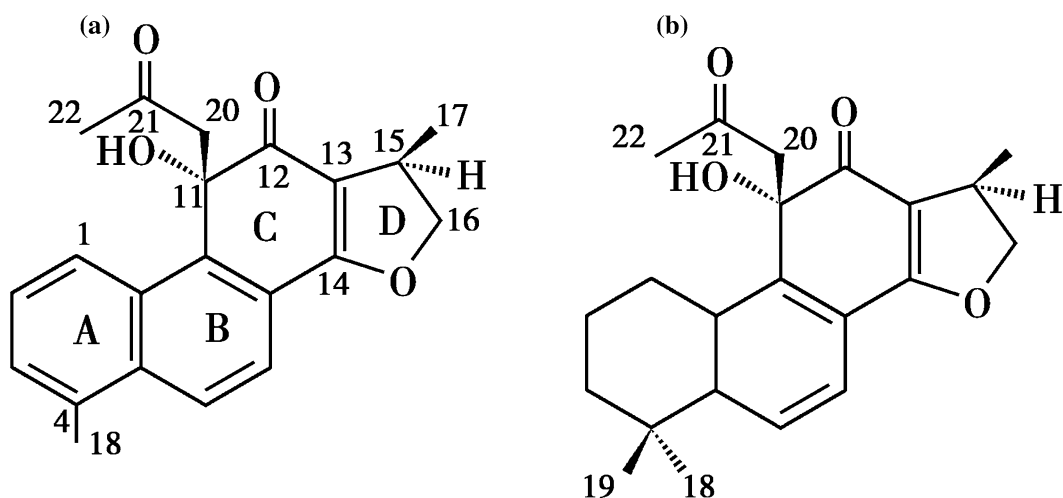
(DPM) $_3$ generated a product with $[\alpha]_{\text{D}} -146.6^\circ$ (CHCl_3 , $c = 0.09$), while the natural existed dihydrotanshinone I was $[\alpha]_{\text{D}} -332.8^\circ$. This result demonstrated that the configuration of C-15 is R.

Danshenol-B (54) is a yellow needle crystal, m.p. 176°C , $[\alpha]_{\text{D}} -131.6^\circ$ (CHCl_3), $\text{C}_{22}\text{H}_{26}\text{O}_4$ (HRMS: 336.1395 m/z 354). The H-NMR spectrum of Danshenol-B shares some similarities with that of cryptotanshinone (see Table 8.14): three methylene protons coupled with each other; two ortho protons of benzene (6-H, 7-H); a fragment of $\text{CH}_3\text{-CH-CH}_2\text{-O}$ (17-H_3 , 16-H_2 , 15-H), as well as two single-peaked methyl groups (18-H_3 , 19-H_3). The C3 unit ($\text{CH}_3\text{-CO-CH}_2$) found in Danshenol-A is also present in Danshenol-B. Therefore, it was assumed that Danshenol-B had a C ring system similar to compound 55. ^1H - ^1H and ^1H - ^{13}C 2D correlation spectra and HMBC confirmed the assumption. The stereochemical structure of Danshenol-B was deduced also based upon the NOE effect: observe the interrelation of 17-H_3 and 22-H_3 in NOE test; use $\text{Eu}(\text{DPM})_3$ to react with cryptotanshinone in a retro-aldol reaction and measure the specific rotation of the product. The result was $[\alpha]_{\text{D}} -56.8^\circ$ (CHCl_3 , $c = 0.09$), while natural cryptotanshinone is $[\alpha]_{\text{D}} -76.5^\circ$. Thus, it is believed that Danshenol-A and Danshenol-B could be formed by aldol condensation in the presence of acetone. However, we could

Table 8.14 ^{13}C -NMR data for Danshenol-A (55), Danshenol-B (54), and some Ref. [33]

C	55	Dihydrotanshinone I, 7	Tanshinone-I	Danshenxinkun A, 39	54	Cryptotanshinone 2	Tanshinone-IIA, 3
1	125.8	124.7	125.1	125.0	29.2	29.6	29.9
2	126.7	130.6	130.5	129.5	19.9	19.3	19.1
3	128.5	128.3	128.9	128.6	38.7	37.7	37.8
4	135.2	135.2	135.0	134.8	35.3	34.8	34.7
5	134.9	132.9	134.8	133.0	151.6	143.6	144.1
6	125.5	133.0	131.9	131.3	127.3	132.5	133.3
7	120.1	118.7	120.4	121.6	122.2	122.5	120.8
8	120.4	118.7	128.2	129.8	120.3	128.8	127.4
9	141.3	153.1	126.2	124.4	140.6	126.1	126.5
10	131.0	129.6	132.2	134.6	137.3	152.1	150.1
11	79.3	183.3	185.3	183.5	79.6	184.0	183.6
12	196.1	207.2	175.8	155.4	196.0	175.5	175.7
13	113.6	120.3	118.4	121.7	112.5	118.2	119.9
14	171.3	162.5	170.4	185.5	171.6	170.8	171.7
15	34.5	122.2	34.7	32.0	34.4	34.6	121.4
16	81.4	142.1	81.7	64.3	81.1	81.5	141.1
17	18.0	8.3	18.8	13.9	17.9	18.7	17.9
18	20.1	19.8	19.9	18.9	32.4	31.7	31.2
19					32.6	31.8	31.2
20	57.3				54.8		
21	204.8				205.1		
22	32.1				32.1		

Note in CDCl_3 - CD_3OD

**Fig. 8.12** Structures of **a** Danshenol-A and **b** Danshenol-B

detect Danshenol-A ($R_f = 0.24$) and Danshenol-B ($R_f = 0.33$) when separating the methanol extract of Danshen on TLC, using benzene-acetic ether (87:13) as the developing solvent, with no acetone involved at all. This obviously shows that the two compounds are not artifacts.

8.3.3.28 NMR Spectrum of Paramiltioic Acid [56]

Paramiltioic acid is a diterpene acid isolated from *S. sinica*, $C_{19}H_{24}O_5$ (EIMS: m/z 332.1532 M^+). The IR spectrum shows two carbonyl groups at 1,761 and 1,717 cm^{-1} ; the former band is due to an $\alpha\beta$ -unsaturated five-membered lactone (δ_c 173.4, s), and the latter one is due to an $\alpha\beta$ -unsaturated carboxylic acid (ν 3,305–2,400, br, and 942 cm^{-1}). In the ^{13}C -NMR spectrum, (δ_c 166.5, s), one methyl group (δ_H 1.77, 3H, d, $J = 1.5$ Hz) is coupled to a vinyl hydrogen (δ_H 7.34, 1H, q, $J = 1.5$ Hz, 12-H) which is located on the lactone ring. HMBC experiments confirm the structure of fragment I. It also suggests the presence of fragments II and III. 1H - 1H COSY spectroscopy shows a crosspeak due to W-type

coupling between 9-H and 7-H. Paramiltioic acid is thus shown to have a spirolactone structure at C-8. The existence of fragments IV, V, and VI is suggested by HMBC experiments. The crosspeaks between 5-H and 6-H, 6-H and 7-H are observed in the 1H - 1H COSY spectrum. These data suggest the existence of an oxabicyclo [4.4.0] decane system in paramiltioic acid. The same system can be seen in norsalvioxide (60) and miltipolone (61), and both have the same ring systems. NOESY tests also show the following crosspeaks: 15- CH_3 and 17-Ha, 5-H and 16- CH_3 , 6-Ha and 7-H, 12-H and 17-Hb, 12-H and 19- CH_3 . The W-type coincidence between 5-H and 17-Hb indicated by 1H - 1H COSY spectrum proves the *trans* configuration of rings A/B. Plane and stereochemical structures are shown in Fig. 8.13.

8.3.4 Mass Spectrometry

Mass spectrometry (MS) is a very convenient and effective way to study the structures of

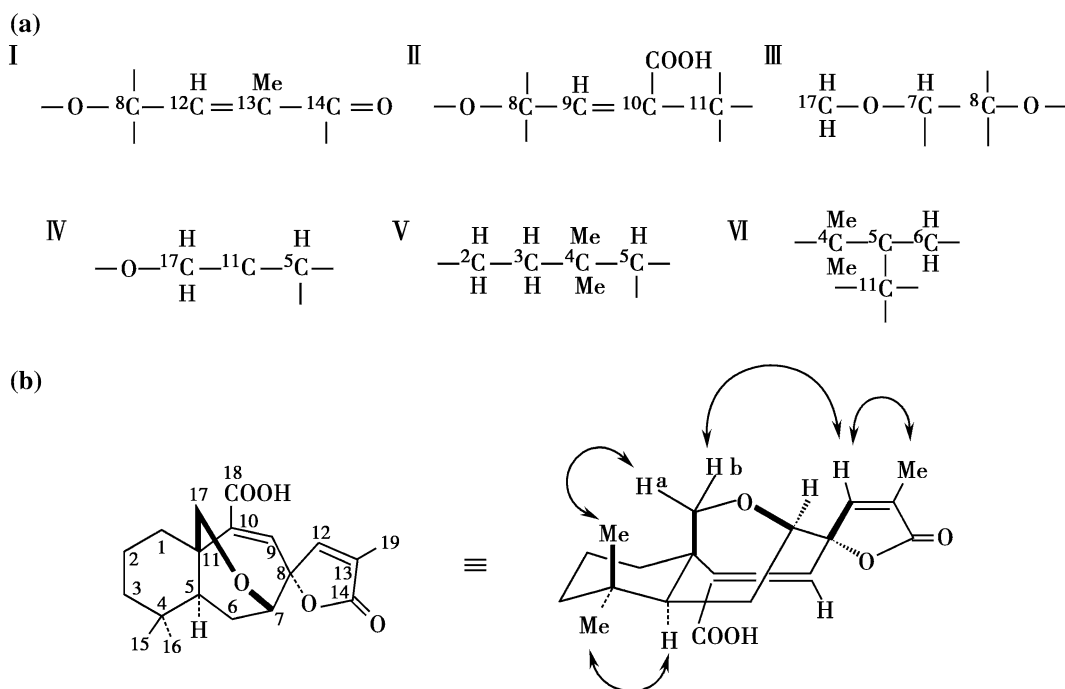


Fig. 8.13 Plane and stereochemical structure of fragments (a) and paramiltioic acid (b)

tanshinone and its related tricyclic diterpenes. A compound's mass spectrum could provide the following structural information in the forms of mass/charge ratio (m/z) and its relative abundance: molecular weight, molecular formula, types of functional groups, and the connecting sequence of the groups. The molecular formula obtained from the MS data can be used to distinguish different types of tanshinones, such as 1,2 o-naphthoquinone and 1,4 p-naphthoquinone. It can also be used to identify the diterpene compounds involved in tanshinone's biosynthesis. For the sake of convenience, the MS data of all diterpene quinones from Danshen with known structures are listed in Tables 8.15 and 8.16. The compound's structural formula can be found by its serial number which is located after each compound's name. In Table 8.15, all the cited MS data were obtained with a JMS-D 300 mass spectrometer. Electron ionization energy: 70 eV, temperature of ion source: 210–230 °C, direct injection, temperature-programmed control of the probe. Resolution: low-resolution $R = 1,000$, high-resolution $R = 5,000$, error: 4–5 m/z . In Table 8.16, the data are from different publications. For some compounds, only one molecular ion peak $[M]$ is listed; for some others, the data are high-resolution MS (HRMS), which is expressed in m/z .

The differences in relative abundance of molecular ion peaks could imply different structure stabilities of tanshinone compounds and different types of ring systems in the compounds. The peak abundance of compounds in which ring A is alicyclic such as tanshinone IIA, cryptotanshinone, and methylenetanshinone can reach 100 %, while the abundance of tanshinone I and dihydrotanshinone I in which ring A is aromatic is only 44.5 and 19.8 %, respectively.

The stability of tanshinone compounds, which are defined as compounds with a furan or dihydrofuran ring besides C ring, is higher than that of tricyclic diterpenes in which the furan rings are substituted by an isopropyl group. The molecular ion peaks of tricyclic diterpene quinones are very weak, for example, the relative abundances of miltirone and miltirone I are m/z 264 ($[M]$, 1.4 %) and m/z 282 ($[M]$, 1.6 %),

respectively. Besides, tricyclic diterpene quinones display a characteristic ion peak of $[M+2]$ in MS.

In addition, Hayashi et al. [57] found that when ring A was alicyclic as in tanshinones IIA, it gave the mass fragment ion peaks **[b]** at m/z 261 by dehydration from the ion peaks **[a]** m/z 279 which did not contain an hydroxyl group. The rearrangement pathway of its dehydration is proposed as follows (Fig. 8.14).

The proposed rearrangement pathway did not clearly show how the C-11 oxygen was lost, or how the hydrogen atom was transferred to C-11 after the deoxygenation. However, as the progress of chemical research on diterpene quinones moves forward, many new compounds have been isolated. To elucidate the dehydration mechanism, the following rearrangement pathway is proposed based on the fact that they have their own way of dehydration due to the differences in structure.

This rearrangement clearly shows the loss of the oxygen atom at C-11 can be attributed first to the transfer of the proton at the position of 1-H on ring A to the oxygen atom at C-11 on ring C through the formation of intermediate **[b]**, followed by the loss of H_2O during the fragmentation process of these compounds. Therefore, the hydrogen at C-1 and oxygen at C-11 seems to be the source of H_2O , which was lost resulting in the formation of a tetracyclic fragment (see Fig. 8.15).

Accordingly, an alicyclic structure is necessary for the loss of oxygen in C-11. The mechanisms of dehydration can be divided into different modes according to the different characteristics of the structure of ring A.

8.3.4.1 Dehydration After the Loss of Side Chain in Ring A

Tanshinone IIA, tanshinone IIB and methyl tanshinonate all belong to type II tanshinones. The only difference among them lies in the side chain in ring A. Before dehydration, the loss of the R side chain in C-4 occurs. For example, tanshinone IIA, tanshinone IIB, and methyl tanshinonate display peaks of ($[M-CH_3]$, 42.5), ($[M-CH_2OH]$, 100) and ($[M-COOCH_3]$, 100), respectively, after the

Table 8.15 The MS data of diterpene quinones and their related compounds in Danshen [9]

Compound	Molecular formula	m/z
Ferrugiol 50	C ₂₀ H ₃₀ O	286([M], 98.4), 271([M-CH ₃], 100), 243([M-C ₃ H ₇], 6.9)
Danshenxinkun B 40	C ₁₈ H ₁₆ O ₃	280([M], 100), 252([M-CO], 1.8), 234([M-CO-H ₂ O], 0.9)
Salviolone 59	C ₁₈ H ₂₀ O ₂	268([M], 58.3), 253([M-CH ₃], 15.5), 225([M-COCH ₃], 17.0)
Miltirone 27	C ₁₉ H ₂₂ O ₂	282([M], 1.6), 267([M-CH ₃], 1.49), 254([M-CO], 49.2), 249([M-CH ₃ -H ₂ O], 1.1)
Δ ¹ Miltirone 29	C ₁₉ H ₂₀ O ₂	280([M], 1.7), 265([M-CH ₃], 0.85), 252([M-CO], 51.1), 247([M-CH ₃ -H ₂ O], 0.65)
Tanshinlactone 46	C ₁₇ H ₁₂ O ₃	264([M], 100), 235([M-CHO], 2.1), 236([M-CO], 0.7), 208 ([M-2CO], 6.5)
Danshenspiroketallactone 42	C ₁₇ H ₁₆ O ₃	268([M], 72), 212([M-C ₄ H ₈], 100), 184([M-C ₄ H ₈ -CO], 45.1)
Miltirone I 28	C ₁₈ H ₁₆ O ₂	266([M + 2], 7.8), 264([M], 1.4), 236([M-CO], 100)
Tanshinone IIA 3	C ₁₉ H ₁₈ O ₃	294([M], 100), 279([M-CH ₃], 42.5), 261([M-CH ₃ -H ₂ O], 76.9)
Δ ¹ -Tanshinone IIA 15	C ₁₉ H ₁₆ O ₃	292([M], 61.4), 277([M-CH ₃], 94.6), 249([M-CH ₃ -CH], 100), 264([M-CO], 4.9)
Methylenetanshinone 8	C ₁₈ H ₁₄ O ₃	278([M], 100), 260([M-H ₂ O], 9.25), 263([M-CH ₃], 18.6), 250([M-CO], 7.7)
Tanshinone I 1	C ₁₈ H ₁₂ O ₃	276([M], 44.5), 248([M-CO], 100)
Methyltanshinonate 6	C ₂₀ H ₁₈ O ₅	338([M], 0.7), 279([M-COOCH ₃], 100), 261([M-COOCH ₃ -H ₂ O], 9.6)
Nortanshinone 13	C ₁₇ H ₁₂ O ₄	280([M], 100), 253([M-CO], 23.5), 234([M-CO-H ₂ O], 4.8)
Cryptotanshinone 2	C ₁₉ H ₂₀ O ₃	296([M], 100), 268([M-CO], 29.1), 281([M-CH ₃], 8.6), 263([M-CH ₃ -H ₂ O], 4.5)
Dihydrotanshinone I 7	C ₁₈ H ₁₄ O ₃	278([M], 19.8), 250([M-CO], 46.9), 235([M-CO, -CH ₃], 100)
Danshenol-A 55	C ₂₁ H ₂₀ O ₄	336([M], 1.6), 318([M-H ₂ O], 0.3), 278([M-C ₃ H ₆ O], 15.6), 250([M-C ₃ H ₆ O, -CO], 47.2), 235([M-C ₃ H ₆ O, -CH ₃], 100)
Tanshinone IIB 4	C ₁₉ H ₁₈ O ₄	310([M], 23.0), 279([M-C ₂ OH], 100), 261([M-CH ₂ OH, -H ₂ O], 19.7)
3α-Hydroxytanshinone IIA 14	C ₁₉ H ₁₈ O ₄	310([M], 100), 295([M-CH ₃], 27.3), 292([M-H ₂ O], 39.7), 277([M-CH ₃ , -H ₂ O], 38.6), 267([M-CH ₃ , -CO], 62.1), 249([267-H ₂ O], 48.7)
Przewaquinone A 19	C ₁₉ H ₁₈ O ₄	310([M], 32.8), 292([M-H ₂ O], 76.3), 277([M-H ₂ O, -CH ₃], 84.3), 249 ([M-H ₂ O, -CH ₃ , -CO], 43.7)
Przewaquinone B 20	C ₁₈ H ₁₈ O ₄	292([M], 43.1), 264([M-CO], 100)
Danshenxinkun A 39	C ₁₈ H ₁₆ O ₄	296([M], 60), 278([M-H ₂ O], 9.7), 265([M-CH ₂ OH], 38.1)
Tanshindiol B 11	C ₁₈ H ₁₆ O ₅	312([M], 26.3), 294([M-H ₂ O], 86.4), 279([M-H ₂ O, -CH ₃], 22.2), 266 ([M-H ₂ O,-CO],100)
Tanshindiol A 10	C ₁₈ H ₁₆ O ₅	312([M], 1.72), 294([M-H ₂ O], 5.1), 281([M-CH ₂ OH], 100), 263([M-CH ₂ OH, -H ₂ O], 8.1)
Tanshindiol C 12	C ₁₈ H ₁₆ O ₅	312([M], 17.8), 294([M-H ₂ O], 66.4), 279([M-H ₂ O, -CO], 100)
Triterpene, Przewanoic acid A	C ₃₀ H ₄₆ O ₄	470([M], 82.7), 455([M-CH ₃], 7.4), 452([M-H ₂ O], 90.9), 425([M-COOH], 7.7), 301(k, 30.5), 232(4.2), 187([232-COOH], 100)
Przewanoic acid B	C ₂₉ H ₄₂ O ₄	454([M], 29.1), 439([M-CH ₃], 5.1), 436([M-H ₂ O], 34.9), 409([M-COOH], 4.57), 300(k.8.2), 285(k-CH ₃ , 2.0), 232(4.1), 187([232-COOH], 100)
Oleanolic acid	C ₃₀ H ₄₈ O ₃	456([M], 0.9), 248(a, 98.4), 203(c, [248-COOH], 100), 441([M-CH ₃], 0.4), 438([M-H ₂ O], 1.8), 411([M-COOH], 0.55)

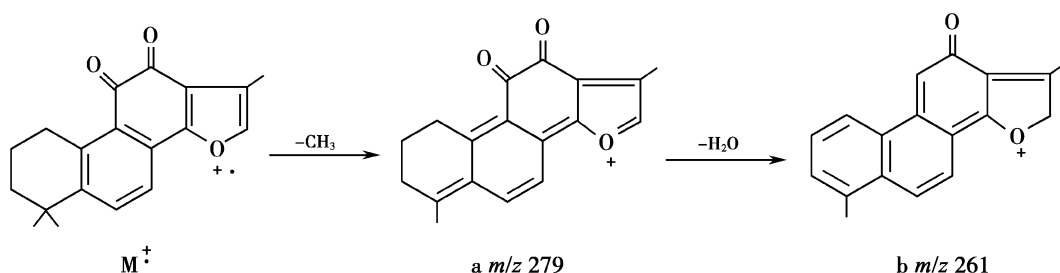
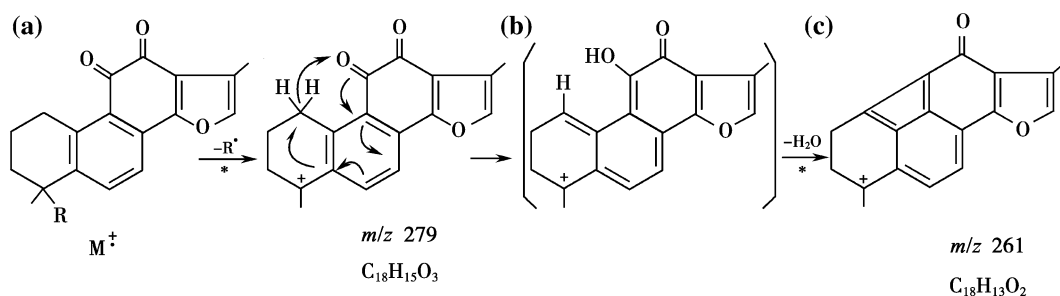
Table 8.16 The MS data of diterpene quinones in Danshen and their related compounds

1-Hydroxytanshinone IIA 5	C ₁₉ H ₁₈ O ₄	310([M], 100), 295(14), 281(11), 278(13), 277(16), 267(15), 249(35)
Tanshinaldehyde II 16	C ₁₉ H ₁₆ O ₄	308([M], 15), 294(3), 280(92), 279(100), 264(17), 261(27), 251(28) HRMS:m/z308.1057
Tanshinaldehyde I 26	C ₁₈ H ₁₀ O ₄	HRMS:m/z290.0579
1,2,15,16-Tetrahydrotanshinone 18	C ₁₈ H ₁₆ O ₃	280([M], 97.1), 278(14.7), 265(12.3), 262(4.2), 252(21.4), 237(72.4), 235(53.3)HRMS:m/z280.117
Przewaquinone C 21	C ₁₈ H ₁₆ O ₄	296([M], 8.58), 281([M-CH ₃], 17.96), 287([M-CH ₃ -CO], 19.88 HRMS:m/z296.1077
Przewaquinone F 22	C ₁₈ H ₁₆ O ₅	312([M], 7.11), 294(10.3), 282(24.3), 281(100), 265(21.4) HRMS:m/ z312.1004
Cryptomethyl-tanshinonate 23	C ₂₀ H ₂₀ O ₅	340([M], 83.4), 338([M-2H], 30), 312([M-CO], 37), 297 ([M- CH ₃ - CO], 47), 281([M-COOCH ₃], 30), 279(55), 263(15), 253(100)
Tanshinol I 24	C ₁₈ H ₁₂ O ₄	292([M], 49), 265(22), 264([M-CO], 100), 247(12), 179(22), 178(28) HRMS:m/z292.0740
Hydroxymethylene tanshinone 25	C ₁₈ H ₁₄ O ₄	HRMS:m/z294.0892
Methylenelmiltirone 30	C ₁₈ H ₁₈ O ₂	266[M]
Methylenelenehydrotanshinone 17	C ₁₈ H ₁₆ O ₃	HRMS:m/z280.1087
1-Hydroxymiltirone 31	C ₁₉ H ₂₂ O ₃	298([M], 15), 283(2), 282(5), 252(46), 237(100), 227(9), 222(16), 214(19), 209(20)
Isotanshinone IIA 34	C ₁₉ H ₁₈ O ₃	294[M]
Isotanshinone I 33	C ₁₈ H ₁₂ O ₃	276[M]
Isocryptotanshinone 35	C ₁₉ H ₂₀ O ₃	296[M]
Isodihydrotanshinone 36	C ₁₈ H ₁₄ O ₃	HRMS:m/z 278.0944[M]
2-Hydroxyisodihydrotanshinone 37	C ₁₈ H ₁₄ O ₄	294([M], 25.5), 266(55.0), 251(100), 195(16.1), HRMS:m/z 294.0907[M]
Isotanshinone IIB 38	C ₁₉ H ₁₈ O ₄	310[M] 292([M-H ₂ O]), 279([M-CH ₂ OH]), 251(279-CO), 223(251- CO)
Danshenspiroketallactone 42	C ₁₈ H ₂₂ O ₃	HRMS:m/z 286.1571
Anhydride of tanshinone IIA 47	C ₁₉ H ₁₈ O ₄	HRMS:m/z 310.1205
Sugiol 52	C ₂₀ H ₂₈ O ₂	HRMS:m/z 300.2065
Arucadiol 53	C ₁₉ H ₂₂ O ₃	HRMS:m/z 298.1565
Danshenol-B 54	C ₂₂ H ₂₆ O ₄	354[M], 311, 296, 268, 253. HRMS:m/z 354.1866
Miltionone I 56	C ₁₉ H ₂₀ O ₄	312([M], 100), 297(7), 284(14), 269(59), 251(14), HRMS:m/z 312.1357
Miltionone II 57	C ₁₉ H ₂₀ O ₄	312([M], 20), 297(5), 284(5), 283(5), 269(35), 268(41), 254(19), 253(100) HRMS:m/z 312.1394
Norsalvioxide 60	C ₁₈ H ₂₄ O ₂	HRMS:m/z 272.1783
Miltipolone 61	C ₁₉ H ₂₄ O ₃	FAB mass peak [M + H ⁺ :m/z 301.1837]
Tanshinone V 62	C ₁₉ H ₂₂ O ₄	314([M], 40), 296([M-H ₂ O], 100), 281([M-H ₂ O-CH ₃], 50), 253([M-H ₂ O-CH ₃ -CO], 100)
Tanshinone VI 63	C ₁₈ H ₁₆ O ₄	296([M], 40), 278([M-H ₂ O], 70), 263([M-H ₂ O-CH ₃], 45), 250([M-H ₂ O-CO], 70), 235([M-H ₂ O-CO-CH ₃], 100)

(continued)

Table 8.16 (continued)

1-Hydroxytanshinone IIA 5	C ₁₉ H ₁₈ O ₄	310([M], 100), 295(14), 281(11), 278(13), 277(16), 267(15), 249(35)
3-Hydroxysalvilenone 64	C ₂₀ H ₂₀ O ₃	HRMS:m/z 308.1432
Salvilenone 65	C ₂₀ H ₂₀ O ₂	HRMS:m/z 292.1406
3-Ketosapriparaquinone 66	C ₂₀ H ₂₄ O ₄	HRMS:m/z 328.1557

**Fig. 8.14** The rearrangement pathway of dehydration in tanshinone IIA proposed by Hayashi, T**Fig. 8.15** The rearrangement and dehydration mechanism of tanshinone I

loss of the R side chain to produce ion [a] at m/z 279. Then, the product of ion [c] at m/z 261 is formed by electronic rearrangement and dehydration (Fig. 8.15). This mechanism was confirmed by detection of the metastable ion and then searching for the mother ion according to the daughter ion by the accelerating voltage scan method.

If ring A is aromatic, and the compounds belong to type I Tanshinones, such as tanshinone I, dihydrotanshinone I, and Przewaquinone B, there are no dehydration peaks, even though the furan ring in Przewaquinone B is linked with a β -hydroxymethyl group. The main fragments of tanshinone type I generate peak [M-CO], which shows as the base peak after the loss of CO (see Table 8.15).

8.3.4.2 Direct Dehydration

We take methylene tanshinquinone and its isomer 1, 2-dihydrotanshinone as examples. The main difference in the spectra of these two compounds is the intensity of the peak after dehydration. The intensity of the produced ion [M-H₂O] of methylene tanshinquinone at m/z 260 is 9.25, while that of 1,2-dihydrotanshinone at m/z 260 is 3.56.

8.3.4.3 Dehydration After the Loss of CO

Because the carbonyl group in C-4 causes the reduction of the activity of hydrogen in C-1, nortanshinone cannot produce the dehydration peak directly, so no ion at m/z 262. However, a strong peak at m/z 252 appears after the loss of carbonyl in C-4. Then, as Fig. 8.16 suggests, the

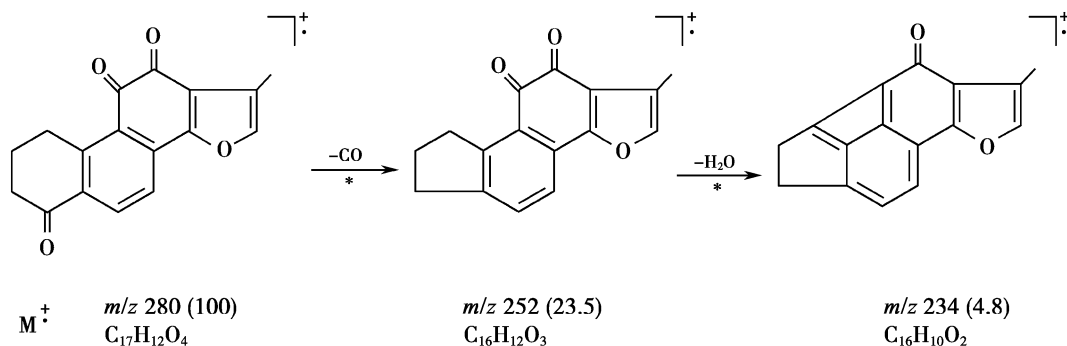


Fig. 8.16 The dehydration mechanism of Nortanshinone

dehydration peak appears after the same rearrangement, though its intensity is relatively weak.

8.3.4.4 The Dehydration Process of Compounds with a Hydroxyl Ring A

3 α -hydroxyltanshinone IIA can display an obvious peak at m/z 292 ([M-H₂O], 39.7), which results from the dehydration of C-1 and C-3. In contrast, the loss of acetic acid occurs in the

corresponding 3-acetoxytanshinone IIA, contributing to the formation of a 1, 3-cyclopropane structure in ring A which induces hydrogen in C-1 to be unable to go through the rearrangement dehydration (Fig. 8.17).

8.3.4.5 The Effect of Ring D on the Dehydration Process

The only difference between cryptotanshinone and tanshinone IIA lies in ring D. tanshinone IIA has a furan ring, while cryptotanshinone has a

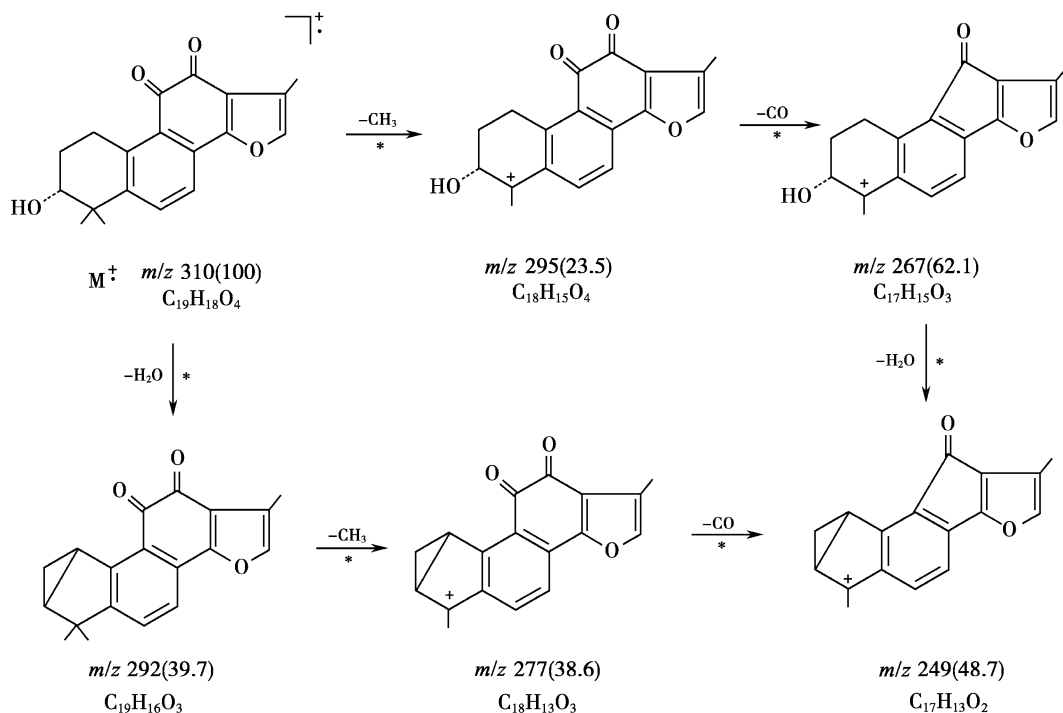


Fig. 8.17 The 1,3 dehydration of 3 α -hydroxyltanshinone IIA

dihydrofuran ring. In fact, cryptotanshinone's chromophore is an *o*-naphthoquinone, which shows a shorter conjugated system than tanshinone IIA, but they have an identical ring A; thus, the dehydration process can occur in both compounds. However, the intensity of cryptotanshinone's dehydration peak is weaker at m/z 263 ($[M-CH_3, -H_2O]$, 4.5) than that of tanshinone IIA m/z 261 ($[M-CH_3, -H_2O]$, 76.9), indicating the conjugated system of ring D influences the intensity of the ion peak produced by dehydration. Although miltirone, one of the tricyclic diterpene quinones, also displays the dehydration peak, its intensity is very weak, m/z 247 ($[M-CH_3, -H_2O]$, 0.65). Interestingly, Przewaquinone A, in which ring A is alicyclic, also displays a strong peak after dehydration m/z 292 ($[M-H_2O]$, 76.3), and this is confirmed by detection of existing metastable ions. However, the corresponding Przewaquinone B could not display the dehydration peak though it possessed the hydroxymethyl group bond to ring D, indicating that the dehydration process does not come from the hydroxymethyl group in C-19.

Therefore, a structure with an alicyclic ring A is necessary for the dehydration of tanshinones. It is also crucial that it possesses two protons in C-1. Take Δ^1 -tanshinone IIA for example. It could not dehydrate because there is only one ethylene proton in ring A. Furthermore, the quinone group attached on ring C is also necessary for dehydration. The main fragmentation pathway of *o*-di-acetoxy derivatives (the reduction product of tanshinone IIA) is the successive loss of two acetoxy groups, yielding the ion with a *o*-phenolic hydroxyl group at m/z 296, followed by giving the ion peak at m/z 281 after the loss of an methyl group. However, it does not show the dehydration peak in the mechanism mentioned above, indicating that the existence of an *o*-phenolic hydroxyl group does not benefit proton rearrangement and dehydration (see Fig. 8.18).

The fragmentation mechanism mentioned above is only suitable for EI (electron impact ionization, occurred in 70 eV). As for the popular electrospray ionization which has a different performance, its fragmentation mechanism still needs further investigation.

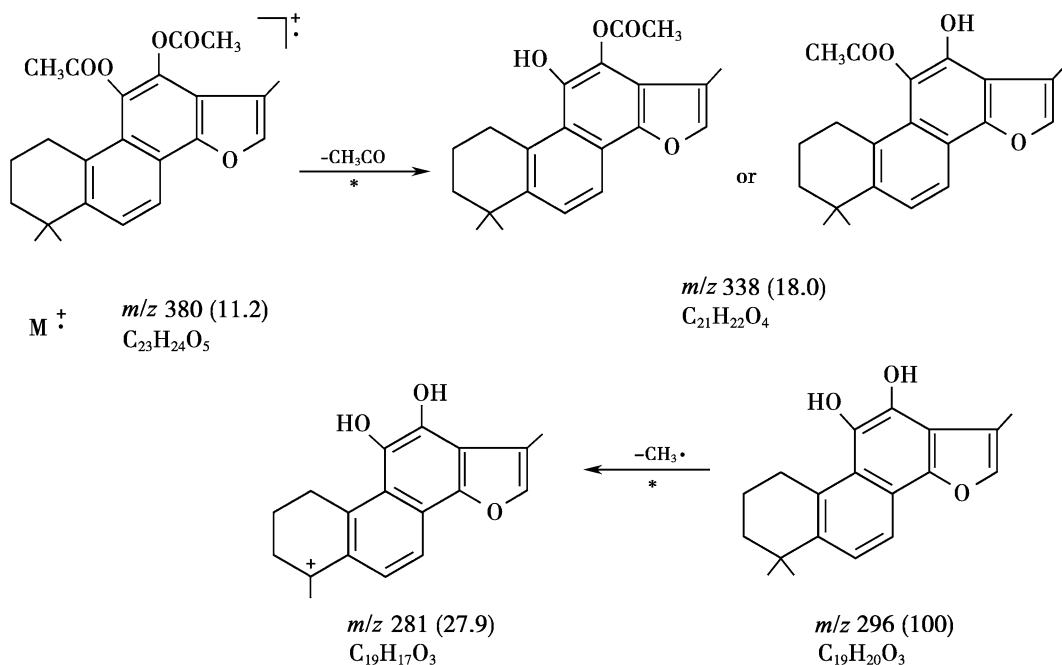


Fig. 8.18 The characteristic of diacetyltanshinone: the successive loss of 2 acetones

Since many tanshinones have the same molecular weight and formula, there are some disadvantages in the identification of compounds by MS only. For example, many compounds share the same molecular weight at m/z 310 and same formula $C_{19}H_{18}O_4$, such as tanshenione IIB, 1-hydroxyl tanshenione IIA, 3 α -hydroxyl tanshenione IIA, Przewaquinone A and isotanshinone IIB. As for tanshenione IIB (4), the characteristic presence of a fragment peak at m/z 261 $[M-CH_2OH-H_2O]$ suggests the presence of a primary alcohol attached to ring A, which could differentiate tanshenione IIB from both 3 α -hydroxyl tanshenione IIA (14) and Przewaquinone A (19). Although both of them display the fragment peak of $[M-H_2O]$ and not the peak of $[M-CH_2OH]$, the molecular peak of 3 α -hydroxyl tanshenione IIA is a base peak while that of abundance of Przewaquinone A is only 32.8 % (Fig. 8.15). They can also be distinguished according to their R_f values which are obtained by proper TLC (Table 8.2). It is difficult to identify 1-hydroxyl tanshenione IIA (5) and 3 α -hydroxyl tanshenione IIA (14) only by MS, while it is helpful to distinguish them by TLC according to their R_f values, which are 0.18 and 0.07, respectively, under the proper conditions [silica-CMC plate, developing solvent: benzene-acetone (95:5)].

8.4 The Physicochemical Properties of Tanshinones

Some physicochemical properties of tanshinones such as their detection characteristics and solubilities have been discussed numerous times in

the section of Extract and Separation. Now we discuss the relationships among their chemical structures, physicochemical properties and bioactivities, or the SAR. Tiny differences in structure may cause considerable effects in physicochemical properties. For example, a remarkable difference can be found between diterpenoid tanshinones with a furan ring or dihydrofuran ring. cryptotanshinone, which possesses a dihydrofuran ring, can react with ferric trichloride in glacial acetic acid solution and form a complex salt $C_{19}H_{20}O_3-FeCl_3$ [3], while tanshinone IIA, which possesses a furan ring, cannot. The solvation effects of *o*-naphthoquinone and chlorides ($ZnCl_2$, $BiCl_3$) in non-aqueous solvents (CH_3NO_2 , CH_3CN) have been reported [58].

In this section, the relationships between the structures of tanshinones and their chemical stabilities, antioxidant activities and solubilities will be discussed briefly.

8.4.1 The Redox Potential of Tanshinones

Tanshinones are categorized chemically as diterpene quinone compounds, belonging to a special tricyclic skeleton system of abietane. Such a structure possesses not only the general characteristics of quinones, but also some particularities, and they are the basis of various bioactivities. Quinones can easily transform into their hydroquinones, due to their similarity in energy level (see Fig. 8.19).

Then, a suitable oxidation-reduction system is constructed. Many characteristics of quinone are due to hydroquinone, which has a tendency to

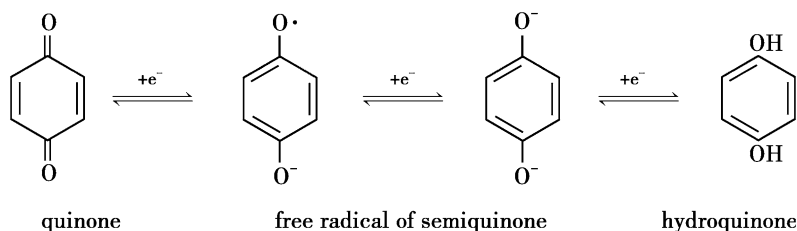


Fig. 8.19 The transformation between quinone and hydroquinone

form aromatic ring systems. The easiness or difficulty of such transformations can be expressed by the redox potential (E°). Some common quinones' E° values (V) are shown in Fig. 8.20; some of them, e.g., 2,3-dichloro-5,6-dicyano-1,4-benzoquinone (DDQ), have an E° value of close to 1.0, which is usually used as an oxidant agent in chemosynthesis dehydrogenation reactions. Generally, 1,2 *o*-benzoquinone and *o*-naphthoquinone's E° values are higher than those of 1,4 *p*-benzoquinone and *p*-naphthoquinone. They are not commonly used because their unstable structures are hard to deal with.

Attention must be paid to ubiquinone, also known as coenzyme (CoQ), which is a liposoluble small molecule residing in the inner membrane of mitochondria, and the basic structure of tanshinone diterpenoids is a tricyclic system made of a naphthoquinone mother nucleus with a ring A, which could be either alicyclic or aromatic. Such a structure is more stable and its E° value is also lower than that of benzoquinone or naphthoquinone. It has been reported that the redox potential values of both *o*-phenanthrenequinone and *p*-phenanthrenequinone, both having a tricyclic system, are between 0.53 and 0.62 V. It is confirmed by experimentation that the dihydrofuran ring of cryptotanshinone could transform to tanshinone IIA through dehydrogenation by reaction with DDQ, and at the same

time, DDQ is hydrogenated to hydroquinone. All of these results show that although tanshinones belong to diterpene quinones, they do have rather large differences in properties. The following is the discussion of the antioxidation effect of tanshinone IIA.

8.4.1.1 The Influence of Tanshinone IIA on Free Radicals of Lipids

In heart and cerebral ischemia reperfusion experiments, the bioactivities of tanshinone IIA, especially the activities on the scavenging of oxygen free radicals, have attracted many biologists' attention. Generally speaking, electron spin resonance (ESR) cannot detect the free radicals due to their short life and low content, so spin entrapment technique must be used at first, in which we use an unsaturated diamagnetism substance, named spin label, to carry out an addition reaction, and then produce free radicals with a longer life, such as DMPO-OH. Finally, we observe the scavenging effect of tanshinone on hydroxide radicals ($\text{OH}\cdot$). The experiment showed that when the dose of tanshinone IIA is between 0.05 and 0.08 mg/ml, it has no scavenging effect on hydroxide radicals. Likewise, in xanthine/xanthine oxidase (X/XO) system, tanshinone IIA shows no scavenging effect on superoxide anions, when the chemoluminescence method was used for detection. However,

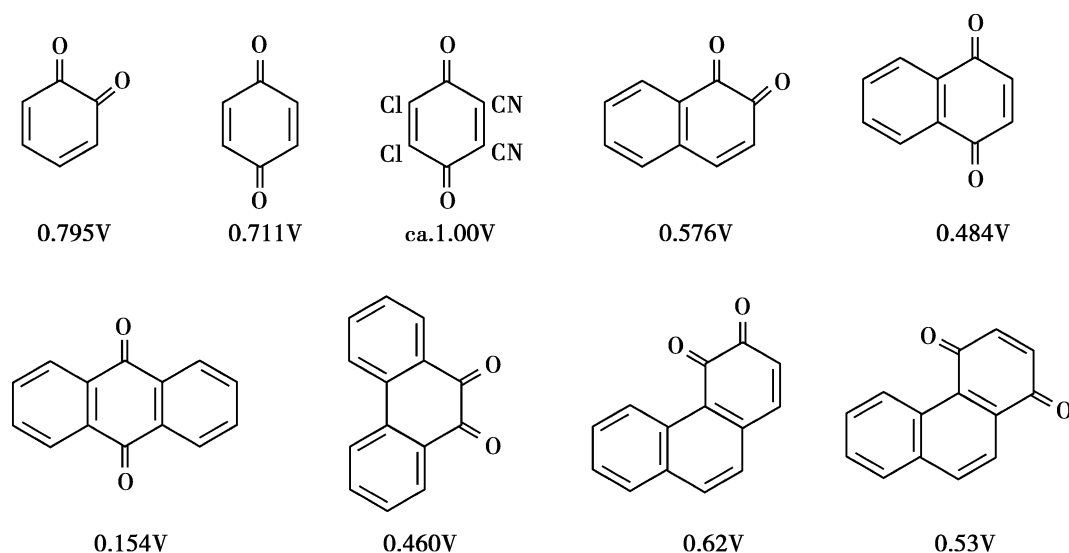


Fig. 8.20 The redox potential E° (V) of some common quinones

tanshinone IIA has a significant scavenging effect on lipid free radicals produced by the cardiac muscle sarcoplasmic reticulum lipid peroxidation reaction induced by (X/XO) system; the clearance rate with a dose of 40 mg is 72 %, and this effect is dose-dependent [59]. Furthermore, the following experiment showed that tanshinone IIA can remove lipid free radicals produced by Fe^{3+} , which induces the lipid peroxidation of the mitochondria membrane. When a dose of 0.8 mg/mg/Pr is given, the clearance rate is nearly 70 % [60]. From these two experiments, we can conclude that tanshinone IIA acts as a chain blocking agent to remove free radicals by inhibiting or breaking off oxidative chains rather than directly removing free radicals. In another experiment, it was found that tanshinone can inhibit the release of oxygen free radicals in human neutrophils. This test is about the inhibition effect on chemoluminescence of human neutrophils induced by phorbol. When the dose of tanshinone I is 5 ng, the inhibition ratio is 57.82 %, and when the dose of tanshinone I is 50 ng, the inhibition ratio is 83.28 %. It was also found that when the dose of tanshinone I is 5 ng/ml, respiratory explosion of human neutrophils induced by N-formyl-methionine-leucine-phenylalanine (fmLP) can be significantly inhibited [61].

8.4.1.2 The Relationship Between the Structure and Antioxidation Activity of Tanshinones

To observe the effect of tanshinones on lipidic free radicals more directly, researchers used diterpene quinones with different chemical structures to prevent the rancidity of fatty acids.

In 1990, Zhang Ke Qin [26] reported that seven quinone compounds isolated from Danshen had an antioxidation effect on lard; among them, dihydrotanshinone I had the highest antioxidant activity. After that, ten different quinone compounds were isolated from Danshen by Weng and Gordon [26]. They investigated their inhibition of the rancidity of lard, and the protectant coefficient P_F was used to describe their abilities of antioxidation. The definition of P_F value is as follows:

$$P_F = \frac{\text{lard} + \text{the duration of induced fat rancidity after given antioxidant}}{\text{the duration of fat rancidity induced by pure lard}}$$

Two known antioxidants, BHA and BHT, were used as a positive control. The results were as follows: the P_F values of dihydrotanshinone I, miltirone I and dehydro-miltirone were 5.5, 5.3 and 4.2, respectively; miltirone and cryptotanshinone were 6.4 and 3.5, respectively; the two known antioxidants, BHA and BHT, were 5.8 and 3.0, respectively.

In order to elucidate the mechanism of tanshinone's antioxidant activity, Weng and Gordon used an unsaturated fatty acid, methyl oleate, whose free radical could react with 9,10-phenanthrenedione. The spectral analysis of the resultant compounds proved the hypothesis proposed by Roberts and Caserio: the antioxidant effect of quinone can react with lipid free radicals $\text{R}\cdot$ to form stable free radicals, which are stabilized by electron delocalization both around the aromatic ring and onto an oxygen atom. Hence, this reaction interrupts the autooxidation chain reaction [26]. To further reveal the mechanism, Baoan et al. [27] compared the electronic structure of a typical tanshinone with that of known antioxidants of vitamin E by using the AM I method of quantum chemical calculation. They proposed the following two scales as the quantum chemical index for evaluating the relative antioxidation activity: complex radical stable energy (CRSE) and radical stable energy (RSE).

$$\begin{aligned} \text{Complex radical stable energy (CRSE)} \\ = E(\text{RH}) + E(\text{AH-R}\cdot) - E(\text{R}\cdot) - E(\text{AH-RH}) \end{aligned}$$

where RH = unsaturated fatty acid in olein; AH = antioxidant; $\text{AH-R}\cdot$ = free radical complex of AH and $\text{R}\cdot$; AH-RH = complex of AH and RH. $E(\text{RH})$, $E(\text{R}\cdot)$, $E(\text{AH-RH})$ and $E(\text{AH-R}\cdot)$ are the total energy of the system of RH, $\text{R}\cdot$, AH-RH and $\text{AH-R}\cdot$, respectively.

Apparently, the more negative CRES is, the more stable $\text{AH-R}\cdot$ and RH are, and the easier it is for $\text{R}\cdot$ to be transformed to $\text{AH-R}\cdot$ and then

scavenged, and accordingly, the stronger AH's antioxidation ability is. Using a control compound as vitamin E which was related to their O–H electron populations, frontier orbitals and decreased energy at the ending state. Although it has only one phenolic hydroxyl group, it has different electronic inductions of O–H due to the difference in the number and position of methyl groups. For example, the differences in the charge distribution and O–H electron populations are also responsible for the difference in the possibility of releasing hydrogen, so that the ability of releasing hydrogen becomes an index of antioxidation and of the ability to scavenge free radicals [62]. Baoan et al. [27] calculated the values of CRSE and RSE based on the addition of the compound butenoic acid to miltirone I, or miltirone and dehydromiltirone (see Fig. 8.21) instead of the addition of the compound of phenanthrenequinone and methyl oleate, as reported by Weng and Gordon [26].

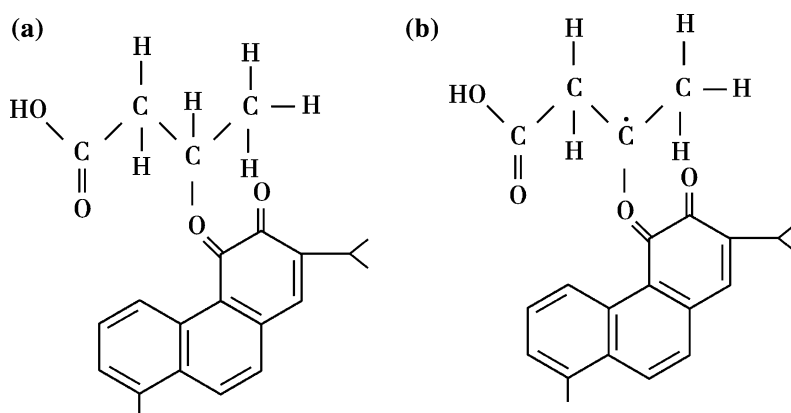
Since neither miltirone I, miltirone nor dehydromiltirone possess phenolic hydroxyl groups, it can only depend on the homolysis of the weakest C–H bond to produce an active H capable of combining with $R\cdot$. After analysis of the structure, the position of isopropyl C_{15} –H attached to ring C is the most suitable choice. Based on the analysis of all the experiments, we think that the reason tanshinone can act as an antioxidant (AH) is because it can react with the free radicals of lipid ($R\cdot$), producing a complex with a low CRSE value. Therefore, we propose that the mechanisms of antioxidative activities should be

classified according to their CRSE and RSE values: If only RES is prominent, then the antioxidants remove $R\cdot$ by supplying active hydrogens. For example, the antioxidation effects of some salvianolic acids in Danshen, such as rosmarinic acid and salvianolic acid B, are achieved by the release of active hydrogens. If only CRES is prominent, the antioxidants remove $R\cdot$ mainly by forming stable radical complexes. The antioxidative effects of many quinones belong to this type. When the values of CRSE and RSE are negative enough, two kinds of pathways to scavenge $R\cdot$ can be used, such as in dihydro-tanshinone-I.

8.4.1.3 Inhibiting the Oxidation of Low-density Lipoprotein by Tanshinones

Low-density lipoprotein (LDL) is composed of a fatty acid and a protein and is in charge of the delivery of cholesterol from the liver and small intestines to other organs. Too much LDL deposited on the endothelium leads to the generation of arteriosclerosis, where LDL is quickly oxidized to its oxidative product (ox-LDL), which causes inflammation and makes arteriosclerosis continuously worsen. LDL is often found in atherosclerotic plaques, so they are used as a marker of angio-sclerotic severity. Niu et al. [63] studied the effect of tanshinone IIA on the LDL oxidation process by oxygen free radicals generated in 4 different pathways: Cu^{2+} , free radicals of superoxide anion, free radicals of $OONO^-$, and oxygen free radicals released by

Fig. 8.21 The complex (a) and free radical complex (b) formed by the reaction between miltirone I and butenoic acid



respiratory explosion from excited macrophages. The experimental results showed that tanshinone IIA can protect LDL from oxidization in the above four different conditions. As an antioxidant, tanshinone IIA itself cannot remove superoxides or free radicals of OONO^- , nor can it react with Cu^{2+} as a chelate. According to the author's presumptions, inhibition of the oxidative process of LDL might be related to non-chemical bonding, combination of tanshinone IIA with LDL directly, thus changing its conformation. One of the pieces of evidence is that tanshinone IIA can increase the negative charges on the surface of LDL, which is reflected by the increase in relative mobility in agarose electrophoresis.

To sum up, the antioxidative activities of diterpene quinone are the reflection of various physicochemical characteristics. The potential of antioxidation depends on the structure of the quinone itself, which is influenced by solvents. In addition, the antioxidative activities of quinones are influenced by ring systems and conjugation systems.

8.4.2 The Chemical Stability of Tanshinones and the Influence of Solvents on Their Structures

Tanshinones are stable in their solid state. Their stabilities in solution depend on the solvents they are dissolved in. Generally speaking, any solvents which can produce free radicals under certain conditions, such as light, can transform tanshinones and produce free radicals. For example, dissolving tanshinones in hexane [10], halocarbon, or unsaturated fatty acids, such as butenoic acid, will cause them to form free radical adducts [27]. Experiments in our laboratory also showed that when tanshinones are dissolved in vegetable oil and exposed to light, they can transform to colorless products. All of these results are consistent with the above conclusion that tanshinones cannot scavenge hydroxyl and superoxide anion free radicals, but they can scavenge lipid free radicals produced by lipid

peroxidation reactions in tissue, such as cardiac muscle sarcoplasmic reticulum.

Tanshinones, including cryptotanshinone, tanshinone IIA, and tanshinone I, fluoresce in a certain range of acidity [64, 65]. The fluorescence is the strongest at a pH of 2–3. Fluorescence intensity is quenched in strong acids or strong bases, and the emission spectrum migrates to blue. At the same time, irreversible changes in the structures of tanshinones occur in strong base conditions. For example, tanshinone I has a strong fluorescent emission peak at 447 nm when radiated by 287 nm UV light in neutral solution. At pH 2–3, the fluorescent emission is stronger, and the position of the peak is the same. At pH < 1, the emission peak shifts to the blue region, and fluorescence intensity is quenched obviously. At pH > 11, the emission peak shifts from 447 to 413 nm and the fluorescence intensity shows an obvious decrease.

8.4.3 The Effects of Rings and Conjugation Systems on the Activity of Quinones

As mentioned above, the quinone structure in tanshinones is responsible for their biological activities. However, there are significant differences in the activities among tanshinones with different structures. For example, dihydrotanshinone-I and Przewaquinone B, both with an aromatic ring A, have great cytotoxic activities, and at the same time, dihydrotanshinone-I can induce apoptosis [66] and enhance X-ray sensitization in some tumor cells [67]. In contrast, tanshinone IIA, with an alicyclic ring A has no cytotoxic activities [68]. In addition, those tricyclic diterpenoid quinones without a furan ring are found possessing many bioactivities. For example, miltirone, in which ring A is alicyclic, can react with the benzodiazepines (Bzs) receptors of the brain. Investigating the SAR shows that ring A of miltirone is the key active center for combining with Bzs receptors, and without ring A, its activity would be reduced to 1/150 [69]. However, miltirone I, whose ring A is aromatic, can inhibit platelet aggregation induced by collagen

and ADP [8], and its antioxidation activity is the strongest among Danshen's diterpenoid quinones. Recently, research has also showed that tanshinone IIA can protect against brain injury induced by cerebral ischemia reperfusion in mice [70]. These results suggest that some diterpenoid quinones of Danshen have potential value for further development. To make these compounds function in vivo, an excellent preparation is needed; to develop an excellent preparation, the following problems need to be solved: solubility, oil–water distribution coefficient, and bioavailability.

8.4.3.1 Factors Affecting Solubility: A Molecular Structure Perspective

The solubilities of tanshinones with different structures differ significantly, and the differences are displayed in terms of the oil–water distribution or the hydrophobic/hydrophilic ratio. These useful parameters can be obtained by calculating the molecular field of tanshinones after geometry optimization to get the most desirable configuration. In order to confirm these parameters, different physicochemical properties of tanshinones can be displayed by some “chromatographic behaviors” directly, and some of the mechanisms of action can also be explained.

The Molecular Field and the Geometry Optimization of Tanshinones

In the classic force field of molecular mechanics, every atom in a molecule is thought to be connected to each other by an independent spring. It maintains natural values of bond length and bond angle. The potential energy in the molecular structure of tanshinones can be expressed by analytic functions. The function of molecular energy usually includes three parts: internal energy, external energy, and adsorptive restriction. Its mathematical description is as follows:

$$E = (E_{\text{bond}} + E_{\text{bend}} + E_{\text{torsion}} + E_{\text{inter}}) \\ + E_{\text{non bond}} + E_{\text{cons}}$$

The four items in parentheses are as follows: The first is the bond stretching energy; the second is the bond angle twisting energy; the third is the dihedral energy; and the fourth is the non-diagonal interaction. All of these four items belong to internal energy. The fifth item represents non-banded interactions, including Van der Waals (VDW) interaction and electrostatic interaction. These two items make up the external energy. The last item represents adsorptive restriction, which is added according to investigative requirements. Since tanshinones are small organic molecules, their molecular force fields include bond flexion, bond angle bending, torsion angle, bond angle crossover, and VDW. In Table 8.17, the calculated values of molecular fields and electrostatic fields of different tanshinones are listed.

The specific calculation is made by application of the Chemistry at HARvard Macromolecular Mechanics (CHARMM) force field, using Powell's method to optimize the geometric structures of Danshen's diterpene quinone molecules. When the value of the root-mean-square deviation of force field is higher than 0.001, it is considered convergence. All calculations were finished in the work station of IRIS-4D-25G [68]. Table 8.18 shows some relevant physicochemical parameters, including dipole moment, VDW and hydrophilic index, which is expressed by the hydrophilic/hydrophobic ratio.

The Hydrophilic/Hydrophobic Ratio

From the hydrophilic/hydrophobic ratios in Table 8.18, the values clearly reflect the hydrophilicity or hydrophobicity of different diterpenoids quinones in Danshen. This physicochemical parameter is very useful in the study, especially in the study of SARs. Hydrophilicity or hydrophobicity can reflect the number and the state of oxygen in diterpenoid quinones and also show the side chain connected to *o*-naphthoquinone. For example, miltirone I, miltirone, and dehydromiltirone do not have a furan ring, which is replaced by a hydrophobic isopropyl group on the C-2 of *o*-naphthoquinone, so their hydrophilic/hydrophobic ratios are 0.1634, 0.1515, and

Table 8.17 The molecular fields of tanshinones

Compounds	Bond energy	Bond angle	Dihedral	Improper	Lennard Jones	Static electricity
Tanshinone IIA	4.474	18.54	13.71	0.2673	11.47	3.398
TanshinoneI	4.133	19.09	12.59	0.0010	13.48	−2.244
Methyl tanshinonate	4.145	18.58	13.64	0.2263	11.50	11.93
Cryptotanshinone	4.181	11.90	11.12	0.6277	11.15	6.757
Dihydrotanshinone I	3.691	12.08	10.39	0.4206	13.05	−1.859
Methylene tanshinquinone	2.799	17.87	13.33	1.766	10.06	0.0038
Przewanone A	4.030	13.92	13.62	0.2742	11.28	2.716
Przewanone B	3.680	14.46	12.60	0.0161	13.33	−2.867
Danshenxinkun A	3.711	6.416	1.755	0.0293	17.83	−27.38
Danshenxinkun B	3.524	6.496	1.755	0.1636	17.71	−28.00
Hydroxyl dihydroisotanshinone	3.670	12.50	10.26	0.4072	12.63	−6.426
Tanshindiol B	3.215	19.57	14.43	0.1157	9.377	−27.66
Miltirone I	3.931	4.198	0.6870	0.0130	16.53	14.99
Miltirone	4.281	3.722	1.802	0.2863	16.53	14.99
Δ^1 -Miltirone	3.944	3.945	3.613	0.5481	13.57	21.26
1,2,15,16-Tetrahydrotanshinone	−2.43	11.36	13.61	1.094	9.944	5.890
Tanshinone-I 2-(N-pyrrolidine-alkyl)	4.686	24.44	25.43	0.3903	15.34	−26.01
Tanshinone12-(N-piperidine-alkyl)	4.934	24.97	13.25	0.116	15.05	−19.79
Tanshinlactone	4.590	17.66	12.59	0.0013	13.66	−19.06

Table 8.18 The Physicochemical parameters of tanshinones and related compounds [68]

Compounds	Dipole moment	VDW	Hydrophilic/hydrophobic	M _w	VDW/M _w
Tanshinone IIA	1.902	259.6237	79/401 = 0.1970	294	0.8830
Tanshinone IIB	1.973	248.2632	110/359 = 0.3064	310	0.8008
Cryptotanshinone	1.159	256.0939	79/405 = 0.1951	296	0.8652
TanshinoneI	0.7891	225.2109	80/377 = 0.2122	276	0.816
Dihydrotanshinone-I	0.8545	235.4458	80/378 = 0.2166	278	0.8469
Hydroxyl dihydroisotanshinone	0.8032	241.0502	80/385 = 0.2078	280	0.8608
Przewanone A	1.637	263.2448	122/370 = 0.3297	310	0.8492
Przewanone B	0.6408	234.6332	122/346 = 0.3526	292	0.8014
Danshenxinkun A	1.186	251.7714	144/365 = 0.3123	296	0.8506
Danshenxinkun B	1.482	248.8484	78/387 = 0.2016	280	0.8887
Miltirone I	2.314	237.4680	66/404 = 0.1634	264	0.8995
Miltirone	1.992	262.2918	65/429 = 0.1515	282	0.9294
Dehydro miltirone	2.333	252.3378	66/425 = 0.1533	280	0.9012
Methyl tanshinonate	2.810	283.5337	117/412 = 0.2840	338	0.8389
Methylene tanshinquinone	0.7697	236.8761	79/384 = 0.2057	278	0.8521
1,2,15,16-Tetrohydrotanshinone	1.716	243.2151	33/225 = 0.1467	294	0.8273

0.1533, respectively. On the other hand, in furan ring-containing compounds such as tanshinone IIA or tanshinone I, the number of oxygens is increased by the furan oxygen, and their hydrophilic/hydrophobic ratios are also increased to 0.1970 and 0.2122, suggesting that the hydrophilicity of tricyclic diterpenoids quinones is lower than that of tanshinone diterpenoid quinones. In tanshinones, tanshinone IIA is one dropheic methyl group less than tanshinone I, so the hydrophilicity of tanshinone I is slightly higher than that of tanshinone IIA. As for przewaquinone A and przewaquinone B, which have four oxygen atoms, because of a hydroxymethyl on the furan ring, their hydrophilic ratios rise to 0.3297 and 0.3526.

The hydrophilic/hydrophobic ratios can be tested by various chromatographies. Of course, the chromatographic behaviors depend not only on the hydrophilicity or hydrophobicity, but also on the local negative charges of atoms. For example, in tanshinone IIA and tanshinone I with *o*-naphthoquinone connecting with a furan ring, as well as all tanshinones with a furan ring, the local electric charge of the oxygen atom in the furan ring is -0.1693 . In contrast, all tanshinones with a dihydrofuran ring, such as cryptotanshinone, dihydrotanshinone I, and 1,2,15,16-tetrahydro-tanshinone, have a local negative charge of the dihydrofuran ring oxygen atom of about -0.2210 [68]. This single difference is sufficient to increase the hydrophilicity and polarity of these compounds. For example, it can influence whether *o*-naphthoquinone could form complex salts with chloride compounds. Such a property can reduce the R_f value (shows its polarity increased) in silica gel adsorption chromatography, or reduce the R_t value (shows its hydrophilicity increased) in reversed-phase column chromatography.

In view of the physicochemical parameters and the chromatographic behaviors, we can conclude that all of the diterpenoid quinones of Danshen are lipophilic hydrophobic compounds. So, it is impossible for them to be dissolved in water or water-based body and tissue fluids. Thus, the problem is how they could be absorbed

and utilized by organisms *in vivo*. Although there are so many reports showing that they possess many bioactivities in *in vitro* tests, such as tanshinone I significantly inhibiting the aggregation of platelets and miltirone reacting with benzodiazepines (Bzs) of the brain; however, in further *in vivo* studies, the results are almost never satisfactory. The reason for that is that the bioavailability *in vivo* is too low, and the concentration in target cells after reaching the tissues is too low to exert bioactivity.

Non-bonded Interactions

In order to fully understand the structural factors affecting the solubility of tanshinones, non-bonded interactions in molecular structure, also named inter-molecular forces, must be considered. The nature of such force is electrostatic interaction, which only plays a role when molecules are close to each other. Another non-bonded interaction is VDW. For instance, the calculated dihedral values of different tanshinones are based on the formula $\Delta = \alpha_1 - \alpha_2$; each tanshinone molecule has plane geometry configuration and delocalized π bonds, which show an increase in intermolecular force, see Table 8.19. Generally, they also easily form crystals with high melting points, except for $^1\Delta$ -dehydro-miltirone, whose melting point is only $71\text{--}75\text{ }^\circ\text{C}$ [14]. When ring A is aromatic, such as in tanshinone I which is a planar surface molecule, $\Delta = 0.06$, and in dihydrotanshinone I, $\Delta = 2.23$. In contrast, if ring A is alicyclic, such as in tanshinone IIA, $\Delta = 12.82$, and in cryptotanshinone, $\Delta = 13.19$. However, in tricyclic diterpenoid quinones without a furan or dihydrofuran ring, such as miltirone I (ring A is a benzene ring), $\Delta = 3.77$. If ring A is alicyclic, such as in miltirone, the value is 8.25.

The VDW of tanshinones with plane geometry configuration (induced dipole-induced dipole interaction) is also very significant. As planar surface molecules, tanshinone I and miltirone I, possess a π - π stacking effect, which can stack together in a face to face or side to face way. This effect can lead to low solubility, which is very obvious in nonpolar solvents such as benzene and

Table 8.19 The dihedral values of tanshinones between α_1 and α_2 planes [69]

Compounds	α_1	α_2	$\Delta = \alpha_1 - \alpha_2$
Tanshinone IIA	168.32	-178.86	12.82
Tanshinone IIB	168.58	177.41	8.83
Przewaquinone A	168.41	179.95	11.54
Methyltanshinone	168.35	179.04	10.69
Cryptotanshinone	169.03	-177.78	13.19
1,2,15,16-tetrahydrotanshinone	-166.02	-179.53	13.51
2-Hydroxy isodihydrotanshinonei	179.64	178.55	1.09
Tanshinonei	179.83	179.77	0.06
Przewaquinone B	176.90	-176.31	6.79
Dihydrotanshinone I	177.46	179.79	2.23
Methylene tanshinquinone	-162.96	-175.05	12.09
Miltirone I	178.39	174.62	3.77
Miltirone	168.25	176.50	8.25
Δ^1 -Dehydromiltirone	165.97	169.69	3.72
Danshenxinkun A	177.52	-0.54	3.02
Danshenxinkun B	-178.30	-4.15	5.85

cyclohexane. Tanshinone IIA or cryptotanshinone also have the same delocalized π bond and π - π stacking due to the existence of *o*-naphthoquinone in the whole structure. As ring A of tanshinone IIA is alicyclic, the effect of π - π stacking is lower than that of tanshinone I, and its solubility in nonpolar solvents such as benzene and cyclohexane is greater than that of tanshinone I.

The values of dipole moments of different tanshinones are influenced by the structure of ring A. Generally, when ring A is aromatic, such as in tanshinone I or dihydrotanshinone-I, their dipole moments are lower than those of compounds in which ring A is alicyclic, such as tanshinone IIA, because of the influence of electricity in benzene (see Table 8.17). One point needs to be emphasized: the crystals of tanshinones isolated from Danshen after purification are actually supermolecules, or supermolecules of crystalline state, formed by the construction of thousands of the same molecules through recognition and rearrangement. In order to exert their biological activity, they must overcome intermolecular forces and reassemble for a new type of

preparation. We emphasize the solubilities of tanshinones because they are very important to their preparations and bioavailability.

The next problem is of what means can be used to test the parameters calculated theoretically. In fact, solubility depends not only on hydrophobicity or hydrophilicity, but also on the local electric charge of compounds, dipole moments, and even molecular three-dimensional images.

8.4.3.2 A Variety of Chromatographic Techniques can Provide a Hydrophobic Index Value of the Different Structures of Tanshinones

Chromatography not only is a useful method to isolate compounds, but also can provide many valuable physicochemical parameters. Each compound's retention time in HPLC or R_f value in TLC can, to some extent, indicate its solubility in certain solvent systems, and it is possible to establish a relationship between the chemical structure and chromatographic behavior of different tanshinones.

Using Reverse HPLC to Obtain Hydrophobicity Data

According to the conditions recommended by *Chinese Pharmacopoeia* (Part I), C18 silica gel is used as the filler, MeOH-H₂O (15:5) as the mobile phase, and the detection wavelength is λ_{\max} 270 nm. 27 peaks are detected from crude extract of Danshen, of which there are four main peaks, and the retention time (R_t) values of dihydrotanshinone I, cryptotanshinone, tanshinone I, and tanshinone IIA are 15.30', 16.47', 20.47', and 25.67', respectively. Among the four compounds, tanshinone IIA and cryptotanshinone have an alicyclic ring A, and tanshinone I and dihydrotanshinone I have an aromatic one. In reversed-phase chromatography, the R_t value depends on the number of hydrophobic groups, for example, tanshinone IIA has one more methyl group than does tanshinone I, and cryptotanshinone has one more methyl group than does dihydrotanshinone I. Therefore, the R_t value of tanshinone IIA is larger than that of tanshinone I, and the R_t value of cryptotanshinone is larger than that of dihydrotanshinone I. The results are in accordance with the hydrophilic/hydrophobic ratio calculated by quantum chemistry. In addition, both cryptotanshinone and dihydrotanshinone I have the structure of *o*-naphthoquinone with a dihydrofuran ring. The partial electric charge of oxygen atoms in dihydrofuran rings is more negative than that of furan rings. In another word, the hydrophilicity of cryptotanshinone is higher than that of tanshinone IIA and the hydrophilicity of dihydrotanshinone I is higher than that of tanshinone I.

Using Partition Chromatography to Reflect Oil–Water Distribution of Different Tanshinones [71, 72]

Tanshinones are water-insoluble lipophilic compounds. Using silica gel as the carrier, N-dimethyl-formamide (DMF) as the stationary phase, and petroleum ether–benzene (8:2) as the mobile phase, partition chromatography results reflect the hydrophobicity of eight different tanshinones. They are arranged by their R_f value to show the degree of hydrophobicity: the R_f value of tanshinone IIA was 0.50, tanshinone I 0.36,

methylene tanshinquinone 0.35, methyl tanshinonate 0.20, cryptotanshinone 0.14, dihydrotanshinone I 0.14, tanshinone IIB 0.02, and tanshinone IIA sodium sulfonate 0. The results demonstrate that tanshinone IIA is the most lipophilic compound among them because its alicyclic ring A has a gem-dimethyl group. When a methyl of the gem-dimethyl is oxidized to become hydroxymethyl, such as in tanshinone IIB, or oxidated to form methyl tanshinonate, the R_f values of both compounds decrease. The R_f value of tanshinone IIA sodium sulfonate is zero because it is an ionic compound which is undissolvable in nonpolar solvents such as petroleum ether and benzene. In addition, both cryptotanshinone and dihydrotanshinone I have a dihydrofuran ring which is less lipophilic than the furan ring of tanshinone IIA and tanshinone I. There is a report showing that tanshinone IIA has no bacteriostasis against *Staphylococcus aureus*, mainly because of its oil–water distribution property. When using CHCl₃ as the solvent, tanshinone IIA could not enter the water-based medium [73]. However, if the solvent is changed to a hydrophilic one, for example, dissolving tanshinone IIA in DMF, so the compound can enter the medium, tanshinone IIA shows bacteriostasis against *S. aureus*.

Chromatography on Thin Film of Polyamide

The total liposoluble components of ethanol extract contain many tanshinones with different polarities. Actually, tanshinones with different structures have different solubilities in ethanol. This point can be demonstrated by letting tanshinones be absorbed to polyamide through hydrogen bonds, then eluting the absorbed tanshinones with ethanol of different concentrations. When developed by 95 % ethanol, the R_f values on thin film of polyamide are listed by their different structures: cryptotanshinone 0.84, tanshinone IIA and tanshinone IIB 0.70, methyl tanshinonate 0.65, dihydrotanshinone I 0.60, methylene tanshinquinone 0.45, and tanshinone I 0.20. Thereby, it is not difficult to see that hydrogen-bonding adsorption between tanshinones and polyamide is related to the number of delocalized π bonds. Comparing the structures of

cryptotanshinone, tanshinone II, methylene tanshinquinone, and tanshinone I, it is found that hydrogen-bonding adsorption is related to the structure of ring A. From alicyclic rings, methenyl groups to benzene rings, the adsorption of hydrogen bonding increases gradually. It is very interesting that the *in vitro* bacteriostasis activity of tanshinones against tuberculosis H₃₇RV could be interfered with by the existence of plasma proteins. The interference is related to the skeleton of ring A in tanshinones [71]. For instance, the minimal inhibitory concentrations of tanshinone IIA and tanshinone I are 0.31 and 0.5 µg/ml, respectively. When 5 % blood serum is dropped into P–B medium, the inhibitory concentrations decrease to 2.5 and 10.0 µg/ml, respectively. The results suggest that the interference of plasma proteins with aromatic ring A-containing tanshinone I is much larger than with alicyclic ring A-containing tanshinone IIA. It means that there are non-bonded interactions between tanshinone and plasma proteins.

8.4.3.3 Thermodynamic Comparison of Tanshinones

Huang et al. [74] studied the Thermodynamics of four typical tanshinone compounds, tanshinone IIA, cryptotanshinone, tanshinone I, and dihydrotanshinone I, in the process of raising the temperature by differential scanning calorimetry, which is a technique for measuring the power difference and temperature relationship between a sample and reference substance at program-controlled temperature. They used type DSC-2C differential scanning calorimetry with a 3,500 data station, manufactured by Perkin–Elmer Company. The heating rate was 10 K/min,

and the range was 20.92×10^{-8} J/s, full scale. In the process of mensuration, take a sample cell of aluminum as a reference charge with nitrogen for protection. Make the standardization of temperature and heat with high pure indium, tin, and lead (purity is 99.999 %) as the primary standard substance. DSC parameters of tanshinone compounds are listed in Table 8.20.

All four tanshinones mentioned above belong to 1,2-o-quinones, but they have the following differences: compounds with an aromatic ring A, such as tanshinone I and dihydrotanshinone I, are classified as group I. Compounds with an alicyclic ring A which is connected with a gem-dimethyl, such as tanshinone IIA and cryptotanshinone, are classified as group II. In addition, although there are some differences between ring A of tanshinone IIA and tanshinone I, both of them have the same furan ring (ring D), while dihydrotanshinone I and cryptotanshinone have the same dihydrofuran ring. In group I compounds, the number of double bonds in ring D of tanshinone I is more than that in dihydrotanshinone I, so it formed a large conjugated system. Similarly, the number of double bonds in ring D of tanshinone IIA is more than that in cryptotanshinone, so its conjugated chain is elongated. In the test of DSC, their melting points and heats of fusion are significantly different due to the difference in their structure. The melting points of compounds in which ring A is alicyclic are lower than in those with an aromatic ring A. However, their heats of fusion are in the opposite situation.

The melting point of tanshinone I, which possesses a delocalization of π electrons, is higher than that of tanshinone IIA, though the D ring in

Table 8.20 The DSC parameters of tanshinones (n = 3)

Compounds	Melting point (K)				Heat of fusion (J/g)				Entropy of fusion [J/(g·K)]
	Measured value		Average value		Measured value		Average value		
Tanshinone IIA	485.8	485.9	486.4	485.7	99.19	98.15	99.98	99.11	0.20
Cryptotanshinone	464.4	465.0	464.5	464.6	87.82	91.46	88.53	89.27	0.19
Tanshinone I	496.6	495.2	495.3	495.4	79.80	79.42	80.67	79.96	0.16
Dihydrotanshinone I	489.9	490.5	490.5	490.3	81.76	76.70	81.05	79.84	0.16

both of them is a furan ring. Similarly, with a dihydrofuran ring D, the melting point of dihydrotanshinone I is higher than that of cryptotanshinone. In the same group I, the melting point of tanshinone I, whose ring D is a furan ring, is higher than that of dihydrotanshinone I, whose ring D is a dihydrofuran ring. The melting point of tanshinone IIA is higher than that of cryptotanshinone. The order of the melting points is

tanshinone I > dihydrotanshinone I > tanshinone IIA > cryptotanshinone

This result suggested that intermolecular force is the key factor to the differences in melting points. The following data also showed that the delocalization of π electrons and intermolecular π - π stacking are the key factors for the melting point. The melting points of tanshinones in which ring A is aromatic are higher than those of tanshinone in which ring A is alicyclic (see Table 8.21).

In the testing the heats of fusion, we could find that the values of the heat of fusion of tanshinone IIA and cryptotanshinone in group II are higher than those of tanshinone I and dihydrotanshinone in group I. As for compounds in the same class, the heat of fusion of tanshinone IIA in which ring A is alicyclic is higher than that of cryptotanshinone. As for tanshinone I and dihydrotanshinone I, both have an aromatic ring, and their heat of fusion is similar. Tanshinones samples display absorption peaks of heat of fusion in DSC plots in the DSC instrument when the temperature is raised by heating, so the heat of fusion (ΔH_m) is defined as the melting point (T_m) at which the crystal transforms to liquid and the

corresponding thermal effect. Given that the system is in balance, we can calculate according to the Thermodynamic formula:

$$\Delta G_m = \Delta H_m - T\Delta S_m$$

We can calculate the values of ΔS_m of four compounds, respectively. In the formula, ΔG_m is free energy (ΔG_m is zero when the state is in balance); ΔH_m is heat of fusion; T_m is melting point; ΔS_m is entropy of fusion. It is very meaningful that the relationship between the structure of tanshinone and the value of entropy is very similar to the relationship between structure and heat of fusion mentioned above. In a word, the values of entropy of compounds with an alicyclic ring are higher than those of compounds with an aromatic ring. As for compounds in the same class, their values of entropy are similar (see Table 8.20).

The phenomenon of miltirone I having great biological activity in vitro, while its activities in vivo are unsatisfactory can be explained by the Thermodynamic determination and discussion of the key factors that influence melting points like intermolecular forces. The reason is because of the change of physicochemical properties induced by non-bonded interactions. Of course, research on the Thermodynamics of tanshinones provide a cue to develop new types of preparations of tanshinones, such as the crystal transform of tanshinones, the state diagram of binary system, and the complex relationship between tanshinone, which is an indissoluble drug, and the coprecipitate of water-soluble high polymers. Thermodynamic research can play its role as a supplementary way to the development of preparation

Table 8.21 The effect of different ring A on the melting point of diterpenoid quinones

Alicyclic ring A tanshinone II-type compounds	Melting point	Benzene ring A tanshinone I-type compounds	Melting point
Miltirone	98.7–99.8	Miltirone I	221–223
Przewaquinone A	173–175	Przewaquinone B	Decomposition at 242–243
Tanshinone IIA	209–210	Tanshinone I	233–234
Cryptotanshinone	191–192	Dihydrotanshinone I	224–225

8.5 The Biosynthetic Pathway of Tanshinone and Its Artifacts

In this section, we focus on the following three aspects: the formation of tanshinones in plants (the process of secondary metabolites), the relationships among tanshinones with different structures, and the influence of environmental conditions on the structures of tanshinones. For example, cryptotanshinone can be converted into tanshinone IIA. tanshinone IIA can be transformed into 1-hydroxytanshinone II by light and oxidation. The latter structural change is attributed to the environment, so we call it an artifact, which means that it does not belong to the original metabolites in plants.

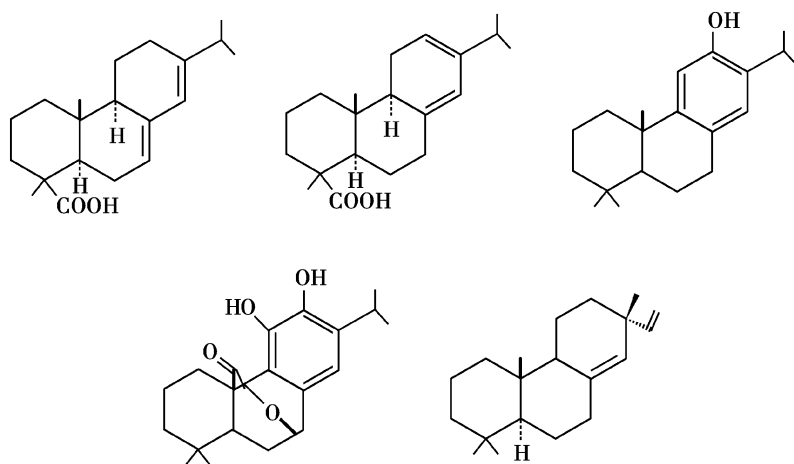
We discuss the original compounds of Danshen's diterpene quinones; in other words, we study how the known diterpenes with an abietane skeleton are transformed into tanshinones, catalyzed by a series of enzymes in a particular species, for example, Danshen (family of *Labiateae*, genus of *Salvia*). As far as we know at present, the types of diterpenes associated with the formation of tanshinones are limited to tricyclic diterpenes with an abietane skeleton, especially abietic acid, ferruginol and carnosol and some isopimaradine (Fig. 8.22). The following explains the process in which 16-hydroxycarnogeninic acid or isopimaradine is transformed into cryptotanshinone.

8.5.1 The Biosynthesis of Cryptotanshinone

In 1993, Luis et al. [75] reported their isolation of C-16 hydroxylated abietane diterpene compounds from *Salvia mellifera* Greene, a plant that grows in California in the United States. Among the isolated compounds are newly discovered 11,12,16-trihydroxyl-20-norabietane-5(10), 8,11,13-ene-1-one, as well as six compounds including 16-hydroxycarnogeninic acid and cryptotanshinone, which had been already identified. To elucidate the biogenetic relationship of these secondary metabolites, Luis et al. proposed that 16-hydroxycarnogeninic acid was transformed into cryptotanshinone through the following pathway (Fig. 8.23).

The key steps of the formation of cryptotanshinone are the demethylation, dehydrogenation, and aromatization of an alicyclic ring B. The demethylation and aromatization of ring B are achieved by the decarboxylation reaction after the hydroxylation on C-7 and the oxidation of the angular methyl group into a carboxylic acid on C-10. Then, the *o*-phenolic hydroxyl group in ring C is oxidized into *o*-quinone, and the electron on the hydroxyl oxygen on C-16 is rearranged to form a dihydrofuran ring. The formation of cryptotanshinone is then completed (Fig. 8.23). Interestingly, tanshinone IIA, the dehydrogenated product of cryptotanshinone, has

Fig. 8.22 The diterpenes associated with the formation of tanshinones



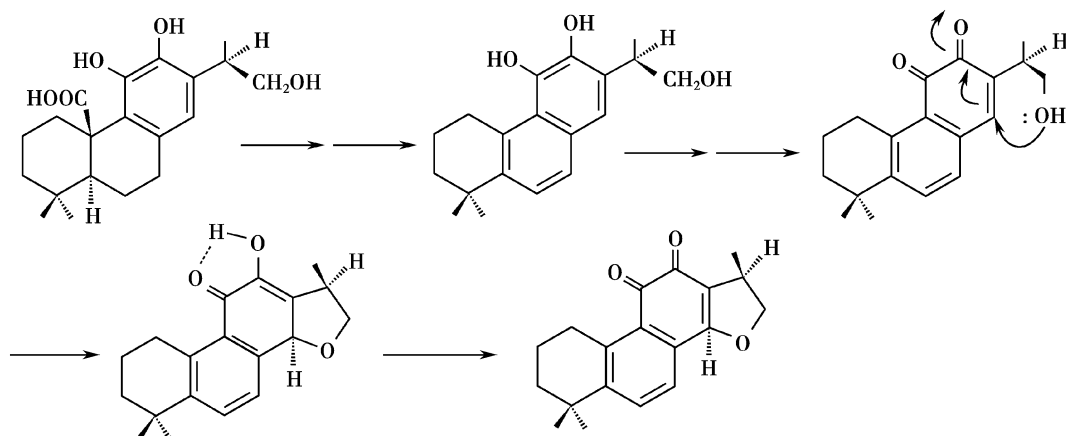


Fig. 8.23 One of the biogenetic pathways of cryptotanshinone

not been isolated from *S. mellifera* yet. Many studies showed that tanshinones, which are contained in *Salvia* in China, are seldom found in many species of *Salvia* in south Europe and northwest Asia, indicating that there is a great influence from geographic situations and species on the formation and accumulation of secondary metabolites. Another biogenetic pathway is described in Fig. 8.24.

This biogenetic pathway is related to the transformation of isopimaradine into cryptotanshinone. The characteristic of this process is that

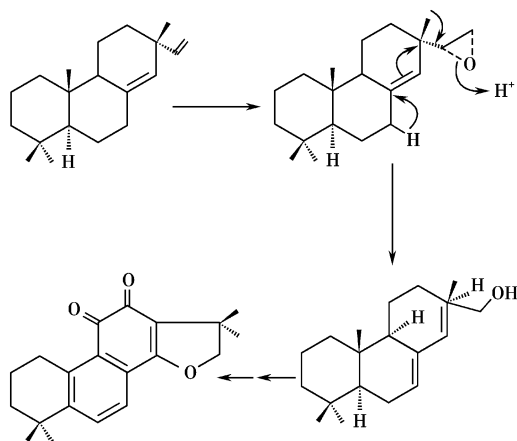


Fig. 8.24 Another biosynthetic pathway of cryptotanshinone

the methyl group at C-13 on ring C is transferred to the double bond of C-15, an abietane skeleton is formed by 1,2 methyl migration from C-13 to C-15 on the double bond, and at the same time, the ring is opened owing to the oxidation of the ethylenic bond, producing the crucial group, 16-hydroxyl. Then, the dihydrofuran ring is formed by the electron rearrangement of oxygen in the hydroxyl of C-16. Thus, cryptotanshinone is formed. Nakanish et al. [6] found that the high content of cryptotanshinone and ferruginol can only be produced in the culture solution of “cell line A” when he studied the tissue culture of Danshen. This was also confirmed in the six cell lines by Miyasaka et al. [76]. The high contents of cryptotanshinone and ferruginol can only be found in the culture solution of cell line A, while ferruginol can be found in other culture solutions of cell lines B–F. When the accumulation of ferruginol in the culture solution was investigated, it was found only in dark conditions, and culture solution without 2,4-auxin had a great benefit on the accumulation of ferruginol. In addition, the details and mechanism of the transformation of ferruginol into cryptotanshinone are worthy of further study and investigation, due to its complex conditions.

8.5.1.1 The Photooxidation Products of Tanshinone IIA (The Formation of Artifacts)

From the figures, we can see that there are a lot of uncertain details in the biosynthetic pathway of tanshinones. However, there is no doubt that abietane, a tricyclic diterpene, is the raw material of biosynthesis. We should distinguish between secondary metabolites and artifacts, because in the isolation process, some artifacts might be mistaken as secondary metabolites. For example, hydroxytanshinone IIA, which was isolated and identified from Danshen as a product in trace amounts, should be regarded as an artifact in light of the research on photooxidation mechanisms. The structure of tanshinone IIA itself is stable, but it also might be transformed to some colorless photooxidation products under some conditions. The most common phenomenon in the laboratory is that most tanshinones on TLC plates, especially samples on the surface of the plates, change their colors from the original orange red to colorless gradually if the plates are exposed to daylight.

Kusumi et al. found that if tanshinone IIA was dissolved in *n*-hexane, exposed to air, and irradiated by 450 W mercury lamp for 2 h, the color of this solution would fade from red, and it would give a white precipitate from which three artifacts (tanshinone IIA anhydride, lactone, and 1-hydroxytanshinone) were isolated by chromatography [10]. A possible mechanism of photooxidation of tanshinone II is outlined in Fig. 8.25.

The first product of the photoreaction of tanshinone IIA is an enolized tanshinone IIA. This product is further oxidized to form a peroxide intermediate of a peroxy ring between rings A and C. The peroxide intermediate is an important product, from which the above-mentioned 3 artifacts are transformed. The migration of the carbonyl group to an electron-deficient oxygen atom leads to the hydroxy tanshinone IIA anhydride, which leads to lactonic acid after molecular rearrangement. The cleavage of the peroxide

hemiacetal ring produces a hydroperoxide, which, after a Baeyer–Villiger reaction, leads to lactone and 1-hydroxy tanshinone IIA.

Lin et al. [77] synthesized tanshinone IIA anhydride and cryptotanshinone anhydride through Baeyer–Villiger reactions and tested their cytotoxicity in tumor cells Colo205, KB and Hep-2. They found that the cytotoxicities of all the anhydride derivatives were lower than those of their parent compounds, tanshinone-I and cryptotanshinone.

8.5.1.2 The Biogenesis of Danshen Lactone and Danshenspiroketallactone

When dealing with the mother liquor of tanshinone IIA, we found that there are some kinds of materials with blue fluorescence in the mother liquor, which are detectable on TLC. Through repeated-column chromatography, two trace amounts of colorless needle crystals were obtained, which were Danshenlactone and Danshenspiroketallactone. The structure of Danshenspiroketallactone was reported by Kong et al. [53] which was confirmed by X-ray, but there have been no reports about the biogenesis of these compounds. Both of them may be biogenetically produced from tanshinone I and dihydrotanshinone I in a manner as shown in Fig. 8.26. An oxidization pathway is necessary for tanshinone I to be transformed into Danshenlactone, and the key step should be the oxidative cleavage of ring C of tanshinone I, from which a decarboxylate is produced. Because of the rupture and shortening of the conjugated system, the absorption in the visible light area disappears and the compound becomes colorless. The cleavage of the furan ring leads to the formation of a di-ketone structure, and the carboxylic acid connected with the keto could form Danshenlactone after β -decarboxylation and other unknown reactions. Because Danshenlactone contains a fragment of coumarin structure, the product shows strong fluorescence.

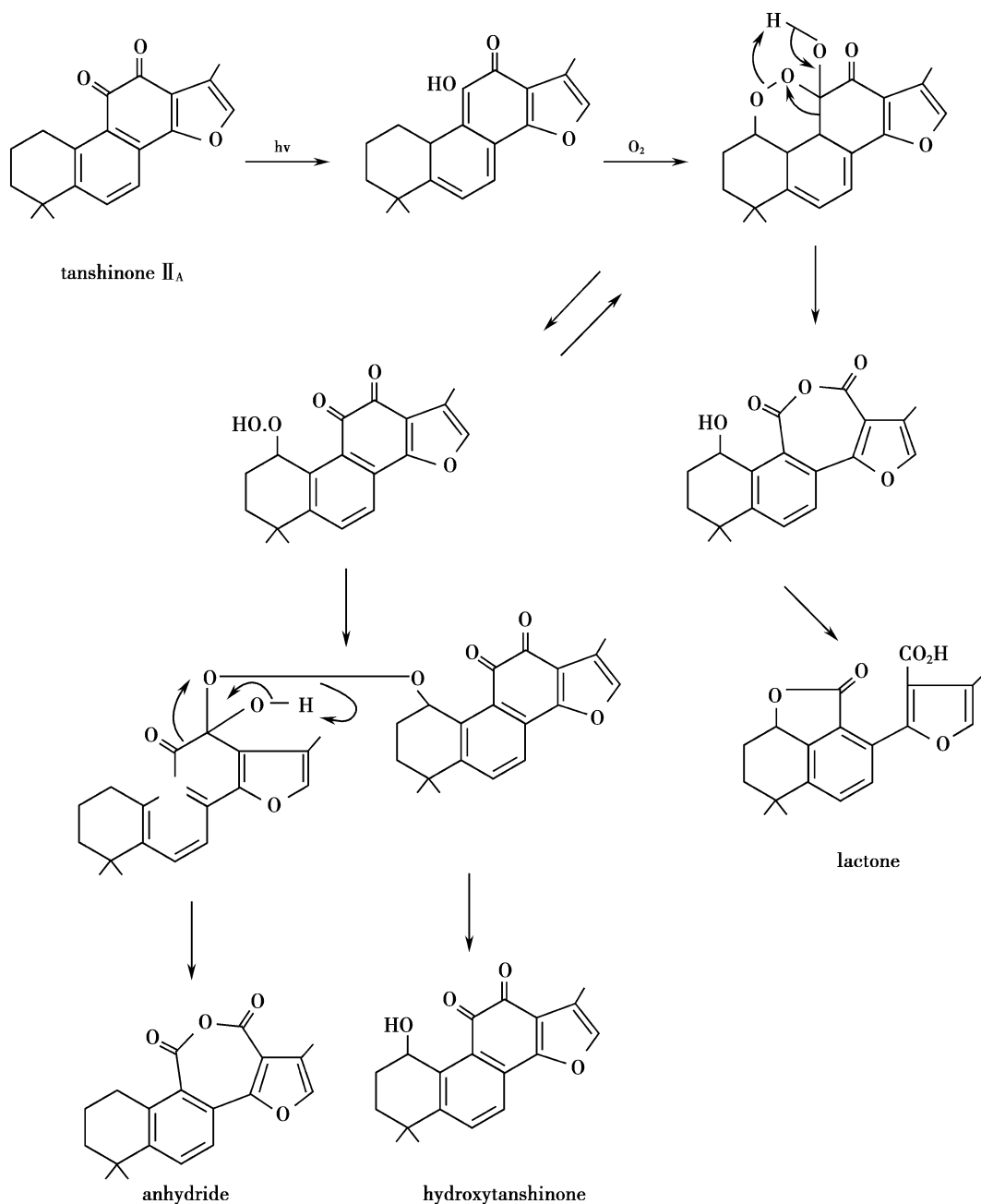


Fig. 8.25 The photooxidation products of tanshinone IIA

8.5.1.3 The Chemical Connection of Secondary Metabolites in Danshen

Among the 3 major tanshinones, tanshinone I can be regarded as a phenanthrenequinone structure

because of its aromatic ring A. However, viewed from the aspect of its biogenesis, tanshinone I is still considered to belong to the diterpenoid quinone compounds, because ring A in the diterpenoid ring system of Danshen's diterpene quinones must

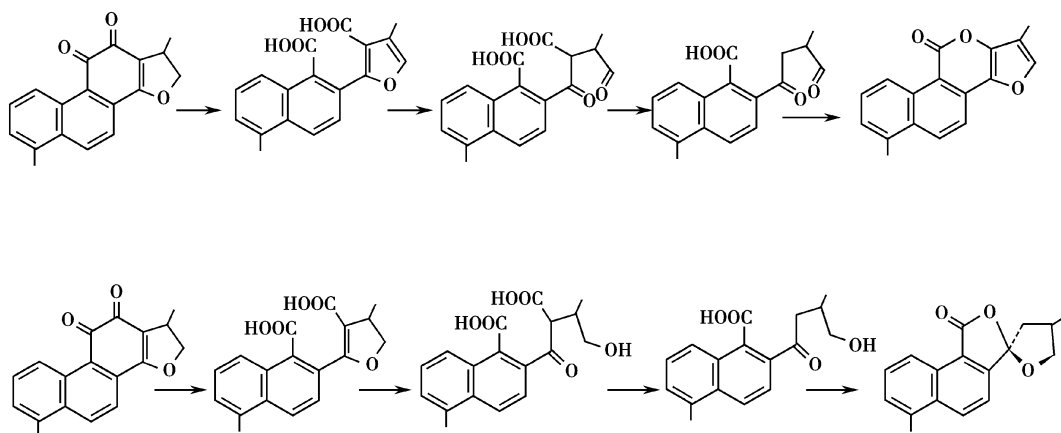


Fig. 8.26 Possible biogenetic pathways of Danshenlactone and Danshenspiroketallactone

be alicyclic, and as abietane's ring system, the ring A is connected with a gem-dimethyl group. So, tanshinone I can only be generated from tanshinone IIA through a series of dehydrogenation and demethylation on its ring A. For example, methylene tanshinquinone and 1,2-dihydrotanshinone I might be the intermediates during the transformation of tanshinone IIA to tanshinone I. Interestingly, the contents of tanshinone I and methylene tanshinquinone in some species like *S. honania* are 0.69 and 0.45 %, respectively, while the content of tanshinone I is only 0.35 %. Similarly, this relationship exists between 1, 2, 15, 16-tetrahydrotanshinone I and dihydrotanshinone I. Furthermore, through dehydrogenation of abietic acid, an abietane-type diterpene could produce 1-methyl-7-isopropyl-9,10-phenanthrene from which 1-methyl-7-isopropyl-9,10-phenanthrenequinone can be

formed by oxidation of KMnO_4 (Fig. 8.27). These results suggest that biogenetically, phenanthrenequinone may be formed by the oxidation of abietane-type diterpenes rather than existing independently.

8.5.1.4 The Formation Order of the Secondary Metabolites

A secondary metabolite should be understood as an active substance in a dynamic process in which the metabolism never stops. It is not difficult to estimate which constituents are major and which are minor components based upon their corresponding accumulated contents in plants. Such information can also shed light on the transformation among the components. Huang et al. [40, 41] investigated the active components in more than twenty varieties of *Salvia*

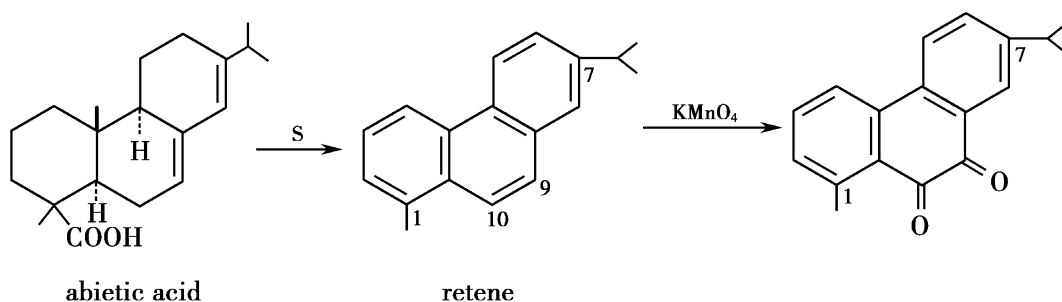


Fig. 8.27 The transformation of abietic acid into 9,10-*o*-quinone

plants in search for new sources of tanshinone IIA. Their results showed that tanshinone IIA is the main diterpenoid quinone in half of *Salvia* species. Particularly, the content of tanshinone IIA in Danshen from Sandong is 0.32 %, while the contents of hydroxyltanshinone II, methyltanshinone, and tanshindiol are 0.001, 0.001, and 0.0001 %, respectively. Because the contents of these components differ so much, it is not difficult to speculate that hydroxyltanshinone II must be the transformed product of tanshinone IIA through photooxidation reactions and that tanshindiol must be the transformed product of tanshinone IIB and 3-hydroxyltanshinone, also through oxidation. As another main constituent in Danshen, cryptotanshinone seems to be derived from 16-hydroxylcarnogeninic acid. The pathway is as follows: a dihydrofuran ring is formed through the electron rearrangement of oxygen in the C-16 hydroxyl after the oxidation and decarboxylation of 16-hydroxylcarnogeninic acid. Then, the ring C is oxidized and cryptotanshinone is formed. tanshinone IIA can be obtained through the dehydrogenation of the dihydrofuran ring in cryptotanshinone. Therefore, from the aspect of biogenesis, all of Danshen's diterpenoid quinones are originated from tricyclic diterpenes, especially abietane-type diterpenes. However, different tanshinones have different oxidation states which can be implied by the ratio of carbon, hydrogen and oxygen in its molecules, such as ferruginol $C_{20}H_{30}O$, cryptotanshinone $C_{19}H_{20}O_3$, tanshinone IIA $C_{19}H_{18}O_3$, methylene tanshinquinone $C_{19}H_{18}O_3$, tanshinone-I $C_{18}H_{12}O_3$, tanshinone IIB $C_{19}H_{18}O_4$, and tanshindiol $C_{18}H_{16}O_5$ (see Table 8.2). The molecular formulas also indicate the formation order of the secondary metabolites, i.e., from molecules with fewer oxygen atoms to ones with more oxygen atoms. Similarly, the ratios of carbon to hydrogen also reflect their oxidation state. For example, from tanshinone IIA to methylene tanshinquinone and to tanshinone I, their carbon-to-hydrogen ratios are not the same.

8.6 Chemical Synthesis of Tanshinones

8.6.1 Total Synthesis of Tanshinone IIA

The total synthesis of tanshinone IIA was reported as early as the 1960s. Ballie and Thomson [78] used 7-methoxyl-1-tetralone as the raw material and went through twelve reactions to get tanshinone IIA. Kakisawa et al. [79] used 2, 3, 4-trimethoxyl-benzoyl-propionic acid as raw material and completed the synthesis in 15 reactions. However, the raw materials used in both methods are hard to obtain, the procedures are too long, and some of the reactions give relatively low yields. Subsequently, Inouye et al. [80] accomplished a total synthesis by the method as follows.

8.6.2 Diene Addition of 3-methoxyl-benzofuran-4,7-diketone

Use 2-acetyl catechol as the starting material, and let the paraquinone intermediate, i.e., 3-methoxy-4,7-benzofurandione, react with 6,6-dimethyl-1-vinyl cyclohexene in a Diels–Alder reaction to form the cycloaddition product. Then, dehydrogenate ring B with alkali to get isotanshinone IIA. To transform isotanshinone IIA to tanshinone IIA, first, transform the furan ring of isotanshinone IIA to the dihydrofuran ring of Isocryptotanshinone by catalytic hydrogenation; second, open the dihydrofuran ring with KOH, then add H_2SO_4 to transform it to cryptotanshinone; finally, dehydrogenate the dihydrofuran ring in the presence of a certain amount of oxidant 2, 3-dichloro-4, 5-dicyanoquinone (DDQ) to get tanshinone IIA (see Fig. 8.28).

As shown in Fig. 8.28, to get furan ring-containing tanshinone IIA, isotanshinone IIA must be transformed further. Such transformations include catalytic hydrogenation, alkalifying ring opening, then acidifying to form the dihydrofuran ring and

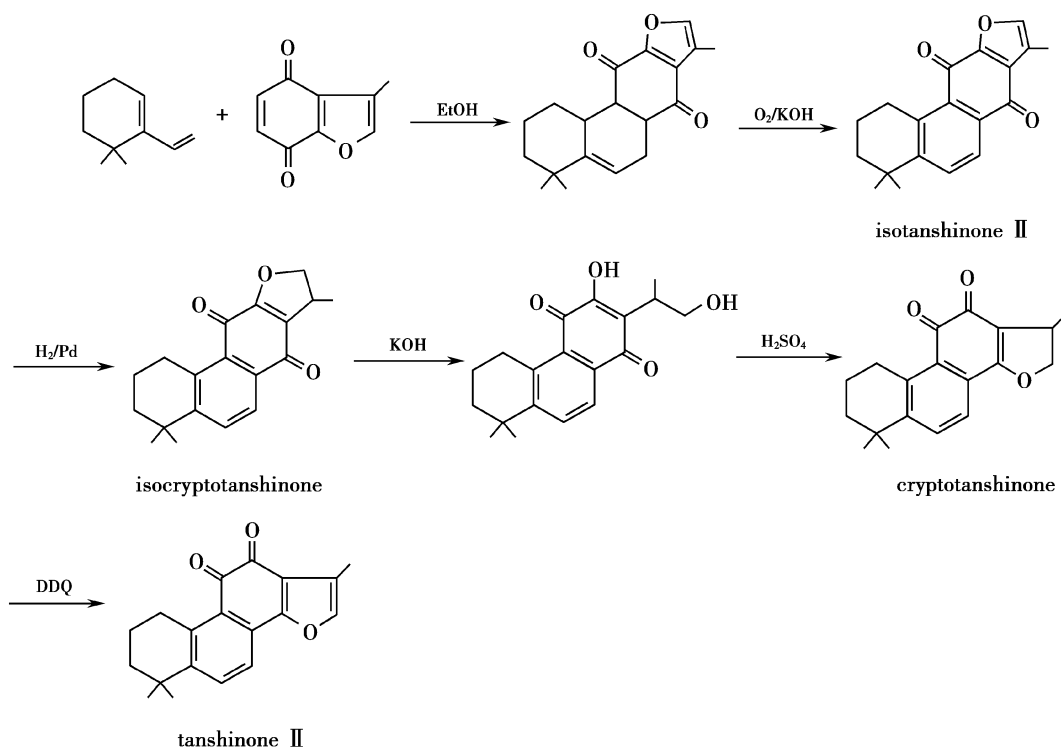


Fig. 8.28 Synthesis of tanshinone IIA: Diels–Alder reaction of 3-methoxy-benzofuran-4,7-diketone and 6,6-dimethyl-1-vinyl cyclohexene

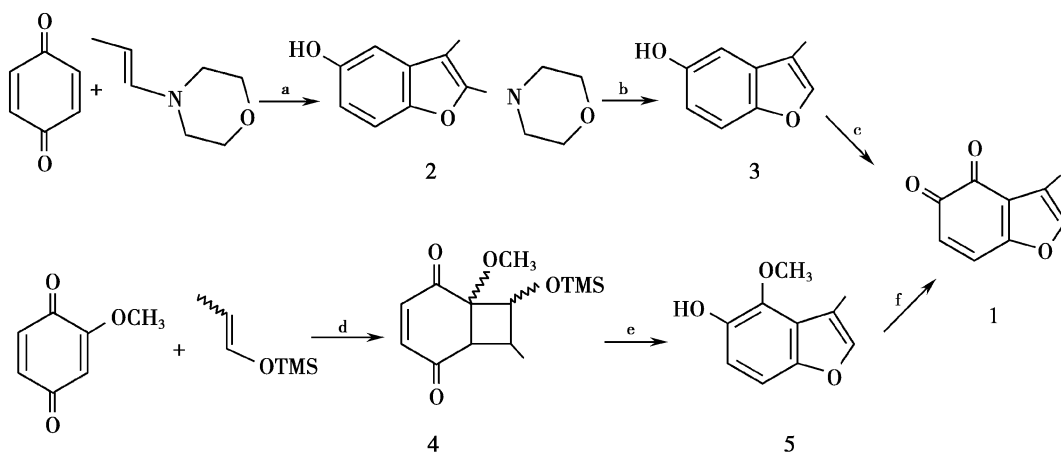


Fig. 8.29 Preparation of dienophile 3-methyl-4,5-benzofurandione (a) 0 °C, benzene, 94 %; (b) 5N HCl/THF, 99 %; (c) Fremy salt, 99 %; (d) Light, benzene, 66 %; (e) p-Ts OH, benzene refluxing, 99 %; (f) NaIO₄

dehydrogenation. The process was circuitous like “S”. At the same time period, Kakisawa et al. isolated three trace isotanshinone compounds

from Danshen, including isotanshinone IIA. It is very likely that the discovery helped the identification of the structure.

8.6.2.1 Diene Addition of 3-methyl-4,5-benzofurandione

To get tanshinone IIA from the product of diene addition in one reaction, dienophile 3-methyl-4,5-benzofurandione is needed. The first step is to prepare this intermediate. The starting material is *p*-benzoquinone, which is widely available. The reactions include Stork enamine condensation reaction, hydrolyzation, and oxidation [81] (see Fig. 8.29). The *o*-quinone (1) is a red solid, m.p. 92–93 °C, stable at room temperature either in the solid state or in ether or benzene solution. In halogenated hydrocarbons (CH_2Cl_2 , CHCl_3) or at elevated temperatures (100 °C), decomposition slowly occurs, though it is stable for 16 h at 80 °C under benzene reflux. Protonic acid can lead to its decomposition.

Table 8.22 lists the results obtained in the cycloadditions with various dienes. Cycloadditions by 3-methyl-4,5-benzofurandione and 6 different diene compounds confirmed that the method has some advantages, i.e., products with *o*-quinone structure can be obtained through one-step reactions, the reaction conditions are mild, generally using benzene as the solvent at low temperature, and the specific conditions are dependent on the diene used (see Table 8.22 for details). The problem of this reaction is that it produces isomerides in different proportions, which causes problems later. In light of this, to reduce the isomerides and improve the yield, ultrasonic catalyzed reaction technology [82] was introduced to the synthesis of tanshinone IIA, Nortanshinone and tanshindiol B. Take tanshinone IIA for example; let 6, 6-dimethyl-1-vinyl cyclohexene and 3-methyl-4,5-benzofurandione react in a Diels–Alder reaction in pure benzene, reflux, 12 h, giving a yield of 53 %. The ratio of tanshinone IIA and its isomeride was 54:45. In the same condition at 45 °C for 2 h, the reaction results of nortanshinone and tanshindiol B are listed in Table 8.22.

In China, Shen et al. [83] reported a similar synthesis method in 1988. The detailed reaction conditions are as follows. 200 mg of 6,6-dimethyl-1-vinyl cyclohexene is added to 50 ml of benzene solution containing 25 mg of 3-methyl-4,5-benzofurandione while stirring. Reflux for

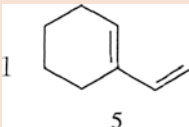
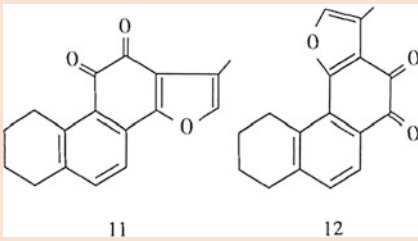
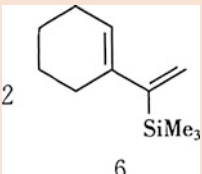
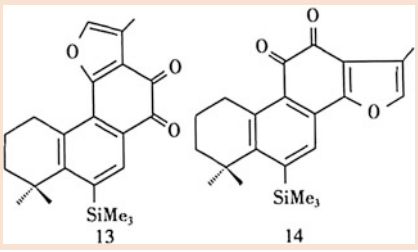
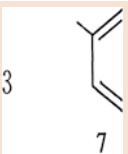
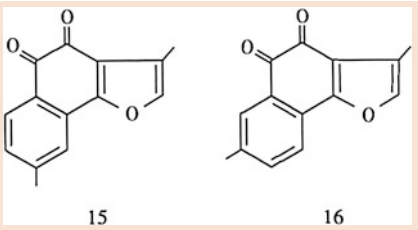
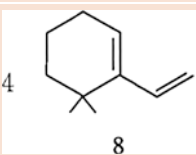
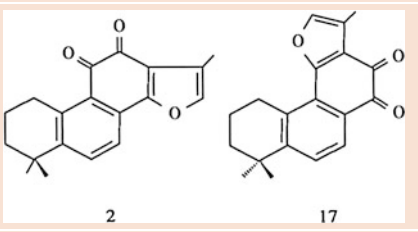
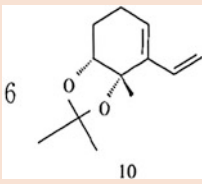
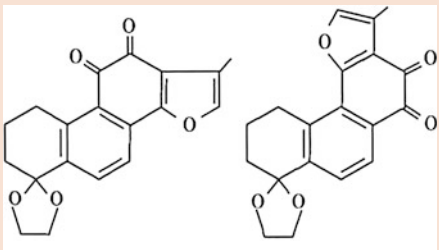
24 h, then add 40 mg of DDQ, and continue refluxing. Concentrate the reactant in vacuo. The residue is subjected to silica gel column chromatography, and tanshinone IIA is obtained by recrystallization in ethanol. The product is confirmed to be tanshinone IIA by IR spectroscopy.

8.6.3 Total Synthesis of Miltionone

The purpose of the total synthesis of miltirone in early years was to confirm the presumed structure. Nasipuri and Mitra [84] began with bromoanisole and obtained miltirone after 10-step reactions (see Fig. 8.30).

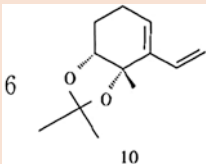
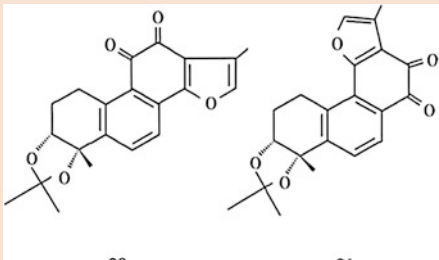
In 1985, Knapp and Sharm used 3-isopropylphthaldione as a dienophile to carry out a cycloaddition reaction with 6,6-dimethyl-1-vinyl cyclohexene and obtained a tricyclic diterpene quinone. They named it rosmariquingone, obviously because they did not know that the compound had been isolated and identified by Kakisawa in 1970 and named “miltirone.” Because of the instability of 3-isopropylphthaldione, the yield was very low, never exceeding 30 %. Lee et al. [85] synthesized miltirone by using ultrasound to catalyze the cycloaddition reaction. Because of the instability of 3-isopropylphthaldione, they used 3-isopropyl catechol as the starting material (see Table 8.31). The catechol was transformed to phthaldione by silver oxide through an ultrasonic in situ reaction at 24 °C for 3 h, and the yield was 93 %, far higher than the 53 % yield obtained without ultrasound. The detailed operating procedure was as follows: Mix 105 mg (0.7 mmol) of 3-isopropyl catechol, 1,200 mg (1.47 mmol) of 6,6-dimethyl-1-vinyl cyclohexene and, 788 mg (3.4 mmol) of Ag_2O , 1.5 ml of absolute alcohol; react at 24 °C catalyzed by ultrasound for 3 h. Detect the completion of the reaction by TLC (CH_2Cl_2 /pet. ether, 1:1). Filter the product, remove the solvent by vacuum distillation, purify by silica gel column, and obtain 184 mg of red crystal with m.p. 94–96 °C, HRMS (EI70 eV) m/z 282.1617 ($\text{MC}_{19}\text{H}_{22}\text{O}_{20}$), and the spectrum of the product is identical to the natural product (Fig. 8.31).

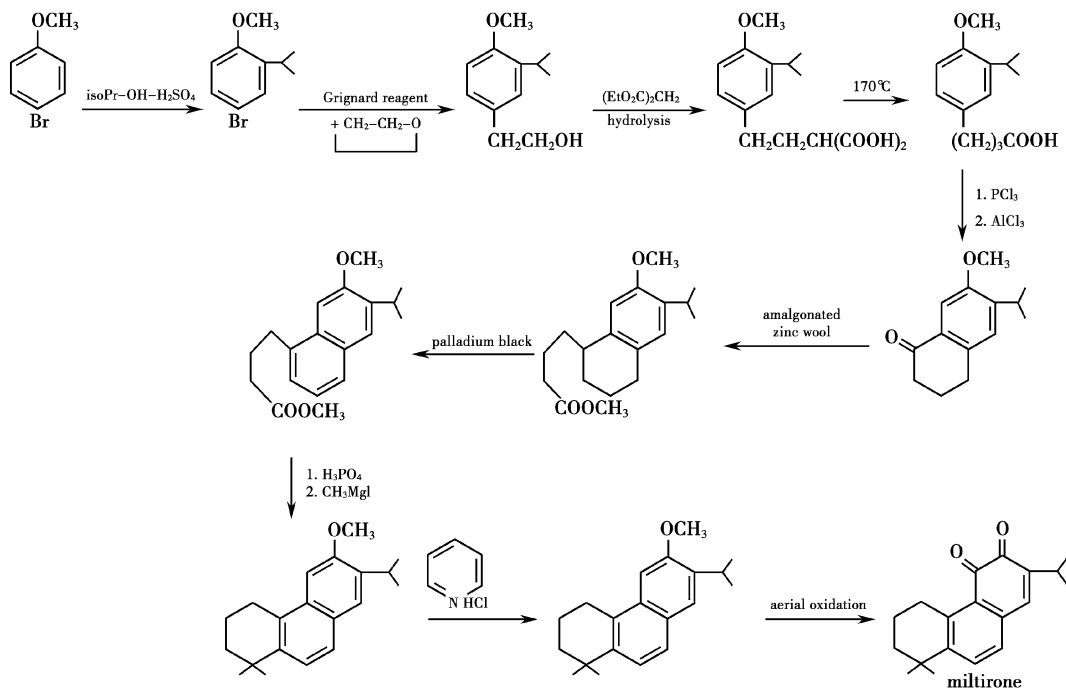
Table 8.22 Addition reactions by 3-methyl-4,5-benzofurandione and different diene compounds

Diene compounds	Reaction conditions	Products	Yield and ratio
1  5	a. benzene, refluxing, 12 h b. MeOH, refluxing, 2 h c. 11 kbar, benzene, room temperature, 2 h d. Eu[fod] ₃ 0.08 equiv, benzene, refluxing, 4 h e. ultrasonic extraction, 45 °C f. ultrasonic extraction, MeOH	 11 12	(11:12) a. 45 (2:1) b. 40 (2.5:1) c. 67 (6:1) d. 31 (10:1) e. 65 (7:2) f. 59 (4:1)
2  6	a. benzene, refluxing, 12 h b. MeOH, refluxing, 4 h c. 11 kbar, MeOH, room temperature, 2 h d. ultrasonic extraction, 45 °C	 13 14	(13:14) a. 18 (3.5:1) b. 28 (3:2) c. 61 (3.5:1) d. 57 (5:1)
3  7	a. benzene, refluxing, 4 h b. ultrasonic extraction, MeOH	 15 16	(15:16) a. 15 (1:1) b. 38 (5:4)
4  8	a. benzene, refluxing, 12 h b. ultrasonic extraction, 45 °C	 2 17	(2:17) a. 53 (54:46) b. 76 (10:3)
6  10	a. benzene, refluxing, 8 h b. 10 kbar, methyl benzene, room temperature, 45 min c. ultrasonic extraction, 45 °C d. ultrasonic extraction, methyl benzene, room temperature, 1 h	 18 19	(18:19) a. 18 (1:1) b. 75 (5:2) c. 65 (8:1) d. 17 (4:3)

(continued)

Table 8.22 (continued)

Diene compounds	Reaction conditions	Products	Yield and ratio
 6	a. benzene, refluxing 8 h b. 10 kbar, methyl benzene, room temperature, 1 h c. ultrasonic extraction, 45 °C	 20 21	(20:21) a. 15 (1:1) b. 73 (7:1) c. 76 (5:1)

**Fig. 8.30** Total synthesis of miltirone

8.6.4 Structural Modification of Tanshinone IIA

Because tanshinone IIA is insoluble in water, it is difficult for it to exert its physiological activity. Qian et al. made a tanshinone IIA derivative, its sodium sulfonate salt, which is a water-soluble compound. The results of pharmacological

testing showed that it could slightly increase rat's heart contractile force in situ. Clinical application of the salt showed that it could alleviate angina pectoris and chest tightness. It also could improve the abnormal electrocardiogram up to 54.7 %. However, the duration of the curative effect was short and the excretion speed was too fast. To find a better water-soluble tanshinone

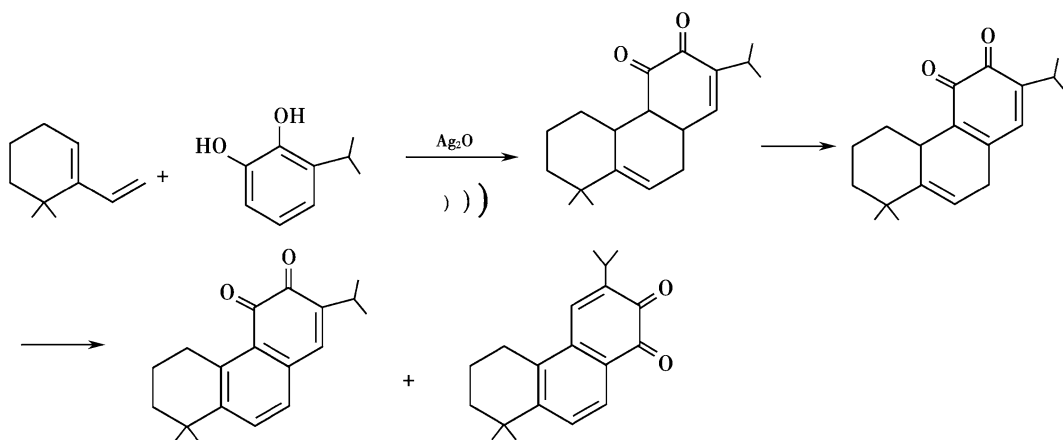


Fig. 8.31 Total synthesis of miltirone began with 3-isopropyl catechol catalyzed by ultrasound

derivative, Sun et al. synthesized Mannich bases of tanshinone I and tanshinone IIA (IX–X) as follows.

8.6.4.1 Synthesis Compound IX

Briefly speaking, compound IX, 4,5-dihydro-2-(diethylamino) methyl-3,9-dimethyl-4,5-diketonephenanthrene[1,2b]furan, is a derivative of tanshinone I whose α -H on the furan ring is displaced by a diethylamino Mannich base. Procedure in detail: dissolve 286 mg of tanshinone I, 160 mg of diethylamine hydrochloride, 45 mg of paraformaldehyde in 5 ml of acetic acid, reflux for 4 h, remove the solvent in vacuum, add the proper amount water, and filter. Alkalize the reddish brown filtrate with 2 N NaOH, then filter, collect the reddish brown solid, wash with water, dry, and obtain 100 mg of product. Recrystallize in tetrahydrofuran and wash with ethanol. The crystal's melting point is 171–173 °C (decompose).

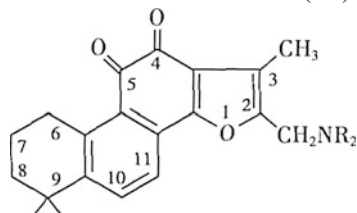
8.6.4.2 Synthesis of 4,5,6,7,8,9-hexahydro-2-(N-pyrrolidinyl)-methyl-3,9-dimethyl-phenanthrene[1, 2b]furan(X a)

Use tanshinone IIA as the starting material and displace its α -H on the furan ring with different NR_2 to get Mannich bases. The following example uses N-pyrrolidinyl. Add 30 g of tanshinone IIA to a cold solution containing 120 ml of acetic acid, 1.56 g of pyrrolidine, and 1.8 g of

36 % formaldehyde. Mix well and incubate in a water bath for 1 h, and heat to 125 °C for 9 h. Add 150 ml of water to dilute the reaction, add 7 g of sodium carbonate to neutralize the solution, filter, wash the precipitate, and dry to get 4 g of product. The product is then purified by column chromatography and recrystallization in acetic ether. Melting point is 160–161 °C. The other Mannich bases of tanshinone IIA are prepared by similar methods; the structures and physical constants are listed in Table 8.23.

8.6.5 Structural Modification of Tanshinone I

The cytotoxicity tests of dihydrotanshinone I, tanshinone IIA, and cryptotanshinone showed that those compounds with an aromatic ring A had higher cytotoxicity than those with an alicyclic ring A [68, 86]. The results also showed that many bioactivities of dihydrotanshinone I were much higher than in tanshinone I. The dihedral angle of the two oxygen atoms in ring C of tanshinone I is nearly 180°, which suggests that the two oxygen atoms were on the same plane. The Mannich bases formed by tanshinone I and different heterocyclic amines not only have different bioactivities, but also different physicochemical parameters. For example, 2-(N-pyrrolidine-alkyl)-tanshinone I, 2-(N-piperidine-alkyl)-tanshinone I, and tanshinone I have

Table 8.23 H-NMR spectrum data for Mannich bases of tanshinone IIA X (a–e)

Compound	NR ₂	MP °C	H-NMR (CDCl ₃ or CCl ₄)						
			C _{7,8} H		C ₃ –CH ₃	C ₆ H	CH ₂ N	C _{10,11} H	NR ₂
Xa		160–160°	1.26 (s)	1.64–1.78 (m) 4H	2.2(s)	3.16 (t) 2H	3.6(s)	7.48(s) 2H	1.64–1.78(m) 4H C _{3,4} H 2.54(m)4H C _{2,5} H
Xb		228–229°	1.34 (s)	1.70(m) 4H	2.24(s)	3.14 (t) 2H	3.56 (s)	7.50(dd)	2.54(m) 4H C _{2,6} H 3.70(m) 4H C _{3,5} H
Xc		229–230°	1.28 (s)	1.48–1.68 (m) 4H	2.18(s)	3.02 (t) 2H	3.38 (s)	7.25–7.4 (dd)2H	1.48–1.68(m) 4HC _{3,4,5} H 2.30–2.49(m) 4H C _{2,6} H
Xd	N(CH ₃) ₂	214–215°	1.20 (s)	1.60(m) 4H	2.12(s)	3.02 (t) 2H	3.28 (s)	7.32(s)	2.12(s)6H N(CH ₃) ₂
Xe		197–198°	1.28 (s)	1.58–1.72 (m) 4H	2.23(s)	3.12 (t) 2H	3.54 (s)	7.48–7.58 (dd)2H	2.30–2.52(m) 8HC _{2,5,3,6} H 2.20(s)3H N-CH ₃

different cytotoxicities (IC₅₀) to P-388 cells: 2.6, 18 and 89 $\mu\text{mol/L}$, respectively. Their dipole moments are 1.646, 0.6323, and 0.7891, respectively. The dihedral angles of the two oxygen atoms in C ring in the three compounds are 14.83, 4.78 and 0.06, respectively [68]. These data indicate that different heterocyclic amines can change not only the solubility and bioactivities of tanshinone I, but in fact also the 3 dimensional structures, as indicated by the dipole moments and the dihedral angles. In addition, we have used some amino acids, such as glycine, aspartic acid, and proline, to make Mannich base derivatives of tanshinone I or tanshinone IIA. The structures of these derivatives are shown in Figs. 8.32 and 8.33.

8.6.5.1 Synthesis of N-4,5-dihydro-3,9-dimethyl-4,5-diketonephenanthrene [1,2b] Furan Sodium Glycinate (A8)

Prepare glycine hydrochloride, mix 100 mg (0.36×10^{-3} mol) of tanshinone I, 30 μl (0.37×10^{-3} mol) of 37 % formaldehyde, 160 mg (1.43×10^{-3} mol) of glycine hydrochloride, and 10 ml of glacial acetic acid in a 50 ml three-necked bottle. Incubate at 60 °C with stirring. Monitor the process of the reaction with TLC. Stop the reaction when it reaches equilibrium, normally in 12 h. Remove the solvent in vacuum, and wash the solid with water until a pH of 7 is reached. The solid is dissolved in Na₂CO₃ solution, pH 8. Remove the insoluble substances by

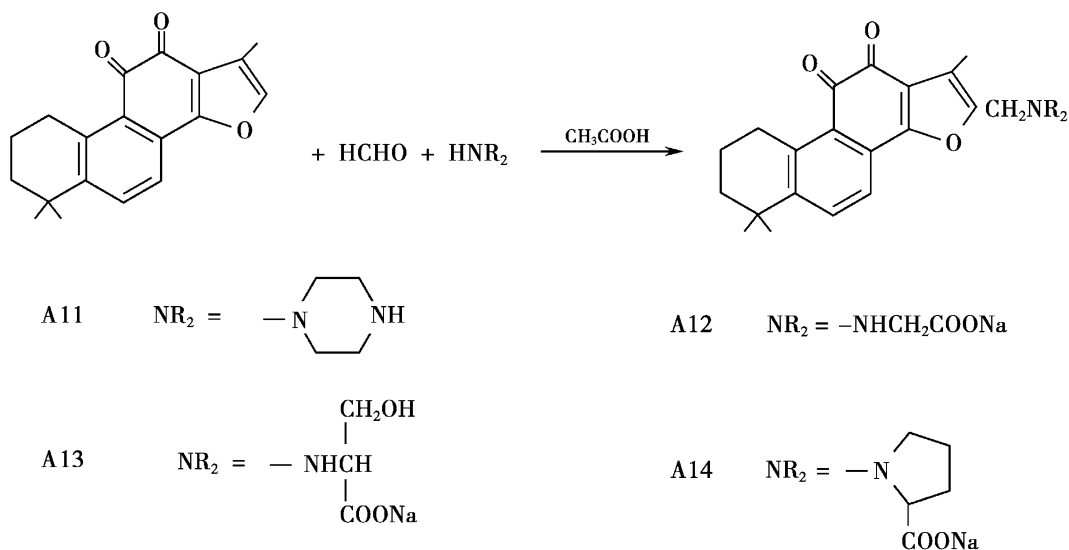
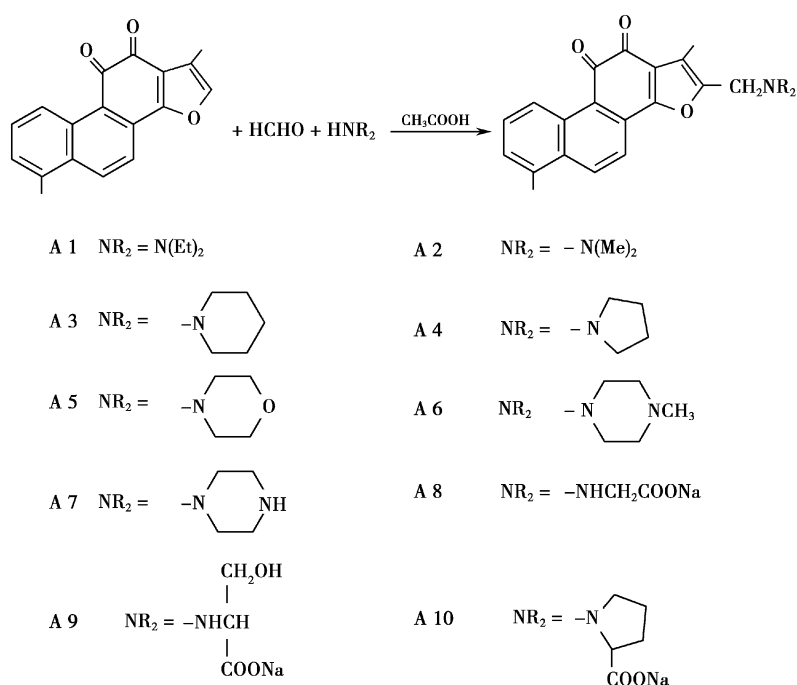


Fig. 8.32 Structure of tanshinone IIA's Mannich bases

Fig. 8.33 Structures of tanshinone I's Mannich bases



filtration, then concentrate the solution and run the sample on a Sephadex LH-20 column. Collect the main fraction, remove the solvent in vacuum, obtaining 60 mg of red powder (A8), m.p. 276–280 °C (decomposed). The product is

dissolvable in water. Mannich bases such as aspartic acid-tanshinone I (A9) and proline-tanshinone I (A10) are also prepared in the same way and the physical constants and spectrum data are listed in Table 8.24.

Table 8.24 Physicochemical constants of tanshinone I’s Mannich bases A1-A10

Compounds	Molecular formula	Mp °C	MS m/z	¹ H-NMR(CDCl ₃ or CD ₃ OD)
A1	C ₂₃ H ₂₃ NO ₃	170–172	361(M)	9.22(1H, d), 7.52(1H, q) 7.32(1H, d), 8.24(1H, d), 7.98(1H, d), 2.26(3H, S), 2.66(3H, S), 3.71(2H, s), 2.63(4H, q), 1.18(6H, t)
A2	C ₂₁ H ₁₉ NO ₃	169–171	333(M)	9.21(1H, d), 7.52(1H, q) 7.32(1H, d), 8.23(1H, d), 7.82(1H, d), 2.27(3H, s), 2.66(3H, s), 3.57(2H, s), 2.38(6H, s)
A3	C ₂₄ H ₂₃ NO ₃	200–201	373(M)	9.17(1H, d), 7.50(1H, q) 7.30(1H, d), 8.21(1H, d), 7.79(1H, d), 2.25(3H, S), 2.61(3H, S), 3.70(2H, s), 2.52(4H, m), 1.64(4H, m), 1.45(2H, m)
A4	C ₂₃ H ₂₁ NO ₃	156–158	359(M)	9.21(1H, d), 7.51(1H, q) 7.31(1H, d), 8.23(1H, d), 7.82(1H, d), 2.27(3H, S), 2.66(3H, S), 3.73(2H, s), 2.69(4H, m), 1.86(4H, m)
A5	C ₂₃ H ₂₁ NO ₄	210–212	375(M)	9.20(1H, d), 7.50(1H, q) 7.30(1H, d), 8.25(1H, d), 7.82(1H, d), 2.24(3H, S), 2.54(3H, s), 3.58(2H, S), 2.24(4H, m), 3.72(4H, m)
A6	C ₂₄ H ₂₄ NO ₃	196–198	388(M)	9.20(1H, S), 7.50(1H, t) 7.30(1H, d), 8.20(1H, d), 7.77(1H, d) 2.25(3H, S), 2.64(3H, S), 3.64(2H, S), 2.57(8H, m), 2.34(3H, S)
A7	C ₂₂ H ₂₂ N ₂ O ₃	177–178	374(M)	9.08(1H, d), 7.39(1H, q) 7.24(1H, d), 8.25(1H, d), 7.71(1H, d), 2.12(3H, S), 2.55(3H, S), 3.61(2H, s), 2.64(4H, m), 3.07(4H, t)
A8	C ₂₁ H ₁₆ NO ₅ Na	276–280	386(M + Na) 402(M + K)	9.05(1H, d), 7.36(1H, t) 7.21(1H, d), 8.25(1H, d), 7.77(1H, d), 2.09(3H, s), 2.52(3H, s), 3.69(2H, s), 3.06(2H, s)
A9	C ₂₂ H ₁₈ NO ₆ Na	238–240	400(M + Na) 416(M + K)	9.60(1H, d), 8.23(1H, d) 7.86(1H, d), 2.35(3H, S), 2.5 l(3H, S), 4.21(2H, q), 4.42(2H, m) 3.98(1H, m)
A10	C ₂₄ H ₂₀ NO ₅ Na	219–221	426(M + Na) 442(M + K)	9.59(1H, d), 7.50(1H, q) 7.26(1H, d), 8.19(1H, d), 7.88(1H, d), 2.49(3H, s), 2.49(3H, s), 2.40(3H, s), 4.09(2H, q), 3.58(1H, t), 3.24(1H, m), 2.61(1H, q) 2.22(2H, m), 1.88(1H, m), 1.71(1H, m)

8.7 Triterpenoids of Danshen

The Tibetan folk drug “Hong Qin Jiao” is the dried roots of *S. Przewalskii* Maxim, which is widely distributed in the western areas of China. It has been reported that its main chemical components are the *o*-naphthaquinone diterpenes, as well as some novel tritepenoids. In another *Salvia* plant, *S. paramiltiorrhiza* Li et Huang, triterpenoids as well as diterpenoids are the main chemical constituents. However, only a few triterpenoids have been isolated from plants of this genus *Salvia*. From *S. triluga* Diels, some triterpenoids have been isolated. In this section, we describe the isolation and elucidation of

przewanoic acid A and przewanoic acid B from *S. Przewalskii*, 2 α ,3 β -24-trihydroxyurs-12-en-28-oic acid and some other known triterpenoids from *S. paramiltiorrhiza*, and euscaphic acid from *S. triluga*.

8.7.1 Isolation and Identification of Przewanoic Acid A and B [87]

Extract 10 kg of dry roots of *S. przewalskii* three times with hot 95 % ethanol. Evaporate the solvent. Run the extract (203 g) on a silica gel column, and elute successively with gradient solution of cyclohexane-CH₂Cl₂-EtOAc. Three triterpenoid compounds are eluted when CH₂Cl₂-

EtOAc ratio reaches 3:1. The yields are 25 mg of oleanolic acid, 10 mg of przewanoic acid A, and 42 mg of przewanoic acid B. When heated, all 3 compounds can react with 5 % phosphomolybdic acid on TLC to form blue black spots, and the R_f values of these triterpenoids are 0.54, 0.80 and 0.62, respectively, which show that their polarities are similar to that of tanshinone IIB, but far are lower than that of tanshindiol (see Table 8.2).

8.7.1.1 Przewanoic Acid A (1)

Colorless needle crystal, m.p. 269–270 °C, $[\alpha]_D^{25} +125^\circ$ (MeOH, c 0.08). HRMS: $M^+ m/z$ 470.3485, $C_{30}H_{46}O_4$. UV λ_{MeOH} nm(log ϵ): 211(3.65), IR ν_{KBr} 3,584, 3,384, 1,695 cm^{-1} . 1H -NMR (400 MHz, pyridine- d_5): δ 5.82(1H, dd, $J = 7.2, 3.6$ Hz), δ 4.29(1H, ddd, $J = 10.7, 4.0, 2.6$ Hz), δ 3.77(1H, d, $J = 2.6$ Hz), δ 0.86, 0.93, 0.94, 1.04, 1.13, 1.20 (s, 3H, six methyl groups). The signal at high-field δ –0.08(dd, 1H, $J = 4.8, 4.8$ Hz) is characteristic of the CH_2 in a cyclopropane. EI-MS (70 eV) m/z (rel.int.): 470 $[M]^+$ (82.8), 455 $[M-CH_3]$ (7.5), 452 $[M-H_2O]$ (90.9), 425 $[M-COOH]$ (7.7). ^{13}C -NMR is shown in Table 8.25.

8.7.1.2 Przewanoic Acid B (2)

Colorless needle crystal, m.p. 258–259 °C, $[\alpha]_D^{25} +103^\circ$ (MeOH; c 0.465). HRMS: $M^+ m/z$ 454.3381, $C_{29}H_{42}O_4$. UV λ_{MeOH} nm(log ϵ): 210(3.65). IR ν_{KBr} 3,426, 1,694, 1,650, 905 cm^{-1} . 1H -NMR (400 MHz, $CDCl_3$): δ 5.58(1H, dd, $J = 7.4, 4.0$ Hz), δ 5.06(1H, s), δ 4.73(s, 1H), δ –0.08(1H, dd, $J = 4.8, 4.8$ Hz). EIMS(70 eV) m/z (rel.int.): 454 $[M]^+$ (29.1), 439 $[M-CH_3]$ (5.1), 436 $[M-H_2O]$ (34.8), 409 $[M-COOH]$ (4.5). ^{13}C -NMR is shown in Table 8.25.

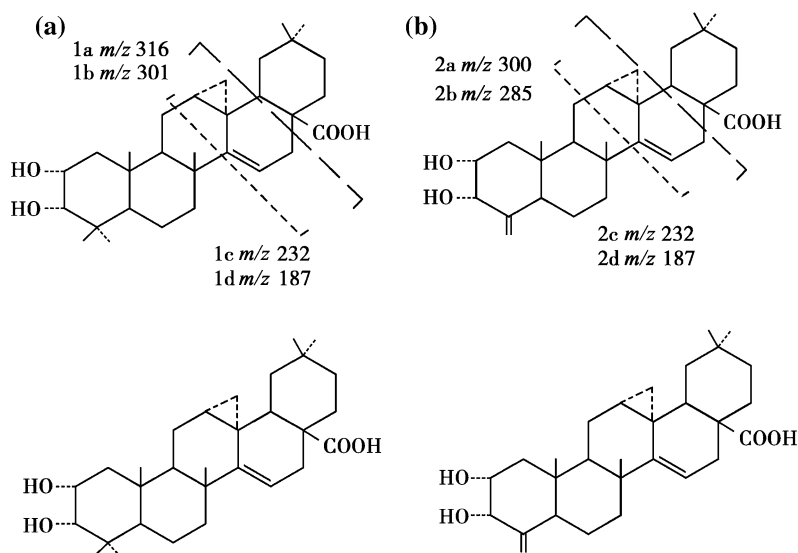
Both przewanoic acid A and przewanoic acid B belong to taraxerene type triterpenes. The common ground between them is the cyclopropane formed on C-12, 13 of ring C, and the main difference between the two is the group attached on ring A: in przewanoic acid A, there is a gem-dimethyl at C-4, while in przewanoic acid B, the gem-dimethyl is replaced by a methylene. The structures are confirmed by fragmentation in mass spectrometry.

The fragment peaks of 2a m/z 300.2062 ($C_{20}H_{28}O_2$) and 2b 285.1848($C_{19}H_{25}O_2$, 2a- CH_3) of przewanoic acid B come from RDA cleavage of ring D, and their mass numbers are

Table 8.25 Data of ^{13}C -NMR spectrum for przewanoic acid A and przewanoic acid B

C	Przewanoic acid A	Przewanoic acid B	C	Przewanoic acid A	Przewanoic acid B
1	42.8t	42.3t	16	31.1t	30.6t
2	66.2d	69.2d	17	52.8s	52.8s
3	79.2d	75.5d	18	34.9d	34.5d
4	38.7s	150.2s	19	38.9t	35.4t
5	48.7d	45.1d	20	29.0s	28.8s
6	19.5t	20.4t	21	34.3t	33.8t
7	35.7t	36.7t	22	31.1t	32.3t
8	38.7s	37.9s	23	29.5q	111.3t
9	48.0d	44.9d	24	17.5q	–
10	37.5s	37.2s	25	17.5q	14.5q
11	18.5t	20.1t	26	22.2q	29.3q
12	14.9d	14.6d	27	11.5t	11.3t
13	23.8s	23.4s	28	179.9s	180.9s
14	156.6s	156.4s	29	32.6q	32.3q
15	118.3d	117.8d	30	22.8q	22.1q

Fig. 8.34 Structures and mass spectra of **a** przewanoic acid A and **b** przewanoic acid B



16 less than the fragment peaks of 1a and 1b, respectively. Fragment peak 2c m/z 232.1473 ($C_{15}H_{20}O_2$) and 2d 187.1462 ($C_{14}H_{19}$, 2c-COOH) come from the cleavage of ring C, which are the same as 1c, 1d (see Fig. 8.34).

8.7.2 Isolation and Identification of Trijuganoic and Euscaphic Acids [88]

Extract 10 kg of *S. trijuga* dry roots with 95 % ethanol. Concentrate the extract and then extract again with EtOAc- H_2O . Concentrate the EtOAc fraction to 0.6 kg, subject to silica gel column, and elute with gradient elution. The euscaphic acid and trijuganoic acid are collected in the methanol fraction.

Euscaphic acid is a colorless powder crystal, m.p. 270–271 °C, HRMS: M^+ , 488.3547, $C_{30}H_{48}O_5$. IR ν_{KBr} : 3,591 cm^{-1} shows a hydroxyl group, a strong and wide peak at 3,570–3,000 cm^{-1} indicates a carbonyl group or an ortho-dihydroxyl groups, an absorption of double bond at 1,464 cm^{-1} , and a carboxy-carbonyl at 1,686 cm^{-1} . 1H -NMR (400 MHz, CD_3OD) shows seven methyl groups: δ 1.35(3H, s), 1.19(3H, s), 0.99(6H, s), 0.93(3H, d, J = 8 Hz), 0.87(3H, s),

0.79(3H, s). ^{13}C -NMR: δ 30.0 q, 27.9 q, 25.7 q, 23.3q, 18.4q, 17.7q, and 17.4q, see Table 8.26.

In Table 8.26, δ 140.8 s and 130.2d suggest two ethylene carbons. RDA cleavage yields fragment a, m/z 264(9.5), and fragment b, m/z 224. The base peak m/z 146 is obtained from fragment a by sequentially removing HCOOH and C_4H_7OH . The 1H -NMR spectrum shows δ 3.93(1H, ddd, J = 2.6, 4.5, 13.3 Hz, -CHOH) and δ 3.31(1H, d, J = 2.6 Hz, -CHOH), which is a group of correlated peaks, while δ 3.93 correlates with δ 2.10(1H, dd, J = 4.5, 13.3 Hz, Ha-1) and δ 1.59(1H, t, J = 13.3 Hz, Hb-1), suggests a fragment of -CHOH-CHOH- CH_2 -, as well as H-28 δ 2.50(1H, s). The structure of the compound is thus established as 2 α ,3 α ,19 α -trihydroxy ursolic acid (euscaphic acid).

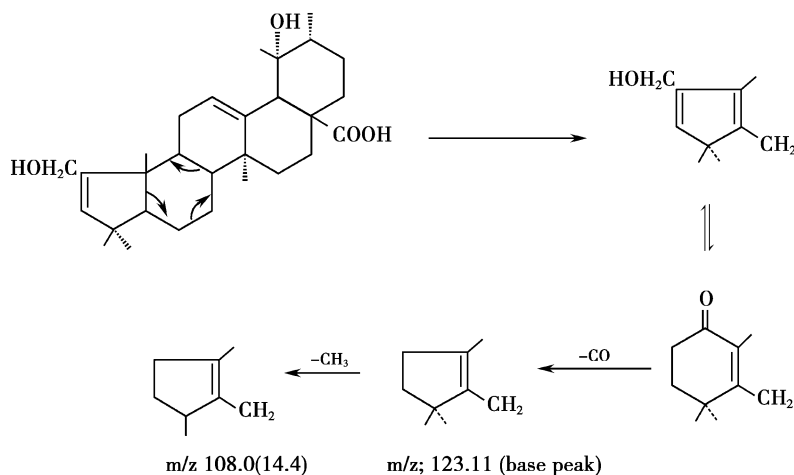
Trijuganoic acid is a colorless powder crystal, m.p. 268–270 °C, HRMS: M^+ , 470.3469, $C_{30}H_{46}O_4$. Comparing with the spectrum of euscaphic acid, something in common can be found. IR ν_{KBr} : 3,591 cm^{-1} , δ_C (74.3, s), δ_H 2.50 (1H, s, H-18) suggests a 19 α -hydroxyl group. EIMS m/z : 146(85) indicated the same C, D, E ring systems. H-NMR (400 MHz, CD_3OD): δ 1.35 (3H, s), 1.19(3H, s), 1.15(3H, s), 1.03(3H, s), 0.95(3H, s), 0.92(3H, d, J = 6.2 Hz), 0.83(3H, s). ^{13}C -NMR: δ 31.1q, 27.9q, 26.2q, 22.6q, 19.9q,

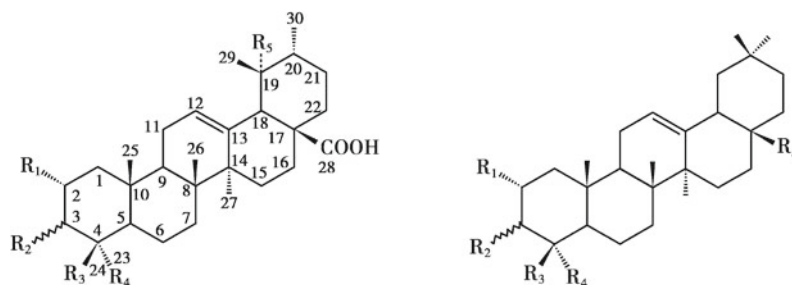
Table 8.26 ^{13}C -NMR spectrum data for trijuganoic and euscaphic acids

C	Trijuganoic acid	Euscaphic acid	C	Trijuganoic acid	Euscaphic acid
1	62.1t	43.3t	16	18.9t	27.4t
2	156.6s	68.0d	17	51.1s	49.8s
3	135.7d	80.9d	18	55.7d	55.9d
4	52.3s	42.1s	19	74.3s	74.4s
5	44.9d	50.1d	20	43.5d	43.9d
6	35.8t	20.1t	21	27.2t	30.4t
7	30.5t	34.9t	22	39.5t	39.8t
8	43.4s	40.2s	23	22.6q	30.0q
9	64.9d	49.0d	24	19.7q	18.4q
10	43.3s	40.2s	25	26.2q	17.7q
11	27.8t	25.5t	26	19.9q	17.4q
12	130.1d	130.2d	27	31.1q	27.9q
13	140.8s	140.8s	28	182.8s	183.1s
14	44.0s	43.5s	29	27.9q	23.3q
15	27.8t	28.1t	30	17.3q	25.7q

19.8q, 17.3q, indicating the existence of seven methyl groups, while two ethylene carbons at δ_c (140.8, s) and (130.1, d) provide evidence that trijuganoic acid is a $\Delta^{12,13}$ pentacyclic triterpene. The main differences between trijuganoic acid and euscaphic acid are the absorption of 1,463, 1,449 cm^{-1} in IR spectra, and ^1H -NMR δ_{H} 5.40 (1H, d, $J = 1.5$ Hz) and δ_c 156.6 s, 135.7, d, which suggest the existence of another double bond in the five-membered ring system because

of its higher tension. There is another group of peaks at δ_{H} 4.18 (1H, dd, $J = 1.5, 12.9$ Hz), δ_{H} 4.08 (1H, dd, $J = 1.5, 12.9$ Hz), δ_c (62.1, t). ^{13}C - ^1H COSY shows the peaks are related and also suggests the existence of a $-\text{CH}_2\text{OH}$ unit, which had long range coupling with an ethylene proton at δ_{H} 5.40, $J = 1.5$ Hz. The fact that the two units can only exist in ring A simultaneously can be demonstrated by the following fragmentation in mass spectrum (see Fig. 8.35).

Fig. 8.35 Structure and mass spectrum of trijuganoic acid



	R ₁	R ₂	R ₃	R ₄	R ₅		R ₁	R ₂	R ₃	R ₄	R ₅
1	OH	β-OH	CH ₂ OH	Me	H	8	H	β-OH	Me	Me	H
2	H	β-OAc	Me	Me	CHO	9	OH	β-OH	Me	Me	H
3	OH	α-OH	Me	Me	H	10	OH	α-OH	CH ₂ OH	Me	COOMe
4	OH	β-OH	Me	Me	H	11	OH	α-OH	Me	CH ₂ OH	COOMe
5	OH	α-OH	Me	Me	OH	12	OH	α-OH	Me	Me	H
6	OH	β-OH	Me	Me	OH	13	OH	β-OH	Me	CH ₂ OH	H
7	OH	α-OH	CH ₂ OH	Me	H	14	OH	β-OH	Me	Me	COOMe

Fig. 8.36 Triterpene acid from *S. paramiltiorrhiza*

8.7.3 Isolation and Identification of Triterpene Acid from *S. Paramiltiorrhiza*

S. paramiltiorrhiza is distributed mainly in Anhui, China. This plant contains little tanshinone, but contains many ursane triterpenes. Seven triterpenes have been isolated from this plant, of which compounds 1, 3, 4, 5, 6, and 7 are ursane type, and only compound 2 is oleanane type (see Fig. 8.36). Now we use compound 1 (2α, 3β-24-trihydroxyurs-12-en-28-oic acid) as an example to describe the process of isolation and identification.

Extract 10 kg of dry roots of *S. paramiltiorrhiza*, purchased from Shucheng, Anhui, with ethanol at room temperature for one week. Evaporate the solvent and obtain 400 g of black viscous paste. Run the sample on silica gel

column, and elute successively with petroleum ether-CHCl₃, CHCl₃-EtOAc, CHCl₃-methanol, methanol. Rerun the fractions eluted with CHCl₃-methanol on silica gel, elute with a gradient CHCl₃-methanol system (99:1–95:5). Collect the following compounds in order of elution: 2 (20 mg), 3 (80 mg), 5 (30 mg), 4 (15 mg), 6 (20 mg), 1 (20 mg), and 7 (25 mg).

Compound 1 was obtained as a colorless crystalline powder, m.p. 255–258 °C, [α]_D +53° (MeOH, c = 0.15). HRMS: M⁺ *m/z* 488.3464, C₃₀H₄₈O₅. ¹³C-NMR spectroscopy shows the presence of one tri-substituted double-bond (δ124.4, d) and (δ138.8, s), and one carboxylic acid group (δ178.2, s). The data and the degree of unsaturation indicate that compound 1 is a pentacyclic triterpene. ¹H-NMR spectroscopy shows the presence of two secondary methyl groups (δ0.80, d, J = 6.6 Hz) and (δ0.91, d, J = 6.4 Hz),

Table 8.27 C-NMR spectrum data of triterpenes from *S. paramiltiorrhiza*

C	1	3	4	5	6	7
1	47.0t	41.7t	49.1t	43.3t	46.9t	41.6t
2	67.0d	64.6d	70.4d	68.0d	67.1d	64.6d
3	83.8d	77.8d	85.3d	80.9d	82.3d	72.5d
4	41.6s	38.4s	41.3s	42.1s	41.3s	41.9s
5	55.3d	47.5d	57.5d	50.1d	54.8d	48.2d
6	18.8t	17.5t	20.3t	20.1t	18.1t	17.9t
7	33.0t	32.6t	35.0t	34.9t	32.6t	33.0t
8	38.9s	39.2s	41.7s	40.2s	38.9s	38.9s
9	46.8d	46.9d	49.9d	49.0d	46.8d	46.8d
10	37.4s	38.3s	40.0s	40.2s	37.5s	37.5s
11	23.1t	22.8t	25.3t	25.5t	23.2t	23.0t
12	124.4d	124.5d	127.5d	130.2d	126.7d	124.5d
13	138.2s	138.2s	140.6s	140.8s	138.6s	138.1s
14	43.0s	41.7s	44.1s	43.5s	46.7s	43.7s
15	27.5t	27.4t	30.0t	28.1t	27.4t	27.4t
16	23.8t	23.7t	26.1t	27.4t	23.8t	23.8t
17	47.2 s	46.7s	49.1s	49.8s	46.8s	47.0s
18	52.3d	52.3d	55.2d	55.9d	53.1d	52.3d
19	38.5d	37.9d	41.2d	74.7s	71.6s	38.4d
20	38.4d	37.7d	41.2d	43.9d	41.1d	38.4d
21	30.1t	30.1t	32.6t	30.4t	28.0t	30.2t
22	36.3t	36.2t	38.9t	39.8t	37.6t	36.3t
23	23.4q	28.8q	30.2q	30.0q	28.8q	22.8q
24	21.8t	21.8q	18.6q	25.7q	17.0q	63.7t
25	16.1q	16.1q	18.3q	17.4q	16.6q	16.5q
26	16.8q	16.8q	18.4q	17.7q	16.9q	16.7q
27	23.3q	23.3q	24.9q	27.9q	23.9q	23.3q
28	178.2s	178.2s	182.4s	183.1s	178.8s	178.2s
29	16.9q	16.9q	18.0q	23.3q	23.2q	16.9q
30	21.0q	21.0q	22.4q	18.4q	16.3q	21.0q

four tertiary methyl groups (δ 0.71, 0.91, 1.02, and 1.07), one hydroxymethyl group (δ 3.26, 1H, d, $J = 10.9$ Hz), (δ 3.72, 1 H, d, $J = 10.9$ Hz) one olefinic proton (δ 5.13, 1 H, t, $J = 2.9$ Hz) and one allylic proton (δ 2.10, 1 H, d, $J = 11.2$ Hz). In the H–H COSY spectrum, the crosspeaks between an olefinic proton (δ 5.13) and allylic methylene protons (δ 1.87, 2H, m), which was also correlated with a proton in (δ 1.48, 1H, m) between two quarternary carbons, suggest the presence of the following partial structure $-\text{CH}-\text{CH}_2-\text{CH}=\text{C}-$.

These data indicate that compound 1 is an urs-12-en type triterpene. The ^{13}C -NMR spectra of compound 1, methyl ursolate (8), and 2 α -hydroxyursolate (9) are quite similar to each other except for the difference in the δ -values and the multiplicities of the signals due to C-2 and C-24 (or C-23) (1; δ 67.0, d), and 63.9(t), 8; the δ (δ 27.3, t) and (δ 15.5, q), and 9; (δ 68.9, d) and (δ 17.0, q). These data also suggest that compound 1 has oxygen- containing functional groups at the positions C-2, C-24 (or C-23), and C-3. This is

further supported by the mass fragment ion peaks at m/z 248 ($C_{16}H_{24}O_2$) and 239 ($C_{14}H_{24}O_3-H$) caused by the retro Diels–Alder (RDA) fragmentation. The coupling patterns of the H-2 and H-3 signals in 1H -NMR of **1** (δ_{H-2} 3.55, 1H, m, $W_{1/2} = 24$ Hz) and $\delta_{H-3} = 2.85$, (1H, d, $J = 9.3$ Hz) indicate that both H-2 and H-3 are axial and that, accordingly, C-2 and C-3 hydroxy groups are α -equatorial and β -equatorial, respectively. Accordingly, compound **1** is determined as 2 α , 3 β -24-trihydroxyurs-12-en-28-oic acid.

In addition, many couples of epimerides like compound **3** and **4**, **5** and **6**, **1** and **7** are isolated from the plant, see Fig. 8.36. For data of C-NMR spectra for ursane-type triterpenes, please see Table 8.27. Further research is needed to study the biological activities of triterpenes from Danshen.

8.8 The Challenges and Opportunities for the Study of Tanshinones in this Century

8.8.1 The Chemical Study of Tanshinone Aims at Finding New Targets

The isolation and purification of tanshinone has been studied for more than 70 years, and all constituents with content greater than 0.00001 % have been isolated and their chemical structures have been elucidated. The chance to find new compounds is minimal, even if we give a great effort toward the isolation of Danshen in the future. What we get from such efforts are most likely a lot of known compounds. Now, how to identify these known compounds quickly is the main problem which needs to be solved. The basic skeleton can be identified by TLC combined with direct chemical reactions even in the crude extract, such as the discrimination between tanshinone I, tanshinone II and cryptotanshinone. The identity of a compound can be further confirmed by ultraviolet absorption spectroscopy. For more complicated structures, infrared spectroscopy and nuclear magnetic resonance

spectroscopy can be used for identification. For example, methyl tanshinonate can be identified by the ester carbonyl infrared absorption. Although the structure of an isolated compound is already known, its biological activities and targets of action are still worthy of in-depth study. The ultimate proposal of phytochemistry study is to find the new biological targets of these constituents. Based on this principle, we could not only clarify the mechanisms of the traditional Chinese medicine Danshen, but also develop new types of drugs. Now, we are in the post-genomics and post-proteomics era, and more attention should be paid to research on the bio-activities of those compounds isolated from Danshen, especially the interactions between these compounds and some proteins with special functions (like the caspase family proteins which can induce cell apoptosis). Thus, we will take some examples to illuminate the points that the development of cell biology and molecular biology provides us with new opportunities and new technologies.

8.8.2 The Biological Activities and the Physicochemical Properties of Compounds

The study of Danshen began from *Emergency Formulas to Keep Up One's Sleeve* and *Liu Juan-zi's Ghost-Bequeathed Formulas*, more than 1,400 years ago. The liposoluble components of Danshen were successfully extracted and named “red ointment” at that time. Since the 1940s, nearly 80 diterpene quinone compounds have been isolated and purified using chemical methods. The most common active constituents are tanshinones (diterpene quinones). Some active compounds have been isolated under the guidance of biological assays, such as Ro-09-0680 with the ability to inhibit platelet aggregation, and miltirone with the ability to tranquilize on the cerebra. But none of them have been developed into new drugs that can be used clinically. One of the reasons for that lies in the insufficient understanding of these compounds' physicochemical properties, which in turn limits

the effort of finding suitable preparations. These are the challenges and opportunities we meet nowadays.

Of course, it is necessary to elucidate the structures of these active components. But it is not enough. First, there is little information on the physicochemical properties of crystals. This topic is so important that we emphasized it in the fourth section of this chapter, including some molecular mechanics and quantum chemistry parameters. Second, although the use of chromatography techniques in chemical experiments is very common, and the obtaining the data of R_f or R_t values of tanshinones is fairly easy; unfortunately, few of these parameters have been used for gathering information such as the oil–water distribution coefficient, the solubility, and the hydrogen bond adsorption to some polymers of these compounds. It needs to be emphasized that a crystal itself is a giant molecule. Among molecules, there are still many non-bonding interactions, such as hydrogen bonds or van der Waals forces. The physicochemical properties of crystal materials cannot be shown fully in a two-dimensional structural formula. For example, even though the R_f values of tanshinone I and tanshinone IIA on the TLC are very close, their solubilities differ a lot because of their different structures. The ring A in tanshinone IIA is alicyclic with a gem-dimethyl, so the intensity of the π – π bond in tanshinone IIA is lower than that in tanshinone I; therefore, the solubility of tanshinone IIA in nonpolar solvents is larger than that of tanshinone I. The non-bonding energy is much lower than the covalent bond energy, but its role in physicochemical properties should not be underestimated. In the 1970s, it was reported that tanshinone IIA had no bacteriostatic action on the resistant *S. aureus* and was not an active component. In that experiment, the researchers neglected the oil–water distribution property of tanshinone IIA and then came to the wrong conclusion. In fact, when tanshinone IIA is dissolved in CHCl_3 , it can no longer be dissolved in agar medium. Just by changing the solvent to a hydrophilic one, such as DMF, in which

tanshinone IIA can be easily dissolved in agar medium, the bacteriostatic action on tolerance *S. aureus* can be observed.

8.8.3 Chemical–biological Research of Tanshinone

The twenty-first century is an era of biology; it has been suggested that new subjects emerged in the “post-genomics” era should be named according to the compound noun X biology, in which X is an adjective, and biology is the stem. So, other non-biological disciplines became adjectives, such as chemical biology, mathematical biology, and computational biology. The “biology” mentioned here refers specifically to the biology emerged in the “post-genomics” era. In light of the prevailing context, we could try to establish a “Natural Product Chemistry-Biology,” which could categorize tanshinone as a class of natural chemicals for biological research. For the time being, it can be called tanshinone chemical biology which mainly focuses on the interactions between small molecules of tanshinones and certain active proteins. Such a subject is not only possible theoretically, but also has been confirmed by preliminary experiments. For example, genes of model organisms have been used for developing drugs on apoptosis. Because the proteins encoded by these genes are so similar, for any single human gene, there is as great of a 50–80 % chance to find a corresponding gene in nematodes or fruit flies. In 2002, the Nobel Prize in Physiology and Medicine was awarded to the subject that found the key genes of regulation of organ development and programmed cell death (PCD) using a nematode model. The choice of a nematode model for such research makes the genetic analysis linked to cell division, differentiation, as well as organ development, and opened possibilities to track a series of processes through microscopic observation. They further confirmed that the new key gene encodes a highly specific protease, called caspase. The word caspase is a short form of the

prefix and suffix of *cysteine aspartic acid specific protease*. The caspase protease family, originated in the research of PCD on nematodes (*c. elegans*), are highly specific protein which can specifically cut the peptide bond of aspartate residues. 11 genes were found related to the PCD, in which *ced3* and *ced4* were considered critical in inducing apoptosis. Later research confirmed that ICE, the homologue of *ced3*, acting as an apoptosis inducer, could be found in all types of mammalian cells including humans. In order to conduct a high-throughput screening for the extraction of Chinese traditional medicine, Dr. Luo Xi and her colleagues from Hong Kong University of Science and Technology in the Chemical Engineering Department established a fluorescence resonance energy transfer (FRET) for the anticancer activity of herbal medicine compounds [89]. The high-throughput screen uses a stable cell line (HeLa-C3) expressing a caspase biosensor, which is an engineered protein consisting of three parts: a donor cyan fluorescent protein (CFP), a 16-amino-acid peptide linker containing the caspase-3 cleavage site, and an acceptor yellow fluorescent protein (YFP).

Sensor C3 : ...CFP...D-E-V-D...YFP

The method of detection is based on the effects of FRET (Cubitt et al. 1995; Heim and Tseien 1996). The basic principle of this method is that in the absence of activated caspase-3 (i.e., under normal growth conditions) the fluorescent emission energy of the excited donor fluorescent protein CFP can be transferred to the acceptor molecule YFP, leading to the emission of yellow fluorescent light. When caspase-3 is activated during apoptosis, the activated protease will cleave the biosensor (CFP-linker-YFP) at the linker peptide containing the recognition sequence for caspase-3, DEVD (Asp-Glu-Val-Asp). Cleavage of the sensor protein abolishes the effect of FRET, resulting in a change in the emission profile of the sensor protein, because fluorescent light is emitted from CFP instead of YFP. Thus, by measuring the fluorescence emission ratio between YFP and CFP, the

amount of activation of caspase-3 in living cells during the process of apoptosis can be detected [90]. To detect the vitality of caspase in a single living HeLa-C3 cell, the fluorescence emission spectrum judged by the Y/C ratio is less than 3. The results showed that HeLa-C3 cells pretreated with tanshinone IIA (20 μ M)-activated caspase-3 enzyme, resulting in a Y/C ratio less than 3 and triggering apoptosis. However, as the control compound, water-soluble tanshinone IIA sulfonic sodium salt (which is introduced a polar sulfonic sodium group) kept the Y/C ratio higher than 5 at the same dose, suggesting failure to activated apoptosis.

Up until now, phytochemical research could not be limited at the level of simple extraction, isolation, and structure determination and could not be confined to subjects within the framework of analysis. Researchers should strive to combine with neighboring disciplines and make more cooperation with each other. Pay more attention to those known compounds. Which targets would they act on? Which biological activities do they have? By virtue of current cell biology and molecular biology techniques, if we combine our chemical knowledge with biological science, it is possible to make a big breakthrough and find the real significant targets, which is what we have anticipated for so long.

References

1. Ge H. A handbook of prescriptions for emergencies, vol. 5. Beijing: The Edition of Photolithograph by People's Medical Publishing House; 1955.
2. Gong QX, Liu J-Z, Gui Y-F Beijing: The Edition of Photolithograph by People's Medical Publishing House; 1955.
3. Urake T. *Pharmaco*. 1941;61(12):482.
4. Okumura Y, Kakisawa H, et al. *Soc Jpn*. 1961;34:895.
5. Urake T. *Tanminon Pharmaco*. 1942;64(12):40.
6. Tsutomu N, Hitoshi M, Masao N, et al. *Phytochemistry*. 1983;22(3):721.
7. Hayashi T, Kakisawa H. *Comm*. 1970;299.
8. Mitsuko O, Morio F, Nobuo S, et al *Chem Pharm Bull*. 1983;31(5):1670.
9. Luo H, J Ji. *Acta Pharm Sin*. 1989;24(5):341.
10. Takenori K, Toshiko K, Hiroshi K et al. *J. Chem. Soc. Perkin Trans. I*. 1976;1716.

11. Hou WL, Jiang J, Mei YW et al. *Chem Pharm Bull.* 1986;34(8):3166.
12. Luo HW, Shaoxing C, Junning L, et al. *Phytochemistry.* 1988;27(1):290.
13. Fang Q, Zhang P, Xue Z. *Acta Chimi Sin.* 1976;34(3):197.
14. Chang HM, Cheng KP, Choang TF, et al. *Bunge (Danshen). J Org Chem.* 1990;55(11):3537.
15. Yang B, Qian M, Qian G, et al. *Acta Pharm Sin.* 1981;16(11):837.
16. Shi YR, Zaesung N, Sung HK et al. *Planta Med.* 1997;63:44.
17. Qian M, Yang B, Gu W et al. *Acta Chimi Sin.* 1978;36(3):199.
18. Kakisawa H, Hayashi T, Okazaki I, et al. *Tetrahedron Lett.* 1968;28:3231.
19. Hou W, Bao J, Mei Y, et al. *Phytochemistry.* 1985;24(4):815.
20. Yang Baojing, Huang Xiulan, Zhou Qianru. *Acta Pharmaceutica Sinica*, 1984, 19(4):274.
21. Lu X, Luo H, Niwa M. *Planta Med.* 1990;56:87.
22. Lu X, Luo H, Ji J, et al. *Acta Pharm Sin.* 1991;26(3):193.
23. Feng B, Li S. *Acta Pharm Sin.* 1980;15(8):489.
24. Li Z, Yang B, Ma G. *Acta Pharm Sin.* 1991;26(3):209.
25. Luo H, Hu X, Wang N et al. *Acta Pharm Sin.* 1988;23(11):830.
26. Weng X-C, Gordon MH *J Agric Food Chem.* 1992;40(8):1331.
27. Gong B, Cheng J, Zheng Q et al. *Study on the quantum chemistry of the antioxidation effect of Danshenquinone III.* 8th edn. Beijing: Atomic Energy Press, 2001. pp. 133–136.
28. Kakisawa H, Hayashi T, Yamazaki T. *Tetrahedron Lett.* 1969;5:301.
29. Kong D, Liu X. *Acta Pharm Sin.* 1984;19(10):755.
30. An R, Wu L, Wen L, et al. *J Nat Prod.* 1987;50(2):157.
31. Michavila A, de la Torre MC. *Phytochemistry.* 1986;25(8):1935.
32. Asari F, Kusum T, Zheng GZ et al. *Chem Soc Jap Chem Lett.* 1990;1885.
33. Yasuhiro T, Rena K, Purusotam B et al. *Chem Pharm Bull.* 1997;45(8):1306.
34. Juan A, Hueso R, Maria L et al. *Phytochemistry.* 1983;22(9):2005.
35. Haro G, Kakisawa H. *Chem Soc Jap Chem Lett.* 1990;1599.
36. Yaki A, Fujimoto K, Tanonaka K et al. *Planta Med.* 1989;55:51.
37. Ikeshiro Y, Mase L, Tomita Y. *Phytochemistry.* 1989;28(11):3139.
38. Lin LZ, Wang XM, Huang XL, et al. *Planta Med.* 1988;54:443.
39. Kusumi T, Ooi T, Hayashi TA. *Phytochemistry.* 1985;24(9):2118.
40. Huang X, Yang B, Huang H et al. *J Integr Plant Biol.* 1980;22(1):98.
41. Huang X, Yang B, Hu Z. *J Integr Plant Biol.* 1981;23(1):70.
42. Liu C, Zhang J, Dai J, et al. *Chin Tradit Pat Med.* 1999;21(8):385.
43. Qian S, Jun J, Zhu L et al. *Chin Wild Plant Res.* 1999;18(1):41.
44. Zhang Y, Liu J, Cui Y, et al. *J South China Univ Technol (Nat Sci).* 1998;26(8):91.
45. Wang H, Wang Q. *J Chin Pharm Univ.* 2002;33(3):219.
46. Chen H, Chen F. *Biotechnol Lett.* 1999;21:701.
47. Chen H, Chen F. *Plant Cell Rep.* 2000;19:710.
48. Shao H, Jing X, Yin L et al. *Chin Trad Pat Med.* 1979;2:8.
49. Shao H, Jing X, Ying L et al. *Nucl Tech.* 1981;5:55.
50. Luo H, Sheng L, Zhang S, et al. *Acta Pharm Sin.* 1983;18(1):1.
51. Xie M, Shen Z. *Acta Pharm Sin.* 1983;18(2):90.
52. Yang Z, Hon P, Chui K, et al. *Tetrahedron Lett.* 1991;32(18):2061.
53. Kong D, Liu X, Teng M et al. *Acta Pharm Sin.* 1985;20(10):747.
54. Yang B, Huang X, Hu Z et al. *Acta Pharm Sin.* 1982;17(7):517.
55. Haro G, Takenori K, Ishitsuka MO, et al. *Tetrahedron Lett.* 1988;29(36):4603.
56. Sun X, Luo H, Tatsuko S, et al. *Tetrahedron Lett.* 1991;32(41):5797.
57. Hayashi T, Inoue Y, Ohashi M, et al. *Organic Mass Spectrometer.* 1970;5:1293.
58. Kazuaki K, Tatsuya T, Yoshio S. *Bull Chem Soc Jpn.* 1982;55(5):1344.
59. Jiang W, Zhao Y, Zhao B et al. *Acta Biophy Sin.* 1994;10(4):685.
60. Zhao Y, Jiang W, Hou J, et al. *Acta Bio Chim Biophys Sin.* 1995;27(6):610.
61. Xu L, Wu Q, B Wang, et al. *Chin J Pathology.* 1994;10(6):635.
62. Shi D, Li L, Liu S et al. *Acta Biophy Sin.* 1999;15(1):193.
63. Niu X, Ichmori K, Yang X, et al. *Free Rad Res.* 2000;33:305.
64. Dong C, Qiao M, Yang Q. *Chin J Spectrosc Lab.* 2000;17(4):369.
65. Li J, Dong C, Yang P. *J Shanxi Univ (Nat Sci Edn).* 2002;25(3):232.
66. Lee DS, Lee SH. *J Biosci Bioeng.* 2000;89(3):292.
67. Li R, Wu Q, Xu S et al. *J Radiat Res Radiat Process.* 1998;16(1):29.
68. Lou H, Wei B, Liu Q, et al. *J Chin Pharm Univ.* 2002;33(1):6.
69. Chang HM, Chui KY, FWL Tan et al. *J Med Chem.* 1991;34:1675.
70. Lam BYH, Lo ACY, Sun X, et al. *Phytomedicine.* 2003;10:286.
71. Luo H, Zheng J, Jiang B et al. *J Chin Pharm Univ.* 1982;18:42.
72. Luo H, Gao J, Zheng J. *J Chin Pharm Univ.* 1988;19(4):258.
73. Zhu J, Luo H. *J Chin Pharm Univ.* 2004;35(4):368.
74. Huang W, Tan F, Luo H. *J Chin Pharm Univ.* 1988;19(2):90.

75. Luis JG, Lucia S. *Tetrahedron*. 1993;49(22):4993.
76. Hitoshi M, Masao N, Toshihiko Y, et al. *Phytochemistry*. 1986;25(3):637.
77. Lin H, Chang W, Chen C. *Chin Pharm J*. 1995;47:77.
78. Ballie AC, Thomson RH. *J Chem Soc(C)*. 1968;48.
79. Kakisawa H et al. *Tetrahedron Lett*. 1968;3783.
80. Inouye Y, et al. *Bull Chem Soc Jpn*. 1969;42:3318.
81. Lee J, Tang J, Snyder JK. *Tetrahedron Lett*. 1987;28(30):3427.
82. Lee J, Snyder JK. *J Am Chem Soc* 1989;111:1522.
83. Shen J, Zhang P, Qiao M. *Acta Pharm Sinica*. 1988;23(7):545.
84. Nasipuri D, Mitra AK. *J Chem Soc Perkin Trans I*. (1973);285.
85. Lee J, Mei HS, Snyder JK. *J Org Chem*. 1990;55(17):5013.
86. Yang D, Luo H. *J Chin Pharm Univ*. 1998;29(4):255.
87. Wang N, Niwa M, Luo HW. *Phytochemistry*. 1988;27(1):299.
88. Sun XR, Luo HW, Sakai T, et al. *Shoyakugaku Zasshi*. 1992;46(3):202.
89. Tian H, Ip L, Luo H, et al. *Brit J Pharmacol*. 2007;150:321.
90. Luo KQ, Yu VC, Pu Y et al. *Biochem Biophys Res Commun*. 2001;283:1054.
91. Li S. *Compendium of material medica*, vol. 12. Beijing: The Edition of Photolithograph by People's Medical Publishing House; 1965.
92. Huang X, Hu Z, Yang B, et al. *Chin Pharm J*. 1981;16(9):534.
93. Ji J, Luo H. *J Chin Pharm Univ*. 1988;19(3):197.
94. Sun C, Bai D, Yao X, Xue B. 1985;20(1):39.
95. Lu X. The Doctoral Dissertation of Beijing Medical University, 1993;20.

Index

Symbols

Δ^1 -miltirone, 141, 147
 Δ^1 -tanshinone IIA, 146
1- hydroxymiltirone, 169
1-hydroxytanshinone II, 149
1-hydroxytanshinone IIA, 146
1, 2-dihydratanshinone, 150
1, 2-dihydratanshinone I, 146, 150
1, 4-paraquinone, 150
1, 4-paraquinone skeleton, 149
1,2,15,16-tetra, 146
2-hydroxy isodihydratanshinone I, 147
2-hydroxyferruginol, 147
3-hydratanshinone IIA, 146
3-hydroxysalvilenone, 147
3-keto-sapriparaquinone, 147
3 α -hydroxytanshinoneia, 141

A

Above-ground part, 57, 59, 60, 61, 63, 65, 73
Adventitious root, 50, 70, 74, 75, 92
Anhydride of cyptotanshinone, 127
Anhydride of tanshinone, 156
Anhydride of tanshinone IIA, 147
Arucadiol, 127, 147, 158, 169

B

Baihua Ganxi Shuwei (white flower sage of western Gansu) (*S. przewalskii* Maxim. var. *alba* X. L. Huang et H. W. Li), 5
Baihua (white flower), 5
Benma Cao, 1
Biexue, 2
Biosynthetic pathway, 110–113, 185–187
Breeding, 90–92, 94, 95
Bud removal, 54–56

C

cDNA chips, 44
Cell culture, 50, 69, 72, 76, 78
Changguan Shuwei (long crest sage) (*S. plectranthoides* Griff.), 7

Chang Shuwei Cao, 1

Chao, 2

Chemical composition variation, 13, 14, 17

Chemical synthesis of tanshinones, 192

Chenghuang Shuwei (orange yellow sage) (*S. aerea* Lev.), 7

Chishen, 1, 2, 4

Chromosomes, 90

Community, 12, 14, 17, 63

Constituents, 14–17, 50, 54, 56, 57, 59, 60, 63, 64, 69, 72–81, 86, 87, 89–92, 94, 95

Counterfeits, 8

Cross-sections, 28

Crown gall, 75, 76, 78, 80–83, 85, 86, 94

Cryptoacetalide, 127, 163, 164

Cryptomethyltanshinoate, 146

Cryptotanshinone, 97, 119–123, 127–132, 135–141, 143, 145, 146, 149, 153, 156, 158, 162–168, 172–175, 177, 179–188, 190, 192, 197, 205

Cu, 2

Cutting, 50, 56, 70, 76

D

Danshinspiroketallactone, 144, 145

Danye (single leaf), 5

Da Zi (bright purple), 4

Dehydromiltirone, 124, 130, 155, 176, 180

Demethylcryptojaponol, 127, 147

Development, 11, 49, 51, 60, 63, 66, 79, 80, 87

Dian (Yunnan), 5

Diene addition of 3-methoxyl-benzofuran-4,7-diketone, 192

Dihydratanshinone, 122, 127, 129, 131, 135–137, 140, 153, 155, 164, 165, 167, 168, 170, 175, 179–184, 189, 190, 197, 198

Dihydratanshinone I, 141, 146, 176, 178, 181, 183

Distribution, 2, 8, 12, 61

E

Ecological and Biological Characteristics, 11

Edition, 1, 3

Embryo sac, 35, 40

Environmental condition, 12, 52, 54, 60

Epi, 145
 Epicryptoacetalide, 147
 Ests, 44, 45

F

Female gametophytes, 35
 Ferruginol, 126, 127, 141, 147, 158, 168
 Five-phase-five-color theory, 2
 Flowering, 54
 Flowers, 2, 3, 5, 9, 10, 90
 Four tones materia medica, 2
 Functional genomics, 44

G

Gansu, 4
 Genuineness, 15, 17, 18, 64
 Germplasm, 89
 Growth, 9, 11, 12, 14, 49, 50, 52, 54, 56–61, 63–66, 71–86, 90, 91

H

Habitat, 2, 12, 13, 50
 Hairy root, 75–80, 94, 95
 Haozhou Zishen, 1
 Hong Gen, 1, 4
 Huanghua Jiaohao (*Incarvillea lutea* Bur. et Franch.) (family: *Bignoniaceae*), 10
 Huanghua Shuwei (yellow flower sage) (*S. flava* Forrest ex Diels), 7
 Hydrotanshinone, 123, 126, 150, 157, 159, 169–171, 179, 190
 Hydroxyferruginol, 127
 Hydroxyisodihydrotanshinone, 153, 169
 Hydroxymethylene tanshinnone, 146
 Hydroxymiltirone, 169
 Hydroxytanshinone II, 149

I

Internal structure, 28
 In vitro, 69, 76, 77, 93
 In vitro seedlings, 70
 IR spectrum, 148–163, 166
 Isocryptotanshinone, 121, 126, 134, 147, 149, 150, 152, 153, 169, 192
 Isodihydrotanshinone, 126, 153, 169, 181
 Isodihydrotanshinone I, 147
 Isotanshinone, 121, 125, 126, 134, 149, 150, 152–154, 169, 173, 179, 192
 Isotanshinone I, 147, 149, 150
 Isotanshinone II, 149, 150
 Isotanshinone IIA, 192
 Isotanshinone IIB, 147
 Isozyme, 42, 43

J

Jiu, 1, 2

K

Ketosapriparaquinone, 170

L

Leaves, 2–4, 6–10, 49, 50, 54–61, 63, 66, 69–73, 77, 81, 90, 91, 93
 Lise Shuwei (dark brown sage) (*S. castanea* Diels), 8
 Lithospermic acid, 98, 99, 103, 105, 108, 116
 Local varieties, 4

M

Macrospores, 35
 Male gametophytes, 40
 Maodihuang Shuwei (foxglove sage) (*S. digitaloides* Diels.), 7
 Maoye Qiaomai Di Shuwei (hairy leaf buckwheat field sage) (*S. kiaometiensis* Lév. *F. pubescens* Sib.), 7
 Methlene miltirone, 147
 Methylene tanshinquinone, 143, 146, 150, 157, 159, 170, 171, 179, 181–183, 190
 Methylenedihydrotanshinone, 146, 159
 Methylenemiltirone, 125
 Methylenetanshinone, 123, 129, 131, 135, 138, 139, 141, 168
 Methyl tanshinonate, 141, 146, 149
 Microelements, 64–66
 Micropropagation, 69
 Microscopic structure, 27
 Microspores, 40
 Miltionone, 127, 162, 169, 176
 Miltionone -I, 147
 Miltionone -II, 147
 Miltipolone, 127, 147, 160–162, 169
 Miltirone, 121–126, 129, 136, 140, 141, 144, 147, 155, 167, 168, 172, 175, 176, 178–181, 184, 185, 195, 205
 Miltirone I, 141, 147, 168, 175, 178, 179, 181
 Miltironei, 141, 179
 Morphological characteristics, 4
 Morphology, 2, 4, 89
 MS data, 167–169
 Mu Yang Ru, 1, 2

N

Nan (southern), 4
 NMR spectrum, 148–164, 166, 196, 199, 201–203
 Norsalvioxide, 127, 147, 166, 169
 Nortanshinone, 141, 146, 156, 157, 171, 192

O

Ol-A, 147
 Ol-B, 147
 Oleanolic acid, 141
 Original plant of Danshen, 4

P

Phenolic acids, 97–99, 101–103, 107, 110, 131
 Photo-oxidation, 187, 188
 Physicochemical parameters of tanshinone, 179
 Planting density, 60–63
 Pollen, 13, 66
 Pollen grains, 31, 32, 35, 40
 Pollination, 31–34
 Primary structures, 28
 Propagation, 18, 49, 50, 69, 70, 72, 75, 79, 80, 82, 91, 93
 Protocatechuic aldehyde, 98, 109, 110, 131
 Przewaquinone, 122, 142, 150, 157, 158, 170, 172, 173, 178, 180
 Przewaquinone A, 141, 146
 Przewaquinone B, 141, 146
 Przewaquinone C, 146
 Przewaquinone F, 146

Q

Qiaomai Di Shuwei (Buckwheat field sage) (*S. Kiao-metiensis* Lév.), 6
 Qiancao (*Rubia cordifolia* L.) (family: *Rubiaceae*), 8

R

RAPD, 13, 91
 R_f values, 182, 183
 Roots, 2–11, 13, 17, 18, 49–52, 54–57, 59, 60, 61, 65, 66, 70–74, 76, 77, 80, 89–91, 93, 95
 Rootstalk division, 49
 Root system, 57, 60–63, 65, 66, 90, 95
 Rosmarinic acid, 98, 99, 102, 103, 108, 132, 176

S

Salvia bowleyana Dunn, 4
Salvia miltiorrhiza, 1, 3, 97, 119
 Salvianolic acid, 97–100, 102–116, 130–132, 142, 176
 Salvianolic acid A, 141
 Salvianolic acid B, 141
 Salvilenone, 128, 147, 148, 170
 Salviolone, 127, 140, 141, 147, 148, 168
 Sanye (three-leaf), 5
 Secondary structures, 29
 Seedlings, 3, 49–53, 57, 58–61, 69–72, 77, 79–82, 90, 93, 94
 Seeds, 3, 11, 18, 49, 51–54, 57, 60, 66, 70, 80, 93
 Shanshen, 1
 Shaomao Ganxi Shuwei (Less hair sage in western Gansu) (*S. Przewalskii* var. *Glabrescens* Stib.), 6
 Shen Nong's classic of the materia medica, 1, 2
 Shuisu Caosu (*Phlomis betonicoides* Diels) (family: *labiatae*), 9

S. miltiorrhiza Bunge F. *alba* C. Y. Wu et H. W. Li, 5
S. miltiorrhiza Bunge var. *charbonnellii* (Léveillé) C. Y. Wu, 5
S. paramiltiorrhiza H. W. Li et X. L. Huang, 6
 Spectral properties, 103
 Sperms, 92
 Spiroketallactone, 141, 145, 147
S. Przewalskii Maxim, 4
S. Przewalskii Maxim. Var. *Mandarinorum* (Diels.) Stib., 4
S. sinica Migo, 6
 Stems, 2, 3, 18, 49, 57, 58, 61, 66, 72, 73, 76, 77, 90, 91, 93, 94
S. trijuga Diels., 5
 Sugiol, 127, 137, 147, 158, 169
 Summer dormancy, 56, 57, 59
S. yunnanensis C. H. Wright, 5

T

Tan, 2
 Tanshenlactone, 122, 123, 146, 159
 Tanshinaldehyde, 1, 146
 Tanshinaldehyde I, 146
 Tanshindiol, 122, 123, 140, 142, 145, 148, 156, 157, 168, 179, 190, 200
 Tanshindiol A, 141, 146
 Tanshindiol B, 141, 146, 192
 Tanshindiol C, 141, 146
 Tanshindiols A, B and C, 145
 Tanshinlactone, 121, 127, 138, 139, 141, 144, 145, 154, 155, 168, 179
 Tanshinol, 14, 15, 55–57, 59–61, 63–65, 67, 68, 89, 91, 122
 Tanshinol I, 146
 Tanshinone, 97, 101, 102, 119–123, 125–132, 134–136, 138–143, 145–148, 151, 152, 154, 155, 157–160, 167–190, 192, 194–200, 204–206
 Tanshinone I, 97, 119–123, 126, 127, 129–133, 135–146, 148–154, 156, 157, 159, 167, 169, 170, 172–175, 177, 178, 180–192, 195–199, 205–207
 Tanshinone II, 141, 145, 149, 150, 183
 Tanshinone IIA, 4–8, 13–15, 51, 56–62, 65, 66, 68, 73, 75, 77, 78, 81, 86, 91, 92, 97, 146, 149, 150, 192
 Tanshinone IIA leaves, 63
 Tanshinone IIB, 183
 Tanshinone V, 147
 Tanshinone VI, 147
 Tanshinonei, 141
 Tetrahydrotanshinone, 122, 159, 169, 179, 181, 189
 Thermodynamic, 183–185
 Tissue culture, 50, 51, 70, 72, 75, 80, 91, 93
 Total synthesis of miltionone, 195
 Total synthesis of miltirone, 194, 195
 Total synthesis of tanshinone IIA, 192
 Transformation, 51, 79, 81, 87, 92–95
 Triterpene, 141
 Tu Huoxiang (local ageratum) (*Agastache* sp.) (family: *labiatae*), 9

U

UV spectrum, [146](#), [148–150](#), [152–162](#)

W

Wan E (Anhui and Hubei), [6](#)

Water soluble components, [97](#), [98](#)

Weilingcai Gen (*potentilla* root) (*Potentilla chinensis* Ser.) (family: *Rosaceae*), [10](#)

X

XH-14, [133](#), [136](#), [137](#)

Xiaku Cao (self-heal) (*Prunella vulgaris* L.) (family: *Labiatae*), [9](#)

Xichan Cao, [1](#)

Xinkun A, [141](#), [147](#)

Xinkun B, [127](#), [141](#), [147](#)

Xinkun C, [147](#)

Xueshan Shuwei (snow mountain sage) (*S. evansiana* Hand.-Mazz.), [8](#)

Y

Yield, [12](#), [13](#), [50](#), [51](#), [54–57](#), [59–64](#), [67](#), [68](#), [74](#), [78](#), [83](#), [86](#), [89](#), [91](#), [95](#)

Yunnaneic acid, [98](#), [99](#), [101](#), [103](#), [106–110](#)

Z

Zhe Wan (Zhejiang and Anhui), [6](#)

Zhu Ma, [1](#), [2](#)

Zhusha Gen (*Ardisia crenata* Sims.) (family: *Myrsinaceae*), [9](#)

Zi, [1](#)

Zi Dangen, [1](#)

Zihua, [1](#), [2](#), [8](#)